Palaeontologia Electronica
palaeo-electronica.org

Sharks and rays (Chondrichthyes: Elasmobranchii) from the Peace River and Tamiami formations (Late Miocene–Early Pliocene) on the submerged continental shelf near Venice, Florida, USA

Harry M. Maisch IV, Martin A. Becker, Victor J. Perez, and Kenshu Shimada

ABSTRACT

The submerged continental shelf near Venice, Sarasota County, Florida, USA, exposes clays and hard-bottom limestones of the Peace River and Tamiami formations (Late Miocene–Early Pliocene). These formations occur in ≤12 m of seawater, within 4.5 km of the modern-day shoreline, because of wave- and current-driven deposition and erosion during glacioeustactic sea-level cyclicity, shifting of the ancestral shoreline, fluvial incision, and storm activity across the shallow shelf since the Miocene. These processes have accumulated residual, fossiliferous lag deposits on the modern seafloor that contain an abundance of elasmobranch remains (primarily isolated teeth of sharks and rays) belonging to at least 45 taxa including: *Squalus* sp., *Isistius triangulus, Heterodontus* sp., *Ginglymostoma cirratum, Carcharias taurus, Otodus megalodon, Parotodus benedinii, Isurus oxyrinchus, Carcharodon carcharias, C. hastalis, Scyliorhinus* sp., *Mustelus* sp., *Galeorhinus* sp., *Hemipristis serra, Galeocerdo aduncus, G. mayumbensis, G. cuvier, Physogaleus contortus, Rhizoprionodon* sp., *Negaprion brevirostris, Carcharhinus* cf. *C. falciformes, C. leucas, C. obscurus, C. plumbeus, C.* cf. *C. altimus, C. perezii, C.* cf. *C. brachyurus*, *C.* cf. *C. porosus*, *Carcharhinus limbatus*, *Carcharhinus brevipinna*, *Sphyrna* cf. *S. zygaena*, *S.* cf. *S. tiburo*, *Rhynchobatus* sp., Rhinobatidae gen. indet., *Pristis* cf. *P. pristis, Anoxypristis* sp., Rajidae gen. indet., *Hypanus* cf. *H. say*, *Hypanus* cf. *H. americanus, Rhinoptera* cf. *R. bonasus*, *Mobula* cf. *M. hypostoma, Mobula* cf. *M. birostris*, *Aetomylaeus* sp., *Myliobatis* sp., and *Aetobatus* cf. *A. narinari*. These elasmobranch remains were collected exclusively by SCUBA diving off the coast of Venice, Florida and provide a unique means to observe taphonomic processes influencing vertebrate fossils on the shallow continental shelf. This represents the most diverse fossil elasmobranch assemblage reported from the state of Florida and is also one of the most diverse assemblages in the late Cenozoic fossil record in the USA. Comparison of the submerged Venice shelf elasmobranchs

Final citation: Maisch, Harry M. IV, Becker, Martin A., Perez, Victor J., and Shimada, Kenshu. 2025. Sharks and rays (Chondrichthyes: Elasmobranchii) from the Peace River and Tamiami formations (Late Miocene–Early Pliocene) on the submerged continental shelf near Venice, Florida, USA. Palaeontologia Electronica, 28(3):a49.
https://doi.org/10.26879/1529
palaeo-electronica.org/content/2025/5629-fossil-sharks-and-rays-venice-florida-usa

with those from land-based exposures in Florida and elsewhere along the Atlantic and Gulf Coastal Plains of the USA also indicates that fossils and submerged formations become geologically younger to the south. Moreover, the Venice taxa provide a unique means to assess the stratigraphic distribution of many well-known and globally occurring elasmobranchs, including large lamniforms and the megatoothed shark, *Otodus megalodon*, as related to habitat shifts along the west coast of Florida since the late Cenozoic.

Harry M. Maisch IV. Department of Marine and Earth Sciences, The Water School, Florida Gulf Coast University, 10501 FGCU Boulevard South, Fort Myers, Florida 33965, USA (corresponding author). hmaisch@fgcu.edu
Martin A. Becker. Department of Environmental Science, William Paterson University, 300 Pompton Road, Wayne, New Jersey 07470, USA. beckerm2@wpunj.edu
Victor J. Perez. Natural and Historic Resources Division, Prince George's County Parks and Recreation, Maryland-National Capital Parks and Planning Commission, Upper Marlboro, Maryland, USA. Victor.Perez@pgparks.com
Kenshu Shimada. Department of Environmental Science and Studies, DePaul University, 1110 West Belden Avenue, Chicago, Illinois 60614, USA; and Department of Biological Sciences, DePaul University, 2325 North Clifton Avenue, Chicago, Illinois 60614, USA; and Sternberg Museum of Natural History, Fort Hays State University, Hays, Kansas 67601, USA; and Scientific Affiliate, Integrative Research Center, Field Museum of Natural History, Chicago, IL 60605, USA. kshimada@depaul.edu

Keywords: climate change; fossil elasmobranchs; Miocene; Peace River Formation; Pliocene; Tamiami Formation

Submission: 28 December 2024. Acceptance: 28 August 2025.

INTRODUCTION

For over 125 years, the diverse marine and terrestrial invertebrate and vertebrate fossil remains occurring throughout Florida have attracted many amateur and professional geologists and paleontologists (e.g., Leidy, 1896; Matson and Clapp, 1909; Brown, 1988; Garcia and Miller, 1998; Sinibaldi, 1998; Kocsis, 2002; Fink, 2004; Portell and Agnew, 2004; Renz, 1999, 2002, 2005). In particular, the central Florida phosphate-mining region, known as "Bone Valley", contains an abundance of vertebrate fossil remains that have been concentrated along with phosphatic clasts (Day, 1886; Wright, 1893; Scott, 1988; Hulbert, 2001). Fossil elasmobranch teeth including those belonging to the megatoothed shark (i.e., *Otodus megalodon* or simply "Megalodon"), are locally abundant in Florida's phosphatic sediments and are highly sought after by collectors and scientists alike (Hulbert, 2001; Renz, 2002; Bryan et al., 2008).

The abundance of fossil shark teeth on publicly accessible beaches and the submerged shallow continental shelf in Venice, Florida, has led this city to become known as the "Shark Tooth Capital of the World" and the host of annual Shark Tooth Festivals (Hine, 2013). The unique occurrence of fossils on this picturesque, west Florida, Gulf of Mexico shoreline also encouraged the publication of numerous fossil collecting and identification guides (e.g., Ayres, 1961; Thomas, 1965; Cartmell, 1988; Marlowe, 2014; Fuqua, 2011, 2017, 2020). However, fossils from Venice have been largely overlooked by the academic paleontological community. The abundance of elasmobranch fossils found in the Venice region is a result of numerous climatically driven sea-level fluctuations that have exhumed, concentrated, and reburied fossil remains since at least the Late Miocene. These fossils can differ in age by ≥5 million years and represent taxa with distinctly different habitat preferences. In this paper, we report for the first time a comprehensive study on the elasmobranch assemblage recovered exclusively by SCUBA diving off Venice, Florida (hereafter referred to as the Venice Elasmobranch Assemblage) and provide insights on the geology, age, and taphonomic history of the shallow continental shelf in the area.

GEOLOGICAL AND PALEONTOLOGICAL BACKGROUND

General Geological Setting

The state of Florida is a carbonate platform composed of Cenozoic marine sediments and rocks that are underlain by Cretaceous and crystalline basement rocks (Hine, 2013). The majority of these calcareous sediments and rocks were subsequently covered by siliciclastic sediments derived from the Appalachian Mountains and transported by rivers flowing southward in response to sea-level regression beginning in the Oligocene (McKinney, 1984; Hine, 1997, 2013; Missimer and Maliva, 2017). This influx of siliciclastic sediment adjoined Florida to the Atlantic and Gulf Coastal Plains of the USA and consequently diminished carbonate deposition and altered ocean current flow (Hine, 2013). In particular, sea-level changes affecting peninsular Florida influenced the flow paths of the ancestral Loop Current and Gulf Stream since the Miocene (Riggs, 1984; Mullins et al., 1987; Snyder et al., 1990; Fountain et al., 1993; Compton, 1997; Scott, 1997).

Peninsular Florida is composed of Cenozoic and Holocene sediments that exhibit structural features including the Peninsular Arch and Ocala Platform (i.e., the Ocala Arch sensu Fountain et al., 1993) which trend in a north-south direction (Fountain et al., 1993; Scott et al., 2001; Hine, 2013). In general, west of the Peninsular Arch, sedimentary layers dip towards the Gulf of Mexico, east of the arch, sedimentary layers dip towards the Atlantic Ocean, and collectively, sedimentary layers also become progressively younger towards the southern portion of the state (Cathcart, 1989; Fountain et al., 1993; Scott et al., 2001; Bryan et al., 2008; Hine, 2013).

Phosphate is relatively common throughout Florida's Cenozoic sediments; however, it is most concentrated in the Peace River Formation that occurs across the central portion of the state (Scott, 1988; Scott et al., 2001). In particular, central Florida contains large, ore-grade phosphate deposits that have been exploited through dredging and mining activities for about 140 years (e.g., Day, 1886; Wright, 1893). These regional phosphate deposits are frequently referred to as "Bone Valley" due to the abundance of vertebrate fossil remains that co-occur with phosphate ore (Matson and Clapp, 1909). The "Central Phosphate District" was established around the Peace River region in Polk and Hillsborough Counties, Florida and has high-grade phosphate ore consisting of boulder to sand-sized clasts (Cathcart, 1989; Scott, 1990; Fountain et al. 1993). However, additional, lower-grade phosphate has also been mined from the "Southern Extension" of the Central Phosphate District that extends into Hardee, Manatee, and DeSoto counties, Florida (Cathcart, 1989; Fountain et al., 1993).

Traditionally, all layers with phosphatic sediments within the Central Phosphate District and Southern Extension were identified as the Bone Valley Formation (sensu Matson and Clapp, 1909); however, the Cenozoic geology of Florida was extensively revised by Scott (1985a, 1985b, 1986, 1988). The "Bone Valley Formation" is now referred to as the Bone Valley Member of the Peace River Formation within the Hawthorn Group and represents a thin, sporadically exposed, extremely rich phosphatic zone containing large clasts in the Central Phosphate District (Cathcart, 1989; Scott, 1988, 1990). The undifferentiated Peace River Formation is comprised of fine-grained sandy, clayey, and phosphatic sediments below and above the Bone Valley Member, and the formation increases in thickness to the south (Cathcart, 1989; Scott, 1990).

The Peace River Formation has been identified as Middle to Late Miocene–Pliocene in age based on vertebrate fossils (Webb and Tessman, 1968; Webb and Crissinger, 1983; Cathcart, 1989) and nannofossils (Covington, 1992). The age of localized Bone Valley Member deposits has been controversial and previously placed within the Miocene or Pliocene because varying amounts of erosion and reworking have influenced individual outcrops (e.g., Matson and Clapp, 1909; Matson, 1915; Simpson, 1930; Cooke, 1945; MacFadden and Webb, 1982; Webb and Crissinger, 1983; Scott, 1988). Currently, the Bone Valley Member is considered to be Pliocene in age and contains Miocene marine fossils that have been reworked along with Pliocene terrestrial fossils in fluvial channel deposits (Webb and Crissinger, 1983; Scott, 1988). Strontium isotope analyses of phosphatic clasts recovered from drill cores in Lee County, Florida indicate that the lower Peace River Formation is ~13–8.5 Ma, whereas the upper Peace River Formation in this region is ~5.23–4.29 Ma (Compton et al., 1993; Missimer, 2001). However, it must be noted that the clasts utilized for strontium analyses were collected downdip (i.e., south of Venice, Sarasota County, Florida) and the strontium-isotope curve flattens near the Miocene–Pliocene boundary providing less reliable chronostrati-

graphic resolution (Missimer, 2001; McArthur et al., 2020).

Younger sediments belonging to the Pliocene Tamiami Formation or various Plio–Pleistocene formations overlie the Peace River Formation in central Florida and also outcrop across much of the southern portion of the state (McCartan and Moy, 1995). The contact between the Peace River and Tamiami formations is erosional and generally identified as a dark-colored, carbonate mud containing concentrations of reworked phosphate, dolomite, and quartz sand (Missimer, 1978, 1992). However, placement of this contact can be difficult because the Peace River and Tamiami formations are lithologically and paleontologically similar, phosphate occurs locally throughout the Tamiami Formation, and the extent of reworking may obscure the contacts between formations (Peck et al., 1979; Scott, 1990; Missimer, 1978, 1992). The Tamiami Formation has been identified as Pliocene in age with the base of the formation identified between ~4.9–4.2 Ma and the upper Plio–Pleistocene boundary identified at ~1.95 Ma in southern Florida (Cathcart, 1989; Missimer, 1978, 1992, 2001).

It is important to note that the geology of southwest Florida has been difficult to decipher because various units, members, and formations have been proposed or identified based on lithostratigraphic or biostratigraphic variations despite the lack of laterally expansive surface exposures or subsurface units (Scott, 1988; Missimer, 1992; McCartan and Moy, 1995). Moreover, additional complications with identifying and correlating the late Cenozoic geology of southwest Florida stem from workers with differing areas of expertise including hydrogeology, lithostratigraphy, biostratigraphy, and sequence stratigraphy. In this study, featuring a time-averaged assemblage of elasmobranch teeth, we utilize a sequence stratigraphic approach and interpret these teeth to be Late Miocene–Early Pliocene in age derived from lag deposits occurring at (or near) the boundary between the Peace River and Tamiami formations. These lag deposits have been further reworked to varying extents across the shallow Venice shelf as a result of wave-based erosion, bottom currents, and fluvial incision of the continental shelf during sea-level lowstands.

Geology of the Submerged Venice Study Area

The shallow continental shelf along the coast of Venice, Florida, is located adjacent to the northwestern portion of the Southern Extension of the Florida phosphate mining district (Fountain et al., 1993; Scott et al., 2001; Hine, 2013). The submerged study area documented in this report occurs south of Venice Inlet and extends towards Manasota Key (Figure 1). Fossil remains were collected within 4.5 km of the present-day shoreline in water depths ranging from ~3–12 m.

The northernmost region of the study area near Venice Inlet contains coarse, pebble to boulder-sized clasts that include megatoothed shark teeth as well as marine and terrestrial mammal bones and teeth. These large litho- and bio-clasts frequently exhibit extensive amounts of abrasion and bioerosion that suggests prolonged winnowing and reworking occurred in this area (e.g., Boessenecker et al., 2014; Maisch et al., 2019a). While it is possible that this localized zone may represent a submerged exposure of the Bone Valley Member of the Peace River Formation, large authigenic phosphate clasts are absent. Instead, it is more likely that the deposit in this zone represents Miocene–Pliocene residuum concentrated from a Plio–Pleistocene fluvial channel that has been further reworked by wave-based erosion from changes in sea-level.

Further south, the abundance of boulder to cobble-sized clasts and large, abraded vertebrate fossils decreases and is replaced by gray-colored, phosphatic, sandy clay exposures occurring on or just below the seafloor. These exposures are frequently blanketed by black, brown, orange, or red-colored, coarse sands with pebble to silt-sized phosphate clasts. Vertebrate fossils, including an abundance of elasmobranch teeth and isolated marine and terrestrial mammal bones and teeth are frequently associated with these phosphatic seafloor deposits. The lithology of these exposures, and in particular the abundance of sand-sized phosphate clasts, is consistent with descriptions of the undifferentiated Peace River Formation (Figures 2–3; Scott, 1988; Cathcart, 1989; Scott, 1990). The undifferentiated Peace River Formation has been identified as Late Miocene, Miocene–Pliocene, or Pliocene in age depending on stratigraphic position, location, and the extent of erosion (Missimer, 1978; Scott, 1988; Scott, 1990).

In contrast, the southernmost portion of the submerged Venice study area in the Manasota Key region exposes low-lying, white to tan-colored limestone hardbottom scarps that are sparsely phosphatic and may occur adjacent to green-gray colored, sandy clays. Fossil remains are less abundant at the southern exposures; however, on average consist of larger marine mammal remains,

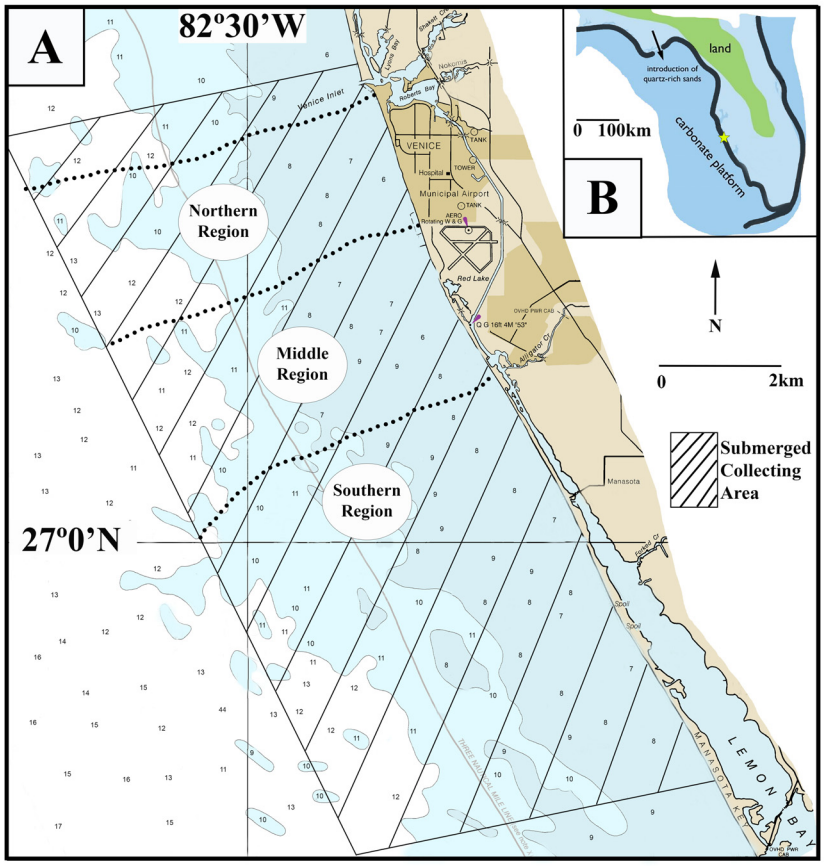

FIGURE 1. Venice, Florida study area. **A,** location map of the Venice, Sarasota County, Florida, USA, coastline and shallow continental shelf modified from NOAA chart #11424. The submerged collecting area from which elasmobranch remains were recovered is demarcated by the parallelogram with diagonal lines and specific collecting zones are labeled as northern, middle, and southern regions. B, inset map of peninsular Florida showing approximate terrestrial surface area across the late Miocene–early Pliocene (green), the location of the ancestral shoreline ~21 ka during the Last Glacial Maximum (dark blue), and the present-day shoreline (light blue) modified from Bryan et al. (2008). Depths in meters. Star in B represents Venice, Florida.

megatoothed shark teeth, and an increased abundance of terrestrial vertebrate remains. The vertebrate fossils and lithology of these southern exposures are consistent with descriptions of the Pliocene Tamiami Formation and indicate that geologically younger sediments are exposed to the south (Figures 1–3; Cathcart, 1989; Missimer, 1978, 1992, 1999; Hulbert, 2001). The increased occurrence of terrestrial mammal remains in the southern region may be associated with localized Pleistocene exposures on the Venice Shelf or these remains may represent bioclasts from younger formations that have been reworked and superimposed on the Tamiami Formation.

Land-based geological data from Florida Geological Survey wells (i.e., W-16814 and W-17488) and geologic mapping in Sarasota County, Florida (e.g., McCarten and Moy, 1995; Green et al., 1997) reinforce our stratigraphic determination of the submerged shallow shelf. Typically, ~7.5 m of Quaternary and Pleistocene surficial sediments blanket the underlying Miocene–Pliocene Peace River Formation that ranges between ~9–18 m thick and overlies the Early–Middle Miocene Arcadia Formation occurring ~18 m below ground in the Venice region.

Brief Review of Paleontology in Florida

Florida has been long known to contain diverse vertebrate and invertebrate fossil assemblages from the Eocene–Pleistocene (Leidy, 1896; Scott and Allmon, 1992; Ward, 1992; Hulbert, 2001; Perez, 2022 and references therein). In particular, the state preserves a wealth of Late Miocene–Pleistocene fossil material that is underrepresented or absent elsewhere across the Atlantic and Gulf Coastal Plains of the USA (Hulbert, 2001; Perez, 2022). Diverse assemblages of

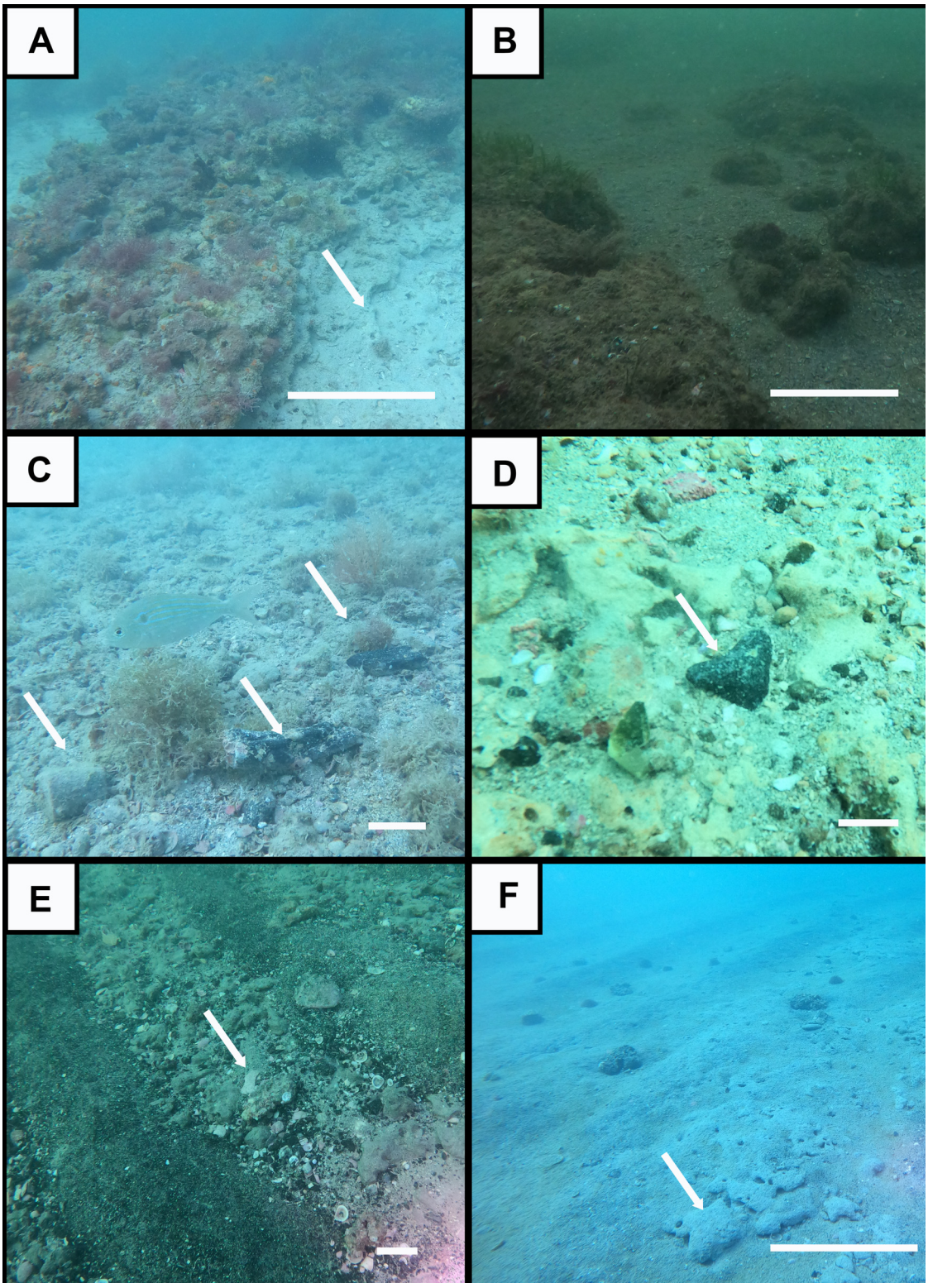

FIGURE 2. Composite of underwater images showing different types of seafloor exposures within the shallow Venice, Florida continental shelf study area. A, hardbottom reef with underlying clay indicated by arrow. B, hardbottom reef scarp with adjacent, boulder-sized rubble. C, cobble-sized pavement with arrows indicating sirenian bone fragments. D, scoured and bioeroded hardbottom limestone with arrow indicating fragmentary *O. megalodon* tooth. E, rubble-sand rows with underlying clay exposure indicated by arrow. F, silty-sand rows with underlying clay exposure indicated by arrow. Scale bars in A–B, F = 1 m; C–E = 5 cm.

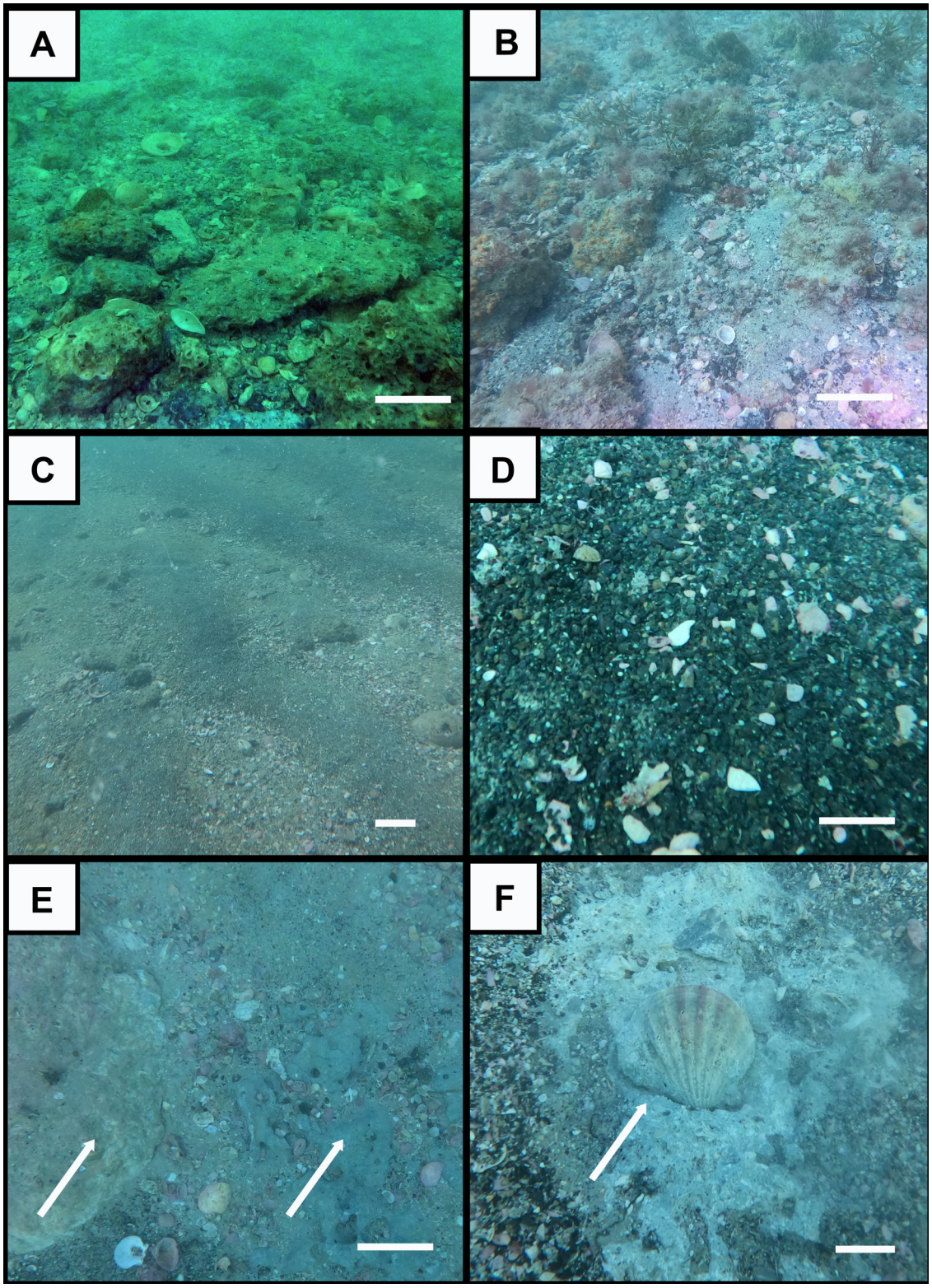

FIGURE 3. Composite of underwater images for the northern (A–B), middle (C–D), and southern (E–F) regions of the shallow Venice, Florida continental shelf study area. A–B, large cobble to boulder-sized rubble pavement deposited adjacent to hardbottom exposures. C–D, pebbly sand rows (C) that frequently contain an abundance of phosphatic debris (D). E–F, low-lying limestone and clay exposures at or near the seafloor containing minor amounts of phosphorite and occasional invertebrate fossils. Note arrows in E indicate limestone and clay exposures and arrow in F indicates in situ Chesapecten sp. Scale bars in A–B, E = 10 cm; C–D, F = 5 cm.

marine and terrestrial invertebrates (e.g., Olsson and Harbison, 1953; Olsson, 1968; Petuch, 1994; Portell, 2004; Portell and Agnew, 2004; Portell et al., 2006; Waller, 2018; Osborn et al., 2020; Petuch and Berschauer, 2021) and marine and terrestrial vertebrates (e.g., Case, 1934; Olsen, 1959; Weigel, 1962; Brodkorb, 1963; Weisbord, 1971; Webb, 1974; Reinhart, 1976; MacFadden and Webb, 1982; Dodd and Morgan, 1992; Morgan, 1994; Morgan and Hulbert, 1995; Scudder et al., 1995; Hulbert, 2001; Bryan et al., 2008; Velez-Juarbe et al., 2016; Perez, 2022) have been reported from Florida and are the focus of many other studies.

Elasmobranchs are the most abundant identifiable vertebrate fossils represented in Florida; however, they have gone largely unreported in professional scientific literature despite public interest and the production of numerous avocational identification guides (e.g., Brown, 1988; Renz, 2002; Fink, 2004; Fuqua, 2011). Several detailed reports on elasmobranchs from specific localities across Florida, as well as a Cenozoic chondrichthyan diversity study for the state exist. Yet, none of these reports specifically feature the Miocene–Pliocene elasmobranch assemblage from Venice (e.g., Olsen, 1964; Scudder et al., 1995; Boyd, 2016; Perez and Marks, 2017; Perez, 2022; Clinton et al., 2023). In this regard, the present study, documenting 45 elasmobranch taxa, makes a significant contribution to the paleontological literature of Florida and, by providing new insights into the marine paleoecology of the eastern Gulf of Mexico during the Late Miocene–Early Pliocene.

FIELD AND LABORATORY METHODS

Elasmobranch teeth were recovered from the shallow Venice continental shelf exclusively while SCUBA diving at various locations, in ~3–12 m of water over the last 10 years by the first author (HMM) (Figure 1). Fossil remains were obtained by surface collecting and bulk sampling at over 50 different locations within the study area. Approximately 200 kg of sediment was bulk sampled from various locations on the shallow Venice continental shelf using plastic containers or fine mesh bags. Bulk sediment samples were sieved in the laboratory through a series of sieves (mesh sizes 10–1 mm) and concentrated sediments were dried and analyzed using a standard binocular microscope. Elasmobranch teeth recovered display varying degrees of taphonomic wear, bioerosion, and encrustation. Selected specimens were cleaned with dilute acetic acid, dental picks, and brushes. Small specimens were imaged using an Olympus SZ61 binocular microscope attached to an Infinity–2 digital Camera and large specimens with a Canon EOS Rebel T5 digital camera. A total of 208 representative elasmobranch teeth and sawfish rostral spines featured in this manuscript were selected from an assemblage of over 10,000 specimens and have been reposited in the collections of the Florida Museum of Natural History (FLMNH) under the catalog numbers UF-VP560804–UFVP561113. The number of reposited specimens for each taxon represented in the systematic paleontology section of this study attests to the overall abundance of these teeth in the Venice Elasmobranch Assemblage. Higher numbers of reposited specimens indicate a greater abundance of teeth; whereas, fewer reposited specimens indicate uncommon or rare occurrences. Given the geologically recent, Late Miocene–Pliocene age of the Venice Elasmobranch Assemblage, and the continuous representation of many taxa in the present-day oceans, our taxonomic analyses focused on mid-Miocene–Recent elasmobranchs found in the Atlantic Ocean, Gulf of Mexico, and eastern Pacific Ocean. Identifications were based on regional and global literature with specific reference to: Compagno (1988), Purdy et al. (2001), Compagno et al. (2005), Voigt and Weber (2011), Castro (2011), Cappetta (2012), Last et al. (2016a), Kent (2018), and Ebert et al. (2021).

SYSTEMATIC PALEONTOLOGY

Class CHONDRICHTHYES Huxley, 1880
Subclass ELASMOBRANCHII Bonaparte, 1838
Cohort EUSELACHII Hay, 1902
Superorder SELACHIMORPHA Nelson, 1984
Order SQUALIFORMES Goodrich, 1909
Family SQUALIDAE Bonaparte, 1834
Genus *SQUALUS* Linnaeus, 1758
Squalus sp.
Figure 4A–B

Referred specimen. One tooth (UF-VP560804).

Description. The tooth crown is labiolingually compressed. It is oblique with a smooth margin and measures 2.24 mm in height and 3.15 mm in width. A short, well-developed distal heel is present and separated from the main crown by a notch. The labial tooth surface contains a centrally located enameloid uvula that projects across the root base. The tooth root is labiolingually compressed, contains a small lingual protuberance near the crown-root interface, and is shorter than the crown height.

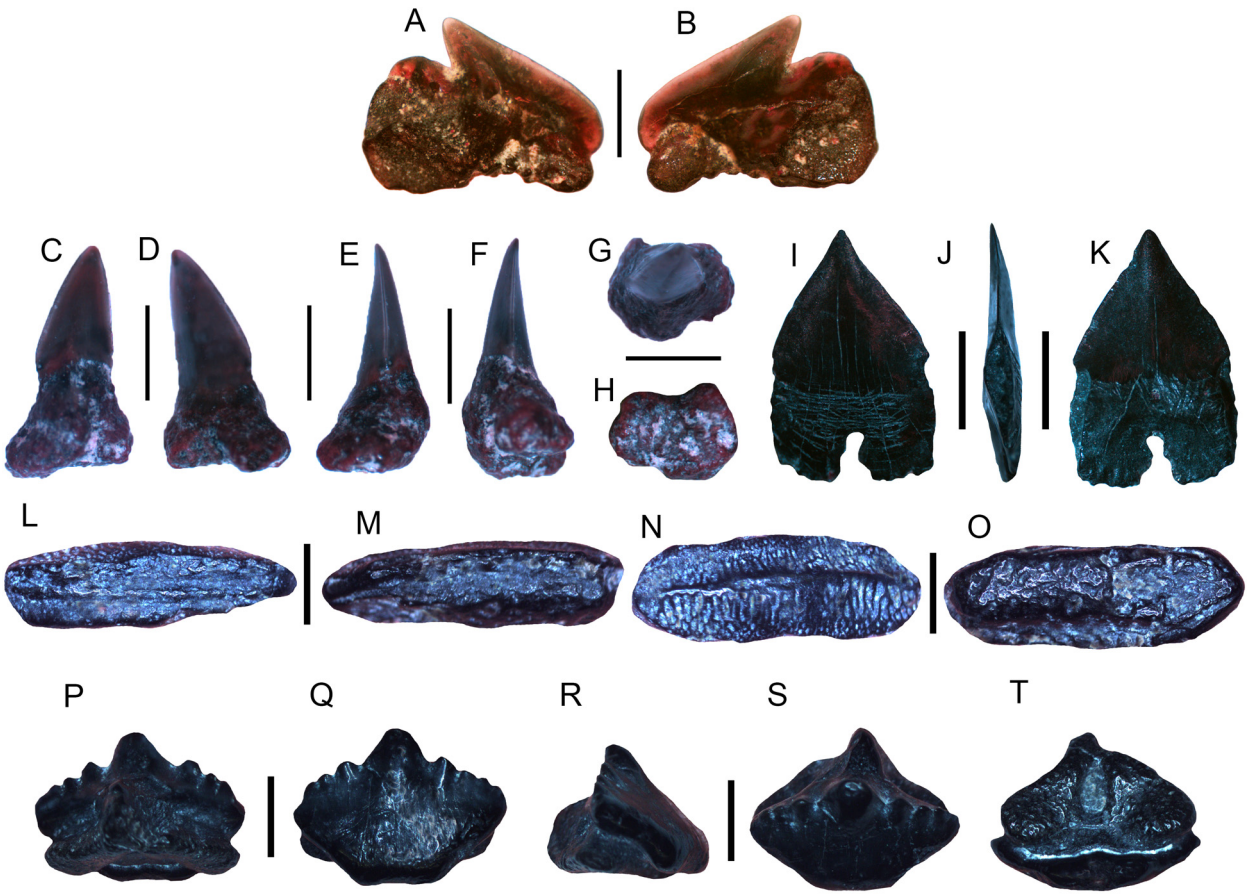

FIGURE 4. Squaliform, heterodontiform, and orectolobiform teeth from the Peace River and Tamiami formations on the shallow Venice, Florida continental shelf. **A–B,** *Squalus* sp. (UF-VP560804). **C–K,** *Isistius triangulus* upper anterior (C–H; UF-VP560805) and lower anterior (I–K; UF-VP560806) teeth. **L–O,** *Heterodontus* sp. molariform tooth (UF-VP560807). **P–T,** *Ginglymostoma cirratum* anterior tooth (UF-VP560808). Orientations = lingual: A, C, I, L, P; labial: B, D, K, M, Q; lateral: E, F, J, R; occlusal: G, N, S; basal: H, O, T. Scale bars: A–K = 1 mm; L–T = 2 mm.

Remarks. This is the first known report of a fossil *Squalus* tooth from Florida. Teeth of *Squalus* sp. can be readily distinguished from those of other elasmobranchs in the Venice assemblage including *Isistius triangulus* (Probst, 1879) and *Rhizoprionodon* sp., because they are small, labiolingually compressed, and have a centrally located enameloid uvula on the labial surface that projects across the root base. The teeth of *Squalus* are similar in both the upper and lower jaws, but the lower teeth are frequently larger than the upper teeth (Castro, 2011; Cappetta, 2012; Perez and Marks, 2017; Perez, 2022). Numerous *Squalus* species are known in the fossil record since the Late Cretaceous, where they are taxonomically diagnosed based on tooth size, labial uvula development, and crown and root morphology (Cappetta, 2012). However, we refrain from species-level taxonomic identification of *Squalus* in the Venice Elasmobranch Assemblage because only a single, fragmentary tooth has been recovered.

Presently, Squalidae is represented by *Cirrhigaleus* and *Squalus* and of these genera, *Squalus* has been subdivided into at least 34 species within three primary subgroups or clades (Ebert et al., 2021). In the present-day Gulf of Mexico, four squalid species are recognized and include: the roughskin spiny dogfish *Cirrhigaleus asper* (Merrett, 1973), the spiny dogfish *Squalus acanthias* Linnaeus, 1758, the Cuban dogfish *Squalus cubensis* Howell Rivero, 1936, and the Gulf dogfish *Squalus clarkae* Pfleger, Grubbs, Cotton, and Daly-Engel, 2018. These taxa are all represented by small-bodied sharks possessing teeth with similar morphologies (Castro, 2011; Ebert et al., 2021).

Although most squalids are known to inhabit outer continental shelf and slope waters and feed upon a variety of invertebrates and small fish, some taxa (e.g., *C. asper* and *S. acanthias*) also venture into shallow continental shelf waters, including bays and river mouths (Castro, 2011; Ebert et al., 2021).

Family DALATIIDAE Gray, 1851
Genus *ISISTIUS* Gill, 1865a
Isistius triangulus (Probst, 1879)
Figure 4C–K

Referred specimens. One upper jaw tooth (UF-VP560805) and one lower jaw tooth (UF-VP560806).

Description. The upper jaw tooth has a narrow, distally inclined cusp and a globular root base, and measures 3.3 mm in height and 1.63 mm in width. The labial and lingual faces are slightly convex, and the margins are smooth. The distal margin is nearly straight, and the mesial margin is convex. The cutting edge of the upper jaw tooth ends abruptly and is separated from the bulbous root base by an elongated tooth neck. The root base is weakly separated into two distinct lobes by a nutritive groove. The lower jaw tooth has a broad, triangular crown and measures 3.19 mm and 1.81 mm in total height and width, respectively. The crown is labiolingually flattened and has smooth cutting edges. The crown and root interface on the distal margin is linear and slightly convex, whereas the crown extends beyond the root base on the mesial margin and forms a slight concavity for interlocking with the adjacent tooth. The root is labiolingually flattened, square in outline, approximately the same height as the tooth crown, and contains a well-developed nutritive groove. The crown-root interface on the lingual surface is relatively straight and equally separates the crown and root in contrast to that observed on the labial face that extends further down onto the root base. A small, centrally located foramen is present on the lingual surface of the root just above the nutritive groove.

Remarks. *Isistius* spp. have a well-developed heterodont dentition where the upper teeth are very small, narrow, and delicate in contrast to the lower teeth that are larger and triangular (Strasburg, 1963; Herman et al., 1989; Adnet, 2006; Cappetta, 2012). The lower teeth of *I. triangulus* can be readily distinguished from those of other elasmobranchs in the Venice assemblage because they are small, extremely labiolingually flattened, and have a thin, square-shaped root base containing a well-developed nutritive groove that can be observed on both the labial and lingual root surfaces. However, in contrast to the larger, more diagnostic lower teeth of *Isistius*, the more delicate and less diagnostic upper jaw teeth are rarely reported in the fossil record (Cappetta, 2012; Perez and Marks, 2017). In fact, the upper tooth of *I. triangulus* identified in this study represents the first report of an upper tooth of *I. triangulus* known globally. Previously, only a single upper tooth attributed to *I.* aff. *I. trituratus* (Winkler, 1874) was described from the Eocene of France (Adnet, 2006). The upper teeth of *Isistius* spp. can be distinguished from those of similar taxa, including *Dalatias* and *Somniosus*, because they have shorter more erect crowns and roots that are more robust (Adnet, 2006; Cappetta, 2012).

Isistius triangulus iis only known from the Miocene–Pliocene of Europe, North America, the Caribbean, Central America, and South America (Antunes and Jonet, 1970; Longbottom, 1979; Laurito Mora, 1996; Adnet, 2006; Kriwet and Klug, 2009; Cappetta, 2012; Carillo-Briceño et al., 2014; Pino, 2014; Perez and Marks, 2017; Szabó et al., 2022, 2023). Upper and lower teeth of *I. triangulus* can be distinguished from those of *I. trituratus* because they typically have a more well-developed nutritive groove that can be seen on both the lingual and labial tooth surfaces and the tooth margin may contain extremely faint serrations (Cappetta, 2012; Perez and Marks, 2017). Moreover, *I. trituratus* teeth have only been reported from the Paleocene–Eocene of Europe, Asia, Africa, and North America (Adnet, 2006; Kriwet and Klug, 2009; Cappetta, 2012; Staube et al., 2015).

Presently, two extant species of *Isistius* are recognized consisting of *I. brasiliensis* (Quoy and Gaimard, 1824) and *I. plutodus* Garrick & Springer, 1964 (Castro, 2011; Ebert et al., 2021). Dental characters that separate these taxa from *I. triangulus* include crowns that are narrower and resemble isosceles rather than equilateral triangles and roots that are longer and more rectangular (Laurito Mora, 1996; Cappetta, 2012; White and Last, 2013; Perez and Marks, 2017; Ebert et al., 2021; Szabó et al., 2023). Both extant *Isistius* taxa have been reported from tropical to subtropical locations around the world; however, *I. brasiliensis* inhabits water depths ranging from 3,700 m to the surface and makes vertical migrations through the water column, whereas *I. plutodus* seems to be restricted to depths of 60–200 m (Kiraly et al., 2003; Zidowitz et al., 2004; Castro, 2011; Ebert et al., 2021). Despite differences in preferred bathymetry, the overall similarities in tooth structure and feeding habits of these sharks earned them the common

name, cookiecutter sharks, and the status as the only known ectoparasitic shark (Papastamatiou et al., 2010; Castro, 2011; Wenzel and Suarez, 2012; Ebert et al., 2021). These sharks possess the largest teeth in proportion to the body size of any known shark species and with their suctorial lips attach themselves to prey items and twist off plugs of flesh leaving behind crater-like wounds (Castro, 2011; Ebert et al., 2021). Cookiecutter sharks have been documented attacking a variety of prey items including large fish (Papastamatiou et al., 2010), marine mammals (Wenzel and López Suarez, 2012), white sharks (Hoyos-Padilla et al., 2013), squid (Strasburg, 1963), rubber sonar devices on nuclear submarines (Compagno et al., 2005), and humans (Minaglia and Liegl, 2024).

In contrast to the upper teeth, the lower teeth of *Isistius* spp. are interlocked, shed together (similar to those of *Squalus* spp.), and also self-ingested possibly as a means of recycling calcium phosphate (Bigelow and Schroeder, 1948a; Strasburg, 1963; Ebert et al., 2021). The ingestion and recycling of teeth by *Isistius* spp. also suggest that these sharks may have been more abundant in shallow marine depositional environments during the late Cenozoic despite the infrequent occurrence of their teeth.

Order HETERODONTIFORMES Berg, 1937
Family HETERODONTIDAE Gray, 1851
Genus *HETERODONTUS* Blainville, 1816
Heterodontus sp.
Figure 4L–O

Referred specimen. One lateral molariform tooth (UF-VP560807).

Description. The lateral molariform tooth measures 6.82 mm in height and 2.70 mm in width. The tooth has a rectilinear appearance with a slightly convex occlusal surface containing a centralized transverse ridge and numerous pits and furrows. The cusp is thicker than the root which it overhangs. The root base contains several foramina, and the central portion is slightly concave.

Remarks. The anterior teeth of *Heterodontus* are typically tricuspid with lateral cusplets that are lower in height than the main cusp, whereas lateral teeth are molariform. In this report, only a single lateral tooth of *Heterodontus* was collected and available for study. This lateral tooth differs from similar molariform teeth in the Venice Elasmobranch Assemblage including those of *Mustelus* sp., *Rhinoptera* cf. *R. bonasus*, and *Myliobatis* sp., because it has a furrowed and pitted occlusal surface with a centralized transverse ridge and a root base that is thin, centrally depressed, and contains several foramina.

Heterodontus taxa were more ubiquitous and are known to have occurred since the Jurassic with numerous fossil taxa having been identified from isolated anterior and lateral teeth (e.g., Case, 1980; Laurito Mora, 1999; Cappetta, 2012; Partarrieu et al., 2018; Ebert et al., 2021). While many reports of *Heterodontus* are left in open nomenclature as *Heterodontus* sp. or *H*. cf. *H. francisci*, two distinct taxa have been reported from the Miocene–Pliocene of the Americas: *H. janefirdae* Case, 1980 and *H. uscarenesis* Laurito Mora, 1999. Anterior teeth of *H. janefirdae* have a single pair of large, spatulate cusplets, whereas anterior teeth of *H. uscarensis* are reported to have as many as two lateral cusplets that are relatively tall compared to the main cusp. Similarly, the molariform lateral teeth of these taxa are reported to exhibit strong ornamentation and transverse ridges that are either mesially displaced or centrally located with a prominent conical apex, respectively (Case, 1980; Laurito Mora, 1999). The molariform lateral tooth specimen of *Heterodontus* from Venice does not appear to be identical to *H. janefirdae* or *H. uscarensis* but more similar to the teeth of *H. francisci* (Girard, 1855) and *H. mexicanus* Taylor and Castro-Aguirre, 1972, due to a centrally located transverse ridge and well-developed occlusal surface ornamentation (Herman et al., 1993; Castro, 2011; Partarrieu et al., 2018; Ebert et al., 2021). Despite these similarities, the prominence of transverse ridges and occlusal surface ornamentation on molariform lateral teeth can vary depending on the ontogenetic stage and functional position of the tooth in the jaws of extant *Heterodontus* spp. (Taylor, 1972; Herman et al., 1993). Due to the infrequent occurrence of *Heterodontus* teeth in the Venice Elasmobranch Assemblage and the variability seen in the teeth of extant taxa, we refrain from lower-level classification until additional specimens and comparative analysis are conducted.

There are presently nine extant species of *Heterodontus* globally (Cappetta, 2012; Ebert et al., 2021). No extant *Heterodontus* spp. are known in the Gulf of Mexico or Atlantic Ocean, but two taxa, the horn shark, *H. francisci* and Mexican horn shark, *H. mexicanus* are recognized along the shallow, rocky Pacific US and Mexican coasts (Castro, 2011; Ebert et al., 2021). Predominantly benthic taxa preferring rocky-reef substrates, horn sharks are known to feed upon a variety of invertebrates including mollusks, crabs, sea urchins, and

squid as well as small fish (Roedel and Ripley, 1950; Castro, 2011; Ebert et al., 2021).

Order ORECTOLOBIFORMES Applegate, 1972
Family GINGLYMOSTOMATIDAE Gill, 1862
Genus *GINGLYMOSTOMA* Müller and Henle, 1837
Ginglymostoma cirratum (Bonnaterre, 1788)
Figure 4P–T

Referred specimens. Four teeth (figured tooth: UF-VP560808 and additional teeth: UF-VP560809–UF-VP560811).

Description. The largest tooth is 4.06 mm in height and 4.15 mm in width and is symmetrical with an erect central main cusp that is flanked by three pairs of lateral cusplets. The labial and lingual faces are smooth, and a rounded apron extends below the crown-root interface on the labial face. The root is hemiaulacorhizous and contains a well-developed lingual protuberance. The root base is flat and contains a well-defined, central foramen within a channel-like furrow.

Remarks. Teeth of *Ginglymostoma cirratum* can be readily distinguished from those of other elasmobranchs in the Venice assemblage because they are small but robust, contain multiple lateral cusplets on both sides of the main cusp, and have a flat root base containing a centrally located foramen within a furrow. *Nebrius* teeth differ from those of *G. cirratum* by having a main cusp that is nearly the same height and size as the cusplets (Cappetta, 2012). Teeth of *Squatina* sp. are also different from those of *G. cirratum* by being thin, conical, and smooth and having thin, widely separated root lobes (Herman et al., 1992; Castro, 2011; Ebert et al., 2021). Teeth of the Miocene taxon *G. delfortriei* Daimeries, 1889, and extant taxon, *G. unami* Del Moral-Flores et al., 2015, although very similar to *G. cirratum*, have a noticeably triangular and erect main cusp surrounded by reduced, coarse or fine cusplets, respectively (Cappetta, 2012; Ebert et al., 2021).

Presently the extant nurse shark, *G. cirratum,* has a restricted range and occurs on the shallow continental shelves on both sides of the tropical and subtropical Atlantic Ocean and Gulf of Mexico. This taxon is typically abundant all year round in shallow waters in tropical Florida and the Caribbean and feeds upon a variety of small vertebrates (primarily fish) and invertebrates (Castro, 2011; Ebert et al., 2021).

Order LAMNIFORMES Berg, 1958
Family CARCHARIIDAE Stone and Shimada, 2019
Genus *CARCHARIAS* Rafinesque, 1810
Carcharias taurus Rafinesque, 1810
Figure 5A–L

Referred specimens. Nine teeth consisting of three anterior, three anterolateral, one intermediate, and two symphyseal teeth (figured teeth: UF-VP560812–UF-VP560816; additional teeth: UF-VP560817–UF-VP560820).

Description. The largest tooth is an anterior tooth that measures 34.81 mm in height and 15.18 mm in width. Symphyseal, anterior, intermediate, and lateral teeth have erect, slender main cusps that widen toward to the base and are flanked by one or two pairs of cusplets. Symphyseal teeth may contain highly reduced cusplets. The labial face is smooth and the lingual face may contain faint apicobasally oriented striations. In most specimens, the cusp is curved lingually although the cusp apex may curve labially giving the tooth a sigmoidal appearance. The tooth roots are holaulacorhizous and well-defined, and broadly spaced root lobes occur in all but symphyseal teeth. Symphyseal tooth roots are mesiodistally compressed and labiolingually thickened. Anterior tooth roots are thin and round and may contain a flattened edge on the basal-most portion of the root lobes. Anterolateral, intermediate, and lateral teeth have wider root lobes that are flattened labiolingually. A pronounced lingual protuberance containing a nutritive groove occurs on all tooth roots.

Remarks. The teeth of the sand tiger shark, *Carcharias taurus,* can be distinguished from those of *I. oxyrinchus,* and lower teeth of *H. serra* in the Venice Elasmobranch Assemblage by the presence of well-developed, narrow main cusps, lateral cusplets, and widely-spaced root lobes. Teeth of *Araloselachus* (*Carcharias*) *cuspidata* (Agassiz, 1843) may also appear similar to those of *C. taurus*; however, anterolateral teeth of *A. cuspidata* have wider main cusps that lack lingual striations and may contain irregular folds in the enameloid margin near the crown-root interface on both the labial and lingual face, have more robust roots, and contain broad, flattened, spade-like lateral cusplets (e.g., Purdy et al., 2001; Cappetta, 2012; Maisch et al., 2015). Teeth from *Odontaspis ferox* (Risso, 1810) and *O. noronhai* (Maul, 1955) are also distinct from those of *C. taurus* because they contain needle-like main cusps and multiple pairs of elongated lateral cusplets or an elongated main cusp with enameloid that connects with the lateral cusplets on the labial surface, respectively (Castro, 2011). Teeth assigned to *C. acutissima* (Agassiz, 1843) are similar to and may in fact be synonymous with those of *C. taurus* (Reinecke et al.,

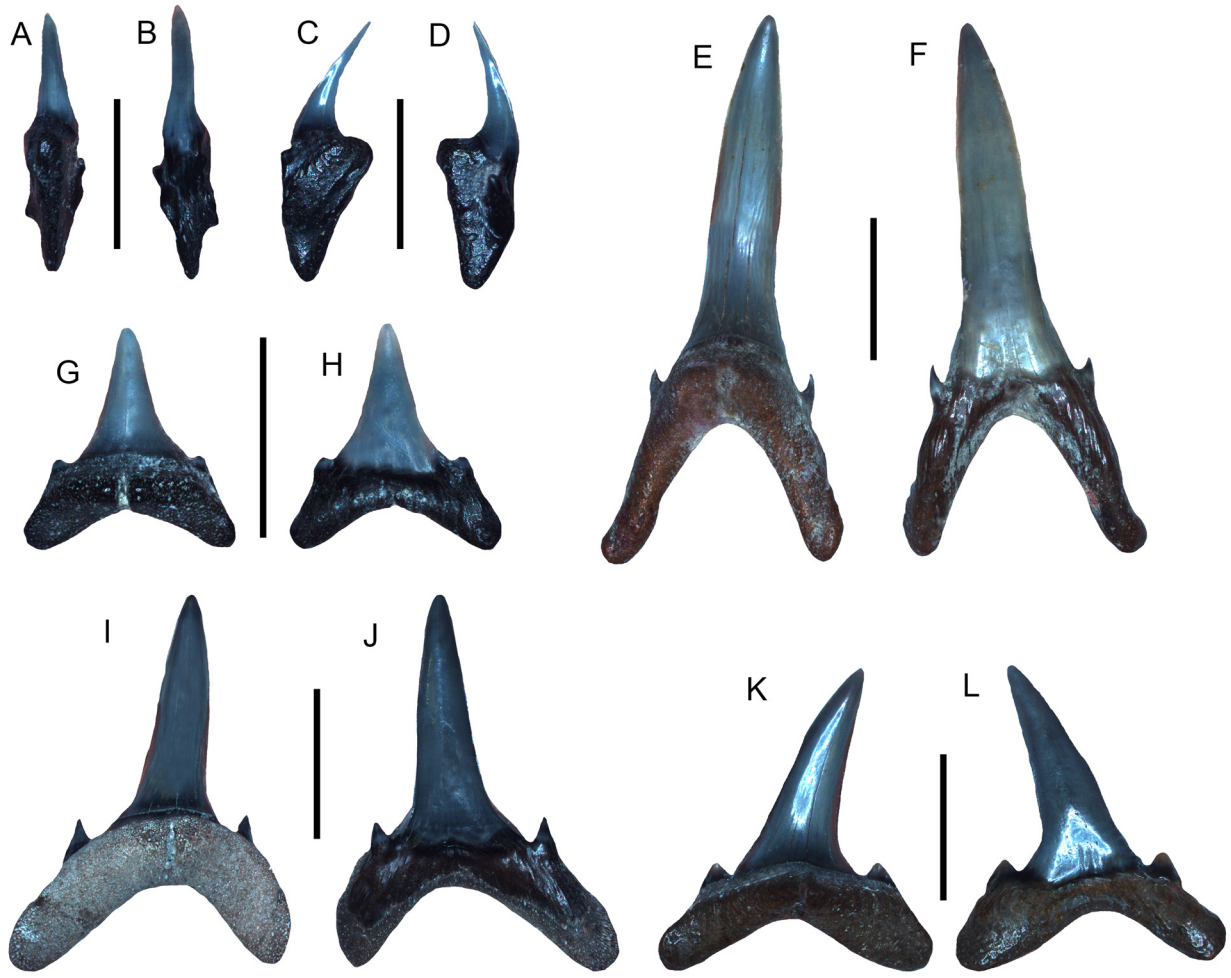

FIGURE 5. Lamniform teeth from the Peace River and Tamiami formations on the shallow Venice, Florida continental shelf. **A–L,** *Carcharias taurus* symphyseal (A–D; UF-VP560812), anterior (E–F; UF-VP560813), intermediate (G–H; UF-VP560814), and anterolateral (I–L; UF-VP560815–UF-VP560816) teeth. Orientations = lingual: A, E, G, I, K; labial: B, F, H, J, L; lateral: C, D. All scale bars = 1 cm.

2011). Additional discussion on the classification of *C. taurus* can be found in papers by Suárez et al. (2006), Reinecke et al. (2011), Cappetta (2012), and Stone and Shimada (2019).

Extensive literature exists on *C. taurus* in the fossil record and modern oceans, although this taxon is typically found in continental shelf waters globally (Ebert et al., 2021). Currently, extant *C. taurus* is less abundant in the Gulf of Mexico than along the US Atlantic coast where it frequently occurs around reefs and shipwrecks and feeds on a variety of fish and invertebrates (Castro, 2011; Ebert et al., 2021).

Family OTODONTIDAE Glikman, 1964
Genus *OTODUS* Agassiz, 1838

Otodus megalodon (Agassiz, 1835)
Figure 6A–L

Referred specimens. Five teeth consisting of two anterior (UF-VP560821–UF-VP560822), one anterolateral (UF-VP560823), and two posterior teeth (UF-VP560824-UF-VP560825).

Description. The largest specimen is an anterior tooth that measures 90.44 mm in height and 61.25 mm in width. The main cusps of the anterior, anterolateral, and posterior teeth have regular and finely serrated tooth margins with convex labial surfaces and slightly convex lingual surfaces. Lateral cusplets are absent. Upper anterior teeth are broad and triangular, whereas lower anterior teeth have a slender and more pointed appearance. Anterolateral and posterior (i.e., distally located lateral) teeth are distally inclined which becomes

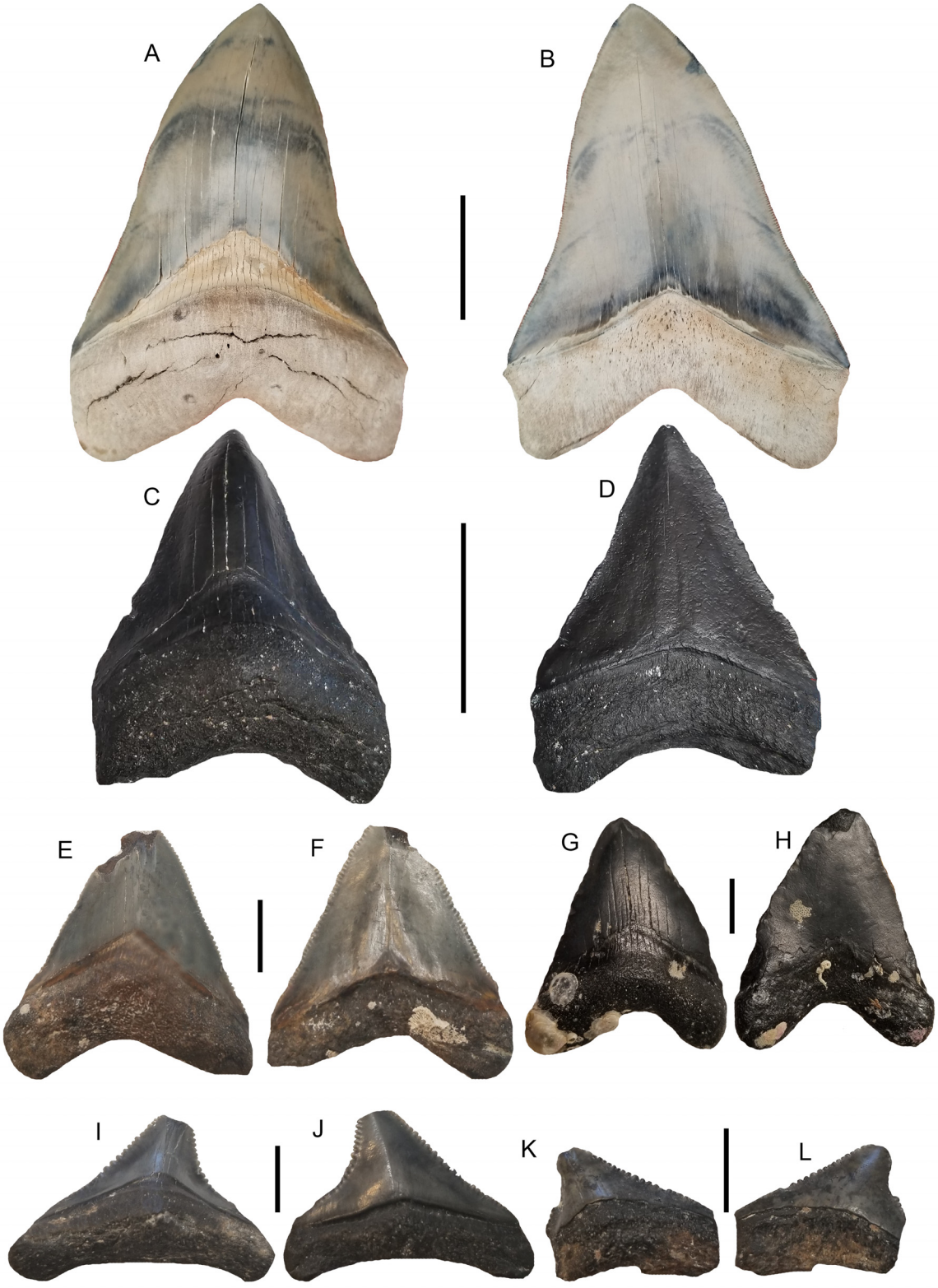

FIGURE 6. Lamniform teeth from the Peace River and Tamiami formations on the shallow Venice, Florida continental shelf. **A–L,** *Otodus megalodon* anterior (C–H; UF-VP560821–UF-VP560823), anterolateral (A–B; private collection of Capt. B. Morrow), and posterior (I–L; UF-VP560824–UF-VP560825) teeth. Note possible feeding damage in E–F and I–J. Orientations = lingual: A, C, E, G, I, K; labial: B, D, F, H, J, L. Scale bars: A–D = 5 cm; E–L = 1 cm.

more pronounced distally. The anterior, anterolateral, and posterior tooth roots are holaulacorhizous with slightly convex lingual faces, slightly concave labial faces, and lack nutritive grooves. Additionally, root lobes become less developed distally.

Remarks. Large teeth frequently exceeding 5 cm in crown height that contain fine, regular serrations and lack lateral cusplets distinguish teeth of *Otodus megalodon* from other taxa found in the Venice Elasmobranch Assemblage including those of *Carcharodon carcharias, C. hastalis,* and *Parotodus benedinii* (e.g., Purdy et al, 2001; Bor et al., 2012; Cappetta, 2012; Ehret et al., 2012; Kent, 2018). Globally, teeth belonging to *O. megalodon* are recognized from Middle Miocene–Lower Pliocene deposits (Cappetta, 2012; Pimiento and Balk, 2015; Pimiento et al., 2016; Perez et al., 2017; Boessenecker et al., 2019; Maisch et al., 2018, 2019a; Perez et al., 2021; Perez, 2022). Although teeth of *O. chubutensis* contain distinct lateral cusplets and have been reported elsewhere along the Atlantic Coastal Plain of the USA, this taxon is known from Early–Middle Miocene deposits and does not occur in the Late Miocene–Pliocene Venice Elasmobranch Assemblage (Perez et al., 2021; Perez, 2022).

Numerous, recent studies on *O. megalodon* have expanded our knowledge of the size (Perez et al., 2021; Shimada, 2021; Shimada et al., 2020, 2021, 2022; 2025), morphology (Sternes et al. 2022, 2024), distribution (Herraiz et al., 2020; Shimada et al., 2022), trophic ecology (Kast et al., 2022; McCormack et al., 2022; 2025), thermophysiology (Griffiths et al., 2023), and extinction (Boessenecker et al., 2019; McCormack et al., 2022) of this enigmatic, macropredatory shark. However, despite our increased understanding of the species, there is still much to be discovered about this unique taxon and its ancestors. With particular reference to Florida and the Venice Elasmobranch Assemblage, it has been suggested that this area served as an *O. megalodon* nursery because teeth belonging to smaller individuals (<5 cm in total height) are frequently recovered in contrast to those belonging to larger individuals (>5 cm in total height) (i.e., Herraiz et al., 2020). However, another explanation for the differences in tooth and body sizes of *O. megalodon* individuals, seen in various assemblages around the world is that the fossil species may have exhibited Bergmann's rule and had different body sizes as a result of latitudinal temperature gradients over time (Shimada et al., 2022). Regardless, geochemical analyses of *O. megalodon* tooth enameloid from various global locations (including Venice, Florida) has shown that this taxon was mesothermic and occupied an extremely high tropic level (i.e., Kast et al., 2022; Griffiths et al., 2023; McCormack et al., 2022; 2025). Additional discussions regarding the classification, paleogeographic distribution, body size and morphology, and trophic ecology of *O. megalodon* can be found in papers by the following authors: Hulbert (2001); Purdy et al. (2001); Nyberg et al. (2006); Cappetta (2012); Ehret et al. (2012); Pimiento et al. (2016); Pimiento and Clements (2014); Pimiento and Balk (2015); Perez et al. (2019, 2021); Sternes et al. (2022, 2024); Pollerspöck and Shimada (2024); and Shimada et al. (2016, 2020, 2021, 2022, 2025).

Genus *PAROTODUS* Cappetta, 1980
Parotodus benedinii (Le Hon, 1871)
Figure 7A–C

Referred specimen. One lateral tooth (UF-VP560835).

Description. The cusp of the lateral tooth is robust, has a D-shaped cross-section, hook-like distal curvature, smooth and flat labial face, and convex lingual face. The cutting edges are complete and no lateral cusplets or serrations are present. The tooth measures 57.39 mm and 34.23 mm in maximum length and width, respectively. The root of the tooth is holaulacorhizous, very robust with basally oriented and rounded root lobes, and contains a large lingual protuberance lacking a nutritive groove.

Remarks. The presence of thick and robust, nonserrated teeth with a distinct hook-like distal curvature distinguishes those of *P. benedinii* from other taxa in the Venice Elasmobranch Assemblage, including *C. hastalis, C. carcharias,* and *O. megalodon*. To date, the most complete and associated dentition of *P. benedinii* consists of 114 teeth and was described by Kent and Powell (1999) from the Pliocene Yorktown Formation at the Nutrien (PCS/Lee Creek) Phosphate Mine. Teeth from this dentition were shown to exhibit unique morphology and placement within the jaws thereby reinforcing the placement of this taxon within its own genus. It has also been suggested that *Parotodus* diverged from *Otodus* and underwent increases in body size across the Cenozoic (Cappetta, 2012). In the Venice Elasmobranch Assemblage and contemporaneous deposits around the world, teeth belonging to *P. benedinii* are less frequently recovered than those of *O. megalodon*, and *C. hastalis* (e.g., Bor et al., 2012; Cappetta, 2012; Maisch et al., 2018; Collareta et al., 2023).

FIGURE 7. Lamniform teeth from the Peace River and Tamiami formations on the shallow Venice, Florida continental shelf. A-C, *Parotodus benedinii* anterior tooth (UF-VP560835). D-E, *Isurus oxyrinchus* anterior tooth (UF-VP560826). F-G, *Carcharodon carcharias* upper anterior tooth (UF-560828). *Carcharodon hastalis* upper anterolateral (H-K, UF-VP560829-UF-VP560830) and lower anterolateral (L-O, UF-VP560831-UF-VP560832) teeth. Orientations = lingual: A, D, F, H, J, L, N; labial: C, E, G, I, K, M, O; lateral: B. All scale bars = 1 cm.

Family LAMNIDAE Müller and Henle, 1838
Genus *ISURUS* Rafinesque, 1810
Isurus oxyrinchus Rafinesque, 1810
Figure 7D–E

Referred specimens. Two fragmentary anterior teeth (figured tooth: UF-VP560826 and additional tooth: UF-VP560827).

Description. The figured anterior tooth is 26.26 mm in height and 11.26 mm in width. The cusp of anterior teeth is erect, angled distally, curved in the lingual direction, and has smooth labial and lingual faces. The anterior tooth roots, although fragmentary, are holaulacorhizous.

Remarks. The extant shortfin mako, *I. oxyrinchus,* is typically pelagic, preys upon a variety of vertebrates, and has a global distribution in temperate,

tropical, and subtropical waters (Castro, 2011; Ebert et al., 2021). Despite mild heterodonty, *I. oxyrinchus* lacks broad, triangular, blade-like anterior teeth, robust lower anterior teeth, and lateral cusplets which distinguishes them from other similar teeth found in the Venice Elasmobranch Assemblage including those belonging to *Carcharias taurus, Carcharodon hastalis,* and *Hemipristis serra* (Purdy et al., 2001; Bor et al., 2012; Cappetta, 2012). Anterior teeth of *I. paucus* Guitart-Manday (1966) are more robust and exhibit less labial recurvature of the main cusp, whereas lateral teeth are more lobate and less labiolingually flattened than those of *I. oxyrinchus*. Additionally, comparative analyses between composite dentitions and modern tooth sets of *I. oxyrinchus* with fossil teeth previously identified as *I. desori* Agassiz, 1843, indicated they are morphologically indistinguishable (e.g., Purdy et al., 2001; Reinecke et al., 2011; Bor et al., 2012). The teeth identified as *I. oxyrinchus* in the Venice Elasmobranch Assemblage are identical to those reported by Purdy et al. (2001), Reinecke et al. (2011), Bor et al. (2012), and Maisch et al. (2015).

Genus *CARCHARODON* Müller and Henle, 1838

Carcharodon carcharias (Linnaeus, 1758)

Figure 7F–G

Referred specimen. One fragmentary upper anterolateral tooth (UF-VP560828).

Description. The main cusp of the upper anterolateral tooth is thin with nearly flat lingual and labial faces. The tooth, although fragmentary, measures 34.64 mm and 16.33 mm in maximum length and width, respectively. The cusp has an irregular and coarsely serrated tooth margin and shows a slight distal inclination.

Remarks. The thin, nearly flat, blade-like morphology, presence of irregular, coarse serrations, and thin, rectilinear root in upper anterolateral teeth distinguish those of *Carcharodon carcharias,* the white shark, from other similar teeth also found in the Venice Elasmobranch Assemblage including *C. hastalis* and *O. megalodon.* Although *C. hastalis* teeth are similar in size and shape to those of *C. carcharias*, *C. hastalis* teeth lack serrations (e.g., Purdy et al, 2001; Cappetta, 2012; Cione et al., 2012; Ehret et al., 2012). Teeth of *Isurus subserratus* (Agassiz, 1843) (formerly *Carcharomodus escheri* and identified as *Cosmopolitodus hastalis* by Purdy et al., 2001, p. 118) have been proposed to represent a transitional form between *C. hastalis* and *C. carcharias* or a distinct taxon that evolved from *I. oxyrinchus* (e.g., Ehret et al., 2009, 2012; Cappetta, 2012; Kriwet et al., 2015; De Schutter et al., 2021). To date, teeth resembling those of *I. subserratus* have not been found in Venice; however, they can be identified based on the presence of broad, triangular crowns with faint, irregular serrations (Purdy et al., 2001; Cappetta, 2012; De Schutter et al., 2021). Numerous reports indicate that *C. carcharias* likely evolved from *C. hastalis*, but this view is not followed by all researchers (e.g., Casier, 1954; De Muizon and De Vries, 1985; Nyberg et al., 2006; Cappetta, 2012). Additional discussions regarding the classification of *C. carcharias* and similar related taxa can be found in papers by Applegate and Espinosa-Arubarrena (1996); Hulbert (2001); Purdy et al. (2001); Nyberg et al. (2006); Cione et al. (2012); Ehret et al. (2012); Cappetta (2012); Staig et al. (2015); Ebersole et al. (2017); Landini et al. (2017a); Kent (2018).

Extant *C. carcharias* occurs in coastal–offshore waters globally and frequently aggregates near rocky coastlines harboring seal populations (Compagno et al., 2005; Ebert et al., 2021). The distribution and behavior of *C. carcharias* in the Gulf of Mexico are poorly understood (Adams et al., 1994; Castro, 2011).

Carcharodon hastalis (Agassiz, 1838)

Figure 7H–O

Referred specimens. Six teeth consisting of three upper anterolateral and three lower anterolateral teeth (figured teeth: UF-VP560829–UF-VP560832 and additional teeth: UF-VP560833–UF-VP560834).

Description. The main cusps of upper anterolateral teeth have labially recurved apices, are broad and triangular, exhibit convex lingual faces and slightly convex to flat labial surfaces, and smooth tooth margins. The largest upper anterolateral tooth measures 38.36 mm in length and 26 mm in width. Lower anterior teeth have cusps with slender, convex labial surfaces, nearly flat lingual surfaces, and labiolingually thickened. The largest lower anterolateral tooth measures 34.72 mm in length and 22.17 mm in width. The anterolateral tooth roots are holaulacorhizous and a nutritive groove with foramina may be present. Lower teeth have wider roots with well-defined, divergent root lobes, in contrast to those of upper anterolateral teeth that are thinner and more labiolingually compressed.

Remarks. The triangular, blade-like anterior tooth morphology, labial recurvature of tooth apices, and absence of serrations distinguish teeth of *C. hastalis* from those of other taxa found in the Venice

Elasmobranch Assemblage including *C. carcharias* and *I. oxyrinchus.* Traditionally, these teeth were identified as *Isurus hastalis*; however, more recent studies have questioned the phylogeny of "*hastalis*" and recognized multiple tooth morphotypes. In particular, narrow and broad-toothed forms of "*hastalis*" have been proposed to represent ontogenetic variation, sexual dimorphism, or evolutionary change in tooth morphology and increase in tooth size from the Middle Miocene–Pliocene, or separate species (Leriche, 1926; Van den Bosch et al., 1975; Van den Bosch, 1978; Purdy al., 2001; Whitenack and Gottfried, 2010; Cione et al., 2012; Landini et al., 2017a; Kent, 2018). Different views on the evolutionary relationship between "*hastalis*" and *Carcharodon carcharias* have also led to complications in the taxonomic classification of this taxon and "*hastalis*" teeth have been placed in one of three genera including *Carcharodon* (e.g., Ehret et al., 2009; 2012; Cione et al., 2012; Staig et al., 2015; Boyd, 2016; Maisch et al., 2018; Perez, 2022), *Cosmopolitodus* (e.g., Glickman, 1964; Ward and Bonavia, 2001; Bor et al., 2012; Cappetta, 2012; Betancort et al., 2016; Ebersole et al., 2017; Collaretta et al., 2017a; Landini et al., 2017a), or *Isurus* (e.g., Uyeno et al., 1990; Applegate and Espinosa-Arrubarrena, 1996; Purdy et al., 2001; Nyberg et al., 2006; Takakuwa, 2014).

Another complication in the proper taxonomic placement of "*hastalis*" derives from weakly and irregularly serrated teeth such as *Isurus subserratus* (*Carcharomodus escheri* (Agassiz, 1843)) and *Carcharodon hubbelli* (Ehret et al., 2012), that are known from late Miocene and early Pliocene stratigraphic horizons. These species have been interpreted to represent either transitional taxa between "*hastalis*" and *C. carcharias*, therefore suggesting a gradual, chronospecific evolutionary lineage or distinct species not directly related to *C. hastalis* (e.g., De Muizon and De Vries, 1985; Nyberg et al., 2006; Ehret et al., 2009, 2012; Cione et al., 2012; Cappetta, 2012; Kriwet et al., 2015; De Schutter et al., 2021). We follow Ehret et al. (2012) and identify these teeth as *Carcharodon hastalis* in the Venice Elasmobranch Assemblage. Additional discussions regarding the classification and paleogeographic distribution of *Carcharodon hastalis* and similar related taxa can be found in papers by Uyeno et al. (1990); Hulbert (2001); Purdy et al. (2001); Nyberg et al. (2006); Bor et al. (2012); Cappetta (2012); Ehret et al. (2009, 2012); Staig et al. (2015); Shimada et al. (2016); Ebersole et al. (2017); Collareta et al. (2017a); Landini et al. (2017a); Kent (2018); and Maisch et al. (2018).

Order CARCHARHINIFORMES Compagno, 1973
Family SCYLIORHINIDAE Gill, 1862
Genus *SCYLIORHINUS* Blainville, 1816
Scyliorhinus sp.
Figure 8A–O

Referred specimens. Three teeth (UF-VP560836–UF-VP560838).

Description. The largest tooth is an anterior tooth measuring 3.12 mm in height and 2.88 mm in width. The cusp is erect, contains two reduced lateral cusplets, and is displaced lingually. The lingual face is slightly convex, whereas the labial face is noticeably convex. The root is robust and has a flat base with a deep nutritive groove.

Remarks. Teeth of *Scyliorhinus* sp. in the Venice Elasmobranch Assemblage may appear similar to the anterior teeth of *Heterodontus* sp., but they possess lateral cusplets that are shorter and less robust. The teeth of *S. boa* Goode and Bean, 1896, are triangular with multiple cusplets and have a broad, triangular root base (Castro, 2011). Teeth belonging to *S. hesperius* Springer, 1966, are similar to those of *S. boa*; however, they have larger primary cusplets, whereas those of *S. retifer* (Garman, 1881) have a single pair of cusplets and a triangular root base. Teeth of *Triaenodon obesus* (Rüppel, 1837) may also appear similar to those of *Scyliorhinus* sp., but upper teeth are small with needle-like main cusps and have cusplets that are connected to the enameloid of the main cusp (Castro, 2011; Ebert et al., 2021). Of these taxa, teeth of the chain dogfish, *S. retifer,* appear most similar to those of *Scyliorhinus* sp. in the Venice Elasmobranch Assemblage. However, we refrain from species-level taxonomic identification because teeth from this taxon are uncommon, only three teeth were collected and available for study, and uncertainties exist regarding intraspecific variation in tooth morphology across *Scyliorhinus* spp. Many extant *Scyliorhinus* taxa are currently known from the Gulf of Mexico and Caribbean region, but most occur in deeper continental shelf and slope waters (Castro, 2011; Ebert et al., 2021).

Family TRIAKIDAE Gray, 1851
Genus *MUSTELUS* Linck, 1790
Mustelus sp.
Figure 8P–Y

Referred specimens. Four teeth (figured teeth: UF-VP560839–UF-VP560840 and additional teeth: UF-VP560841–UF-VP560842).

Description. The largest tooth is 2.49 mm in height and 1.29 mm in width. The occlusal face is weakly convex, has a distinct longitudinal ridge that

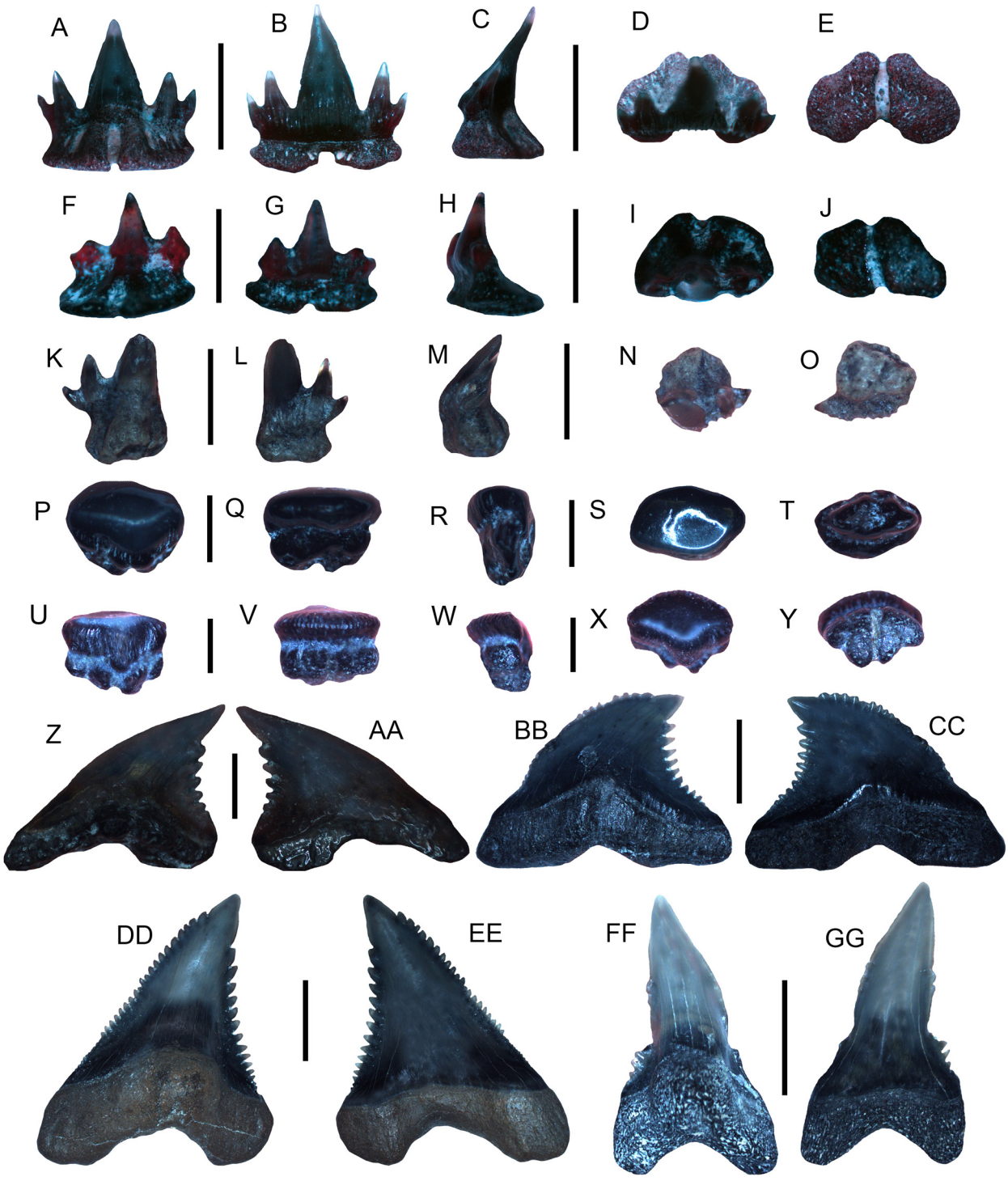

FIGURE 8. Carcharhiniform teeth from the Peace River and Tamiami formations on the shallow Venice, Florida continental shelf. **A–O,** *Scyliorhinus* sp. (UF-VP560836–UF-VP560838). **P–Y,** *Mustelus* sp. molariform teeth (UF-VP560839–UF-VP560840). **Z–AA,** *Galeorhinus* sp. lateral tooth (UF-VP560843). **BB–GG,** *Hemipristis serra* upper lateral (BB–CC; UF-VP560844), upper anterolateral (DD–EE; UF-VP560845); and lower anterior (FF–GG; UF-VP560846) teeth. Orientations = lingual: A, F, K, P, U, Z, BB, DD, FF; labial: B, G, L, Q, V, AA, CC, EE, GG; lateral: C, H, M, R, W; occlusal: D, I, N, S, X; basal: E, J, O, T, Y. Scale bars: A–E, Z–AA = 2 mm, F–Y = 1 mm; BB–GG = 5 mm.

is mesodistally oriented, and overhangs the root base. The labial face contains faint furrows near the crown-root interface, whereas the lingual face contains a distinct central uvula. The tooth root is typically very thin and contains a central nutritive furrow on the basal surface.

Remarks. The teeth of *Mustelus* sp. in the Venice Elasmobranch Assemblage can be differentiated from those of *Heterodontus*, *Rhynchobatus*, *Rhinobatos*, and *Hypanus* based on the presence of an ovular shape, occlusal surface ridge, furrows near the crown-root interface, and thin roots. Currently, many *Mustelus* taxa are known from the Atlantic and Gulf Coastal Plains of the USA and along western North America, Central America, and South America (Castro, 2011; Ebert et al., 2021). These taxa typically inhabit various bathymetries and have teeth that are morphologically similar (Castro, 2011; Ebert et al., 2021). Teeth of *M. albipinnis* Castro-Aguirre et al., 2005 have centrally elongated crowns that are conical in shape, whereas those of *M. norrisi* Springer, 1939, are flattened in the apicobasal direction, have rhombus to diamond-shaped occlusal surfaces that are low cusped in the upper jaw and slightly convex in the lower jaw (Castro, 2011). The teeth of *M. canis* (Mitchill, 1815) are rhomboidal–trilobate in outline and have raised central portions surrounded by faint ridges and grooves near the root base (Castro, 2011; Ebert et al., 2021). Upper teeth of *M. sinusmexicanus* Heemstra, 1997, have a slightly convex occlusal surface with a central ridge and may have a lobate appearance in contrast to lower teeth that are relatively flat or weakly convex (Castro, 2011). *Mustelus dorsalis* Gill, 1864, teeth have a conical main cusp atop a rounded–ovular root base and appear similar to those of *M. higmani* Springer and Lowe, 1963, that also exhibit scalloped enamaloid at the crown-root interface (Ebert et al., 2021). Similarly, teeth of *M. henlei* Gill, 1863, can be distinguished from those of *Mustelus* sp. in the Venice Elasmobranch Assemblage because they have distinct cusps, tooth shoulders, and a visible nutritive groove (Ebert et al., 2021). The teeth of *Mustelus* sp. in the Venice Elasmobranch Assemblage appear most similar to those of the smooth dogfish, *M. canis,* the Florida dogfish, *M. norrisi*, and the gulf smooth houndshark, *M. sinusmexicanus*. As a result, we refrain from species-level identification due to similarities in tooth morphology and uncertainties in dental variation related to ontogenetic and sexual heterodonty in these *Mustelus* taxa.

Presently, the distributions of these extant taxa are as follows: the smooth dogfish, *M. canis*, occurs in the western Atlantic and is seasonally abundant in southern regions during the winter (Dodrill, 1977; Heemstra, 1997; Castro, 2011), the Florida dogfish, *M. norrisi*, occurs from the Gulf of Mexico to Brazil and is seasonally abundant along the Florida coast (Clark and von Schmidt, 1965; Heemstra, 1997; Castro, 2011), and the gulf smooth houndshark, *M. sinusmexicanus*, is known from the Gulf of Mexico but the limits of its distribution are unknown (Heemstra, 1997; Castro, 2011). The maximum size for these taxa ranges between 100 and 150 cm, and all are known to be opportunistic bottom feeders that prey upon a variety of invertebrates (e.g., crabs, shrimp, lobster, worms) and small fish (Heemstra, 1997; Castro, 2011).

Genus *GALEORHINUS* Blainville, 1816

Galeorhinus sp.

Figure 8Z–AA

Referred specimens. One tooth (UF-VP560843).

Description. The tooth is labiolingually compressed and measures 7.33 mm in height and 6.19 mm in width. The cusp is distally inclined with a nearly straight, smooth mesial margin and a coarsely serrated distal margin. The root is labiolingually compressed, and a weakly defined nutritive groove is present on the lingual surface.

Remarks. The teeth of *Galeorhinus* sp. appear very similar to those of *Hemipristis serra* that also occur in the Venice Elasmobranch Assemblage; however, they have a nearly straight, smooth mesial margin, thinner roots, and smaller overall size. The upper anterior teeth of *Paragaleus* differ from those of *Galeorhinus* because they have a more mesiodistally compressed cusp that has a straight mesial edge and are much smaller in size. Similarly, *Hemigaleus* teeth differ from those of *Galeorhinus* because they have a prominent nutritive groove on the lingual root surface. While the teeth of *Galeorhinus* sp. in the Venice Elasmobranch Assemblage bear some resemblance to those of the extant taxon, *G. galeus* (Linnaeus, 1758), they are mesiodistally wider and do not exhibit a concave mesial margin. Presently, the extant school shark, *G. galeus,* occurs along the western coast of the USA and Mexico, but this taxon has not been reported in the Gulf of Mexico or along eastern North America (Castro, 2011; Ebert et al., 2021).

Family HEMIGALEIDAE Hasse, 1879

Genus *HEMIPRISTIS* Agassiz, 1835

Hemipristis serra Agassiz, 1835
Figure 8BB–GG

Referred specimens. Four teeth consisting of three upper anterolateral and one lower anterior tooth (figured teeth: UF-VP560844–UF-VP560846 and additional tooth: UF-VP560847).

Description. The largest upper anterolateral tooth measures 36.81 mm in height and 24.54 mm in width. The cusps of upper anterolateral teeth are triangular, coarsely serrated, and distally inclined. Serrations on the distal margin are larger than those on the mesial margin and increase in size toward the cusp apex but terminate slightly below the apex. The roots of upper anterolateral teeth are holaulacorhizous, tall, and have well-developed lingual protuberances containing nutritive grooves. The mesial root branches are flatter and taper to a point, whereas the distal branches have rounded lobes. The cusp of the lower anterior tooth is long, robust, sigmoidal, and bent lingually. The lower tooth margin is smooth, and the cutting edge is limited to the apical portion of the cusp. A pair of short, irregular lateral cusplets occurs on the distal and mesial tooth shoulders. The root of the lower anterior tooth is holaulacorhizous, and mesiodistally compressed, and contains a robust lingual protuberance.

Remarks. Teeth of *H. serra* display strong dignathic heterodonty allowing distinction between upper and lower jaw positions where upper teeth are broad, coarsely serrated, distally inclined, and contain relatively thin roots in contrast to lower teeth that are narrow and erect and have thicker roots with a more well-developed lingual protuberance (Purdy et al, 2001; Cappetta, 2012). In particular, upper anterolateral teeth are distally-hooked, contain coarse serrations that increase in size towards the cusp apex on the distal margin, and have thin roots with lingual protuberances and are in direct contrast to lower anterior teeth that have slender cusps and robust roots (Purdy et al., 2001; Cappetta, 2012; Kent, 2018). These distinct tooth morphologies distinguish *H. serra* from other similar teeth also found in the Venice Elasmobranch Assemblage including *Galeorhinus* sp., *Galeocerdo aduncus* Agassiz, 1843, and *Galeocerdo cuvier* (Perón and Lesueur, 1822). Teeth of *Prionace glauca* (Linnaeus, 1758) (i.e., *Carcharhinus glaucus* (Linnaeus, 1758), *Sensu* da Silva Rodrigues-Filho et al., 2023) may also appear similar to those of *H. serra* although they exhibit finer serrations and less distal inclination, and lower teeth are more triangular (Castro, 2011; Ebert et al., 2021). The Eocene species, *H. curvatus* Dames, 1883, has upper teeth with serrations that increase in size towards the cusp apex on both the mesial and distal tooth margins (Cappetta, 2012). Upper teeth from the extant taxon *H. elongata* (Klunzinger, 1871) are typically more elongate, have finer serrations, and are mesiodistally thinner than those of *H. serra*.

Hemipristis serra is an extinct taxon that had a nearly global, mid-latitudinal distribution during the middle to late Cenozoic and increased in size between the Miocene and Pliocene prior to its extinction in the Pleistocene (Purdy et al., 2001; Chandler et al., 2006; Cappetta, 2012; Lin et al., 2022). However, presently only a single extant species, *H. elongata*, is known from inner continental shelf habitats in the Indo-Pacific and feeds on cephalopods and a variety of fish (Ebert et al., 2021).

Family GALEOCERDONIDAE Poey, 1875
Genus *GALEOCERDO* Müller and Henle, 1838
Galeocerdo aduncus Agassiz, 1843
Figure 9A–H

Referred specimens. Four teeth of which two teeth represent the broad-toothed form (UF-VP560848–UF-VP560849) and two teeth represent the narrow-toothed form (UF-VP560850–UF-VP560851).

Description. Teeth have two distinct morphologies: 1) a broad form (Figure 9A–D) and 2) a narrow form (Figure 9E–H). The largest tooth representing the broad-toothed form measures 16.64 mm in length and 19.24 mm in width, whereas the largest tooth representing the narrow-toothed form measures 20.96 mm in length and 20.57 mm in width. The crown of the narrow-toothed form has fine serrations with a flat labial face and a convex lingual face. The cusp is angled distally, and a weakly developed distal notch separates the main cusp from the distal shoulder that contains coarse, compound serrations. Teeth of the broad-toothed form are wider and shorter with coarse, simple, and irregular serrations on the mesial and distal cutting edges. The distal shoulder is separated from the main cusp by a notch and contains large, compound serrations. The tooth roots are holaulacorhizous and more exposed on the lingual side with a short nutritive groove.

Remarks. Teeth of *G. aduncus* may appear similar to those of *G. cuvier, G. mayumbensis,* and *Physogaleus contortus* that also occur in the Venice Elasmobranch Assemblage; however, they can be distinguished on the basis of having broad- and narrow-toothed forms that only have compound

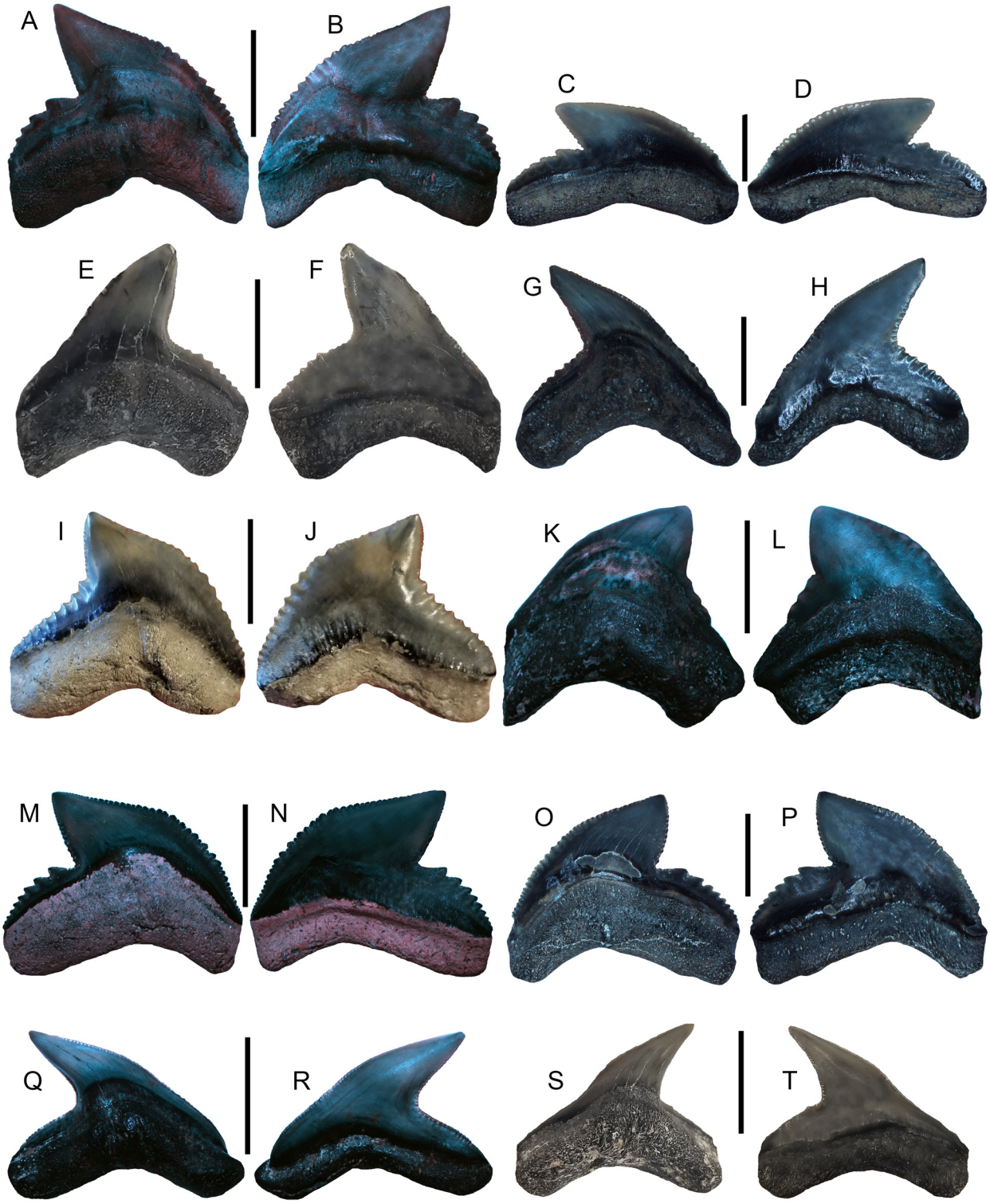

FIGURE 9. Carcharhiniform teeth from the Peace River and Tamiami formations on the shallow Venice, Florida continental shelf. *Galeocerdo aduncus* broad-toothed form (**A–D,** UF-VP560848–UF-VP560849) and narrow-toothed form (**E–H,** UF-VP560850–UF-VP560851). **I–L,** *Galeocerdo mayumbensis* (UF-VP560852–UF-VP560853). **M–P,** *Galeocerdo cuvier* (UF-VP560854–UF-VP560855). **Q–T,** *Physogaleus contortus* (UF-VP560856–UF-VP560857). Orientations = lingual: A, C, E, G, I, K, M, O, Q, J; labial: B, D, F, H, J, L, N, P, R, T. Scale bars: A–B, E–F, I–N = 1 cm; C–D, G–H, O–T = 5 mm.

serrations on the distal margin (Cappetta, 2012; Kent, 2018; Maisch et al., 2018; Türtscher et al., 2021). In light of these recent studies, we identify teeth belonging to three *Galeocerdo* taxa in the Venice Elasmobranch Assemblage: 1) the narrow- and broad-toothed forms of *G. aduncus* with compound serrations on only the distal margin; 2) *G. mayumbensis* for broad teeth with steeply inclined, coarsely serrated distal shoulders; and 3) *G. cuvier* for large, broad teeth with a distinct distal shoulder and compound serrations on all margins. The distinction between *G. aduncus* and *G. cuvier* on the basis of compound serration abundance and location was presented by Kent (2018) who also identified the broad and narrow tooth morphologies of *G. aduncus* (resembling *G. cuvier* and *P. contortus*, respectively) from the Miocene Calvert Cliffs of Maryland, USA. Other researchers have suggested that the teeth of *G. aduncus* and *P. contortus* may represent sexual dimorphism or upper and lower jaw teeth (i.e., dignathic heterodonty) of the same species (Applegate, 1978, 1992; Ward and Bonavia, 2001; Türtscher et al., 2021). However, some European Miocene localities are known to contain an abundance of the broad-toothed form of *G. aduncus* and lack or infrequently contain teeth identified as *P. contortus* (Reinecke et al., 2011; Bor et al., 2012; Cappetta, 2012). Broad *G. aduncus* teeth appear very similar to those of *G. cuvier* but are typically smaller in size, lack compound serrations on the main cutting edges, and are commonly reported from the early to Middle Miocene–Mio/Pliocene boundary, whereas those of *G. cuvier* have been primarily reported since the Pliocene for teeth with compound serrations on all margins. Similarly, narrow *G. aduncus* teeth closely resemble those of *P. contortus* and both taxa are known to occur in the Miocene (Kent, 2018; Türtscher et al., 2021). Kent (2018) distinguished between the narrow-toothed and broad-toothed forms of *G. aduncus* and *P. contortus* on the basis that: 1) narrow teeth of *G. aduncus* contain coarse, compound serrations on the distal heel and have a less sigmoidal profile; 2) broad teeth of *G. aduncus* resemble those of *G. cuvier* but lack compound serrations on the distal margin; and 3) teeth of *P. contortus* have thickened roots and crowns that are sigmoidal with comparatively finer serrations along the entire tooth margin. These interpretations were supported by the recent morphometric analyses of Türtscher et al. (2021). As a result, we identify teeth belonging to both the narrow and broad-toothed forms of *G. aduncus* in the Venice Elasmobranch Assemblage. We also note that the distribution of *G. aduncus* is likely more widespread than presently recognized because many prior studies in Florida and the USA have identified the narrow-toothed forms of *G. aduncus* as *P. contortus* (e.g., Perez, 2022). Additional information on the taxonomy of *Galeocerdo* and *Physogaleus* species can be found in the work by Cappetta (2012), Kent (2018), and Türtscher et al. (2021).

Galeocerdo mayumbensis
Darteville and Casier, 1943
Figure 9I–L

Referred specimens. Two teeth (UF-VP560852–UF-VP560853).

Description. The largest tooth measures 23.18 mm in height and 27.20 mm in width. The tooth crown is broad and erect. Both the lingual and labial faces are convex, and tooth serrations are compound. The distal shoulder is not well-developed or separated from the main crown, is steeply inclined, and contains noticeably coarser serrations. Coarse serrations also occur on the lower and central portion of the mesial cutting edge which is curved outwards. The tooth root is holoaulachorhizous and weakly separated. The labial root surface is slightly concave, and the lingual root surface is convex and contains a short nutritive groove.

Remarks. The presence of a broad crown, steeply inclined distal shoulder, and coarse serrations on the curved mesial cutting edge and distal shoulder distinguishes teeth of *G. mayumbensis* from other similar teeth also found in the Venice Elasmobranch Assemblage including those of *G. aduncus* and *G. cuvier.* Teeth of *G. mayumbensis* were previously assigned to *G. aduncus* (e.g., Cigala-Fulgosi and Mori, 1979; Marsili et al., 2007); however, the validity of this taxon was confirmed by Andrianavalona et al. (2015) and Türtscher et al. (2021). Although the teeth of *G. mayumbensis* are frequently confused with those of *G. cuvier* because they are commonly found in the same deposits and are similar in size, the presence of a steeply inclined distal shoulder with coarse serrations can be used to distinguish *G. mayumbensis* from *G. cuvier.* In contrast to the teeth of *G. cuvier* and *G. aduncus,* those of *G. mayumbensis* are relatively uncommon in the Venice Elasmobranch Assemblage and are instead more frequently collected in central Florida (HMM personal observation). According to Türtscher et al. (2021), *G. mayumbensis* is known from the Early Miocene–Mio/Pliocene boundary.

Galeocerdo cuvier (Perón and Lesueur, 1822)
Figure 9M–P

Referred specimens. Two teeth (UF-VP560854–UF-VP560855).

Description. The largest lateral tooth measures 17.70 mm in height and 22.00 mm in width. The crown of the lateral tooth is smooth with a flat labial surface and convex lingual surface. The cusp is angled distally and contains a distinct distal notch that separates the main cusp from the distal shoulder. All tooth margins contain well-developed, compound, and coarse serrations that decrease in size towards the cusp apex. The lateral tooth root is holaulacorhizous, robust, and more exposed on the lingual surface where a nutritive groove is present.

Remarks. The presence of coarse, compound serrations on all tooth margins, a thick root with a lingual protuberance containing a shallow nutritive groove, and a larger overall size distinguishes teeth of the tiger shark, *G. cuvier,* from other similar teeth also found in the Venice Elasmobranch Assemblage including those of *H. serra, G. aduncus,* and *G. mayumbensis* (Bor et al., 2012; Cappetta, 2012; Kent, 2018). At the PCS Phosphate Mine, Purdy et al. (2001) identified similar teeth as *G.* cf. *G. cuvier* on the basis that some basal and apical mesial cutting edges are straight creating an obtuse angle that is usually only seen in juveniles and not adults of the modern species. The teeth of *G. aduncus* appear very similar to those of *G. cuvier;* however, teeth from this taxon are smaller in size, only have compound serrations on the distal shoulder, have two tooth morphotypes, and are commonly reported from the Oligocene–Mio/Pliocene boundary (Cappetta, 2012; Maisch et al., 2015, 2018; Kent, 2018; Türtscher et al., 2021). Teeth of *G. mayumbensis* may appear similar to those of *G. cuvier* because they are robust and contain coarse, compound serrations; however, they typically have taller crowns, straight to weakly concave distal shoulders, and weakly separated root lobes (e.g., Andrianavalona et al., 2015; Türtscher et al., 2021).

Of the *Galeocerdo* taxa represented in the Venice Elasmbranch Assemblage, teeth of *G. cuvier* are the most frequently collected. Although typically reported from the Late Miocene/Mio–Pliocene boundary, *G. cuvier* has also been identified from the Middle Miocene of Hungary (Szabó et al., 2023) and Florida (Türtscher et al., 2021). The Hungarian report of *G. cuvier* from the Middle Miocene is represented by a single, fragmentary tooth residing in a private collection (Szabó et al., 2023, p. 59), whereas 37 teeth reposited in publicly accessible museum collections were analyzed from Florida (Türtscher et al., 2021). The majority of the teeth analyzed from Florida were collected from phosphate mines and adjacent waterways in Polk, Hardee, and DeSoto counties. In this region, varying amounts of erosion and reworking have occurred, and most of these fossil assemblages derive from the Late Miocene and Miocene–Pliocene-aged Peace River Formation and Bone Valley Member of the Peace River Formation. Additionally, a specimen identified as *G. cuvier* and utilized by Türtscher et al. (2021) was reported from the “Arcadia River, Florida” for which there is no such location. However, the Peace River, a well-known fossil-bearing waterway in central Florida, does run through the town of Arcadia, and this specimen may have derived from here. As a result of the complex stratigraphy, erroneous locality information of at least one proposed Middle Miocene *G. cuvier* tooth specimen from central Florida, and privately held specimens from Hungary, the validity of *G. cuvier* occurring in the Middle Miocene requires additional study that is beyond the scope of this report. Additional information on the taxonomy of *Galeocerdo* and *Physogaleus* species can be found in work by Cappetta (2012), Kent (2018), and Türtscher et al. (2021).

Extant *G. cuvier* is known in shallow marine deposits since the Late Miocene (and potentially the Middle Miocene: i.e., Türtscher et al., 2021; Szabó et al., 2023). This taxon has a global distribution although it is most frequently reported in temperate and tropical continental shelf regions where it is known to be an opportunistic predator that feeds upon a variety of vertebrates including fish, elasmobranchs, turtles, and marine mammals (e.g., Dudley et al., 2000; Compagno et al., 2005; Wirsing et al., 2007; Castro, 2011; Aines et al., 2018; Ebert et al., 2021; Türtscher et al., 2021).

Genus *PHYSOGALEUS* Cappetta, 1980
Physogaleus contortus (Gibbes, 1849)
Figure 9Q–T

Referred specimens. Two lateral teeth (UF-VP560856–UF-VP560857).

Description. The largest lateral tooth measures 17.19 mm in height and 20.35 mm in width. The main cusp is smooth with a flat labial face and convex lingual face, angled distally, and has a sigmoidal profile. The distal tooth margin contains a weakly developed distal notch and serrated shoulder. Serrations on tooth margins are fine, with those of the distal shoulder becoming slightly coarser, and compound serrations are not present.

The tooth root is holaulacorhizous and contains a nutritive groove in the center of a robust lingual protuberance, and a greater root surface area is exposed on the lingual surface.

Remarks. The presence of an elongated cusp with a sigmoidal profile, finely serrated tooth margins, and a robust root bearing a lingual protuberance with nutritive groove distinguishes teeth of *P. contortus* from other similar teeth also found in the Venice Elasmobranch Assemblage, such as *Galeocerdo aduncus* and *G. cuvier*. Taxonomic reassessment has placed this taxon in the genus *Physogaleus* rather than *Galeocerdo* based on robust roots, narrow, erect, and sigmoidal cusps, and finely serrated tooth margins (e.g., Ward and Bonavia, 2001; Reinecke et al., 2011; Bor et al., 2012; Cappetta, 2012; Kent, 2018). Kent (2018) and Türtscher et al. (2021) further distinguished *P. contortus* from a narrow-toothed form of *G. aduncus* on the basis that *P. contortus* teeth have fine serrations on all margins and a sigmoidal crown. However, these studies do not discuss the possibility of sexual heterodonty or other variations in *P. contortus*. In the Venice Elasmobranch Assemblage, *P. contortus* teeth are infrequently recovered and can be identified by the presence of a sigmoidal crown and lack of coarse serrations.

Family CARCHARHINIDAE Jordan and Evermann, 1896

Genus *RHIZOPRIONODON* Whitley, 1929

Rhizoprionodon sp.

Figure 10A–V

Referred specimens. Twenty teeth (11 figured teeth: UF-VP560858–UF-VP560868 and nine additional teeth: UF-VP560869–UF-VP560877).

Description. The largest anterolateral tooth measures 1.6 mm in height and 1.88 mm in width. The cusps of anterolateral teeth are slender, needle-like, and distally inclined, and contain a complete cutting edge. The distal heel is pronounced and is generally smooth but several irregular serrations are present in some teeth (e.g., Figure 10J–V). The labial tooth face overhangs the root and displays a convex ridge parallel to the root base, whereas the lingual face is nearly flat. The root is holauchorhizous and rectilinear and contains a nutritive groove.

Remarks. The presence of small teeth with slender main cusps, well-defined distal heels, and absence of regular serrations distinguishes *Rhizoprionodon* sp. from other similar teeth in the Venice Elasmobranch Assemblage, including *P. contortus, Carcharhinus* spp., *Sphyrna* cf. *S. zygaena,* and *S.* cf. *S. tiburo.* The teeth of *Rhizoprionodon* sp. can generally be distinguished from those of *Scoliodon* sp. by the lack of the labial crown base overhanging the root and steeply inclined main cusps that overhang the distal root margin. *Sphyrna* spp., including *S. lewinii,* may have teeth similar to those of *Rhizoprionodon;* however, teeth from these taxa are generally larger and contain thicker crowns that are not sigmoidal. Although many *Rhizoprionodon* taxa exist, those with teeth most similar to those in the Venice Elasmobranch Assemblage include: *R. longurio* Jordan and Gilbert, 1882, that have small, smooth-margined, distally inclined teeth with a distal heel that may contain faint crenulations; *R. terraenovae* (Richardson, 1836) that has small, thin teeth with margins that may be smooth, faintly, or irregularly serrated, and may also contain irregular serrations on the distal heel; and *R. porosus* (Poey, 1861) that has distally inclined teeth with a nearly straight mesial edge, and may have faintly serrated or crenulated distal heels (Castro, 2011; Ebert et al., 2021).

At least three extant *Rhizoprionodon* (sharpnose shark) taxa (i.e., *R. terraenovae*, *R. porosus*, and *R. longurio*) are currently known to occur along the southeastern USA, Gulf Coastal Plain, Caribbean, Central America, western North America, and northern South America and feed upon a variety of small fish and invertebrates (Castro, 2011; Ebert et al., 2021). *Rhizoprionodon* teeth in the Venice Elasmobranch Assemblage exhibit morphologies consistent with all of these extant taxa, suggesting that multiple species were present during the Miocene–Pliocene and deposition of the Peace River and Tamiami formations. Moreover, inter- and intraspecific variations in the tooth morphology of extant genera, including *Scoliodon, Loxodon,* and *Rhizoprionodon,* are further complicated by sexual dimorphism and ontogenetic heterodonty (Springer, 1964; Cappetta, 2012; Ebersole et al., 2023). As such, we refrain from species-level taxonomic identification at the present time.

Genus *NEGAPRION* Whitley, 1940

Negaprion brevirostris (Poey, 1868)

Figure 11A–H

Referred specimens. Four teeth consisting of three upper anterolateral (UF-VP5610–UF-VP561016) and one lower anterior tooth (UF-VP560878).

Description. The largest tooth is a lower anterior tooth that measures 19.04 mm in height and 21.07 mm in width. The cusps of the upper anterolateral teeth are erect, have complete, smooth cutting edges, a nearly flat labial face and convex lingual

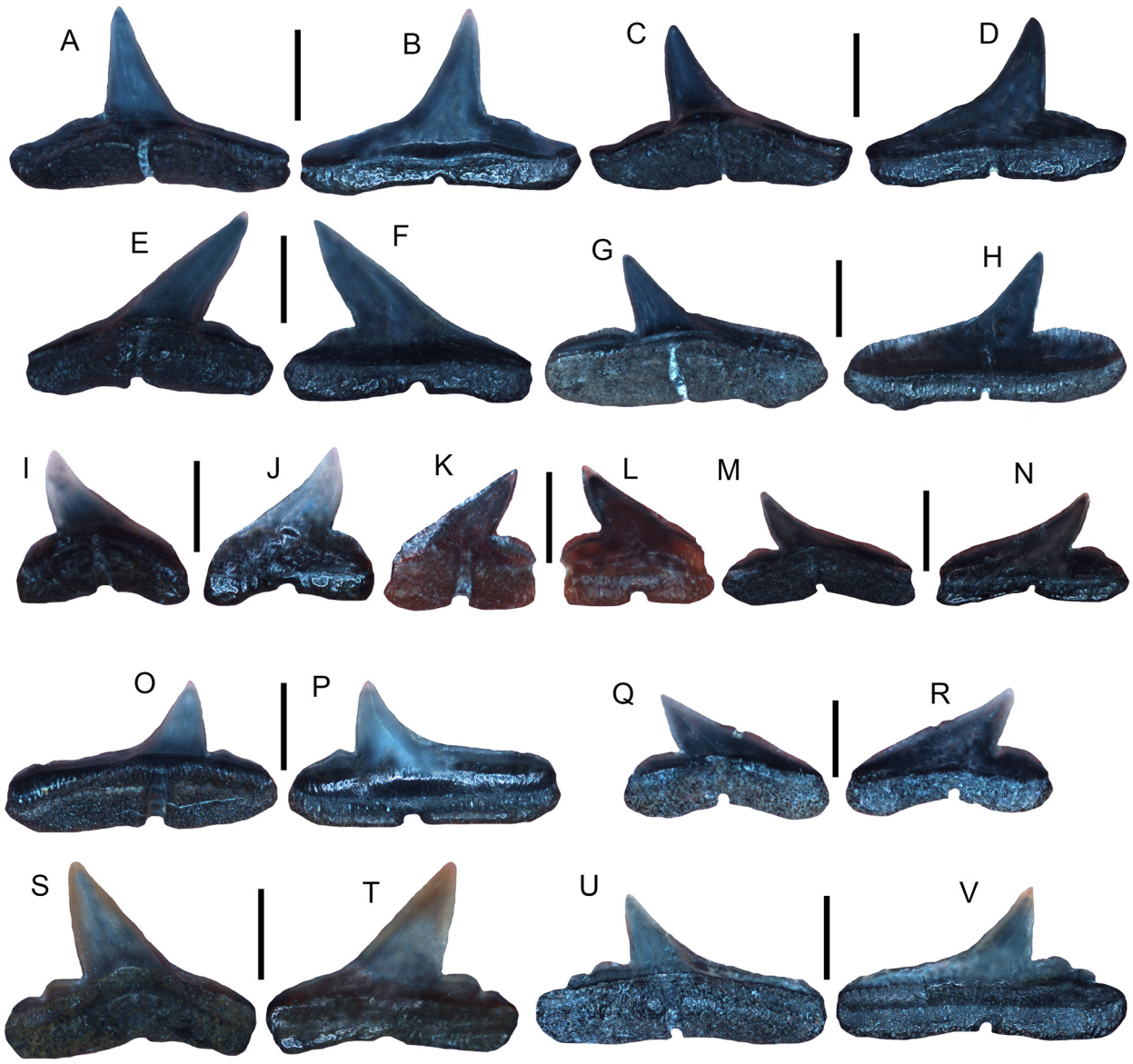

FIGURE 10. Carcharhiniform teeth from the Peace River and Tamiami formations on the shallow Venice, Florida continental shelf. **A–V,** *Rhizoprionodon* sp. teeth (UF-VP560858–UF-VP560868). Orientations = lingual: A, C, E, G, I, K, M, O, Q, J, U; labial: B, D, F, H, J, L, N, P, R, T, V. Scale bars: A–F, J–V = 2 mm; G–R = 1 mm.

face, and well-developed tooth shoulders that are separated from the main cusp by notches and contain low, faint serrations. The cusps of lower anterior teeth are erect, have a noticeably convex lingual face and a slightly convex labial face, and lack well-defined tooth shoulders. The tooth roots are holaulachorhizous and widely divergent, may have a flattened basal edge on the lingual face, and contain a faint nutritive groove. The roots of lower anterior teeth are similar to those of upper teeth except they are generally more rounded in shape.

Remarks. The presence of erect teeth with a smooth cusp and well-developed, faintly serrated tooth shoulders distinguishes those of the lemon shark, *N. brevirostris*, from other similar teeth also found in the Venice Elasmobranch Assemblage, including *Carcharias taurus* and *Carcharhinus* spp. *Negaprion brevirostris* teeth differ from those of *N. eurybathrodon* (Blake, 1862) because upper anterior teeth display larger, more erect crowns and

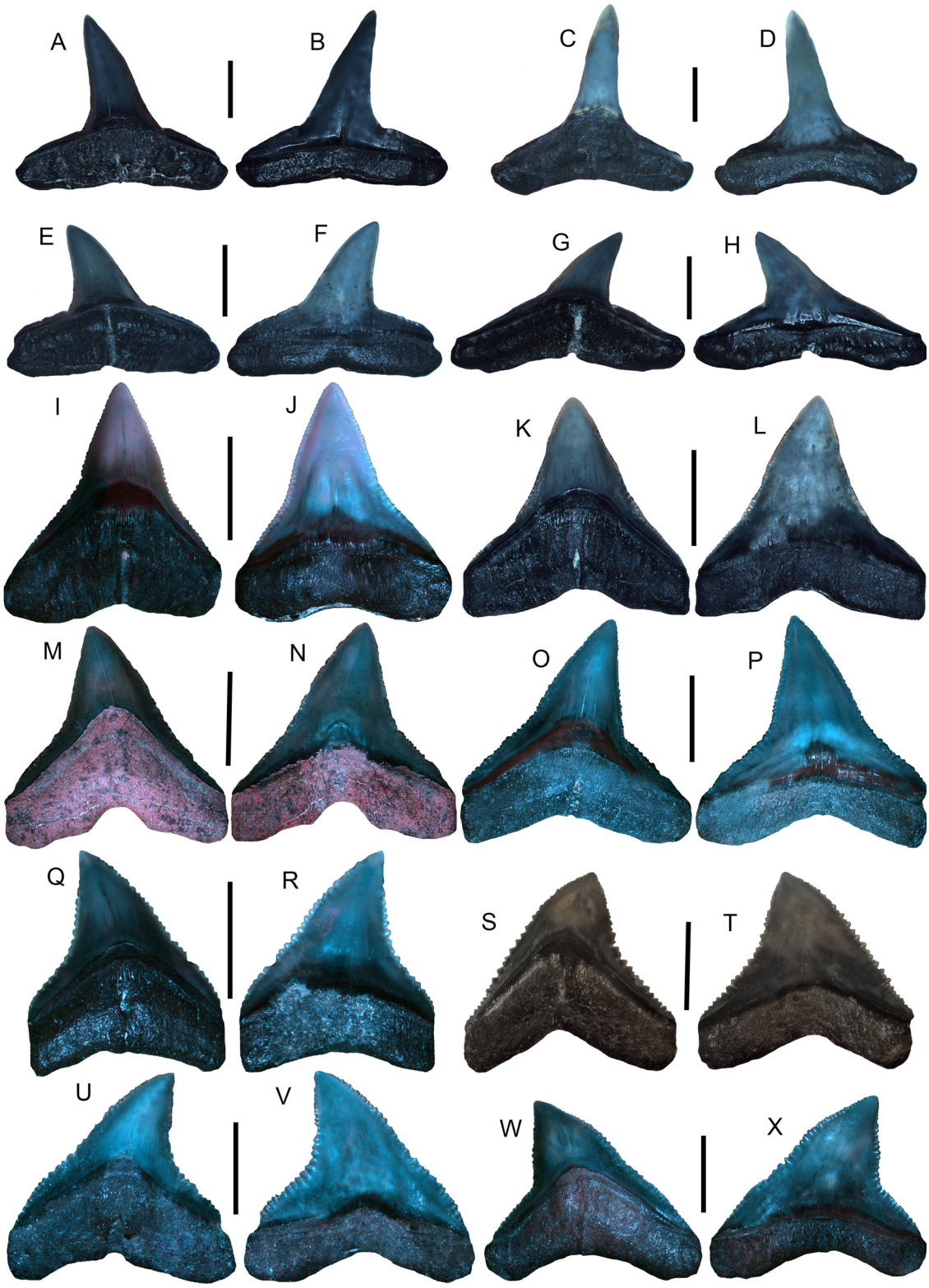

FIGURE 11. Carcharhiniform teeth from the Peace River and Tamiami formations on the shallow Venice, Florida continental shelf. **A–H,** *Negaprion brevirostris* anterolateral teeth (UF-VP560878; UF-VP561014–UF-VP561016). **I–P,** *Carcharhinus leucas* upper anterolateral teeth (UF-VP561019–UF-VP561022). **Q–X,** *Carcharhinus obscurus* upper anterolateral teeth (UF-VP561031–UF-VP561034). Orientations = lingual: A, C, E, G, I, K, M, O, Q, S, U, W; labial: B, D, F, H, J, L, N, P, R, T, V, X. All scale bars = 5 mm.

contain well-developed, partially serrated tooth shoulders (Cappetta, 2012; Maisch et al., 2018). Kent (2018) identified *N. eurybathrodon* as an uncommon taxon from the Miocene Calvert Cliffs of Maryland following Purdy et al. (2001) who indicated *N. brevirostris* was a junior synonym of *N. eurybathrodon*. This view is not widely accepted and currently, two extant *Negaprion* taxa are recognized, *N. brevirostris* in the western Atlantic and Gulf of Mexico and *N. acutidens* (Rüppell, 1837) in the Indian and western Pacific Oceans that has upper teeth with faintly serrated, less-developed tooth shoulders (Compagno et al., 2005; Castro, 2011; Ebert et al., 2021). Additional discussions regarding the classification of *N. brevirostris* can be found in papers by White (1955); Antunes and Jonet (1970); Longbottom, 1979; Purdy et al. (2001); Ward and Bonavia (2001); Kocsis (2007); Bor et al. (2012); Cappetta (2012); and Kent (2018).

Extant *N. brevirostris* is especially common in shallow continental shelf waters along the southeastern USA, Gulf of Mexico, and Caribbean and feeds predominantly on fish and crustaceans (Castro, 2011; Ebert et al., 2021). Important nursery areas have been documented for this taxon, including the southeastern coast of the USA from South Carolina–Florida, as well as the Bahamas (Springer, 1950a, Morrissey and Gruber, 1993; Castro, 2011).

Genus *CARCHARHINUS* Blainville, 1816
Carcharhinus cf. *C. falciformis*
(Bibron in Müller and Henle, 1839)
Figure 12A–D

Referred specimens. Two upper anterolateral teeth (UF-VP561017–UF-VP561018).

Description. The larger of the two teeth measures 14.97 mm in height and 15.56 mm in width. The cusp of the anterolateral tooth is triangular and erect and serrations become coarser near the base of the cusp and on the tooth shoulders. Serrations on the tooth shoulders are separated from the main cusp by a notch. The labial tooth face is nearly flat, and the lingual face is slightly convex. The tooth root is holaulacorhizous and labiolingually compressed and contains a shallow nutritive groove on the lingual face.

Remarks. Isolated teeth of *Carcharhinus* spp. are notoriously difficult to identify; however, upper jaw teeth exhibit a greater degree of variation between species. The presence of coarser serrations on upper anterolateral tooth shoulders that are separated from progressively finer serrations on the main cusp by a notch distinguishes teeth of the silky shark, *C. falciformis,* from those of other carcharhiniform taxa also found in the Venice Elasmobranch Assemblage. Despite similarities in tooth shape and size with other taxa including *C. leucas, C. obscurus,* and *C. plumbeus,* the distinct notch that separates between the tooth shoulder and main cusp in teeth of *C. falciformis* is a diagnostic feature, and this taxon is likely more abundant in Venice than presently known. Additional discussions on *C. falciformis* and related taxa can be found in works by Garrick (1982); Compagno (1988); Naylor and Marcus (1994); Grace (2001); Purdy et al. (2001); Carnevale et al. (2006); Reinecke et al. (2011); Voigt and Weber (2011); Cappetta (2012); Marsili (2007); Carrillo-Briceño et al. (2016a); Kent (2018); and Ebert et al. (2021).

Extant *C. falciformis* occurs globally in mid-latitudinal waters and typically preys upon a variety of fish and invertebrates (Castro, 2011). Adults of this taxon typically frequent offshore surface waters and may be found among swordfish and schooling tuna, whereas juveniles are more abundant in shallow waters, especially during the warmer months (Strasburg, 1958; Branstetter, 1981, 1987; Castro, 2011).

Carcharhinus leucas (Müller and Henle, 1839)
Figure 11I–P

Referred specimens. Twelve anterolateral teeth (figured teeth: UF-VP561019–UF-VP561022 and additional teeth: UF-VP561023–UF-VP561030).

Description. The largest figured tooth is an anterolateral tooth that measures 21.30 mm in height and 21.74 mm in width. The cusp of upper anterior teeth is erect, triangular, and finely serrated along the entire margin whereas the cusps of anterolateral teeth exhibit mesiodistally thinner cusps that are distally inclined. The labial face of the cusp of upper anterior and anterolateral teeth is nearly flat, whereas the lingual face is convex and contains a well-developed tooth neck between the cusp and root base. The roots of upper anterior teeth are broad, have widely spaced root lobes, and contain a deep, centrally located nutritive furrow that extends from the base of the root toward the center of the root. The roots of anterolateral teeth are similar but their lobes are reduced in size. Roots in teeth from both upper jaw positions also display a concave U-shaped, arch-like depression between the root lobes, and the lateral edges of the root lobes are typically straight.

Remarks. Extensive literature exists on the bull shark, *C. leucas*, in the fossil record (e.g., Cap-

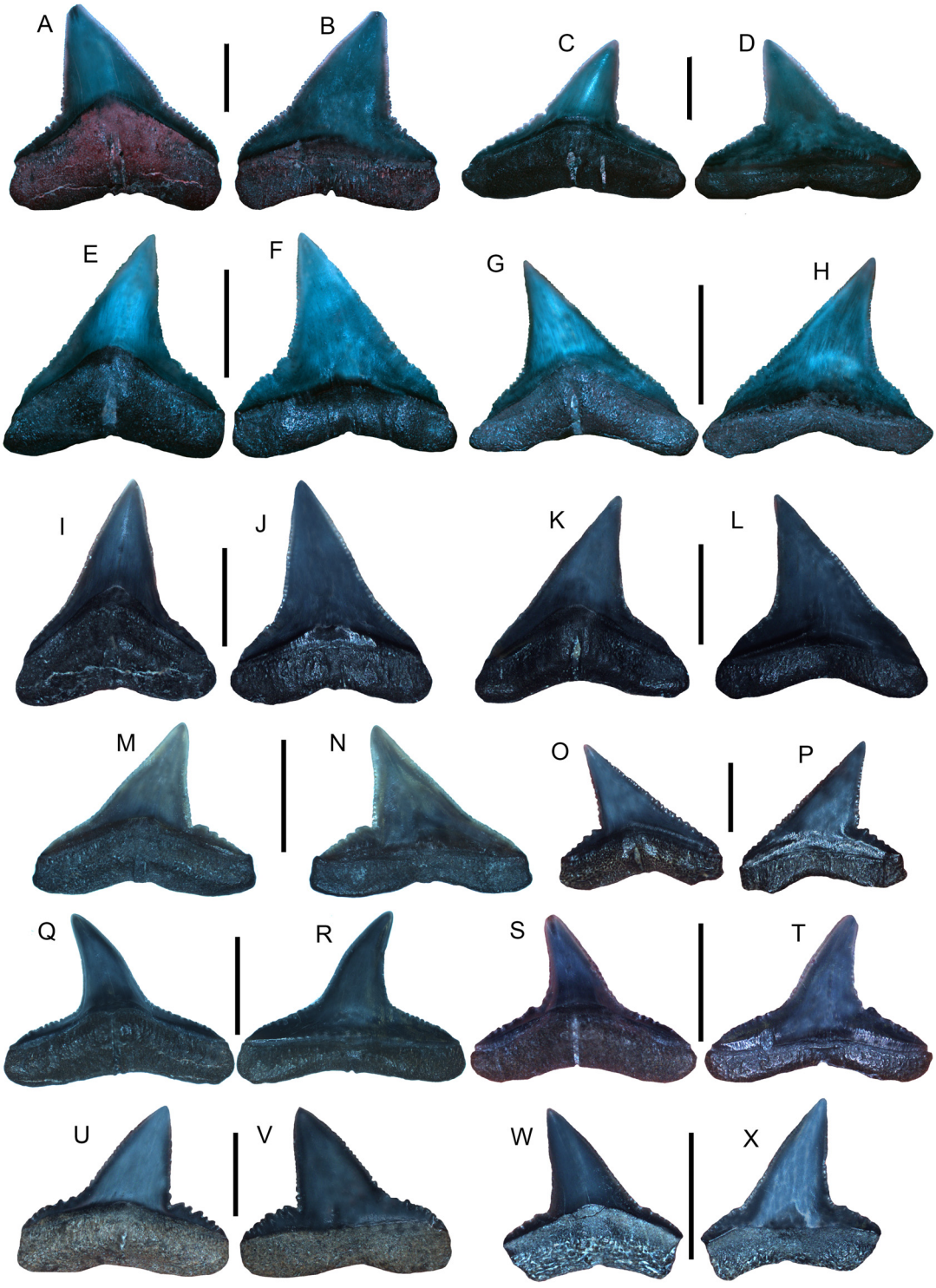

FIGURE 12. Carcharhiniform teeth from the Peace River and Tamiami formations on the shallow Venice, Florida continental shelf. **A–D,** *Carcharhinus* cf. *C. falciformis* upper anterolateral teeth (UF-VP561017–UF-VP561018). **E–H,** *Carcharhinus* cf. *C. plumbeus* upper anterolateral teeth (UF-VP561043–UF-VP561044). **I–L,** *Carcharhinus* cf. *C. altimus* upper anterior lateral teeth (UF-VP561815–UF-VP561816). **M–P,** *Carcharhinus* cf. *C. perezii* upper anterolateral teeth (UF-VP561039–UF-VP561040). **Q–T,** *Carcharhinus* cf. *C. brachyurus* upper anterolateral teeth (UF-VP561047–UF-VP561048). **U–X,** *Carcharhinus* cf. *C. porosus* upper anterolateral teeth (UF-VP561819–UF-VP561820). Orientations = lingual: A, C, E, G, I, K, M, O, Q, S, U, W; labial: B, D, F, H, J, L, N, P, R, T, V, X. Scale bars: A–N, Q–X = 5 mm; O–P = 2 mm.

petta, 2012; Kocsis et al., 2015; Kent, 2018). Upper teeth belonging to *C. leucas* can be distinguished from those of other carcharhiniforms in the Venice Elasmobranch Assemblage, by the presence of broad, triangular cusps that are regularly and finely serrated, and roots that contain a U- or arched-shaped depression between lobes and have straight lateral edges. Despite these characteristics, *C. leucas* upper teeth may still appear very similar to those of *C. obscurus*; however, they typically have finer serrations along most of the tooth margin and a more distinct U-shaped depression between root lobes. Additionally, *C. galapagensis* (Snodgrass and Heller, 1905) teeth can be distinguished from those of *C. leucas* because they have coarser and more irregular serrations on the lower portion of the cusp and are typically taller than they are wide. The anterior teeth of *C. longimanus* may also appear similar to those of *C. leucas*; however, they are more erect and distinctly triangular in shape with serrations that are coarser along the entire margin. For additional discussions on *C. leucas* and related taxa see: Garrick (1982); Compagno (1988); Naylor and Marcus (1994); Grace (2001); Purdy et al. (2001); Carnevale et al. (2006); Castro (2011); Reinecke et al. (2011); Voigt and Weber (2011); Cappetta (2012); Marsili (2007); Carrillo-Briceño et al. (2015a); Kent (2018); and Ebert et al. (2021).

Extant *C. leucas* has a global distribution although is typically found in continental shelf and brackish waters in tropical and subtropical regions where it is preys upon a wide variety of vertebrates (e.g., Compagno et al., 2005; Castro, 2011; Ebert et al., 2021). Currently, *C. leucas* occurs throughout the Gulf of Mexico from deep waters to coastal estuary systems, including those along Florida's west coast (Castro, 2011; Curtis et al., 2011; Ebert et al., 2021). Interestingly, these estuary systems presently support many other juvenile and subadult elasmobranch taxa that also occur in Venice Elasmobranch Assemblage, suggesting that similar coastal habitats have existed along southwest Florida since at least the Miocene/Pliocene (Yeiser et al., 2008; Ortega et al., 2009; Heupel and Simpfendorfer, 2008, 2011; Hunt and Doering, 2013; Dawdy et al., 2022).

Carcharhinus obscurus (Lesueur, 1818)
Figure 11Q–X

Referred specimens. Eight upper anterolateral teeth (figured teeth: UF-VP561031–UF-VP561034 and additional teeth: UF-VP561035–UF-VP561038).

Description. The largest figured anterolateral tooth is 19.08 mm in height and 21.26 mm in width. The cusp of upper anterolateral teeth is broad, triangular, and regularly serrated along the entire margin with serrations increasing in size near the base of the cusp. The labial face is nearly flat, whereas the lingual face is convex and contains a well-developed tooth neck near the base of the cusp. The roots of upper anterolateral teeth are broad with relatively straight lobes that are widely separated by a concavity. The lingual root face exhibits a well-developed nutritive furrow that is present from the root base to the center portion of the root.

Remarks. In the Venice Elasmobranch Assemblage, carcharhiniform teeth belonging to the dusky shark, *C. obscurus*, and the bull shark, *C. leucas,* are very similar and are frequently confused with each other. However, upper teeth from these taxa typically exhibit morphological differences that include the presence of regular, finely serrated margins and a well-developed U-shaped concavity separating the root lobes in *C. leucas* and more coarsely serrated lower cusp margins and a shallower concavity separating the root lobes in *C. obscurus*. Additionally, teeth of *C. galapagensis* may appear similar to those of *C. obscurus*, but they are more coarsely and irregularly serrated near the crown-root interface, have root lobes that are generally more rounded, and are typically taller than they are wide. Anterolateral teeth of *C. falciformis* may also bear some resemblance to those of *C. obscurus*; however, they have a distinct notch that separates serrations on the tooth shoulders from those on the main cusp. Additional discussions on *C. obscurus* and related taxa can be found in papers by Garrick (1982); Compagno (1988); Naylor and Marcus (1994); Grace (2001); Purdy et al. (2001); Carnevale et al. (2006); Castro (2011); Reinecke et al. (2011); Voigt and Weber (2011); Cappetta (2012); Marsili (2007); Carrillo-Briceño et al. (2015a); Kent (2018); and Ebert et al. (2021).

Extant *C. obscurus* occurs on most tropical and subtropical continental shelves globally and is known to prey upon a variety of fish and invertebrates (Castro, 2011; Hoffmayer et al., 2014). Whereas some *C. obscurus* individuals exhibit site fidelity in the Gulf of Mexico and along the Atlantic Coastal Plain of the USA, others are known to migrate over greater ranges (Cortes et al., 2006; Hoffmayer et al., 2014).

Carcharhinus perezii (Poey, 1876)
Figure 12M–P

Referred specimens. Four upper anterolateral teeth (figured teeth: UF-VP561039–UF-VP561040 and additional teeth: UF-VP561041–UF-VP561042).

Description. The largest upper anterolateral tooth measures 7.19 mm in height and 9.67 mm in width. The crown of the upper anterolateral tooth contains an erect cusp and completely serrated cutting edge with serrations finer near the apical region and coarser near the base of the cusp. The labial tooth face is nearly flat, the lingual face is convex, and both surfaces are smooth. The roots are holaulacorhizous and contain a shallow nutritive groove on the lingual face.

Remarks. The presence of fine serrations that become coarser near the base of the cusp and continuously progress onto the tooth shoulders without a notch distinguishes the teeth of *C. perezii* (Caribbean reef shark) from those of other carcharhiniforms in the Venice Elasmobranch Assemblage. Although *C. acronatus* teeth may be similar in size and overall shape to those of *C. perezii*, they are narrower, more erect, and finely serrated or smooth in more distally located teeth (Castro, 2011; Voight and Weber, 2011). Fossil teeth previously identified as *C. priscus* (Agassiz, 1843) also appear similar to those of *C. perezii* although they have finer serrations along the entire tooth margin and are typically smaller in size (Reinecke et al., 2011; Voight and Weber, 2011; Kent, 2018; Maisch et al., 2018). The teeth identified as *C. perezii* in the Venice Elasmobranch Assemblage are all distally inclined, finely serrated along the main cusp, and more coarsely serrated on the distal tooth shoulder, making them appear identical to those imaged by Voight and Weber (2011). Extant *C. perezii* is most known from shallow continental shelf waters of the western Atlantic; however, the taxon has also been reported from the Gulf of Mexico where it preys upon a variety of fish and invertebrates (Castro, 2011; Driggers et al., 2011; Voight and Weber, 2011; Ebert et al., 2021). Additional discussion on *C. perezii* and similar related taxa can be found in works by Compagno (1988); Naylor and Marcus (1994); Purdy et al. (2001); Kocsis (2007); Marsili (2007); Castro (2011); Reinecke et al. (2011); Voight and Weber (2011); Bor et al. (2012); Cappetta (2012); Kent (2018); and Ebert et al. (2021).

Carcharhinus plumbeus (Nardo, 1827)
Figure 12E–H

Referred specimens. Four upper anterolateral teeth (figured teeth: UF-VP561043–UF-VP561044 and additional teeth: UF-VP561045–UF-VP561046).

Description. The largest figured upper anterolateral tooth measures 15.75 mm in height and 13.17 mm in width. The cusps of upper anterolateral teeth are thin, triangular, and contain fine, regularly spaced serrations and have a nearly straight mesial margin. Teeth progressing from mesial to distal jaw positions develop a distinctly concave distal margin although still contain fine, regularly spaced serrations on the tooth margins. The labial surface is smooth whereas lingual surface is weakly convex although both surfaces are smooth. The roots of anterolateral teeth are thin and arched and contain a well-developed nutritive groove on the lingual face.

Remarks. The presence of labiolingually thin, mesiodistally broad, finely serrated upper teeth with well-developed nutritive grooves on the lingual root surface distinguishes teeth of the sandbar shark, *C. plumbeus*, from those of other carcharhiniform taxa also found in the Venice Elasmobranch Assemblage. The teeth of *C. plumbeus* appear most similar to those of *C. altimus* but are broader, and more distally inclined. Juvenile teeth of *C. leucas* may also appear similar to those of *C. plumbeus*; however, they are more robust and have clearly separated root lobes (Castro, 2011; Voight and Weber, 2011). Similarly, the teeth of *C. acronatus* are distinct from those of *C. plumbeus* because they typically have small, finely serrated, and narrow main cusps in anterior teeth, partially serrated to smooth cusps in distally located teeth, and teeth in all positions possesses a distinct distal shoulder (Voight and Weber, 2011).

Extant *C. plumbeus* exists along most mid-latitudinal continental shelves and preys upon a variety of vertebrates and invertebrates (Castro, 2011; Ebert et al., 2021). This taxon has complex migratory patterns and utilizes multiple areas for nurseries along the Atlantic and Gulf Coastal Plains of the USA, ranging from Great South Bay, Long Island, New York, to the northern Gulf of Mexico (Springer, 1960; Castro, 2011).

Carcharhinus cf. *C. altimus* (Springer, 1950b)
Figure 12I–L

Referred specimens. Four upper anterolateral teeth (figured teeth: UF-VP561815–UF-VP561816

and additional teeth: UF-VP561817–UF-VP561818).

Description. The largest figured upper anterolateral tooth is 15.51 mm in height and 13.68 mm in width. Upper anterolateral teeth are broad, finely serrated, and have elongated, triangular cusps. The labial face is slightly convex whereas the lingual face is nearly flat. The tooth root is thin, root lobes are weakly separated, and a well-developed nutritive groove is present on the lingual face.

Remarks. The bignose shark, *Carcharhinus altimus*, frequents deeper tropical–subtropical, mid-latitudinal continental shelf waters; however, this taxon has been reported in shallower shelf waters globally (Castro, 2011; Ebert et al., 2021). This taxon is known to make seasonal migrations along the Atlantic Coastal Plain of the USA where it feeds upon a variety of a variety of vertebrates and invertebrates, including chimaeras, smaller elasmobranchs, and cephalopods (Springer, 1950b; Kohler et al., 1998; Castro, 2011; Ebert et al., 2021). We identify labiolingually thin, mesiodistally broad, erect, and finely serrated upper teeth with well-developed nutritive grooves on the lingual root surface as *C.* cf. *C. altimus* in the Venice Elasmobranch Assemblage. The teeth of *C. plumbeus* appear most similar to those of *C.* cf. *C. altimus* but are less erect and exhibit a greater degree of distal inclination. Kent (2018) identified *C.* cf. *C. altimus* from the Miocene Calvert Cliffs of Maryland but indicated that these teeth are typically small and uncommon and may in fact represent those of *C. acronatus* (Poey, 1860). Teeth of *C. acronatus* are typically small, anterior teeth are finely serrated with narrow main cusps, distally located teeth are partially serrated to smooth, and teeth in all positions contain a distinct distal shoulder that is relatively thin in contrast to those of *C. altimus* (Castro, 2011; Ebert et al., 2021; Voight and Weber, 2011). In the Venice Elasmobranch Assemblage, we tentatively identify *C. altimus* because these teeth can appear very similar to those of *C. plumbeus.*

Carcharhinus cf. *C. brachyurus* (Günther, 1870)
Figure 12Q–T

Referred specimens. Four upper anterolateral teeth (figured teeth: UF-VP561047–UF-VP561048 and additional teeth: UF-VP561049–UF-VP561050).

Description. The largest figured upper anterolateral tooth measures 8.98 mm in height and 11.57 mm in width. The upper anterolateral tooth cusps are narrow, scythe-shaped, distally inclined, and finely serrated with serrations that may become more irregular near the base of the cusp. The labial face is convex, and the lingual face is nearly flat. The tooth roots are nearly flat on the labial face and weakly convex on the lingual face and have widely divergent lobes, and the basal root face is nearly flat. A well-developed nutritive groove is present on the lingual root face.

Remarks. The presence of narrow, oblique, finely serrated upper teeth with well-developed nutritive grooves on the lingual root surface distinguishes teeth of the copper shark, *C. brachyurus*, from those of other carcharhiniform taxa also found in the Venice Elasmobranch Assemblage. Teeth of *C. limbatus* and *C. brevipinna* appear most similar to those of *C. brachyurus* but are generally smaller and less oblique and have finer and more regularly spaced serrations. Additionally, the cusp apex of the upper teeth in *C. brachyurus* typically has a distinct distal curvature not seen in the teeth of the other *Carcharhinus* spp. in the Venice Elasmobranch Assemblage (Garrick, 1982; Castro, 2011). Teeth of *C. brachyurus* were considered synonymous with those of *C. priscus* (Agassiz, 1843) by Purdy et al. (2001) and Marsili (2007); however, additional analysis by Reinecke et al. (2011) showed that *C. priscus* teeth are morphologically distinct from those of *C. brachyurus* and other taxa. Maisch et al. (2015) and Kent (2018) identified *C. priscus* from the early and Middle Miocene of the Atlantic Coastal Plain of the USA for small, distally inclined, and finely serrated teeth lacking a distinct distal curvature of the cusp apex. The teeth identified as *C. brachyurus* in the Venice Elasmobranch Assemblage are distinct from those of *C. priscus* and appear identical to those identified by Marsili (2007) and Landini et al. (2017a, 2017b).

Extant *C. brachyurus* is known to prey upon a variety of vertebrates and invertebrates, including schools of fish and squid, and has been reported from the continental shelf waters of eastern and western South America, western Africa, the Mediterranean, Australia, Japan, and China. Although reports indicate that this taxon likely occurs in the Gulf of Mexico and is more widespread than presently documented, its presence in North American waters is currently not known (Castro, 2011; Ebert et al., 2021).

Carcharhinus limbatus
(Valenciennes in Müller and Henle, 1839)
Figure 13A–D

Referred specimens. Three upper anterolateral teeth (figured teeth: UF-VP561051–UF-VP561052 and additional tooth: UF-VP561053).

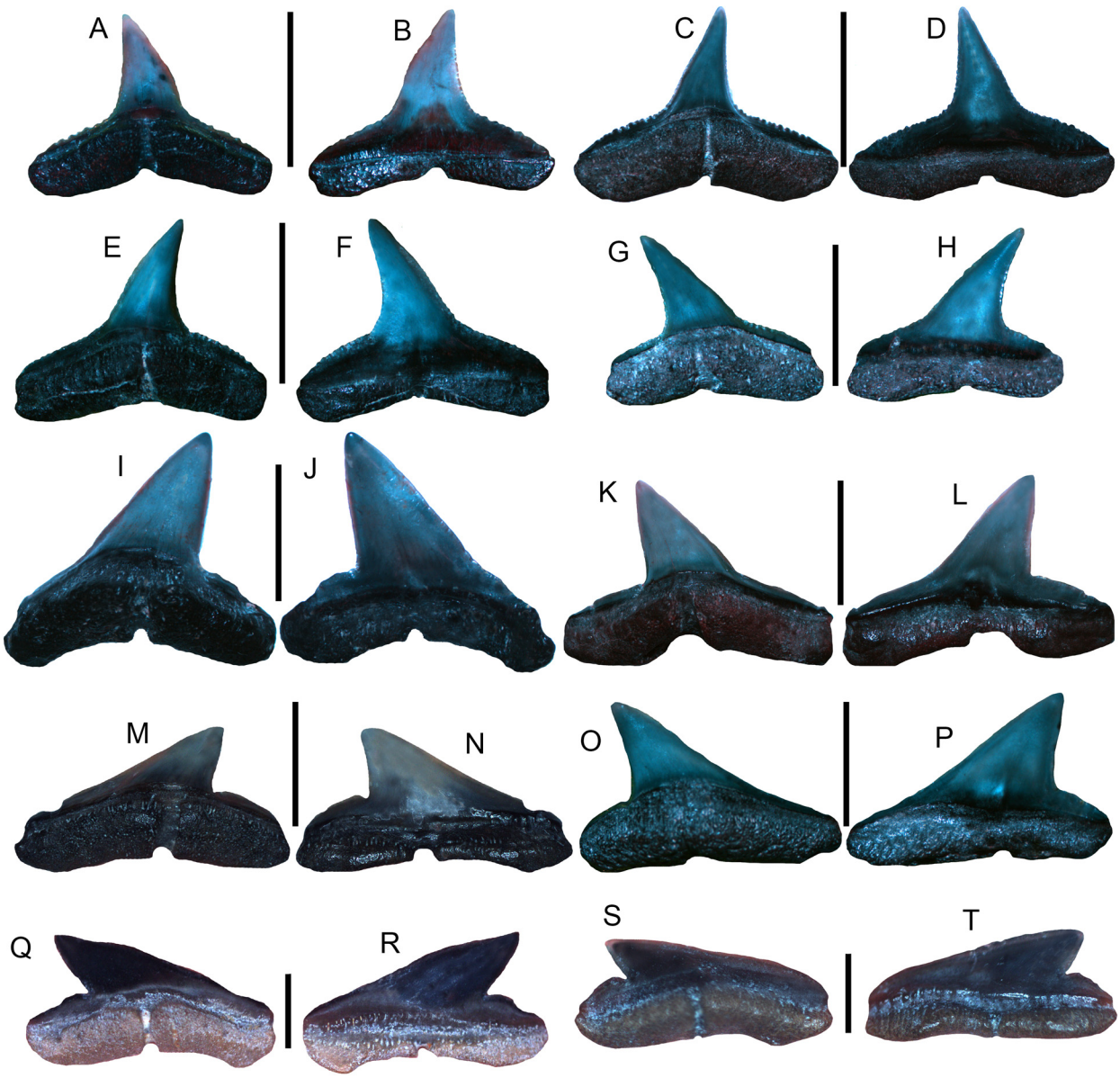

FIGURE 13. Carcharhiniform teeth from the Peace River and Tamiami formations on the shallow Venice, Florida continental shelf. **A–D,** *Carcharhinus* cf. *C. limbatus* upper anterolateral teeth (UF-VP561051–UF-VP561052). **E–H,** *Carcharhinus* cf. *C. brevipinna* upper anterolateral teeth (UF-VP561054–UF-VP561055). **I–P,** *Sphyrna* cf. *S. zygaena* teeth (UF-VP561058–UF-VP561061). **Q–T,** *Sphyrna* cf. *S. tiburo* teeth (UF-VP561062–UF-VP561063). Orientations = lingual: A, C, E, G, I, K, M, O, Q, S; labial: B, D, F, H, J, L, N, P, R, T. Scale bars: A–P = 5 mm; Q–T = 2 mm.

Description. The largest figured upper anterolateral tooth measures 8.06 mm in height and 10.94 mm in width. Upper anterolateral teeth are narrow, cusps are erect or slightly oblique, and serrations are fine and uniform on the central part of the cusp but become slightly coarser and irregular near the base of the cusp and on the tooth shoulders. The labial face is nearly flat, and the lingual face is weakly convex. Anterolateral tooth roots are thin and narrow with widely divergent lobes and contain a nutritive groove on the lingual face. A nutritive groove gap can also be seen in labial view.

Remarks. The presence of upper teeth that are small, erect, and narrow, have finely serrated main cusps with more coarsely serrated tooth shoulders, and exhibit a nutritive groove on the lingual root

surface distinguishes teeth of the blacktip shark, *C. limbatus,* from those of other carcharhiniform taxa also found in the Venice Elasmobranch Assemblage. Teeth of *C. brevipinna* and *C. brachyurus* appear very similar to those of *C. limbatus* but typically have finer, more regular tooth serration patterns. Additionally, *C. brevipinna* teeth are more erect with their serration size typically being very fine along the tooth margin except near the root base, and *C. brachyurus* teeth have distinctly distally curved cusp apices (Castro, 2011; Voight and Weber, 2011; Ebert et al., 2021).

Extant *C. limbatus* occurs globally along mid-latitudinal continental shelves and preys primarily upon small vertebrates including bony fish and elasmobranchs (Castro, 2011; Voight and Weber, 2011; Ebert et al., 2021). In the Gulf of Mexico and waters surrounding Florida, migratory aggregations of *C. limbatus* frequently occur in the summer months and have been documented entering feeding frenzies on concentrated food sources (Castro, 2011; Ebert et al., 2021).

Carcharhinus brevipinna
(Müller and Henle, 1839)
Figure 13E–H

Referred specimens. Four anterolateral teeth (figured teeth: UF-VP561054–561055 and additional teeth: UF-VP561056–UF-VP561057).

Description. The largest figured upper anterolateral tooth measures 9.40 mm in height and 11.66 mm in width. Upper anterolateral teeth are narrow, cusps are erect, and serrations are very fine and may exhibit a slight increase in size along the cusp onto the tooth shoulders. The labial face is nearly flat, and the lingual face is weakly convex. Anterolateral tooth roots are thin and narrow with widely divergent lobes and contain a nutritive groove on the lingual face. The gap of the nutritive groove is also partly visible in labial view.

Remarks. Isolated teeth of *Carcharhinus* spp. are notoriously difficult to identify; however, upper jaw teeth exhibit a greater degree of variation between species. The presence of small, erect, narrow, finely serrated upper teeth distinguishes the teeth of the spinner shark, *C. brevipinna,* from those of other carcharhiniform taxa also found in the Venice Elasmobranch Assemblage. The coarseness of serrations gradually increases along the cusp toward the tooth shoulders of *C. brevipinna* teeth in contrast to the teeth of *C. limbatus* that only show slightly coarser serrations on their shoulders (Castro, 2011; Voight and Weber, 2011; Ebert et al., 2021). Teeth of *C. isodon* can also be distinguished from those of *C. brevipinna* because they have very slender, smooth cusps that may contain irregular serrations on the distal tooth shoulder. In contrast to the teeth of *C. acronatus*, those of *C. brevipinna* have cusps that are much narrower rather than blade-like and do not have a defined distal shoulder (Voight and Weber, 2011).

Extant *C. brevippina* occurs nearly globally along mid-latitudinal continental shelves, primarily preys upon fish and other small vertebrates, and commonly forms migratory schools in the Gulf of Mexico similar to *C. limbatus* (Castro, 2011; Ebert et al., 2021). The possibility also exists that a subspecies between Pacific and Atlantic populations may be present because the Pacific representatives have a larger body size and teeth that are generally longer than those of the Atlantic type (Voight and Weber, 2011).

Carcharhinus cf. *C. porosus*
(Ranzani, 1839)
Figure 12U–X

Referred specimens. Four anterolateral teeth (figured teeth: UF-VP561819–UF-VP561820 and additional teeth UF-VP561821–UF-VP561822).

Description. The largest figured anterolateral tooth measures 7.80 mm in height and 10.10 mm in width. The cusps of the upper anterolateral teeth are distally inclined and finely serrated and exhibit a coarsely or irregularly serrated distal tooth shoulder. The labial face is convex, and the lingual face is nearly flat. The tooth root is thin, root lobes are separated by a depression, and a nutritive groove occurs on the lingual face.

Remarks. Isolated teeth of *Carcharhinus* spp. are notoriously difficult to identify; however, upper jaw teeth exhibit a greater degree of variation between species. The presence of a finely serrated main cusp with coarser serrations on the tooth shoulders separates the teeth of the smalltail shark, *C.* cf. *C. porosus*, described here from those of similar taxa including *C.* cf. *C*. *acronatus*, *C. perezii*, and *Rhizoprionodon* sp. that also occur in the Venice Elasmobranch Assemblage. In particular, the teeth of *C. perezii* appear very similar to those of *C. porosus*; however, they have finer serrations on all margins and typically possess a less developed distal shoulder with finer serrations. The teeth identified as *C.* cf. *C. porosus* in this study appear nearly identical to those of anterolateral teeth provided as line drawings in Castro (2011; p. 460) and images of upper anterior teeth provided by Voight and Weber (2011).

Extant *C. porosus* is known to prey upon a variety of small vertebrates and invertebrates including fish and shrimp on the continental shelf and in estuaries along the west coast of Mexico and South America, eastern South America, and the West Indies but is noticeably absent around the Caribbean Islands and those offshore western South America (Castro, 2011; Ebert et al., 2021). Although historically reported from various locations throughout the Gulf of Mexico, at present, *C. porosus* has only been reported from the southern Gulf of Mexico (Castro, 2011; Ebert et al., 2021).

Genus *SPHYRNA* Rafinesque, 1810
Sphyrna cf. *S. zygaena*
(Linnaeus, 1758)
Figure 13I–P

Referred specimens. Four anterolateral teeth (UF-VP561058–UF-VP561061).

Description. The largest anterolateral tooth measures 10.89 mm in height and 12.78 mm in width. The crowns of anterolateral teeth are smooth and labiolingually flattened and possess a complete cutting edge. The labial face is nearly flat, and the lingual face is slightly convex. The cusp is angled distally and is separated from the distal heel by a notch. The root is thin and holaulachorhizous and exhibits a deep nutritive groove.

Remarks. The smooth hammerhead, *Sphyrna zygaena,* represents one of the larger extant sphyrnid taxa known globally and preys upon a variety of vertebrates, including other elasmobranchs and bony fish (Castro, 2011; Ebert et al., 2021). The presence of smooth, erect cusps and well-developed distal heels distinguishes the teeth of *S.* cf. *S. zygaena* described here from those of similar taxa in the Venice Elasmobranch Assemblage, such as *S. tiburo*, *Rhizoprionodon* sp., and *Carcharhinus* spp. Studies on sphyrnids document little to no ontogenetic heterodonty, allowing for differentiation among the *Sphyrna* species such as *S. media* (Springer, 1940) containing smaller teeth with gracile cusps, *S. integra* (Probst, 1878) with teeth having low distal heels, *S. lewini* (Griffith and Smith, 1834) with teeth possessing gracile cusps and labiolingually compressed roots with well-developed nutritive grooves, and *S. mokarran* (Rüppell, 1837) with erect, finely-serrated teeth (e.g., Purdy et al., 2001; Castro, 2011; Cappetta, 2012; Bor et al., 2012; Ebert et al., 2021). Purdy et al. (2001) identified *S. laevissima* (Cope, 1867) as a junior synonym of *S. zygaena*; however, Reinecke et al. (2011) and Kent (2018) determined that these taxa are morphologically distinct. In particular, *S. laevissima* can be distinguished based on upper teeth with broader crowns and shorter distal heels and lower teeth being shorter and more triangular (Reinecke et al., 2011; Kent, 2018). A morphological gradient between the late Miocene and Pliocene was also documented by Reinecke et al. (2011), suggesting that *S. zygaena* may have evolved from *S. laevissima*. We assign the Venice specimens to *S.* cf. *S. zygaena* based on the presence of mesiodistally widened, non-serrated cusps, well-developed distal heels, enlarged nutritive groove, and a labiolingually compressed structure, following Purdy et al. (2001), Castro (2011), and Cappetta (2012).

Extant *S. zygaena* occurs globally in temperate and subtropical waters and is rare or absent in tropical environments (Castro, 2011; Ebert et al., 2021). Although reported from the east coast of Florida and the Florida Keys, this taxon is not presently known from the Gulf of Mexico (Castro, 2011; Ebert et al., 2021).

Sphyrna cf. *S. tiburo* (Linnaeus, 1758)
Figure 13Q–T

Referred specimens. Two anterolateral teeth (UF-VP561062–UF-VP561063).

Description. The larger anterolateral tooth is 1.93 mm in height and 3.94 mm in width. The cusp is low and distally inclined and has a smooth margin and well-developed distal tooth shoulder. The labial face is convex, and the lingual face is nearly flat. The cusp height is nearly the same as the thickness of the root. The root is thin and exhibits a well-developed nutritive groove on the lingual surface, and the lateral-most edge of each root lobes is angled outward.

Remarks. The bonnethead shark, *Sphyrna tiburo*, can be found in various habitats and water qualities including sandy shoals, river mouths, estuaries, and seagrass beds with clear or turbid waters, forms small, migratory schools, and preys upon a variety of invertebrates and small vertebrates including crabs, shrimp, and fish (Castro, 2011; Ebert et al., 2021; Gonzalez et al., 2024). The presence of smooth, low, and distally inclined cusps with short distal heels distinguishes teeth of *S.* cf. *S. tiburo* identified here from those of similar taxa in the Venice Elasmobranch Assemblage, such as *S.* cf. *S. zygaena* and *Rhizoprionodon* sp. Teeth of *S. corona* (Springer, 1940) can also be distinguished from those of *S. tiburo* because they have thinner and more erect cusps (Castro, 2011; Ebert et al., 2021). Similarly, the teeth of *S. lewini* and *S. media* can be distinguished from those of *S. tiburo* because they are more erect and the tooth

cusps may contain notches or crenulations (Castro, 2011).

While the extant bonnethead, *Sphyrna tiburo*, was long considered to consist of a single taxon in most warm waters in the western hemisphere, including the Gulf of Mexico, recent morphometric and genetic analyses indicate that *S. tiburo* in fact represents a species complex (Gonzalez et al., 2024). As such, two species are now recognized in the western Atlantic, *S. tiburo* and *S. alleni* Gonzalez, Postaire, Driggers, Caballero, and Chapman, 2024 and one species, *S. verpertina* Springer, 1940, is currently recognized in the eastern Pacific (Gonzalez et al., 2024).

Superorder BATOMORPHII Cappetta, 1980
Order RHINOPRISTIFORMES Naylor et al., 2012
Family RHINIDAE Müller and Henle, 1841
Genus *RHYNCHOBATUS* Müller and Henle, 1837
Rhynchobatus sp.
Figure 14A–T

Referred specimens. Ten teeth (figured teeth: UF-VP561064–UF-VP561067 and additional teeth: UF-VP561068–UF-VP561073).

Description. Teeth are small and have a low, globular appearance. The largest figured tooth measures 3.71 mm in height and 3.89 mm in width and has an occlusal surface that shows faint furrows and a weakly developed transverse ridge. The labial face is rounded, and the enameloid overhangs the root base. The lingual face contains a broad, centrally located uvula that extends over the root base and separates the occlusal surface into two lobes. The root is thinner than the cusp, and the basal face is bisected by a well-developed nutritive groove containing a foramen.

Remarks. The genus *Rhynchobatus* belongs to a group of rays commonly known as wedgefishes. The presence of small teeth with a globular occlusal surface containing a transverse ridge, a single lingual protuberance, and a thin root base distinguishes teeth of *Rhynchobatus* sp. described here from those of Rhinobatidae gen. indet., *Hypanus* spp., *Mustelus* sp., and *Pristis* cf. *P. pristis* oral teeth that also occur in the Venice Elasmobranch Assemblage. In particular, the teeth of *Rhynchobatus* sp. are frequently larger than those of *Rhinobatos* and have only a single prominent lingual uvula (Antunes and Balbino, 2007; Cappetta, 2012; Reinecke et al., 2023). Although pristid oral teeth also contain only a single lingual uvula, they are more mesiodistally compressed, and their root is not as thin or lingually displaced as in the teeth of *Rhynchobatus* sp.

Although historically separated into distinct families (e.g., Herman et al., 1997; Cappetta, 2012), Last et al. (2016a) recommended that extant wedgefish should be placed in a single family (Rhinidae) that consists of three genera (*Rhina*, *Rhynchobatus*, and *Rhynchorhina*) with a total of 10 species. Of the teeth from extant taxa imaged by Herman et al. (1997) and Reinecke et al. (2023), those of *Rhynchobatus lübberti* Ehrenbaum, 1915, and *R. djiddensis* (Forsskal, 1775) appear most similar to those of *Rhynchobatus* sp. in the Venice Elasmobranch assemblage because they exhibit a partially pitted to smooth occlusal surface with a lingually displaced transverse ridge and a thin, lingually displaced root. However, teeth identified as *R. pristinus* (Probst, 1877), that are reported in Miocene and Miocene/Pliocene European and Central and South American elasmobranch assemblages, also appear very similar to the teeth of *Rhynchobatus* sp. identified from Venice because they have a lingually displaced transverse ridge and root base as well as a partially pitted occlusal surface (e.g., Cappetta, 1970; Antunes and Balbino, 2007; Cappetta, 2012; Carrillo-Briceño et al., 2016a; 2019; Laurito Mora and Valerio, 2021). Although the Venice *Rhynchobatus* sp. teeth could belong to *R. pristinus*, *R. lübberti*, *R. djiddensis*, or yet an undescribed fossil species, heterodonty is known to occur in extant *Rhynchobatus* taxa such that teeth may vary in size depending on their location in the jaw and age, and teeth from juveniles may lack occlusal surface ornamentation (Herman et al., 1997; Cappetta, 2012; Reinecke et al., 2023). Due to these complications and the lack of detailed, comparative studies on extant and extinct *Rhynchobatus* taxa, we conservatively identify the fossil teeth described here as *Rhynchobatus* sp.

Presently, no extant *Rhynchobatus* taxa or any other wedgefish are known to occur in the Gulf of Mexico or western Atlantic. The nearest extant representative with morphologically similar teeth to those of *Rhynchobatus* sp. in the Venice Elasmobranch Assemblage is *R. lübberti*, the African wedgefish, that occurs along the northwest–central African coast. Like most other *Rhynchobatus* taxa, *R. lübberti* is benthic, occurs in shallow marine environments, and preys upon small to medium-sized vertebrates (including myliobatiforms) and invertebrates (Last et al., 2016a; Dean et al., 2017).

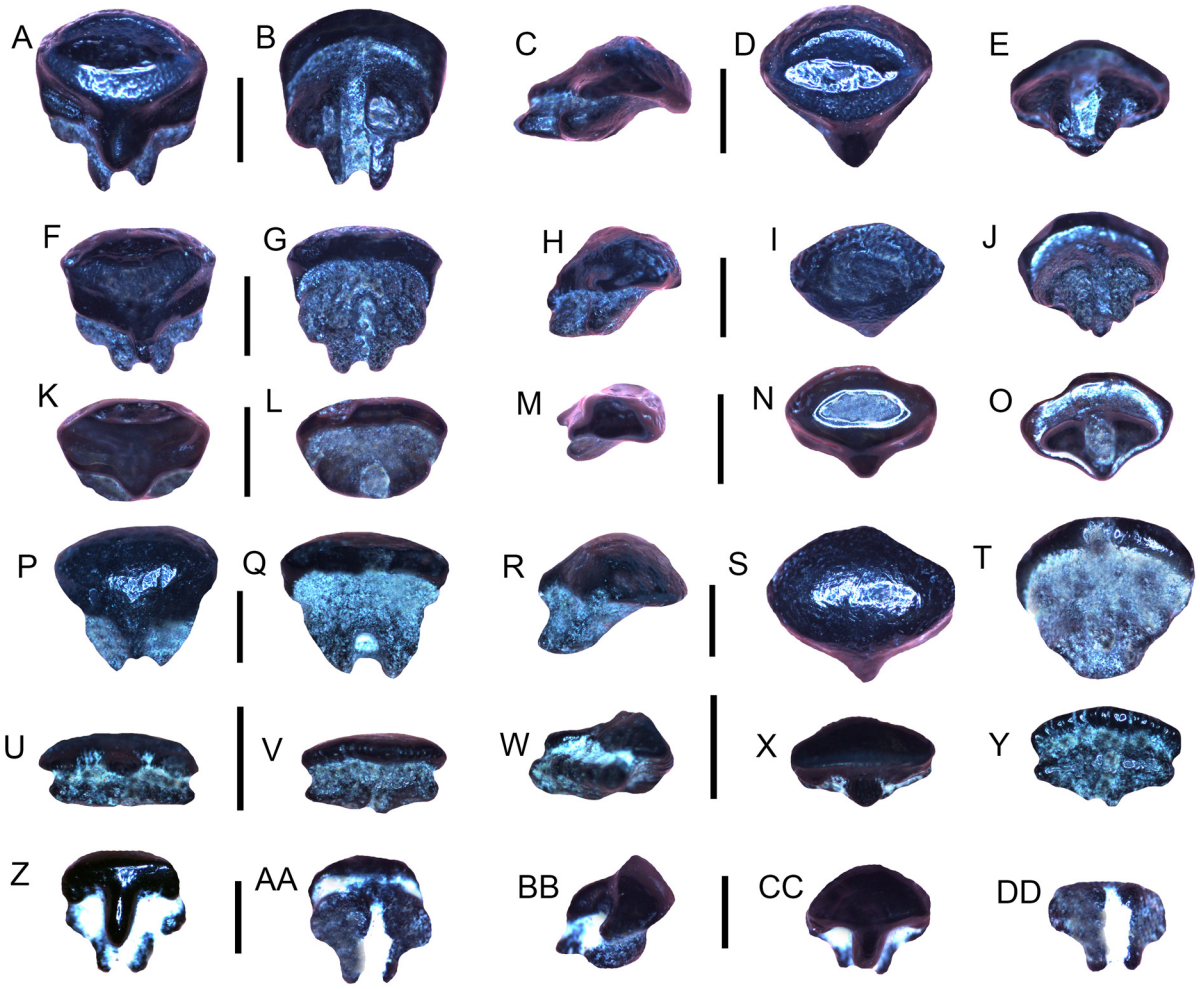

FIGURE 14. Rhinopristiform teeth from the Peace River and Tamiami formations on the shallow Venice, Florida continental shelf. **A–T,** *Rhynchobatus* sp. (UF-VP561064–UF-VP561067). **U–DD,** *Rhinobatos* sp. (UF-VP561074–UF-VP561075). Orientations = lingual: A, F, K, P, U, Z; labial: B, G, L, Q, V, AA; lateral: C, H, M, R, W, BB; occlusal: D, I, N, S, X, CC; basal: E, J, O, T, Y, DD. All scale bars = 1 mm.

Family RHINOBATIDAE Bonaparte, 1835
Rhinobatidae gen. indet.
Figure 14U–DD

Referred specimens. Two teeth (UF-VP561074–UF-VP561075).

Description. Teeth are very small and have an apicobasally compressed, globular appearance. The largest tooth measures 1.33 mm in height and 1.66 mm in width and has a smooth occlusal surface. The labial face extends over the root base whereas the lingual face contains an elongated, centrally located uvula that occurs between two secondary protuberances. A nutritive foramen occurs near both secondary protuberances at the crown-root junction. The root is displaced lingually, and the basal surface exhibits a well-developed nutritive groove with a large, centrally located foramen.

Remarks. Rhinobatids are guitarfish and contain taxa with very small teeth with a globular occlusal surface containing a primary lingual uvula flanked by secondary uvulae that can distinguish them from teeth of *Rhynchobatus* sp., *Hypanus* spp., *Mustelus* sp., and *Pristis* cf. *P. pristis* that also occur in the Venice Elasmobranch Assemblage. Although very similar, *Rhynchobatus* sp. teeth are frequently larger and can be distinguished from those of "*Rhinobatos"* because they have only one prominent lingual uvula (Herman et al., 1997; Cappetta, 2012; Reinecke et al., 2023). Similarly, the oral teeth of *P. pristis* and *P. pectinata* have a central, elongated uvula, lack secondary uvulae, and have a mesiodistally compressed morphology compared to *Rhinobatos* teeth (Cappetta, 2012; Reinecke et al., 2023). Teeth of the fanrays,

Platyrhina sinensis (Bloch and Schneider, 1801) and *Platyrhinoidis triseriata* (Jordan and Gilbert, 1880), may also appear similar to those of *Rhinobatos*; however, they are taller and have a more developed separation between the crown and root or are more globular with less-developed uvulae, respectively (Herman et al., 1997). Additionally, fossil remains of *Platyrhinoidis* have not been reported, and those of *Platyrhina* have only been reported in the Eocene and present-day (Herman et al., 1997; Cappetta, 2012; Last et al., 2016a).

Cappetta (2012) indicated that it is extremely difficult to taxonomically identify isolated *Rhinobatos* teeth, and many fossil *Rhinobatos* taxa may be synonymized or placed in separate genera. In recent genetic and morphological analyses of guitarfish (Rhinobatidae) by Last et al. (2016a), a total of three genera (*Acroteriobatus*, *Rhinobatos*, and *Pseudobatos*) and 31 valid species are identified. While many of these taxa have been documented along western Central America and South America, only one extant taxon, *P. lentiginosus* (Garman, 1880), is represented in the Gulf of Mexico. An additional species, *P. percelleus* (Walbaum, 1792), is known to occur along northern South America and part of the Caribbean; however, this taxon's presence in the Gulf of Mexico is uncertain (Bigelow and Schroeder, 1953; Last et al., 2016a). As presented by Last et al. (2016a), no *Rhinobatos* taxa presently occur in the Gulf of Mexico, along the Atlantic Coastal Plain of the USA, or along the west coast of central and South America, and the nearest representative of this genus, *R. rhinobatos* (Linnaeus, 1758), occurs along the west coast of Africa. As such, we identify these teeth as Rhinobatidae gen. indet. in the Venice Elasmobranch Assemblage and note that they appear similar to those of *P. lentiginosus* and *R. rhinobatos* (*sensu* Bigelow and Schroeder, 1953; Herman et al., 1997). Although presently having different global distributions, the extant freckled guitarfish, *P. lentiginosus* (Garman, 1880), and the common guitarfish, *R. rhinobatos* (Linnaeus, 1758), are known to be benthic, coastal species that prey upon a variety of invertebrates, particularly mollusks and crustaceans (Last et al., 2016a).

However, detailed, published images of teeth belonging to many other extant *Rhinobatos*, *Acroteriobatus*, and *Pseudobatos* species are not presently available and variable degrees of sexual heterodonty have been documented in "*Rhinobatos"* taxa. Further complications with identification of isolated teeth may be a result of seasonal heterodonty (i.e., differences in tooth morphology between the sexes during mating season) such that the teeth of females and males generally exhibit flat, low crowns except during the mating season where male teeth may exhibit taller, pointed crowns (e.g., Herman et al., 1997; Everhart, 2007; Underwood and Cumbaa, 2010; Cappetta, 2012; Bice and Shimada, 2016). As a result, it is extremely difficult to accurately identify fossil or modern "*Rhinobatos*" teeth, and it is clear that additional, comprehensive comparative studies are needed (e.g., Cappetta, 2012; Last et al., 2016a).

Family PRISTIDAE Bonaparte, 1838
Genus *ANOXYPRISTIS*
White and Moy-Thomas, 1941
Anoxypristis sp.
Figure 15A–L

Referred specimens. Three rostral spines (UF-VP561076–UF-VP561078).

Description. Rostral spines are elongated and dorsoventrally compressed. The largest figured rostral spine measures 18.32 mm long, is 6.37 mm wide near the spine base, and is 2.68 mm thick dorsoventrally. The anterior spine margin is typically straight and more convex than the posterior spine margin that may be distally curved near the apex. A faint, barb-like curvature may be present on the posterior margin near the apical portion of smaller spines. Faint longitudinal lines extend from the spine base toward the upper portion of the spine and may be crossed by irregularly spaced, perpendicular bands. The spine base is ovular in cross-section and contains numerous pits.

Remarks. The presence of rostral spines that are thin and blade-like, may be posteriorly curved, and are convex on the anterior and posterior edges distinguishes rostral spines of *Anoxypristis* sp. described here from *Pristis* cf. *P. pristis* that also occurs in the Venice Elasmobranch Assemblage. These same morphological characteristics of rostral spines, in addition to internal rostral morphology, also differentiate *Anoxypristis* sp. from all other extant sawfish taxa (i.e., *P. pristis*, *P. pectinata*, *P. zijsron*, and *P. clavata*). Numerous fossils of *Anoxypristis* sp. have been described, many initially as distinct *Pristis* spp., from isolated, and often fragmentary, rostral spines including *A. aethiopicus* (Darteville and Casier, 1943), *A. mucrodens* (White, 1926), and *A. fajumensis* (Stromer, 1905), among others (Cappetta, 2012; Cappetta and Case, 2016; Ebersole et al., 2019). However, the type species for these taxa derive from the Eocene of Africa and Europe, some of which may in fact be synonymous (Cappetta and Case, 2016). Several

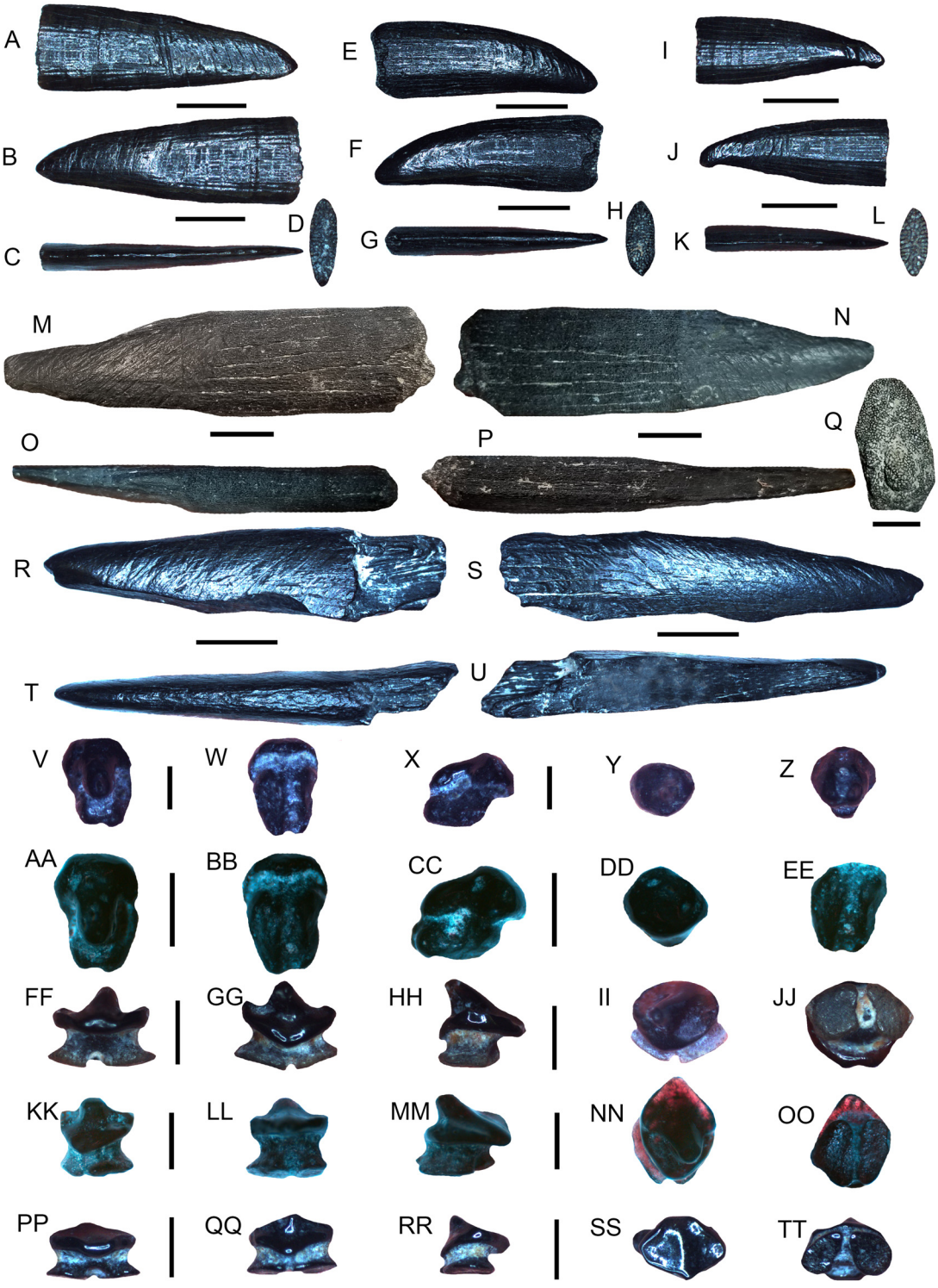

FIGURE 15. Rhinopristiform rostral spines and teeth and rajiform teeth from the Peace River and Tamiami formations on the shallow Venice, Florida continental shelf. **A–L,** *Anoxypristis* sp. rostral spines (UF-VP561076–UF-VP561078). **M–U,** *Pristis* cf. *P. pristis* rostral spines (UF-VP561823–UF-VP561824). **V–EE,** *Pristis* sp. teeth (UF-VP561825–UF-VP561826). **FF–TT,** Rajidae gen. indet. teeth (UF-VP561079–UF-VP561081). Orientations = dorsoventral: A–B, E–F, I–J, M–N, R–S; lateral: C, G, K, X, CC, HH, MM, RR; anterior: O, R; posterior: P, U; basal: D, H, L, Q, Z, EE, JJ, OO, TT; lingual: V, AA, FF, KK, PP; labial: W, BB, GG, LL, QQ; occlusal: Y, DD, II, NN, SS. Scale bars: A–L, Q–U = 5 mm; M–P = 1 cm; V–TT = 1 mm.

reports on Miocene–Pliocene chondrichthyans also document *Anoxypristis* based on isolated rostral spines; however, these remains are typically uncommon and identified as *Anoxypristis* sp. or *Pristis* sp. (e.g., Purdy et al., 2001; Sharma and Patnaik, 2013; Carrillo-Briceño et al., 2015b; Boyd, 2016; Collareta et al., 2017b, 2017c; Kent, 2018; Fialho et al., 2019; Perez, 2022; Pollerspöck and Unger, 2022).

Known as the knifetooth sawfish, extant *Anoxypristis* is represented by only one species, *A. cuspidate* (Latham, 1794), that is restricted to shallow coastal seas of the Indo-Pacific Oceans and feed primarily on small fish and invertebrates (Compagno and Last, 1999; Faria et al., 2013; Last et al., 2016a). The Venice *Anoxypristis* sp. rostral spines bear some resemblance to those of the Eocene taxa and the extant species, *A. cuspidata* (Latham, 1794), but they are narrower, have a more consistent width, and lack well-developed apical barbs (Compagno and Last, 1999; Cappetta, 2012; Cappetta and Case, 2016). It is currently uncertain if these Venice *Anoxypristis* rostral spines derive from a distinct, previously overlooked late Cenozoic fossil taxon or represent ontogenetic variation present in a previously described species. As such, we identify these rostral spines conservatively as *Anoxypristis* sp.

Pristis cf. *P. pristis* (Linnaeus, 1758)
Figure 15M–EE

Referred specimens. Two rostral spines (UF-VP561823–UF-VP561824) and two oral teeth (UF-VP561825–UF561826).

Description. Each rostral spine is dorsoventrally compressed, displays a rounded anterior tooth edge, and flattened, posterior spine edge containing a shallow groove. The largest rostral spine measures 51.46 mm long, is 13.62 mm wide near the spine base, and is 7.10 mm thick dorsoventrally. The dorsal and basal spine faces contain longitudinal furrows that extend from the spine base to the apex. The spine base has a porous texture. The oral teeth are globular and elongated in the anteroposterior direction and have a transverse ridge that separates the well-developed lingual uvula from the labial crown surface. The largest oral tooth is 1.4 mm tall and 0.92 mm wide. A single nutritive foramen occurs on either side of the lingual uvula near the crown-root junction. The labial face of the oral teeth is convex, and the crown overhangs the root base. The root extends beyond the lingual crown surface and is bisected with a nutritive groove, and a single, central nutritive foramen is also present.

Remarks. The presence of rostral spines that are large, posteriorly curved, and have a shallow groove on the posterior surface and small, globular and anteroposterior elongated oral teeth, distinguishes the largetooth sawfish, *P.* cf. *P. pristis*, described here from *Anoxypristis* sp. that also occurs in the Venice Elasmobranch Assemblage. Presently, *P. pristis* is one of four *Pristis* spp. recognized globally (i.e., *P. pristis*, *P. pectinata*, *P. zijsron*, and *P. clavata*) based on genetic and morphological studies (Faria et al., 2013; Dulvy et al., 2016; Byler, 2017). Although the rostral spines of *A. cuspidata* and *Pristiophorous* spp. may appear similar to those of *Pristis* spp., they have thinner, more hook-like rostral spines with different internal structures (Wueringer et al., 2009; Welton et al., 2015; Byler, 2017; Nevatte et al., 2017). Regarding the rostral spines of other extant pristids, those of *P. pectinata* appear most similar to those of *P. pristis* but are thinner, compressed in the anteroposterior direction, and may not exhibit a shallow groove on the posterior spine surface. Similarly, the rostral spines of *P. zijsron* and *P. clavata* are also thinner and more triangular and acutely pointed than those of *P. pristis* (Byler, 2017). The identification of *P.* cf. *P. pristis* in the Venice Elasmobranch Assemblage is also supported by the presence of oral teeth that are small, globular, and anteroposteriorly elongated and have a well-developed lingual uvula and transverse ridge on the occlusal surface. The Venice *Pristis* oral teeth, although infrequent, appear similar to those of *P. pristis* figured by Cappetta (2012) in contrast to the oral teeth of *P. pectinata* figured by Herman et al. (1997) and Reinecke et al. (2023). In particular, the globular and mesiodistally compressed form of *P. pectinata* oral teeth contrasts with that of *P. pristis* that is typically broader, more erect, and have a lingual uvula that extends almost the same length as the root base (Cappetta, 2012).

As indicated by Cappetta (2012) and Kent (2018), numerous *Pristis* taxa, including *P. aquitanicus* Delfortrie, 1871, *P. atlanticus* Zbyszewski, 1947, and *P. caheni* Dartevelle and Casier, 1959, have been identified since the Eocene from isolated and/or fragmentary rostral spines across the North Atlantic. However, the degree of ontogenetic and intraspecific variation present in rostral spines from these taxa as well as their overall similarity with extant taxa, has not been assessed (Herman et al., 1997; Purdy et al., 2001; Cappetta, 2012). Although rostral spines in the Venice Elasmo-

branch Assemblage identified as *P.* cf. *P. pristis* all exhibit a groove along the posterior edge and are larger in size than those identified as *Anoxypristis* sp., we tentatively identify the isolated remains as *P.* cf. *P. pristis* due to the lack of articulated rostra from the Miocene–Pliocene of Florida and uncertain degree of ontogenetic variation in *P. pristis* rostral spines.

The extant largetooth sawfish, *P. pristis*, is known to occur in localized populations in mid-latitudinal shelf regions globally and prey upon numerous vertebrates and invertebrates (Breder, 1952; Faria et al., 2013; Fernandez-Carvalho et al., 2014). In particular, *P. pristis* has been reported from the west coast of Mexico, Central America, and in northern and eastern South America (Faria et al., 2013; Last et al., 2016a). Although *P. pristis* has been historically reported from the Gulf of Mexico, its presence is unconfirmed (e.g., Faria et al., 2013; Seitz and Waters, 2018).

Order RAJIFORMES Berg, 1940
Family RAJIDAE Blainville, 1816
Rajidae gen. indet.
Figure 15FF–TT

Referred specimens. Three teeth consisting of two male teeth (UF-VP561079–UF-VP561080) and one female tooth (UF-VP561081).

Description. Teeth of Rajidae gen. indet. are known to exhibit marked sexual heterodonty. Males have teeth with narrow, erect cusps in contrast to the teeth of females that have relatively short, flattened crowns. The largest tooth of Rajidae gen. indet. in the Venice Elasmobranch Assemblage is a male tooth that is 1 mm in height and 0.86 mm in width. In male teeth, the elongate cusp is centrally located and angled lingually, the crown overhangs the root base, the labial face forms a rounded, convex lip, and the lingual face may bear a central concavity along the margin. The root of male teeth is lingually displaced and consists of two well-developed lobes with relatively flat basal faces. The root lobes may extend beyond the lingual crown face. In contrast, female teeth have a low, lingually directed crown that slightly overhangs the root base. The female tooth identified in this study (Figure 14PP–TT) is 0.67 mm in height and 1.68 mm in width. In occlusal view, a shallow depression is present between the central portion of the crown and the lateral crown edges. Similar to the roots of male teeth, those of females are displaced lingually and separated into two distinct lobes with flat basal faces, but the roots do not extend beyond the lingual crown face.

Remarks. Rajids are skates. The small-sized teeth with lingually displaced root lobes that have either a narrow, centralized cusp, or a short, lingually displaced crown distinguish male and female teeth of rajids from those of *Hypanus* cf. *H. say*, *Hypanus* cf. *H. americanus*, *Pristis* cf. *P. pristis* oral teeth, *Mobula* cf. *M. hypostoma*, and *M.* cf. *M. birostris* that also occur in the Venice Elasmobranch Assemblage. The male and female teeth of Rajidae gen. indet. described here differ from those of *Atlantoraja* (*Raja*) *ceciliae* (Steurbaut and Herman, 1978) and *R. gentili* (Joleaud, 1912) because teeth from these taxa have a wider, centrally located cusp and thinner crowns or completely lack cutting edges, respectively (Cappetta, 1970; Ward and Bonavia, 2001; Reinecke et al., 2011; Bor et al., 2012; Reinecke, 2015). The teeth of *Dipturus* (*Raja*) *casieri* (Steurbaut and Herman, 1978) resemble those of Rajidae gen. indet. in the Venice Elasmobranch Assemblage because they exhibit a conical, centrally located, and lingually inclined cusp, a crown that overhangs the root base in male teeth and female teeth, and diverging, lingually displaced roots with flat basal faces (Bor et al., 2012). However, the teeth of *D.* (*R.*) *casieri* also appear similar to those identified as *Raja* sp. and interpreted to be those of *D.* (*R.*) *laevis* (Mitchill, 1815) by Purdy et al. (2001). While male teeth exhibit a consistent cuspidate morphology, female teeth of *D. laevis* possess low, lingually displaced crowns or nearly flat occlusal faces that have a polygonal outline (Bigelow and Schroeder, 1948b; Purdy et al., 2001).

Although many fossil skate teeth have been assigned to "*Raja*", the family Rajidae is extremely diverse with at least 17 genera and 154 species, many of which occur in cold, deep waters on continental slopes and abyssal plains (Last et al., 2016a). In particular, Last et al. (2016a) indicated that at least four species of skates are presently known to occur in shallow (<100 m) continental shelf waters of the Gulf of Mexico including: *Dipturus olseni* (Bigelow and Schroeder, 1951), *Leucoraja lentiginosa* (Bigelow and Schroeder, 1951), *Rostroraja eglanteria* (Lacepéde, 1800), and *R. texana* (Chandler, 1921). Six additional taxa also occur in adjacent shallow waters of the Atlantic Coastal Plain of the USA and western Central America and include: *D. laevis* (Mitchill, 1815), *L. erinaca* (Mitchill, 1825), *L. garmani* (Whitely, 1939), *L. ocellata* (Mitchill, 1815), *R. equatorialis* (Jordan and Bollman, 1889), and *R. velezi* (Chirichigno, 1973). Interestingly, no extant taxa belonging to *Raja* are known to occur in the Gulf of Mexico or

along the Atlantic Coastal Plain of the USA. The teeth of Rajidae gen. indet. described in this report bear some resemblance to those of *Dipturus* and *Leucoraja*. However, the infrequent occurrence of these teeth in the Venice Elasmobranch Assemblage, uncertain degree of ontogenetic and sexual variation, and lack of ample modern comparative specimens makes their specific taxonomic identification extremely difficult. As a result, we conservatively assign these teeth to Rajidae gen. indet. until a larger sample size of fossil and modern specimens can be studied.

Order MYLIOBATIFORMES Compagno, 1973
Family DASYATIDAE Jordan and Gilbert, 1879
Genus *HYPANUS* Rafinesque, 1818
Hypanus cf. *H. say* (Lesueur, 1817)
Figure 16A–NN

Referred specimens. Ten teeth consisting of five low-crowned, female type teeth (UF-VP561827–UF-VP561831), three cuspidate male type teeth (UF-VP561834–UF-VP561836), and two additional teeth (UF-VP561832–UF-VP561833).

Description. "Dasyatid-like" teeth, including those of *Hypanus*, are known to be highly variable and exhibit sexual dimorphism. In general, the tooth crowns of females are globular in shape and the tooth crowns of males are triangular, elongated, and hook-like. Using these general characteristics, we identify teeth from both female and male *Hypanus* cf. *H. say* in the Venice Elasmobranch Assemblage. The largest, low-crowned, female type tooth measures 3.17 mm in length and 2.92 mm in height. Female teeth have a slightly convex, globular and quadrangular shape, occlusal surfaces that contain an abundance of small surface pits and a U-shaped lingual visor that is subdivided into two marginal faces by a dorsoventral ridge. The bilobate roots of female teeth may extend slightly beyond the lingual visor and have round, peg-like basal surfaces that are gently inclined in the posterior direction. In contrast, the largest, cuspidate male type tooth figured measures 2.09 mm in length and 1.89 mm in height. Male teeth have elongated, triangular to slightly conical, hook-like crowns that are smooth on the lingual surface, irregularly pitted and furrowed on the labial surface, and are lingually inclined. The roots of male teeth begin on the lingual half of the crown base, are short and peglike, angled in the posterior direction, and protrude slightly beyond the lingual surface.

Remarks. "Dasyatid-like" teeth are frequently recovered in the Venice Elasmobranch Assemblage; however, they have highly variable morphologies and exhibit differing degrees of dignathic, ontogenetic, and sexual heterodonty, as well as seasonal variations (Kajiura and Tricas, 1996; Kajiura et al., 2000; Herman et al., 1998, 1999, 2000; Rangel et al., 2014; Cappetta, 2012; Underwood et al. 2015; Reinecke et al., 2023). Recently, Last et al. (2016a, 2016b) conducted phylogenetic studies supported by morphological data that indicated the family Dasyatidae consists of four major subfamilies (Dasyatinae, Neotrygoninae, Urogymninae, and Hypolophinae) and 89 recognized species. In particular, the subfamily Dasyatinae consists of eight genera, including *Dasyatis* and *Hypanus*. *Hypanus* is a resurrected stingray genus that was previously considered to be a junior synonym of *Dasyatis* and now consists of eight species, most of which occur in the western Atlantic and eastern Pacific (Last et al., 2016a, 2016b). Currently *Dasyatis* has been reduced to a group of five species that occur in the eastern Atlantic, Mediterranean, and southwest Indian Ocean (Last et al., 2016a, 2016b). Despite an updated analysis of extant stingray taxonomy, very few reports have documented the dental morphology of these taxa making the identification of isolated fossil teeth extremely difficult (Bigelow and Schroeder, 1953; Herman et al., 1998; Cappetta, 2012; Reinecke et al., 2023). To date, over 70 species have been identified as belonging to *Dasyatis* from isolated fossil teeth with a "dasyatid-design" (Cappetta, 2012). Many of these fossil taxa likely belong to other genera besides *Dasyatis*, represent sexual heterodonty or other tooth variations in specific species, and some might be synonymized with extant species (Ward, 1979; Kajiura and Tricas, 1996; Kajiura et al., 2000; Cappetta, 2012; Rangel et al., 2014; Reinecke et al., 2023).

Teeth identified as *Hypanus* cf. *H. say* in the Venice Elasmobranch Assemblage can be differentiated from those of other taxa including *Hypanus* cf. *H. americanus, Mustelus* sp., *Rhynchobatus* sp., *Rhinobatos* sp., as well as other "dasyatids" by their small size, a slightly convex, furrowed occlusal surface, short lingual visor that may be separated into two marginal faces, and lingually displaced and peg-like roots that represent female and immature male teeth. Mature male teeth of this taxon have enlarged, triangular to slightly conical cusps that may bear a dendritic–furrowed labial surface. However, teeth belonging to the extant taxa *H. americanus* (Hildebrand and Schroeder, 1928) and *H. sabinus* (Lesueur, 1824) are very similar to those of *H.* cf. *H. say*. Teeth of *H.*

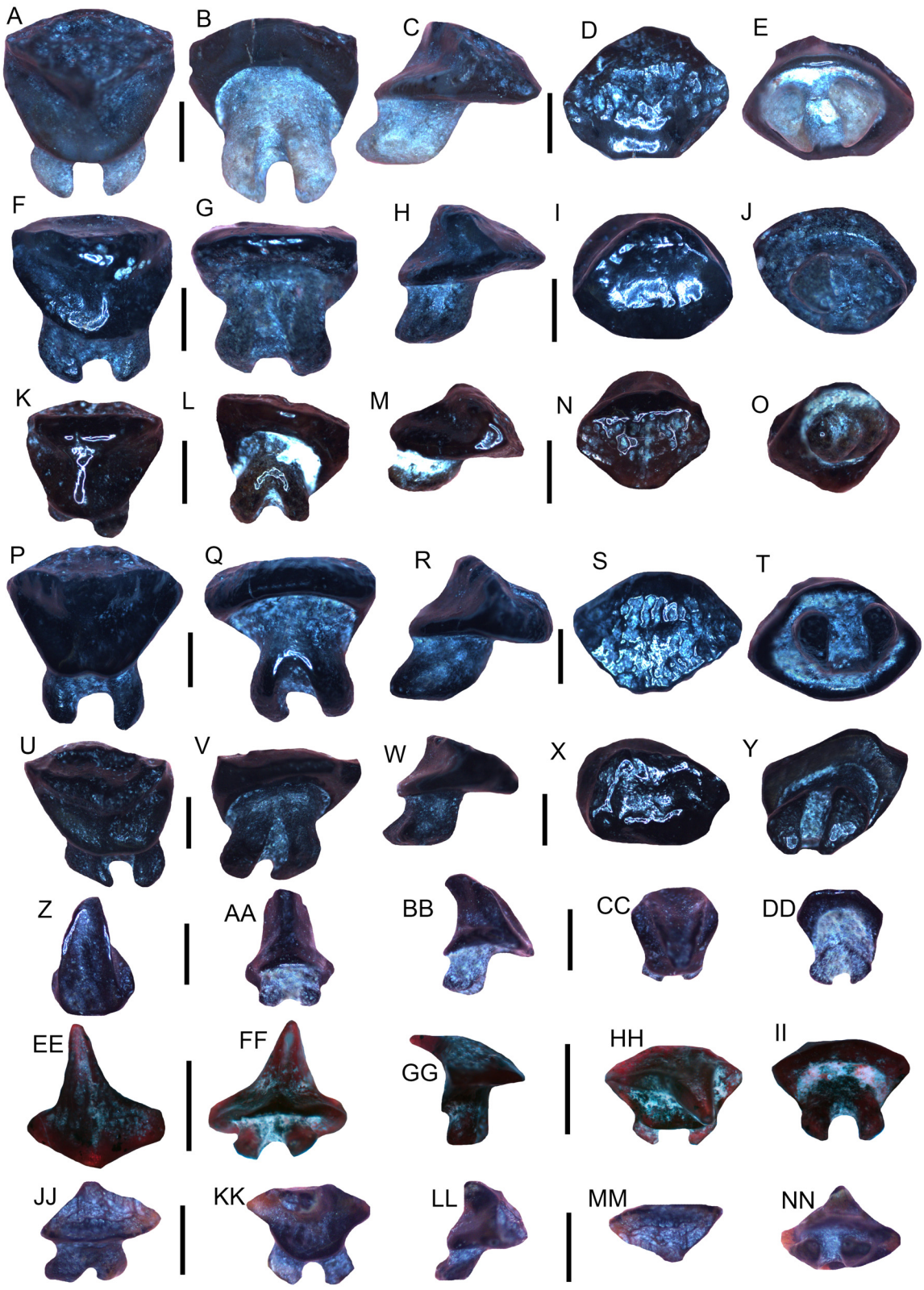

FIGURE 16. Myliobatiform teeth from the Peace River and Tamiami formations on the shallow Venice, Florida continental shelf. **A–NN,** *Hypanus* cf. *H. say* teeth (UF-VP561827–UF-VP561831; UF-VP561834–UF-VP561836). Orientations = lingual: A, F, K, P, U, Z, EE, JJ; labial: B, G, L, Q, V, AA, FF, KK; lateral: C, H, M, R, W, BB, GG, LL; occlusal: D, I, N, S, X, CC, HH, MM; basal: E, J, O, T, Y, D, II, NN. All scale bars = 1 mm.

americanus typically have low crowns that are slightly pitted or furrowed and as long as they are wide in females and immature males, whereas those of mature males typically exhibit a broader, triangular cusp that may contain an irregular and central furrow on the labial face that is either smooth or exhibits a dendritic furrowed pattern (Bigelow and Schroeder, 1953; Berkovitz and Shellis, 2017; Reinecke et al., 2023). In contrast, teeth of *H. sabinus* may be more polygonal–globular in females and immature males, whereas teeth of mature males typically exhibit a basally widened, apically narrow, elongated, and greatly lingually inclined cusp that may contain furrows on the labial face (Bigelow and Schroeder, 1953; Kajiura and Tricas, 1996). *Pteroplatytrygon violacea* (Bonaparte, 1832) teeth are distinct from those of *H.* cf. *H. say*, because they are mesiodistally elongated and dorsoventrally compressed, have triangular to spade-like crowns that are not pitted on the cusp apex in male teeth, and also frequently have an enlarged, ellipse-shaped nutritive foramen between the root lobes (Herman et al., 1998; 2000). Other morphologically similar taxa presently occurring within or in proximity to the Gulf of Mexico include *H. guttatus* (Bloch and Schneider, 1801), *H. dipterurus* (Jordan and Gilbert, 1880), and *H. longus* (Garman, 1880). These taxa also have teeth similar to *H.* cf. *H. say*. However, extant jaw and tooth samples from both females and males or high-resolution published tooth images from these taxa are currently not available.

Previously identified fossil teeth similar to those of *H.* cf. *H. say* include *Bathytoshia probsti* (Cappetta, 1970), *Dasyatis rugosa* (Probst, 1877), *D. strangulata* (Probst, 1877), and *D. dianapizarroae* Laurito Mora, 1999. However, teeth from *B. probsti* and *D. rugosa* are most frequently reported from Oligocene–Miocene localities and have occlusal surfaces that are noticeably more furrowed and pitted than those of *H.* cf. *H. say* in the Venice Elasmobranch Assemblage (Cappetta, 1970; Bor et al., 2012; Reinecke, 2015; Reinecke and Radwański, 2015; Kent, 2018; Reinecke et al., 2023). In contrast, teeth identified as *D. dianapizarroae* Laurito Mora, 1999 from the Miocene–Pliocene of Costa Rica appear somewhat similar to those of *H*. cf. *H. say*; however, it is not clear how distinct *D. dianapizarroae* teeth are from the numerous extant taxa found in the Gulf of Mexico and western Atlantic leaving this taxon's validity in question. Purdy et al. (2001) documented both *D. say* and *D.* cf. *D. americana* from the Miocene–Pliocene of North Carolina. However, several different types of tooth morphologies are represented in their study and only male teeth of *D*. cf. *D. americana* were identified. Dasyatid teeth are extremely common in Neogene marine deposits throughout Florida and, in fact, are the most common elasmobranch species present in the late Miocene Montbrook Fossil Site (Perez, 2022).

The extant bluntnose stingray, *Hypanus say* (Lesueur, 1817), southern stingray, *Hypanus americanus* (Hildebrand and Schroeder, 1928) and Atlantic stingray, *Hypanus sabinus* (Lesueur, 1817) occur in shallow continental shelf waters of the western Atlantic and Gulf of Mexico (Bigelow and Schroeder, 1953; Kajiura and Tricas, 1996; Last et al., 2016a). These taxa have similar tooth morphologies, prey, and habitat preferences, and as a result, we tentatively identify *Hypanus* cf. *H. say* in the Venice Elasmobranch Assemblage (e.g., Bigelow and Schroeder, 1953; Kajiura and Tricas, 1996; Last et al., 2016a). This interpretation is in agreement with extant teeth of *Hypanus say*, where the teeth in Figure 16 of this study correspond well with those figured in Reinecke et al. (2023; Plates 64 C1–C5; 65 C1–C5; 66 B1–B5; 66 C1–C5; 66 D1–D5; 67 B1–B5 and C1–C5).

Hypanus cf. *H. americanus*
(Hildebrand and Schroeder, 1928)
Figure 17A–NN

Referred specimens. Ten teeth consisting of four low-crowned, female-type teeth (UF-VP561837–UF-VP561840), four cuspidate male-type teeth (UF-VP561843–UF-VP561846), and two additional teeth (UF-VP561841–UF-VP561842).

Description. Similar to the description of *Hypanus* cf. *H. say* above, the male and female teeth of *H. americanus* are also known to be highly variable and exhibit sexual dimorphism. In general, the tooth crowns of females are globular in shape, and the tooth crowns of males are triangular, elongated, and hook-like. In the Venice Elasmobranch Assemblage, two additional tooth morphotypes distinct from those of *H.* cf. *H. say* are represented, and they are interpreted to correspond to female and male teeth of *H.* cf. *H. americanus*. The largest figured female tooth measures 2.62 mm in length and 3.08 mm in height. Female teeth have a convex, globular and quadrangular shape, occlusal surfaces that contain an abundance of small surface pits and a U-shaped lingual visor that is subdivided into two marginal faces by a dorsoventral ridge. The bilobate roots of female teeth may extend slightly beyond the lingual visor and have round, peg-like basal surfaces that are gently inclined in the posterior direction. In contrast, the

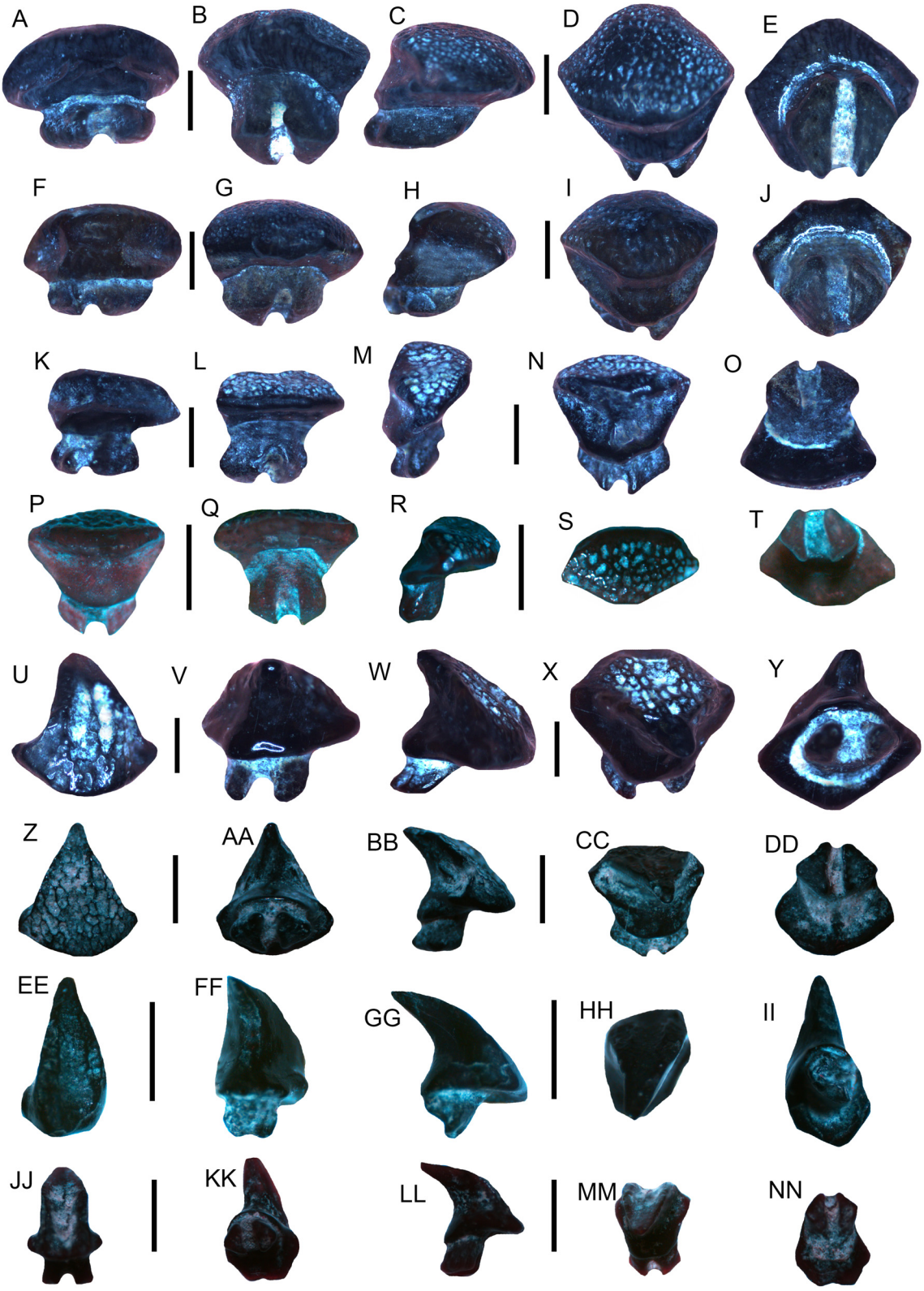

FIGURE 17. Myliobatiform teeth from the Peace River and Tamiami formations on the shallow Venice, Florida continental shelf. **A–NN,** *Hypanus* cf. *H. americanus* teeth (UF-VP561837–UF-VP561840; UF-VP561843–UF-VP561846). Orientations = lingual: A, F, K, P, U, Z, EE, JJ; labial: B, G, L, Q, V, AA, FF, KK; lateral: C, H, M, R, W, BB, GG, LL; occlusal: D, I, N, S, X, CC, HH, MM; basal: E, J, O, T, Y, D, II, NN. All scale bars = 1 mm.

largest male tooth measures 1.94 mm in length and 1.89 mm in width. Male teeth have elongated, triangular to slightly conical, hook-like crowns that are smooth on the lingual face, irregularly pitted and furrowed on the labial face, and are lingually inclined. The roots of male teeth begin on the lingual half of the crown base, are short and peg-like, angled in the posterior direction, and protrude slightly beyond the lingual surface.

Remarks. Teeth identified as *H.* cf. *H. americanus* in the Venice Elasmobranch Assemblage can be differentiated from those of other taxa including *H.* cf. *H. say*, *Mustelus* sp., *Rhynchobatus* sp., *Rhinobatos* sp., as well as other "dasyatids" by their small size, a convex, pitted occlusal surface, short lingual visor that is frequently separated into two marginal faces, and lingually displaced and peg-like roots that represent female and immature male teeth. Mature male teeth of this taxon have enlarged, triangular to slightly conical cusps that may bear a pitted labial surface or appear smooth. However, teeth belonging to the extant taxa, *H. say* (Lesueur, 1817) and *H. sabinus* (Lesueur, 1824), are very similar to those of *H.* cf. *H. americanus*. As seen in Figure 16 of this study and Plates 64–67 of Reinecke et al. (2023), teeth of *H.* cf. *H. say* typically have low crowns that are furrowed or only slightly pitted and typically as long as they are wide in females and immature males, whereas those of mature males typically exhibit a broader, triangular cusp that may contain an irregular, centralized furrow on the labial surface or a dendritic appearance (Bigelow and Schroeder, 1953; Berkovitz and Shellis, 2017; Reinecke et al., 2023). In contrast, *H. sabinus* teeth may be more polygonal–globular in female and immature males, whereas teeth of mature males typically exhibit a basally widened, apically narrow, elongated, and greatly lingually inclined cusp that may contain furrows on the labial surface (Bigelow and Schroeder, 1953; Kajiura and Tricas, 1996). *Pteroplatytrygon violacea* (Bonaparte, 1832) teeth are distinct from those of *H.* cf. *H. americanus*, because they are mesiodistally elongated and dorsoventrally compressed, have triangular to spade-like crowns that are not pitted on the cusp apex in male teeth, and also frequently have an enlarged, ellipse-shaped nutritive foramen between the root lobes (Herman et al., 1998; 2000; Reinecke et al., 2023). *Bathotoshia centroura* (Mitchill, 1815) teeth are also distinct from those of *H*. cf. *H. americanus* due to the presence of irregular furrows and pits on the occlusal and upper lingual surfaces and a more elongated lingual visor (Reinecke et al., 2023). It is also important to note that, although many taxonomic descriptions of *Dasyatis* and *Hypanus* teeth utilize occlusal surface ornamentation as a distinguishing feature, this characteristic alone should not be relied upon to distinguish among taxa. In particular, occlusal surface ornamentation is frequently abraded from feeding activity and further reduced or even removed from taphonomic reworking and abrasion of fossil specimens (Reinecke et al., 2011; Bor et al., 2012; Cappetta, 2012).

Fossil taxa that have been identified based on teeth similar to those of *H.* cf. *H. americanus* include *Bathytoshia probsti* (Cappetta, 1970), *Dasyatis rugosa* (Probst, 1877), *D. delfortrieri* Cappetta 1970, and *D. dianapizarroae*. Of these taxa, teeth from *B. probsti* and *D. rugosa* typically have occlusal surfaces that are much more heavily furrowed and biostratigraphic ranges typically restricted to the Oligocene–Early Miocene of Europe (Cappetta, 1970; Bor et al., 2012; Reinecke, 2015; Reinecke and Radwański, 2015; Kent, 2018; Reinecke et al., 2023). Teeth of *D. delfortrieri* are similar to those of *D. rugosa* but have more regularly spaced ridges and pits on the occlusal surface, a completely wrinkled lingual surface, and *D. delfortrieri* was likely extinct by the Middle Miocene (Reinecke et al., 2005, 2008, 2011; Kent, 2018). *Dasyatis dianapizarroae* Laurito Mora, 1999, from the Miocene–Pliocene of Costa Rica appear somewhat similar to those of *H*. cf. *H. americanus* identified in this study due to the pitted or weakly furrowed, flat to slightly globular occlusal surfaces. However, it is not clear how distinct the teeth of *D. dianapizarroae* are from those of the numerous extant taxa found in the Gulf of Mexico and western Atlantic including *H. americanus* that is known to occur off the present-day coast of Costa Rica (Last et al., 2016a). Purdy et al. (2001) identified a single male tooth of *H.* cf. *H. americanus* that is scoop-like and lingually inclined and exhibits a well-developed, centralized furrow on the labial surface that compares favorably with those in the Venice Elasmobranch Assemblage, and also contrasts with male teeth of *H. say* that are more triangular in shape and have irregularly pitted or furrowed occlusal surfaces.

Currently, a variety of extant stingrays with similar tooth morphologies and prey preferences occur in the Gulf of Mexico (see *H. say* remarks section). However, those that frequent shallow continental shelf waters include the southern stingray *H. americanus* (Hildebrand and Schroeder, 1928), Atlantic stingray *H. sabinus* (Lesueur, 1817), and bluntnose stingray *H. say* (Lesueur, 1817) (Bigelow

and Schroeder, 1953; Kajiura and Tricas, 1996; Last et al., 2016a). As a result of the variety in stingray dentitions and overlapping ranges of modern taxa, we conservatively identify our materials to *H.* cf. *H. americanus* in the Venice Elasmobranch Assemblage (e.g., Bigelow and Schroeder, 1953; Kajiura and Tricas, 1996; Last et al., 2016a).

Family RHINOPTERIDAE Jordan and Evermann, 1896

Genus *RHINOPTERA* Cuvier, 1829

Rhinoptera cf. *R. bonasus* (Mitchill, 1815)

Figure 18A–Q

Referred specimens. Eight specimens consisting of median and lateral teeth and an isolated pavement plate (figured teeth: UF-VP561082–UF-VP561083; UF-VP561088; UF-VP561087, and additional teeth: UF-VP561084–UF-VP561086; UF-VP561089).

Description. The largest specimen is represented by a median tooth that measures 26.88 mm wide, 6.41 mm thick, and 5.53 mm tall. The crowns of median and lateral teeth have nearly flat and smooth hexagonal occlusal surfaces, are mesodistally elongated, and have crowns that are noticeably thicker than the roots. The base of the tooth crown overhangs the root on all but the lingual side, and the crown edges are heavily wrinkled forming dorsoventral furrows. The root is polyaulacorhizous and contains equidimensional nutritive grooves.

Remarks. The presence of mesiodistally elongated, nearly flat crowns with hexagonal occlusal surfaces and crowns that are noticeably thicker than the roots distinguish the cownose ray, *R.* cf. *R. bonasus*, teeth described here from those of *Myliobatis* sp. and *Aetomylaeus* sp., which also occur in the Venice Elasmobranch Assemblage. Median and lateral teeth of *Rhinoptera* sp. are also frequently similar in size, and they have angular edges with irregular, vertical ridges that correspond with the articular surfaces of adjoining teeth (e.g., Nishida, 1990; Herman et al., 2000; Hulbert, 2001; Purdy et al., 2001; Cappetta, 2012; Hovestadt and Hovestadt-Euler, 2013). The number of median and lateral teeth in extant *Rhinoptera* is known to be highly variable, and as a result, specific identifications of fossil material based on isolated teeth or tooth plates are difficult (Kent, 2018). Although the *Rhinoptera* teeth in the Venice Elasmobranch Assemblage resemble those of *R. bonasus*, several other *Rhinoptera* species are known to occur in the western Atlantic and eastern Pacific including *R. brasiliensis* Müller, 1836 and *R. steindachneri* Evermann and Jenkins, 1891, respectively; however, because distinctions among taxa are subtle (Last et al., 2016a), we conservatively identify the teeth described here as *R.* cf. *R. bonasus*. In the Gulf of Mexico and along the Atlantic Coastal Plain of the USA, extant *R. bonasus* is known to seasonally migrate in large schools and feeds upon a wide variety of invertebrates and small vertebrates (Schwartz, 1990; Neer et al., 2005; Collins et al., 2007; Last et al., 2016a; Ogburn et al., 2018; Bangley et al., 2021).

Family MOBULIDAE Bonaparte, 1838

Genus *MOBULA* Rafinesque, 1810

Mobula cf. *M. hypostoma* (Bancroft, 1831)

Figure 18R–FF

Referred specimens. Three teeth (UF-VP561090–UF-VP561092).

Description. Teeth are small and delicate having a lingually inclined, cuspidate to comb-like crown. The largest tooth is 1.73 mm wide and 1.51 mm in height. The crown may have a single cusp or be divided into multiple cusps of slightly different heights. The labial face may contain irregular folds or furrows, and the lingual face is typically smooth. The crown is wider and taller than the root base. The root base may contain two peg-like lobes or be subdivided into two or more lobes separated by nutritive grooves.

Remarks. *Mobula hypostoma* is the lesser devil ray, and the extant form is known from the southeastern USA, Gulf of Mexico, Caribbean, and eastern coast of South America in continental shelf waters (Stevens et al., 2018). It is a small (~125 cm wide) planktivorous mobulid species and occasionally travels in small groups or even larger schools (Last et al., 2016a; Stevens et al., 2018; White et al., 2018). *Mobula* teeth are highly variable within individual species, exhibiting various degrees of ontogenetic, sexual, monognathic, and dignathic heterodonty, but the Venice teeth are most similar to those of *M. hypostoma* and thus are identified as *M.* cf. *M. hypostoma* (e.g., Notarbartolo-di-Sciara, 1987; Adnet et al., 2012; Cappetta, 2012). The small, delicate, lingually inclined teeth with bi- or multi-lobate roots distinguish teeth of *Mobula* cf. *M. hypostoma* described here from those of other batoids in the Venice Elasmobranch Assemblage including *M.* cf. *M. birostris*, *Rhynchobatus, Rhinobatos, Hypanus,* and *Rajidae* gen. indet. Prior studies have indicated that *Mobula* diverged from *Rhinoptera* in the Oligocene, and additional short pulses of speciation occurred in the Middle Miocene and Pliocene–Pleistocene (e.g., Adnet et al., 2012; Poortvliet et al., 2015; White et al., 2018).

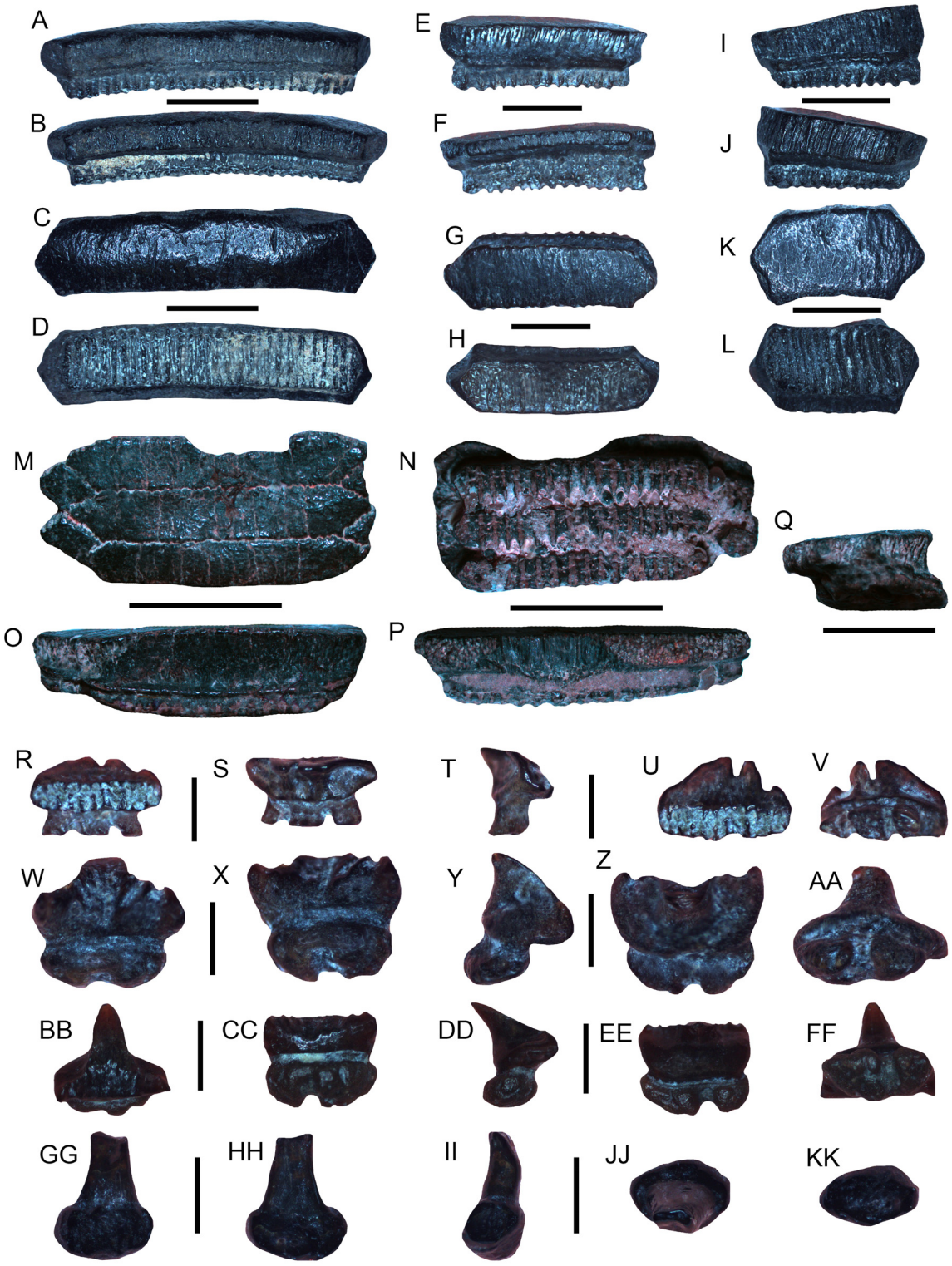

FIGURE 18. Myliobatiform teeth from the Peace River and Tamiami formations on the shallow Venice, Florida continental shelf. *Rhinoptera* cf. *R. bonasus* median teeth (**A–H,** UF-VP561082–UF-VP561083); lateral teeth (**I–L,** UF-VP561088–UF-VP561089); partial pavement plate (**M–Q**, UF-VP561087). **R–FF,** *Mobula* cf. *M. hypostoma* (UF-VP561090–UF-VP561092). **GG–KK,** *Mobula* cf. *M. birostris* (UF-VP561093). Orientations = lingual: A, E, I, O, R, W, BB, GG; labial: B, F, J, P, S, X, CC, HH; occlusal: C, G, K, M, U, Z, EE, JJ; basal: D, H, L, N, V, AA, FF, KK; lateral: Q, T, Y, DD, II. Scale bars: A–L = 5 mm; M–Q = 1 cm; R–KK = 1 mm.

Cappetta (1970) recognized three Miocene *Mobula* species from France (*M. loupianensis*, *M. pectinata*, and *M. fragilis*). They are all identified as valid taxa by Adnet et al. (2012) and are also reported in the Miocene of Maryland (Kent, 2018). The teeth of *M*. cf. *M. hypostoma* described here can be distinguished from those of *M. loupianensis* because they have more ornamented or irregular crenulations on the labial face (Herman et al., 2000; Adnet et al., 2012; Cappetta, 2012; Reinecke and Radwański, 2015). The teeth of *M. pectinata* are similar to those of *M. loupianensis* although they have slightly folded labial faces and the distal and mesial most portions of the cusp are extended in the direction of the main cusp (Cicimurri and Knight, 2009; Adnet et al., 2012). The teeth of *M. fragilis* are readily distinguished from other mobulid taxa because they have a lingually inclined, comb-like cusp (Adnet et al., 2012; Szabó et al., 2022).

Mobula lorenzolizanoi was identified from the Late Miocene–Early Pliocene of Costa Rica by Laurito Mora (1999), but the validity of this taxon from this locality has been questioned due to overall similarities in labial face folding and transverse crest ornamentation with *M. thurstoni* (Lloyd, 1908) (White et al., 2018). Laurito Mora (1999) also identified *M.* cf. *M. hypostoma* from this same Costa Rican assemblage which was the oldest known example of this extant taxon. The occurrence of *M*. cf. *M hypostoma* in the Venice Elasmobranch Assemblage further supports a Miocene–Pliocene existence of *M. hypostoma*.

Mobula cf. *M. birostris* (Walbaum, 1792)
Figure 18GG–KK

Referred specimens. Two teeth (figured tooth: UF-VP561093 and additional tooth: UF-VP561094).

Description. Teeth are small and erect. The largest tooth is 2.16 mm tall and 1.80 mm wide. The labial and lingual faces are convex, and the occlusal surface is flat, displaced lingually, and overhangs the lingual tooth surface. The upper surface and edges of the occlusal surface may be irregular or crenulated. The tooth roots are bulbous and stalk-like. The root base is wider than the upper portion.

Remarks. *Mobula birostris* is the oceanic manta ray, which is the largest extant ray species (i.e., up to ~700 cm wide) and currently occurs along most mid-latitudinal continental shelves and oceanic islands as well as the Gulf of Mexico (Stevens et al., 2018). This planktivorous taxon is typically pelagic where it travels in small groups or even larger schools although occasionally frequents shallow shelf waters (Last et al., 2016a; Stevens et al., 2018; White et al., 2018). As with other mobulids, teeth of *M. birostris* are known to exhibit various degrees of ontogenetic, sexual, monognathic, and dignathic heterodonty (e.g., Adnet et al., 2012); thus, we conservatively identify the teeth described here as *M.* cf. *M. birostris*.

The small-sized, stalk-like teeth with bulbous roots distinguish teeth of *Mobula* cf. *M. birostris* described here from those of other batoids in the Venice Elasmobranch Assemblage including *M.* cf. *M. hypostoma, Rhynchobatus, Rhinobatos, Hypanus* spp., and Rajidae gen. indet. Although previously classified as *M. birostris*, genetic and morphological analyses by White et al. (2018) synonymized *Manta* with *Mobula*. Teeth of *M. mobula* may appear similar to those of *M*. cf. *M*. *birostris*; however, they can be distinguished because the occlusal surface is less ornamented, and they have well-developed nutritive grooves on the basal root face (Herman et al., 2000; Adnet et al., 2012).

Family MYLIOBATIDAE Bonaparte, 1838
Genus *AETOMYLAEUS* Garman, 1908
Aetomylaeus sp.
Figure 19A–GG

Referred specimens. Three fragmentary pavement plates (UF-VP561095–UF-VP561097) and six isolated teeth consisting of four median teeth (UF-VP561098–UF-VP561101) and two lateral teeth (UF-VP561102–UF-VP561103).

Description. The largest tooth plate, although fragmentary, measures 47.59 mm long, 28.81 mm in maximum width, and 13.38 mm in maximum occlusobasal thickness and consists of only median teeth. The largest isolated tooth is a fragmentary median tooth that measures 12.65 mm in height, 46.59 mm in width, and 9.92 mm thick, and the largest isolated lateral tooth measures 19.40 mm in width, 6.53 mm in height, and 8.89 mm thick. Partial pavement plates preserve primarily median teeth and some lateral teeth. Median and lateral teeth are well-interlocked, median teeth are taller and thicker, and lateral teeth are compressed and the occlusal surface is nearly as large as the root base. The basal surface of pavement plates exposes tooth roots that are lingually displaced in relation to the occlusal surface. The crowns of the median teeth are mesiodistally elongated, smooth, arcuate, convex, and the lateralmost edge is flat and tapered to a point. The crowns of lateral teeth are mesiodistally compressed and labiolingually extended and the occlusal surfaces are irregular diamond- to rhombus-shaped. The crowns of

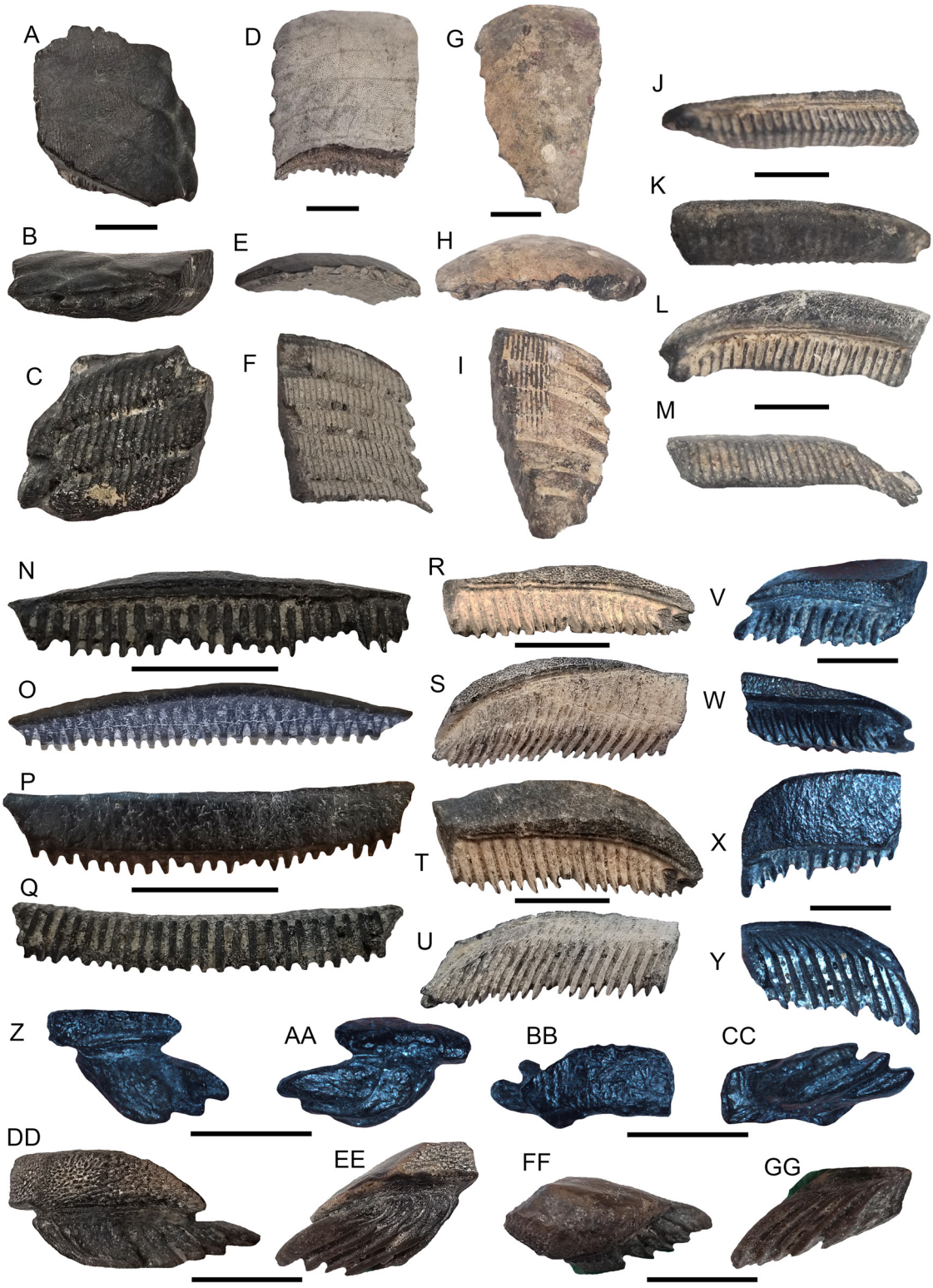

FIGURE 19. Myliobatiform teeth from the Peace River and Tamiami formations on the shallow Venice, Florida continental shelf. *Aetomylaeus* sp. pavement plates (**A–I**, UF-VP561095–UF-VP561097); median teeth (**J–Y,** UF-VP561098–UF-VP561101); lateral teeth (**Z–GG,** UF-VP561102–UF-VP561103). Orientations = occlusal: A, D, G, L, P, T, X, BB, FF; lateral: B, E, H; basal: C, F, I, M, Q, U, Y, CC, GG; lingual: J, N, R, V, Z, DD; labial: K, O, S, W, AA, EE. All scale bars = 1 cm.

median and lateral teeth are thick relative to the tooth roots and overhang the root on all but the lingual face. In cross-section, the crowns have a rhombus-like shape. Median and lateral tooth roots are robust, medially thickened, polyaulacorhizous and contain numerous, nutritive grooves that are easily visible on the basal and lingual root faces and extend beyond the lingual tooth face.

Remarks. *Aetomylaeus* is an eagle ray genus, consisting of seven extant species recognized globally that typically occur in shallow marine environments where they feed upon a variety of invertebrates and small vertebrates (White, 2014; Last et al., 2016a). In the Gulf of Mexico, the roughskin eagle ray, *A. asperrimus* (Gilbert in Jordan and Evermann, 1898), has been reported, but its abundance and distribution are not well known (Last et al., 2016a). The specimens of *Aetomylaeus* sp. described here are represented by medially thickened, mesiodistally elongated median teeth with convex occlusal surfaces, rhombus-like cross sections, and roots that extend beyond the lingual tooth surface. These characteristics distinguish the teeth from those of other similar batoids in the Venice Elasmobranch Assemblage including *Aetobatus* sp., *Rhinoptera* cf. *R. bonasus*, and *Myliobatis* sp. Teeth of *Aetobatus* sp. appear most similar to those of *Aetomylaeus* sp., but they lack lateral teeth, possess lower pavement teeth that are chevron-shaped, and have exceptionally elongated roots and relatively smooth and uniform labial and lingual faces (Herman et al., 2000; Cappetta, 2012; Hovestadt and Hovestadt-Euler, 2013; Villafaña et al., 2019). The teeth of *Pteromylaeus* sp. were previously identified as being similar to those of *Myliobatis* sp. with the exception of having arched median teeth (Purdy et al., 2001; Cappetta, 2012; Kent, 2018). However, this distinction made *Pteromylaeus* teeth nearly identical to taxa previously identified as *Aetomylaeus*. Subsequent molecular and morphological studies have found *Pteromylaeus* to be deeply nested within *Aetomylaeus*, and thus *Pteromylaeus* has been synonymized with *Aetomylaeus* (Aschliman, 2011; Naylor et al., 2012; White, 2014; Last et al., 2016a). Hence, fossil teeth of *Aetomylaeus* are likely more widespread than previously reported (Villafaña et al., 2019).

Fossil taxa with teeth similar to those of *Aetomylaeus* include *Pseudoaetobatus casieri* Cappetta, 1986, *P. belli* Cicimurri and Ebersole, 2015, and *P. undulatus* Cicimurri and Ebersole, 2015. These taxa have all been reported from the Eocene for median teeth that are gently arched, centrally thickened, laterally flattened for articulation with lateral teeth, and having roots that are slightly displaced lingually (Cappetta, 2012; Hovestadt and Hovestadt-Euler, 2013; Cicimurri and Ebersole, 2015). The lateral teeth of *Pseudeoaetobatus* may be equidimensional with square–rhombus shapes or have rounded distal margins, and lateral teeth of *P. undulatus* have undulatory occlusal surfaces (Cicimurri and Ebersole, 2015). Teeth belonging to *Aetobatus cappettai* Antunes and Balbino, 2006 and *A. arcuatus* (Agassiz, 1843) may also appear similar to those of *Aetomylaeus* sp. in the Venice Elasmobranch Assemblage. Although *A. cappettai* is presently considered a valid taxon identified in Late Neogene deposits based on median teeth with thin and flat occlusal surfaces, thickening in the central portion of the tooth, tall roots that are not extensively lingually displaced, and well-defined nutritive grooves, these teeth may in fact represent those of juvenile *Aetobatus narinari* (e.g., Reinecke et al., 2011; Cappetta, 2012; Hovestadt and Hovestade-Euler, 2013; Fiahlo et al., 2019; Collareta et al., 2021). Similarly, *A. arcuatus* has curved–chevron-shaped median teeth with noticeably thickened central portions, nearly vertical lateral tooth margins that do not taper to a point, and the absence of lateral teeth (Reinecke et al., 2011; Bor et al., 2012; Cappetta, 2012).

As with many fossil batoids, various species have been identified for fragmentary specimens, isolated teeth, or upper and lower jaw teeth belonging to the same taxon (Cappetta, 2012; Hovestadt and Hovestadt-Euler, 2013; Kent, 2018). The highly variable dental morphology of pavement teeth belonging to extant batoid genera, including *Aetomylaeus*, makes the identification of isolated fossil median and lateral pavement teeth extremely difficult (Nishida, 1990; Herman et al. 2000; Antunes and Balbino, 2006; Cappetta, 2012; Hovestadt and Hovestadt-Euler, 2013; Cicimurri and Ebersole, 2015; Collareta et al., 2021). In Venice, we have yet to recover intact, well-preserved pavement plates or large isolated median teeth of *Aetomylaeus*. As such, we refrain from species-level taxonomic identification of isolated *Aetomylaeus* sp. teeth in the Venice Elasmobranch Assemblage until further studies are conducted on fossil and extant specimens.

Genus *MYLIOBATIS* Cuvier, 1816

Myliobatis sp.

Figure 20A–BB

Referred specimens. Nine specimens consisting of one fragmentary pavement plate (UF-VP561104) and eight isolated teeth consisting of

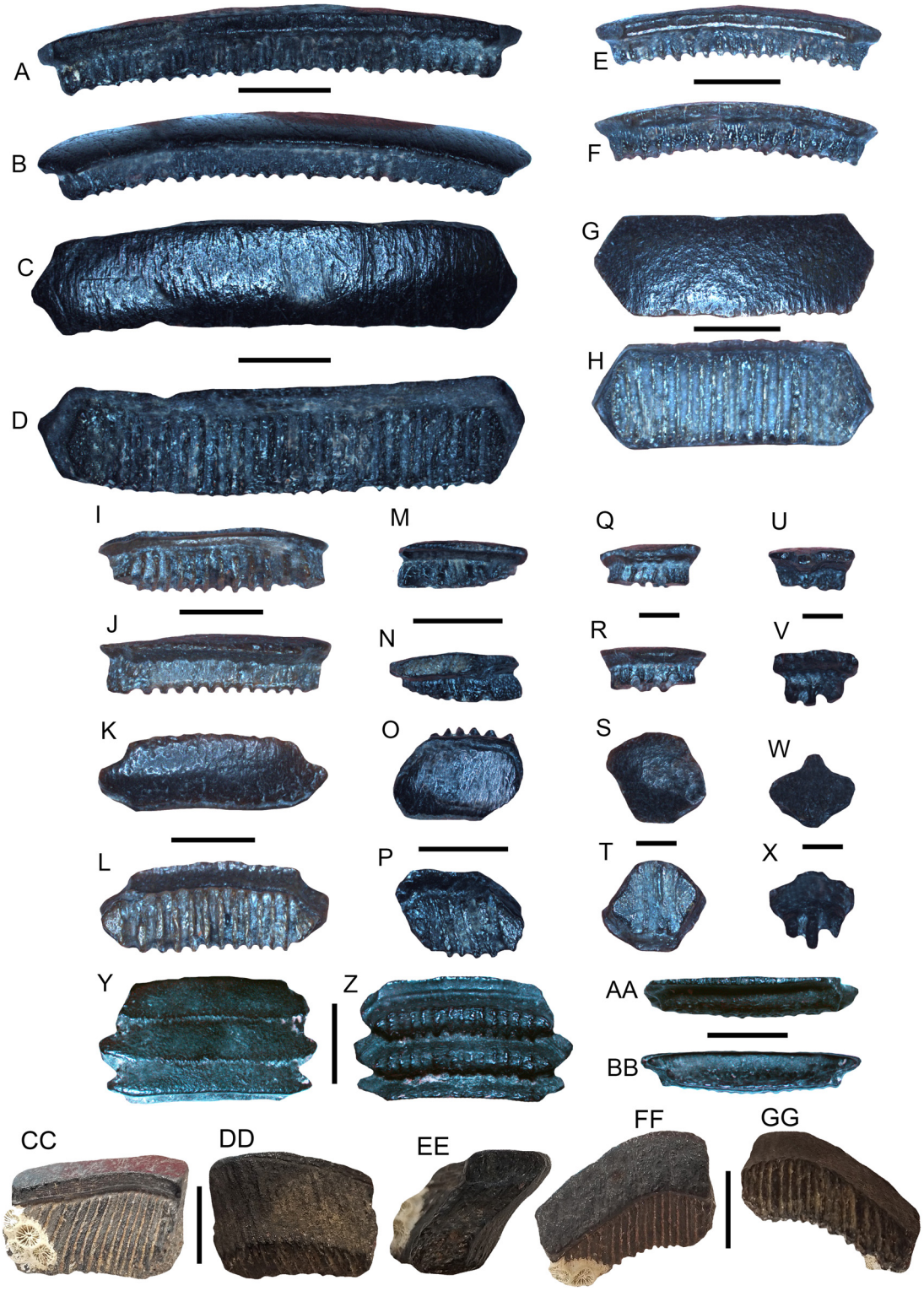

FIGURE 20. Myliobatiform teeth from the Peace River and Tamiami formations on the shallow Venice, Florida continental shelf. **A–BB,** *Myliobatis* sp. median teeth (A–L; UF-VP561105–UF-VP561107), lateral teeth (M–X; UF-VP561109–UF-VP561111), and partial pavement plate (Y–BB; UF-VP561104). **CC–GG,** *Aetobatus* cf. *A. narinari* lower pavement tooth (UF-VP561113). Orientations = lingual: A, E, I, M, Q, U; AA, CC; labial: B, F, J, N, R, V; BB, DD; lateral: EE; occlusal: C, G, K, O, S, W, Y, FF; basal: D, H, C, P, T, X, Z, GG. Scale bars: A–P = 5 mm; Q–X = 2 mm; Y–GG = 10 mm.

four median teeth (UF-VP561105–UF-VP561108) and four lateral teeth (UF-VP561109–UF-VP561112). Figured specimens: UF-VP561104–UF-VP561107; UF-VP561109–UF-VP561111 and additional teeth: UF-VP561108; UF-VP561112.

Description. The fragmentary pavement plate measures 14.43 mm in width, 8.42 mm in height, and 2.75 mm in thickness and consists of only median teeth. The largest isolated tooth is a median tooth that measures 30.13 mm in width, 6.90 mm in height, and 3.99 mm in thickness. The crowns of the median and lateral teeth are mesiodistally elongated, smooth, slightly arcuate, weakly convex, and roughly hexagonal in occlusal view. The crowns are thin relative to the tooth roots and overhang the root on all but the lingual face. Median and lateral tooth roots are polyaulacorhizous and contain numerous, roughly equidimensional, nutritive grooves.

Remarks. *Myliobatis* is another eagle ray genus with 11 extant species that are recognized globally and typically occur in shallow marine environments (White, 2014; Last et al., 2016a). In the Gulf of Mexico and western Atlantic, the bullnose eagle ray, *M. freminvillei* Lesueur, 1824, is relatively abundant and known to feed upon a variety of invertebrates and small vertebrates (Last et al., 2016a). The southern eagle ray, *M. goodei* Garman, 1885, also occurs in the western Atlantic, but this species is currently not known from the Gulf of Mexico. The teeth of *Myliobatis* sp. described here are represented by a mesiodistally elongated form with multiple nutritive grooves, flat to slightly convex occlusal surfaces, and crowns that are thin relative to the root base. These features distinguish them from those of other similar batoids in the Venice Elasmobranch Assemblage including *Rhinoptera* cf. *R. bonasus* and *Aetomylaeus* sp. In particular, the teeth of *Myliobatis* sp. lack thickened and arched median teeth, lack thickened and lingually displaced roots, and may contain irregular ornamentation on the lingual tooth surface (Cappetta, 2012; Villafaña et al., 2019). Median teeth of *Myliobatis* also possess angular edges that correspond with the articular surfaces of adjoining lateral teeth distinguishing them from *Aetobatus* sp. which do not have lateral teeth (e.g., Herman et al., 2000; Cappetta, 2012). Additionally, *Aetomylaeus* sp. have median teeth with curved or arched margins that adjoin with lateral teeth and thickened roots that distinguish them from *Myliobatis* sp. (e.g., Herman et al., 2000; Cappetta, 2012; Hovestadt and Hovestadt-Euler, 2013). The highly variable dental morphology of pavement teeth belonging to extant genera including *Myliobatis*, *Rhinoptera*, and *Aetomylaeus* makes the identification of isolated fossil median and lateral pavement teeth extremely difficult (Nishida, 1990; Herman et al. 2000; Cappetta, 2012). As such, we refrain from species-level taxonomic identification of isolated pavement teeth of *Myliobatis* sp. in the Venice Elasmobranch Assemblage until further studies are conducted on fossil and extant specimens.

Family AETOBATIDAE White and Naylor, 2016
Genus *AETOBATUS* Blainville, 1816
Aetobatus cf. *A. narinari* (Euphrasen, 1790)
Figure 20CC–GG

Referred specimens. One fragmentary pavement tooth (UF-VP561113).

Description. The fragmentary pavement tooth measures 19.97 mm in width, 15.89 mm in height, and 6.25 mm in occlusobasal thickness. The occlusal surface is thin and flat. The lingual surface is concave and composed mainly of a well-developed, elongated root base that has nutritive grooves with a comb-like appearance. The distal portions of the occlusal surface curve in the posterior direction. The labial surface is convex and composed mainly of the well-developed, comb-like root base. In profile view, the root is noticeably displaced in the lingual direction.

Remarks. *Aetobatus* is yet another eagle ray genus composed of five extant species: *A. narinari* (Euphrasen, 1790), *A. flagellum* (Bloch and Schneider, 1801), *A. ocellatus* (Kuhl in Van Hasselt, 1823), *A. laticeps* (Gill, 1865b), and *A. narutobiei* (White, Yamaguchi and Furumitsu, 2013). The white-spotted eagle ray, *A. narinari,* was once thought to have a global distribution, but recent parasitological and molecular analyses concluded that this taxon is in fact restricted to the western Atlantic and ranges between Florida and Brazil (Marie and Justine, 2005; Richards et al., 2009; Last et al., 2016a; White and Naylor, 2016; Sales et al., 2019). A similar species, *A. laticeps*, has been assigned to the eastern Pacific Ocean lineage of *Aetobatus* and likely separated from *A. narinari* around 1.41 Ma (Sales et al., 2019). The pavement teeth of *Aetobatus* described in this paper are distinct by the presence of a mesiodistally elongated form, thin, flat occlusal surface, and elongated, well-developed lingually inclined root base with comb-like nutritive grooves readily. These characteristics distinguish them from other similar batoids in the Venice Elasmobranch Assemblage such as *Aetomylaeus*, *Myliobatis*, and *Rhinoptera*. Teeth of *Aetomylaeus*, particularly fragmentary median pavement teeth, may appear

very similar to those of *Aetobatus*, but those of *Aetomylaeus* generally have thicker occlusal surfaces, shorter roots that are not as lingually displaced, and lateral edges that flatten and taper to a point for articulation with lateral pavement teeth. No lateral teeth are present in *Aetobatus,* and pavement teeth are typically elongated such that they are only slightly inclined posteriorly in the upper jaw and chevron-shaped in the lower jaw (Herman et al., 2000; Cappetta, 2012; Hovestadt and Hovestadt-Euler, 2013; Villafaña et al., 2019).

Several fossil taxa have been described with teeth similar to those of *Aetobatus* cf. *A. narinari* in the Venice Elasmobranch Assemblage including: *Pseudoaetobatus* spp., *Aetobatus cappettai*, and *Aetobatus arcuatus*. *Pseudoaetobatus* spp. have only been reported from the Eocene and are more similar to *Aetomylaeus* because they have centrally thickened, weakly curved median teeth, irregular lateral teeth, and median and lateral teeth with roots that are only slightly displaced lingually (Cappetta, 2012; Cicimurri and Ebersole, 2015). In contrast, the teeth of *A. cappettai* and *A. arcuatus* have been reported from the late Neogene and appear quite similar to those of *Aetobatus narinari* (Reinecke et al., 2011; Bor et al., 2012; Cappetta, 2012; Fiahlo et al., 2019; Collareta et al., 2021). Median teeth of *A. cappettai* typically have thin and flat occlusal surfaces, a thickened central tooth region, tall roots that are not extensively lingually displaced, and well-defined nutritive grooves; however, the validity of this taxon is questionable as these teeth are similar to those of juvenile *A. narinari* (e.g., Reinecke et al., 2011; Cappetta, 2012; Hovestadt and Hovestadt-Euler, 2013; Fiahlo et al., 2019; Collareta et al., 2021). The median teeth of *A. arcuatus* exhibit well-developed curvature or a chevron shape in the lower jaw, whereas upper jaw teeth are less arched, are noticeably thickened in the central portion of the tooth, and the lateral tooth margins are nearly vertical and do not taper to a point (Reinecke et al., 2011; Bor et al., 2012; Cappetta, 2012). The degree of median tooth curvature has been shown to be highly variable between upper and lower jaws, between the same species, and among different taxa and is therefore not a useful taxonomic character (e.g., Reinecke et al., 2011). Because of the uncertainties, we conservatively identify the single fragmentary specimen described here to as *A*. cf. *A. narinari. Aetobatus narinari* is presently restricted to the western Atlantic and primarily feeds on invertebrates along the shallow continental shelf (Last et al., 2016a; Cahill et al., 2023). This species also exhibits seasonal, southerly migrations to waters ~≥23°C including the Gulf of Mexico (Bassos-Hull et al., 2014; DeGroot et al., 2021; Conan et al., 2023).

The specimen reported in this study as *Aetobatus* cf. *A. narinari* is the only definitive chevron-shaped *Aetobatus* tooth collected by the lead author over the last decade of diving in Venice, Florida. Although similarities in the median teeth between *Aetomylaeus* and *Aetobatus* can make their identification difficult based on isolated, fragmentary pavement teeth, no distinctly chevron-shaped teeth of *Aetobatus* were recovered in association with teeth identified as *Aetomylaeus* sp. This suggests that *Aetobatus* was a much less frequent inhabitant of the shallow west Florida continental shelf, in contrast to *Aetomylaeus* sp. and other batoids in the Venice Elasmobranch Assemblage, during the Miocene–Pliocene.

DISCUSSION

Composition and Paleoecology of the Venice Elasmobranch Assemblage

The Venice Elasmobranch Assemblage described in this report consists of 45 taxa from eight orders, 19 families, and 28 definitive genera and is remarkably similar to the extant elasmobranch assemblage occurring in the Gulf of Mexico (Figures 4–20; Tables 1–5; Bigelow and Schroeder, 1948a, 1948b, 1953; Castro, 2011; Last et al., 2016a; Carrier, 2017; Ebert et al., 2021). Taxa represented primarily constitute a mixture of globally ubiquitous carcharhiniforms (19 species), lamniforms (six species including the extinct megatoothed shark, *O. megalodon*), and myliobatiforms (eight species) (e.g., Compagno et al., 2005; Castro, 2011; Cappetta, 2012; Last et al., 2016a; Ebert et al., 2021). Teeth from taxa in the Venice Elasmobranch Assemblage exhibit morphologies that form grasping/clutching/crushing and cutting/slicing dentitions well-suited for feeding on invertebrates, fish, and marine mammals (e.g., Purdy et al., 2001; Castro, 2011; Cappetta, 2012; Ebert et al., 2021). Many of the Venice elasmobranchs are indicative of nutrient-rich, nearshore marine environments. However, the availability of deeper water to the west is supported by the occurrence of taxa including *Squalus* sp., *I. triangulus*, *O. megalodon*, *C. carcharias*, *C. hastalis*, *I. oxyrinchus*, *P. benedinii*, *Mobula* spp., and *Aetobatus* cf. *A. narinari* that are known to frequent neritic and pelagic habitats and are capable of large-scale, open-ocean migrations (e.g., Purdy, 1998; Purdy et al., 2001; Compagno et al., 2005; Castro, 2011; Cappetta, 2012). Notice-

TABLE 1. Distribution of the Miocene–Pliocene elasmobranchs reported from Venice, Florida within the present-day Gulf of Mexico and Western North Atlantic Ocean. † = globally extinct species.

Comparison of the Venice Elasmobranch Assemblage to Modern Assemblages in the USA				
Genus	**Species**	**Venice Shelf, Florida Peace River and Tamiami Fms., Miocene–Pliocene (This Study)**	**Present-day Gulf of Mexico (Castro, 2011; Last et al., 2016a; Carrier, 2017; Ebert et al., 2021)**	**Present-day Western North Atlantic Ocean (Bigelow and Schroeder, 1948; 1953; Castro, 2011; Last et al., 2016a; Ebert et al., 2021)**
Squaliformes				
Squalus	sp.	X	X	X
† *Isistius*	*triangulus*	X		
Heterodontiformes				
Heterodontus	sp.	X		
Orectolobiformes				
Ginglymostoma	*cirratum*	X	X	X
Lamniformes				
Carcharias	*taurus*	X	X	X
† *Otodus*	*megalodon*	X		
† *Parotodus*	*benedinii*	X		
Isurus	*oxyrinchus*	X	X	X
Carcharodon	*carcharias*	X	X	X
† *Carcharodon*	*hastalis*	X		
Carcharhiniformes				
Scyliorhinus	sp.	X	X	X
Mustelus	sp.	X	X	X
Galeorhinus	sp.	X		
† *Hemipristis*	*serra*	X		
† *Galeocerdo*	*aduncus*	X		
† *Galeocerdo*	*mayumbensis*	X		
Galeocerdo	*cuvier*	X	X	X
† *Physogaleus*	*contortus*	X		
Rhizoprionodon	sp.	X	X	X
Negaprion	*brevirostris*	X	X	X
Carcharhinus	cf. *C. falciformis*	X	X	X
Carcharhinus	*leucas*	X	X	X
Carcharhinus	*obscurus*	X	X	X
Carcharhinus	*perezii*	X	X	X
Carcharhinus	cf. *C. brachyurus*	X	Likely	
Carcharhinus	cf. *C. plumbeus*	X	X	X
Carcharhinus	cf. *C. altimus*	X	X	X
Carcharhinus	*limbatus*	X	X	X
Carcharhinus	*brevipinna*	X	X	X
Carcharhinus	*porosus*	X	X	
Sphyrna	cf. *S. zygaena*	X	X	X
Sphyrna	cf. *S. tiburo*	X	X	X
Rhinopristiformes				
Rhynchobatus	sp.	X		

TABLE 1 (continued).

Comparison of the Venice Elasmobranch Assemblage to Modern Assemblages in the USA				
Genus	**Species**	**Venice Shelf, Florida Peace River and Tamiami Fms., Miocene–Pliocene (This Study)**	**Present-day Gulf of Mexico (Castro, 2011; Last et al., 2016a; Carrier, 2017; Ebert et al., 2021)**	**Present-day Western North Atlantic Ocean (Bigelow and Schroeder, 1948; 1953; Castro, 2011; Last et al., 2016a; Ebert et al., 2021)**
Rhinobatos	sp.	X		
Anoxypristis	sp.	X		
Pristis	cf. *P. pristis*	X	X	
	Rajiformes			
"Raja"	sp.	X	X	X
	Myliobatiformes			
Hypanus	cf. *H. americana*	X	X	X
Hypanus	cf. *H. rugosa*	X	X	X
Rhinoptera	cf. *R. bonasus*	X	X	X
Mobula	cf. *M. hypostoma*	X	X	X
Mobula	cf. *M. birostris*	X	X	X
Aetomylaeus	sp.	X	?	?
Myliobatis	sp.	X	X	X
Aetobatus	cf. *A. narinari*	X	X	X

ably absent from the Venice Elasmobranch Assemblage are taxa with distinct, planktivorous or deep-water, abyssal–pelagic affinities such as *Hexanchus*, *Alopias*, *Megachasma*, *Cetorhinus*, and *Rhincodon* that have been reported from other Cenozoic localities in Florida and along the Atlantic and Gulf Coastal Plains of the USA (e.g., Purdy et al., 2001; Compagno et al., 2005; Castro, 2011; Cappetta, 2012; Kent, 2018; Ebert et al., 2021; Perez, 2022). With continued sampling, it is likely that some of these taxa as well as others (e.g., *Notorynchus, Squatina, Alopias, Rhincodon, Gymnura*) that have been reported from other Miocene–Pliocene localities in Florida and elsewhere across the Atlantic and Gulf Coastal Plains may be added to the Venice Elasmobranch Assemblage.

Of the 45 taxa currently represented in the Venice Elasmobranch Assemblage, eight are extinct globally (i.e., *I. triangulus*, *O. megalodon*, *C. hastalis*, *P. benedinii*, *H. serra*, *G. aduncus*, *G. mayumbensis*, and *P. contortus*), three extant genera (*Heterodontus*, *Rhynchobatus*, and *Anoxypristis*) are no longer represented in the Gulf of Mexico, and three taxa (*C. brachyurus*, *Pristis* cf. *P. pristis*, and *Aetomylaeus* sp.) have uncertain extant distributions, but likely occur in the Gulf of Mexico (Table 1). Differences between the Miocene–Pliocene and present-day elasmobranch assemblage in the Gulf of Mexico can likely be attributed to changes in shallow marine habitat, emergence of peninsular Florida, the closure of the Central American Seaway, and fluctuations in ocean circulation patterns as a result of tectonic and climatic changes during the late Cenozoic (e.g., Schneider and Schmitter, 2006; Lessios, 2008; Lunt et al., 2008; Hine, 2013; O'dea et al., 2016; Perez et al., 2017; Perez, 2022; Haq and Ogg, 2024).

Teeth from the Venice Elasmobranch Assemblage range in size from ~1.0 mm to >10 cm in height. However, in contrast to other submerged continental shelf lag deposits (i.e., Maisch et al., 2018; 2019a), elasmobranch teeth measuring ≤1 cm are frequently represented in the Venice Elasmobranch Assemblage (e.g., Maisch et al., 2023, 2024). Among the Venice Elasmobranch Assemblage, carcharhiniform and myliobatiform teeth, including those from *Carcharhinus* spp., *N. brevirostris*, and *Myliobatis* sp., are the most abundant macrofossil elements (>1 cm), whereas the most common microfossil remains (<1 cm) belong to *Rhizoprionodon* and *Hypanus* as well as numerous osteichthyan taxa. Elasmobranch teeth in the Venice Assemblage also co-occur with the bones and teeth of marine mammals (e.g., whales, porpoises,

TABLE 2. A comparison of the Venice Elasmobranch Assemblage with middle–late Miocene, Miocene–Pliocene, and Pliocene elasmobranch assemblages reported from Florida, USA. † = globally extinct species. **A**= Venice Shelf, Peace River and Tamiami Fms., Miocene–Pliocene (This Study), **B**= Torreya Fm., Middle Miocene, Gadsen County (Soto and MacFadden, 2014; Soto, 2016), **C**= Gainesville Creeks, Coosawhatchie Fm., Gainesville, Alachua County, Middle Miocene–Pliocene (Boyd, 2016), **D**= Love Bone Bed, Alachua Fm., Archer, Alachua County, Late Miocene (Webb et al., 1981), **E**= Montbrook Fossil Site (likely reworked Hawthorn Group), Williston, Levy County, Miocene–Pliocene (Ziegler et al., 2019), **F**= Manatee County Dam, Bone Valley Member, Peace River Fm., Bradenton, Manatee County, Pliocene (Webb and Tessman, 1968), **G**= Hickey Creek, Tamiami Fm., Alva, Lee County, Pliocene (Morgan and Pratt, 1983), **H**= Palmetto Fauna, Peace River Formation, Central Phosphate District, Polk, Hardee, Hillsborough, Manatee Counties, Miocene–Pliocene (Simons et al., 2014), **I**= Cookiecutter Creek, Tamiami Fm., North Port, Sarasota County, Pliocene (Perez and Marks, 2017). X*=Taxa identified to the genus level or as a similar species.

Miocene–Pliocene Elasmobranch Assemblages in Florida, USA										
Genus	**Species**	**A**	**B**	**C**	**D**	**E**	**F**	**G**	**H**	**I**
Squaliformes										
Squalus	sp.	X								
† *Isistius*	*triangulus*	X								X
Heterodontiformes										
Heterodontus	sp.	X				X				
Orectolobiformes										
Ginglymostoma	*cirratum*	X	X*	X*		X*			X*	X
Lamniformes										
Carcharias	*taurus*	X		X*		X	X		X	X
† *Otodus*	*megalodon*	X	X	X	X	X	X		X	X
† *Parotodus*	*benedinii*	X								
Isurus	*oxyrinchus*	X				X			X	X
Carcharodon	*carcharias*	X								X
† *Carcharodon*	*hastalis*	X	X	X	X	X	X	X	X	X
Carcharhiniformes										
Scyliorhinus	sp.	X								
Mustelus	sp.	X								
Galeorhinus	sp.	X				X				
† *Hemipristis*	*serra*	X	X	X	X	X	X	X	X	X
† *Galeocerdo*	*aduncus*	X	X	X			X			
† *Galeocerdo*	*mayumbensis*	X	X	X						
Galeocerdo	*cuvier*	X	X			X	X	X	X	X
† *Physogaleus*	*contortus*	X	X	X	X	X			X	X
Rhizoprionodon	sp.	X	X	X	X	X	X	X	X	X
Negaprion	*brevirostris*	X	X	X	X	X	X		X	
Carcharhinus	cf. *C. falciformis*	X		X		X			X	
Carcharhinus	*leucas*	X	X*	X	X	X	X	X	X	
Carcharhinus	*obscurus*	X								
Carcharhinus	*perezii*	X		X		X				
Carcharhinus	cf. *C. brachyurus*	X				X			X	
Carcharhinus	cf. *C. plumbeus*	X		X					X	
Carcharhinus	cf. *C. altimus*	X								
Carcharhinus	*limbatus*	X		X		X				
Carcharhinus	*brevipinna*	X		X						
Carcharhinus	*porosus*	X								

TABLE 2 (continued).

Miocene–Pliocene Elasmobranch Assemblages in Florida, USA										
Genus	**Species**	**A**	**B**	**C**	**D**	**E**	**F**	**G**	**H**	**I**
Sphyrna	cf. *S. zygaena*	X	X	X*		X*			X*	
Sphyrna	cf. *S. tiburo*	X								
Rhinopristiformes										
Rhynchobatus	sp.	X		X		X			X	
Rhinobatos	sp.	X		X	X				X	
Anoxypristis	sp.	X		X					X	X
Pristis	cf. *P. pristis*	X	X*	X		X				
Rajiformes										
"Raja"	*sp.*	X				X				
Myliobatiformes										
Hypanus	cf. *H. americana*	X	X	X		X			X	X
Hypanus	cf. *H. say*	X								
Rhinoptera	cf. *R. bonasus*	X	X	X		X			X	
Mobula	cf. *M. hypostoma*	X				X				
Mobula	cf. *M. birostris*	X								
Aetomylaeus	sp.	X		X					X	
Myliobatis	sp.	X	X	X		X	X	X		X
Aetobatus	cf. *A. narinari*	X	X						X	

and dugongs) that occasionally exhibit bite marks (i.e., *Linichnus* and *Knethichnus* isp.) from predation or scavenging and can be attributed to various carcharhiniform sharks as well as large lamniform sharks including *O. megalodon* and *C. hastalis* (e.g., Godfrey et al., 2018; Maisch et al., 2018). Additionally, bones and teeth of Plio–Pleistocene terrestrial mammals (e.g., horses, mastodons, and mammoths) and reptiles (e.g., turtles, alligators, and crocodiles) frequently co-occur with marine vertebrate remains on the shallow Venice shelf. All vertebrate remains occurring on the Venice shelf exhibit varying degrees of taphonomic wear and bioerosion, and further attest to extensive episodes of weathering, erosion, and time-averaging on the shallow continental shelf since the Miocene (Figures 2–3).

Taphonomy of the Venice Elasmobranch Assemblage

Teeth belonging to the 45 taxa represented in the Venice Elasmobranch Assemblage exhibit distinctly different degrees of preservation (Figure 2D, Figures 4–20). While many of the specimens included in this study are represented by well-preserved teeth, the vast majority of teeth collected exhibit varying degrees of taphonomic wear including fragmentation, polish/abrasion, bioerosion, and increased phosphatization (often exhibited by a darker coloration). These same observations regarding vertebrate fossil preservation have been documented in the Purisima Formation of coastal California (Boessenecker et al., 2014) and the Pungo River and Yorktown formations exposed in Onslow Bay, North Carolina, USA (Maisch et al., 2019a). At these locations, the preservation state of vertebrate fossil remains in the shallow marine environment is dependent on the: 1) amount of time the remains spend on or near the seafloor; 2) frequency of climatically driven sea-level changes; 3) intensity of current-driven erosion and reworking from fairweather and storm wavebase, and 4) bottom currents (Boessenecker et al., 2014; Maisch et al., 2019a).

Fossil elasmobranch remains on the shallow continental shelf along Venice, Florida, are also frequently concentrated with fossil bones and teeth from various marine mammals, terrestrial mammals, reptiles, birds, and bony fishes with distinctly different habitat preferences. These types of fossil concentrations are regarded as lag deposits and represent the mixing of durable remains, including vertebrate fossils, from different habitats, over several hundred thousand to several million years of

TABLE 3. A comparison of the Venice Elasmobranch Assemblage with other Miocene and Early Pliocene elasmobranch assemblages reported from the USA. For Onslow Bay and the Nutrien Mine: M = Miocene; P = Pliocene; * = identified to only the genus level or different species name utilized; † = globally extinct species.

Miocene–Pliocene Elasmobranch Assemblages ACP, USA						
Genus	**Species**	**Venice Shelf, Florida Peace River and Tamiami Fms., Miocene–Pliocene (This Study)**	**Onslow Bay, NC Pungo River and Yorktown Fms. Early Miocene–Pliocene (Maisch et al., 2018)**	**Nutrien Mine, NC Pungo River and Yorktown Fms. Early Miocene–Pliocene (Purdy et al., 2001)**	**Carmel Church Quarry, VA Calvert Fm. Middle Miocene (Hastings and Dooley, 2017)**	**Calvert Cliffs, MD Calvert, Choptank, and St. Marys Fms. Late Early–Late Miocene (Kent, 2018)**
Squaliformes						
Squalus	sp.	X		XP		X
† *Isistius*	*triangulus*	X		X *.		
Heterodontiformes						
Heterodontus	sp.	X				
Orectolobiformes						
Ginglymostoma	*cirratum*	X		XM*		
Lamniformes						
Carcharias	*taurus*	X	XP	XP	X	X
† *Otodus*	*megalodon*	X	XP	XMP	X	X
† *Parotodus*	*benedinii*	X	XP	XP		X
Isurus	*oxyrinchus*	X	XMP	XMP		X
Carcharodon	*carcharias*	X	XP	XP		X
† *Carcharodon*	*hastalis*	X	XP	XP	X	X
Carcharhiniformes						
Scyliorhinus	sp.	X		XMP		X
Mustelus	sp.	X		XM		X
Galeorhinus	sp.	X		XMP		
† *Hemipristis*	*serra*	X	XMP	XMP	X	X
† *Galeocerdo*	*aduncus*	X	XM	XM* .	X *	X
† *Galeocerdo*	*mayumbensis*	X				
Galeocerdo	*cuvier*	X	XP	XP		
† *Physogaleus*	*contortus*	X	XM	XM	X	X
Rhizoprionodon	sp.	X	XMP	XM		X
Negaprion	*brevirostris*	X	XP	XMP	X *	X*
Carcharhinus	cf. *C. falciformis*	X	XMP	XM		X
Carcharhinus	*leucas*	X		XMP	X *	X
Carcharhinus	*obscurus*	X		XP		
Carcharhinus	*perezii*	X		XMP		X
Carcharhinus	cf. *C. brachyurus*	X		XM		
Carcharhinus	cf. *C. plumbeus*	X		XMP		X
Carcharhinus	cf. *C. altimus*	X				X
Carcharhinus	*limbatus*	X				
Carcharhinus	*brevipinna*	X				
Carcharhinus	*porosus*	X				
Sphyrna	cf. *S. zygaena*	X		XMP	X*	X*
Sphyrna	cf. *S. tiburo*	X				

TABLE 3 (continued).

Miocene–Pliocene Elasmobranch Assemblages ACP, USA						
Genus	**Species**	**Venice Shelf, Florida Peace River and Tamiami Fms., Miocene–Pliocene (This Study)**	**Onslow Bay, NC Pungo River and Yorktown Fms. Early Miocene–Pliocene (Maisch et al., 2018)**	**Nutrien Mine, NC Pungo River and Yorktown Fms. Early Miocene–Pliocene (Purdy et al., 2001)**	**Carmel Church Quarry, VA Calvert Fm. Middle Miocene (Hastings and Dooley, 2017)**	**Calvert Cliffs, MD Calvert, Choptank, and St. Marys Fms. Late Early–Late Miocene (Kent, 2018)**
Rhinopristiformes						
Rhynchobatus	sp.	X				X
Rhinobatos	sp.	X		XM		
Anoxypristis	sp.	X		XP		X*
Pristis	cf. *P. pristis*	X		XP *		
Rajiformes						
"Raja"	sp.	X		XP		X
Myliobatiformes						
Hypanus	cf. *H. americana*	X		XM		
Hypanus	cf. *H. say*	X		XMP*		X
Rhinoptera	cf. *R. bonasus*	X		XM*		X*
Mobula	cf. *M. hypostoma*	X		MP*		X*
Mobula	cf. *M. birostris*	X				
Aetomylaeus	sp.	X			X *	X *
Myliobatis	sp.	X			X	
Aetobatus	cf. *A. narinari*	X		XMP *	X	X *

time as a result of climatically driven sea-level fluctuations (e.g., Purdy et al., 2001; Boessenecker et al., 2014; Maisch et al., 2015, 2018, 2019a, 2019b). Similar lag deposit fossil assemblages have been reported globally during the Late Cretaceous–Cenozoic and provide valuable information on taxonomic diversity, taphonomy, and the correlative properties of lag deposits and elasmobranch remains (e.g., Shimada, 1987; Becker et al., 1996, 1998, 2006; Cumbaa et al., 2010; Reinecke et al., 2011; Bor et al., 2012; Boessenecker et al., 2014; Maisch et al., 2014, 2015, 2019a, 2019b, 2021).

It is also noteworthy that a culturally significant Native American burial site was discovered on the shallow Venice continental shelf in 2016 by SCUBA divers while searching for fossil shark teeth (Florida Department of State; Herald Tribune; Kimel, 2019). This burial site, now referred to as the Manasota Key Offshore Site, has been dated to be ~7,200 years old placing it in the Archaic Period, and based on the abundance of peat, is interpreted to represent a freshwater pond that was present when sea-level was ~10 m lower (Price, 2023). This pond was once present above Miocene–Pliocene deposits, and vertebrate fossils have subsequently been eroded and transported across this area which further emphasizes the extremely dynamic nature of the shallow continental shelf.

Major storms, including tropical storms and hurricanes, can also have drastic impacts on the shallow continental shelf, including the Gulf of Mexico (e.g., Hine and Belknap, 1986; Mearns et al., 1998; Morton, 1988; Walker and Plint, 1992; Goodbred and Hine, 1995; Posey et al., 1996; Renaud et al., 1996, 1997; Riggs et al., 1998; Hine et al., 2003). Within the last 150 years alone, 87 tropical storms have passed across or within 100 km of Venice, Florida (and 131 storms have occurred within 150 km) (NOAA Historical Hurricane Tracks). These storms are known to yield increased rainfall, runoff, wave heights, bottom currents, and tidal ranges, among many other impacts (e.g., Ball et al., 1967; Doyle et al., 1995; Matyas and Cartaya, 2009; Smith et al., 2009; Frazier et al., 2010; Stockdon et al., 2012; Ercolani et al., 2015; So et al., 2019; Martin and Muller, 2021). Direct observations from SCUBA diving on the

TABLE 4. A comparison of the Venice Elasmobranch Assemblage with late Miocene, Miocene–Pliocene, and Pliocene elasmobranch assemblages from Central and South America. Note that taxonomic diversity is highly variable among assemblages, some species names have since been revised, and diversity differences may stem from taxonomic splitting and lumping. † = globally extinct species. **A**= Peace River and Tamiami Fms., Miocene– Pliocene, FL (This Study), **B**= Chagres Fm., Late Miocene, Panama (Carrillo-Briceño et al., 2015), **C**= Gatun and Chucunaque Fms., Late Miocene, Panama (Pimiento et al., 2013; Perez et al., 2017), **D**= Curré Fm., Late Miocene, Costa Rica (Laurito and Valerio, 2008), **E**= Pisco Fm., Late Miocene, Peru (Landini et al., 2017a,b), **F**= Uscari Fm., Miocene– Pliocene, Costa Rica (Laurito, 1999; Laurito and Valerio, 2021), **G**= Onzole–Bahia Fms., Late Miocene– Pliocene, Ecuador (Longbottom, 1979; Carrillo-Briceño et al., 2014), **H**= Tirabuźon Fm., Pliocene, Mexico (Lira-Beltrán et al., 2020), **I**= Urumaco Sequence (Soccorro, Urumaco, and Codore Fms.), Miocene–Pliocene, Venezuela (Carrillo-Briceño et al., 2015), **J**= Horcón Fm., Pliocene, Chile (Carrillo-Briceño et al., 2013). X*=Taxa identified to the genus level or as a similar species.

Miocene–Pliocene Elasmobranch Assemblages in Central and South America											
Genus	**Species**	**A**	**B**	**C**	**D**	**E**	**F**	**G**	**H**	**I**	**J**
Squaliformes											
Squalus	sp.	X	X				X		X		
† *Isistius*	*triangulus*	X	X*				X	X			
Heterodontiformes											
Heterodontus	sp.	X	X*				X*		X*		X*
Orectolobiformes											
Ginglymostoma	*cirratum*	X		X*							
Lamniformes											
Carcharias	*taurus*	X	X*			X		X*			
† *Otodus*	*megalodon*	X	X	X		X	X	X	X	X	
† *Parotodus*	*benedinii*	X							X		
Isurus	*oxyrinchus*	X		X	X*	X	X*				X
Carcharodon	*carcharias*	X							X		X
† *Carcharodon*	*hastalis*	X	X			X					
Carcharhiniformes											
Scyliorhinus	sp.	X					X				
Mustelus	sp.	X	X	X			X*		X		
Galeorhinus	sp.	X	X*						X*		X*
† *Hemipristis*	*serra*	X	X	X	X		X	X	X	X	
† *Galeocerdo*	*aduncus*	X		X		X	X				
† *Galeocerdo*	*mayumbensis*	X									
Galeocerdo	*cuvier*	X	X	X					X	X	
† *Physogaleus*	*contortus*	X		X		X					
Rhizoprionodon	sp.	X	X	X			X*	X	X*	X	
Negaprion	*brevirostris*	X	X	X				X	X	X	
Carcharhinus	cf. *C. falciformis*	X		X			X				
Carcharhinus	*leucas*	X	X	X	X*	X	X*	X*	X	X	
Carcharhinus	*obscurus*	X	X	X					X	X	
Carcharhinus	*perezii*	X		X							
Carcharhinus	cf. *C. brachyurus*	X	X			X			X		X
Carcharhinus	cf. *C. plumbeus*	X	X	X						X	
Carcharhinus	cf. *C. altimus*	X									
Carcharhinus	*limbatus*	X							X		
Carcharhinus	*brevipinna*	X		X					X		
Carcharhinus	*porosus*	X								X	

TABLE 4 (continued).

Miocene–Pliocene Elasmobranch Assemblages in Central and South America											
Genus	**Species**	**A**	**B**	**C**	**D**	**E**	**F**	**G**	**H**	**I**	**J**
Sphyrna	cf. *S. zygaena*	X	X*	X	X*	X	X	X*	X	X	
Sphyrna	cf. *S. tiburo*	X									
Rhinopristiformes											
Rhynchobatus	sp.	X		X			X*			X	
Rhinobatos	sp.	X					X		X		
Anoxypristis	sp.	X				X*					
Pristis	cf. *P. pristis*	X					X			X*	
Rajiformes											
"Raja"	sp.	X					X*		X		X*
Myliobatiformes											
Hypanus	cf. *H. americana*	X		X*	X*		X*	X*	X*	X*	X*
Hypanus	cf. *H. say*	X									
Rhinoptera	cf. *R. bonasus*	X		X*	X*		X*		X*	X*	
Mobula	cf. *M. hypostoma*	X		X*			X	X*	X*		
Mobula	cf. *M. birostris*	X					X				
Aetomylaeus	sp.	X								X*	
Myliobatis	sp.	X	X	X*	X	X		X	X	X	X*
Aetobatus	cf. *A. narinari*	X		X*	X*	X*		X*	X*		

Venice continental shelf following several recent storms, including Saffir-Simpson Scale Category 5 Hurricane Ian in 2022 and Category 1 Hurricane Debbie in 2024, have shown that while additional fossil remains are exhumed from the seafloor in some locations, other areas experience increased sedimentation and become deeply buried in silt and fine sand. This variability is likely the result of bathymetric changes, the depth of wave base, and the direction of prevailing winds and currents with respect to each storm.

Overall, the tectonic and oceanographic conditions influencing Florida during the late Cenozoic were like those of today, and it is inferred that similar types of tropical storms would also have regularly occurred in this region during the Late Miocene–Pliocene (Riggs, 1979, 1984). This is supported by the abundance of phosphorite in the Peace River Formation exposed in Venice and across central Florida that formed as a result of nutrient enrichment, high productivity, erosion, concentration, and reburial of sediments on the shallow continental shelf from storm activity and climatically driven sea-level changes (Riggs, 1979, 1984; Compton et al., 1993; Compton, 1997; Hine, 2013). Collectively, it is reasonable to assert that many present-day processes affecting the shallow Venice continental shelf would have also occurred throughout much of the late Cenozoic and contributed to the formation of these highly fossiliferous lag deposits and the abundance of elasmobranch remains.

Biostratigraphy and Correlative Properties of the Venice Elasmobranch Assemblage

The time-averaged Venice Elasmobranch Assemblage contains 45 distinct taxa and represents the most diverse assemblage reported from a specific collecting locality currently known in Florida (Perez, 2022). Additionally, the Venice assemblage is also one of the most diverse late Cenozoic elasmobranch assemblages known from the USA and is similar to those reported from the Early–Middle Miocene Calvert Cliffs in Maryland (50 elasmobranch taxa), as well as the Early–Middle Miocene (46 elasmobranch taxa) and Early Pliocene (36 elasmobranch taxa) assemblages in the Nutrien Mine from Aurora, North Carolina (Purdy et al., 2001; Kent, 2018). Moreover, the high taxonomic composition of the Venice Elasmobranch Assemblage makes it one of the more diverse late Cenozoic elasmobranch assemblages known globally (e.g., Cappetta, 2012; Kent, 2018; Maisch et al., 2018; Lin et al., 2021). A comparison

TABLE 5. Global Miocene–Pliocene occurrence of the Venice elasmobranch taxa. † = globally extinct species. References utilized: **Atlantic Coastal Plain and Gulf Coastal Plain, USA** (Kimmel and Purdy, 1984; Purdy et al., 2001; Boessenecker et al., 2018; Kent, 2018; Maisch et al., 2018; Perez, 2022); **Western North America** (Boessenecker, 2011, 2016; Boessenecker et al., 2014; Lira-Beltrán et al., 2020); **Caribbean, Central, and South America** (Davies, 1964; Gillette, 1984; Applegate, 1986; Long, 1993; Iturralde-Vinent et al., 1996; Flemming and McFarlane, 1998; Nieves-Rivera et al., 2003; Laurito Mora, 1999, 2004; Apolín et al., 2004; Portell et al., 2008; Cione et al., 2011, 2012; Ehret et al., 2012; Pimiento et al., 2013; Collareta et al., 2017a,2017b, 2017c; Landini et al., 2017a; MacFadden et al., 2017; Perez et al., 2017; Carrillo-Briceño et al., 2014, 2015a, 2015b, 2016a, 2016b, 2018, 2019; Laurito Mora and Valerio, 2008, 2021; Laurito Mora et al., 2022); **Africa** (Cook et al., 2010; Ávila et al., 2012; Pawellek et al., 2012; Govender and Chinsamy, 2013; Andrianavalona et al., 2015; Betancort et al., 2016); **Europe** (Holec et al., 1995; Antunes et al., 1999; Antunes and Balbino, 2004; Cappetta and Cavallo, 2006; Carnevale et al., 2006; Kocsis, 2007; Marsili, 2007; Marsili et al., 2007; Cigala-Fulgosi et al., 2009; Vialle et al., 2011; Cappetta, 2012; Reinecke and Radwánski, 2015; Szabó and Kocsis, 2016; Fialho et al., 2019, 2021; Collareta et al., 2021; Szabó et al., 2021, 2023); **Asia** (Itoigawa and Nishimoto, 1974; Uyeno, 1978; Sahni and Mehrotra, 1981; Goto et al., 1984; Shimada, 1987; Sharma and Patniak, 2013, 2014; Kocsis et al., 2018; Razak and Kocsis, 2018; Sharma et al., 2021); **Australia** (Pledge, 1967; Kemp, 1991).

Subcontinent/ Continent		ACP, GCP	WNA	Carib., CA, SA	Africa	Europe	Asia	Australia
Squaliformes								
Squalus	sp.	X	X	X		X	X	
† *Isistius*	*triangulus*	X		X		X		
Heterodontiformes								
Heterodontus	spp.	X	X	X			X	X
Orectolobiformes								
Ginglymostoma	*cirratum*	X		X		X		
Lamniformes								
Carcharias	*taurus*	X		X	X	X	X	X
† *Otodus*	*megalodon*	X	X	X	X	X	X	X
† *Parotodus*	*benedinii*	X		X	X	X	X	X
Isurus	*oxyrinchus*	X	X	X	X	X	X	X
Carcharodon	*carcharias*	X	X	X	X	X	X	X
† *Carcharodon*	*hastalis*	X	X	X	X	X	X	X
Carcharhiniformes								
Scyliorhinus	sp.	X		X	X	X		
Mustelus	sp.	X	X	X		X		X
Galeorhinus	sp.	X	X	X		X		
† *Hemipristis*	serra	X		X	X	X	X	X
† *Galeocerdo*	*aduncus*	X		X	X	X	X	X
† *Galeocerdo*	*mayumbensis*	X		X	X		X	
Galeocerdo	*cuvier*	X	X	X	X	X	X	X
† *Physogaleus*	*contortus*	X		X		X	X	X
Rhizoprionodon	spp.	X	X	X	X	X	X	X
Negaprion	*brevirostris*	X	X	X	X	sp.	X	
Carcharhinus	cf. *C. falciformis*	X		X		X	X	X
Carcharhinus	*leucas*	X	X	X	X	X	X	
Carcharhinus	*obscurus*	X	X	X	X	X		
Carcharhinus	*perezii*	X		X		X		
Carcharhinus	cf. *C. brachyurus*	X	X	X		X	X	X
Carcharhinus	cf. *C. plumbeus*	X		X		X		X

TABLE 5 (continued).

Subcontinent/ Continent		ACP, GCP	WNA	Carib., CA, SA	Africa	Europe	Asia	Australia
Carcharhinus	cf. *C. altimus*	X						
Carcharhinus	cf. *C. limbatus*	X	X	X				
Carcharhinus	cf. *C. brevipinna*	X	X	X				
Carcharhinus	cf. *C. porosus*	X		X				
Sphyrna	spp.	X	X	X	X	X	X	X
Sphyrna	cf. *S. zygaena*	X	X	X		X	X	
Sphyrna	cf. *S. tiburo*	X						
Rhinopristiformes								
Rhynchobatus	sp.	X		X	X	X	X	
Rhinobatos	sp.	X	X	X	X	X	X	
Anoxypristis	sp.	X		X	X	X	X	X
Pristis	cf. *P. pristis*	X		X			X	X
Rajiformes								
"Raja"	spp.	X	X	X		X	X	
Myliobatiformes								
Hypanus	spp.	X	X	X		X	X	X
Rhinoptera	cf. *R. bonasus*	X	X	X		X	X	
Mobula	cf. *M. hypostoma*	X		X		X		
Mobula	cf. *M. birostris*	X		X				
Aetomylaeus	spp.	X		X	X	X	X	
Myliobatis	spp.	X	X	X	X	X	X	X
Aetobatus	cf. *A. narinari*	X	X	X	X		X	

of the 45 taxa in the Venice Elasmobranch Assemblage with other Miocene, Miocene–Pliocene, and Early Pliocene assemblages in Florida and along the Atlantic Coastal Plain of the USA are listed in Tables 2–3, respectively. The data in Table 2 indicate that in Florida: 1) only three taxa (i.e., *C. hastalis*, *H. serra*, and *Rhizoprionodon* sp.) occur in all eight of the Middle Miocene–Pliocene assemblages; 2) six taxa (i.e., *O. megalodon*, *C. hastalis*, *H. serra*, *P. contortus*, *Rhizoprionodon* sp., and *N. brevirostris*) occur in the two Middle/Late Miocene assemblages; 3) fifteen taxa (i.e., *Ginglymostoma* sp., *Carcharias* sp., *O. megalodon*, *C. hastalis*, *H. serra*, *P. contortus*, *Rhizoprionodon* sp., *N. brevirostris*, *C. falciformis*, *C. leucas*, *Sphyrna* sp., *Rhynchobatus* sp., *Hypanus* (*Dasyatis*) sp., *Rhinoptera* sp., and *Myliobatis* sp.) occur in all three Miocene–Pliocene assemblages; and 4) five taxa (i.e., *C. hastalis*, *H. serra*, *G. cuvier*, *Rhizoprionodon* sp., and *Myliobatis* sp.) occur in all three Pliocene assemblages.

There are several locations that contain Miocene and Early Pliocene marine vertebrate assemblages in the USA, but there are no other contemporaneous elasmobranch assemblages spanning the Miocene–Pliocene boundary currently known elsewhere along the Atlantic and Gulf Coastal Plain of the USA with the exception of Florida (Tables 2–3). While there are several Early Miocene, Late Pliocene, and Pleistocene elasmobranch assemblages known along the Atlantic and Gulf Coastal Plains of the USA, the Venice Elasmobranch Assemblage reported in this study is interpreted to be Late Miocene–Early Pliocene in age. As seen in Table 3, several definitive, late Early/Middle Miocene and Early Pliocene assemblages are known from this region, and all are located along the Atlantic Coastal Plain, between North Carolina and Maryland (Purdy et al., 2001; Hastings and Dooley, 2017; Kent, 2018; Maisch et al., 2018). At least eight taxa (i.e., *C. taurus*, *O. megalodon*, *C. hastalis*, *H. serra*, *G. adun-*

cus, *P. contortus*, *Negaprion* sp., and *Carcharhinus* spp.) occurring in the Venice Elasmobranch Assemblage have also been reported from these four Miocene and Pliocene assemblages along the Atlantic Coastal Plain of the USA.

The nearest well-documented Late Miocene or Miocene–Pliocene boundary elasmobranch assemblages are known from Central and South America and border either the eastern Pacific Ocean or Caribbean Sea (e.g., Laurito Mora, 1999; Pimiento et al., 2013; Landini et al., 2017a; MacFadden et al., 2017; Perez et al., 2017; Carrillo-Briceño et al., 2013, 2014, 2015a, 2015b; 2019). As seen in Table 4, many of these assemblages have high taxonomic diversity similar to the Venice Elasmobranch Assemblage; however, compositional variations are more apparent. The Caribbean assemblages represented by the Upper Miocene Chagres, Gatun, and Chucunaque formations of Panama and the Miocene–Pliocene Uscari Formation from Costa Rica, share six common taxa (i.e., *O. megalodon*, *Mustelus* sp., *H. serra*, *Carcharhinus* spp., *Rhizoprionodon* sp., and *Sphyrna* sp.) with the Venice Elasmobranch Assemblage. When viewed collectively, a comparison of assemblages situated along western Central and South America and linked with the eastern Pacific Ocean have only one common taxon: *Myliobatis* sp. (including Myliobatidae indet.). A generic comparison among all nine Central and South American assemblages included in Table 4 also yields only a single common taxon, *Carcharhinus.* However, the elasmobranchs documented at individual western Central and South American localities, when compared with the Venice Elasmobranch Assemblage, does indicate that many genera and even species occurred throughout the entire region. Variations in the taxonomic composition of these assemblages is likely a product of paleobathymetry, shallow marine habitat, paleotemperature, taphonomy (including rates of deposition), collecting techniques, taxonomic classification, and proximity to different ocean basins (e.g., eastern Pacific vs. Caribbean Sea). Moreover, these same biases are also apparent in assemblages across the state of Florida and along the Atlantic Coastal Plain of the USA where some assemblages are only known from species lists within prior publications focusing on other fossil remains (e.g., Webb et al., 1981; Morgan and Pratt, 1983; Perez and Marks, 2017), conference abstracts (e.g., Soto and MacFadden, 2014; Ziegler et al., 2019), or from faunal lists provided by museums. The stratigraphic placement and degree of reworking occurring in some of these assemblages are also poorly constrained, and additional complications exist due to taxonomic discrepancies among researchers, the lack of adequate morphological comparative data of modern taxa for enhancing taxonomic identifications, and the lack of microtooth collection or identification. As a result, comprehensive taxonomic reports, such as the present study, are critical to further understanding the diversity, distribution, and evolution of marine vertebrate groups in the late Cenozoic.

As seen in Tables 1–5, many elasmobranchs in the Venice assemblage have biostratigraphic ranges that span across the Miocene–Pliocene boundary and some are still represented in the modern oceans. Although this reduces the utility of these taxa in fine-tuned biostratigraphic analyses, the occurrence of extinct species can help constrain the age of the Venice Elasmobranch Assemblage. In particular, as seen in Table 5, the eight globally extinct taxa in the Venice Elasmbranch Assemblage (i.e., *I. triangulus, O. megalodon, C. hastalis, P. benedinii, H. serra, G. aduncus, G. mayumbensis,* and *P. contortus*) have well-known, global Miocene and Early Pliocene records and only *H. serra* is presently known from post-Zanclean (i.e., Lower Pleistocene) deposits as confirmed by radiometric dating (e.g., Purdy et al., 2001; Cappetta, 2012; Boessenecker et al., 2018; Kent, 2018; Maisch et al., 2018; Perez, 2022). Similarly, of the three extant taxa no longer present in the Gulf of Mexico or western Atlantic (i.e., *Heterodontus* sp., *Rhynchobatus* sp., and *Anoxypristis* sp.), only *Rhynchobatus* sp. is known from post-Pliocene (i.e., Lower Pleistocene) deposits (Scudder et al., 1995; Cappetta, 2012). The Late Miocene–Early Pliocene age interpretation of the Venice Elasmobranch Assemblage is also reinforced by prior stratigraphic and strontium isotope studies across southwest Florida that indicate the Peace River Formation is primarily Middle–Late Miocene to Pliocene in age (Scott, 1988; Compton et al., 1993; Missimer, 1992, 1999, 2001), whereas the Tamiami Formation is generally regarded as Early–Late Pliocene (Zanclean–Piacenzian) although may extend to the Plio–Pleistocene boundary (~1.95 Ma) in southern Florida (Missimer, 1992, 2001).

These correlations are especially unique for the submerged Venice shelf region because the nearest, well-documented land-based exposures of the 1) Peace River Formation are present in the Central Phosphate Mining District and its southern extension, which are located ~90 km north–north-

east of the Venice region in this present study, and 2) Tamiami Formation occurs in subsurface excavations and river exposures near North Port, Florida, located ~12 km east of this Venice study region (Perez and Marks, 2017). Moreover, the geographic separation of the land-based exposures from our submerged study region indicates that the Peace River and Tamiami formations submerged off the coast of Venice are diachronous with those occurring to the east across central Florida (e.g., McCartan and Moy, 1995; Green et al., 1997; Guertin et al., 2000; Locker et al., 2003).

Effects of Climate Change, Sea-Level Fluctuations, and Closure of the Central American Seaway

Effects of climate and sea-level change. During the late Cenozoic, much of central and southern peninsular Florida was submerged as a result of higher sea-levels from warmer global climates and reduced ice volume in the northern and southern hemispheres (Compton et al., 1993; Allmon et al., 1996; Hine, 2013; Missimer and Maliva, 2017). Prior studies have documented multiple, large-scale marine transgressions during the Miocene–Pliocene, including the Mid-Miocene Climatic Optimum (MMCO) ~18–15 Ma and the Middle Pliocene Warm Period (MPWP) ~3 Ma (e.g., Riggs, 1984; Hine, 2013; Hine et al., 2017; Miller et al., 2020; Haq and Ogg, 2024). The MMCO resulted in global temperatures ~5° C higher and sea-level that ranged between 50–150 m higher on average than present (e.g., Zachos et al., 2008; Herold et al., 2011, 2012; Hamon et al., 2013; Miller et al., 2020; Haq and Ogg, 2024). Similarly, global temperatures during the MPWP are interpreted to have been on average 1–2°C warmer, whereas sea-levels were ~25 m and possibly as much as 50 m higher than present (e.g., Williams et al., 2009; Karas et al., 2017; Zhang et al., 2019; Miller et al., 2020; Haq and Ogg, 2024). A minimum of 25 sea-level regressions have been documented since the MMCO with some having amplitudes as much as 50 m, and 18 of the regressive episodes are interpreted to have been equal to, or lower than, present-day sea-level (Haq and Ogg, 2024). Interestingly, 12 regressions are reported to have occurred between ~11 and 3 Ma with major sequence boundaries identified as NMe2, NZa1, and NZa2 across the Miocene–Pliocene boundary at 5.7, 4.6, and 4.15 Ma, respectively (Haq and Ogg, 2024).

As is evident from the late Cenozoic eustatic curve, sea-level fluctuations were frequent, occasionally high-amplitude, capable of causing large-scale changes to the shallow marine environment, and intricately linked to changes in global climate (Zachos et al., 2001, 2008; Miller et al., 2020; Westerhold et al., 2020; Haq and Ogg, 2024). Sea-level transgression across the already partially submerged Florida peninsula would have increased shallow marine shelf area, likely including a greater abundance of seagrass beds, mangrove islands, and estuary systems that are ideal for many marine vertebrates, including elasmobranchs (e.g., Clark and Schmidt, 1965; Snelson and Williams, 1981; Heck et al., 2003; Castro, 2011). These increases in shallow marine habitats along peninsular Florida during the Miocene–Pliocene may have also supported critical elasmobranch nursery areas for some taxa similar to those documented along the Florida coastline today (e.g., Snelson and Williams, 1981; Heupel et al., 2006; Ortega et al., 2009; Poulakis et al., 2011; Hunt and Doering, 2013; Papastamatiou et al., 2015).

In contrast, sea-level regression would have effectively shifted shallow marine habitats seaward and increased fluvial incision on the exposed continental shelf (e.g., Hine and Snyder, 1985; Talling, 1998; Boss et al., 2002; Cunningham et al., 2003; Fagherazzi et al., 2004; Scott, 2011; Hine, 2013). The extent of habitat reduction is linked with the amplitude of sea-level change and is also dependent on the continental shelf gradient (i.e., the broad, gently dipping western Florida shelf or the narrow, steeply dipping eastern Florida shelf) (e.g., Talling, 1998; Browning et al., 2008; Hine, 2013; Maisch et al., 2019a). The rate of sea-level regression and habitat change is also important to consider as more gradual habitat shifts may enable organisms to adapt, while more rapid changes may exert additional survival pressures on marine organisms including elasmobranchs (e.g., Hallam and Wignall, 1999; Attrill and Power, 2002; Ludt and Rocha, 2015; Sorenson et al., 2014).

Effects of Central American Seaway closure. In addition to the global climatic and sea-level changes occurring during the Miocene–Pliocene, an important oceanographic event was in progress: the closure of the Central American Seaway (CAS). It is generally accepted that tectonic activity beginning ~15 Ma led to the gradual closure of the CAS with the full formation of the Isthmus of Panama occurring ~2.8 Ma (e.g., O'Dea et al., 2016, and references therein, but also see Montes et al., 2015 and Bacon et al., 2015 for differing interpretations of early CAS closure). Varying lines of evi-

dence including marine microfossils, dispersal of terrestrial mammals, molecular divergence estimates, and global coupled climate-marine ecosystem models suggest that a complex, multi-stage process of CAS closure occurred (Knowlton et al., 1993; Coates et al., 2004; Schneider and Schmittner, 2006; Lessios, 2008; Lunt et al., 2008; Leigh et al., 2014; O'Dea et al., 2016). A simplified summary of this process includes: 1) narrowing and shallowing of the seaway in the Middle Miocene ~15 Ma; 2) continued shoaling and loss of a deep-water connection between the Pacific and Atlantic with the occurrence of numerous islands separated by straits in the late Miocene ~9 Ma; and 3) complete CAS closure and Isthmus of Panama formation ~2.8 Ma. Isotopic signatures and climate models also indicate that progressively less water was exchanged from the Pacific to the Atlantic, which caused increases in surface water salinity in the Caribbean and Atlantic, Atlantic deep water to become nutrient poor, and strengthening of the Gulf of Mexico Loop Current, Gulf Stream, and thermohaline circulation began in the Middle Miocene (e.g., Mullins et al., 1987; Lear et al., 2003; Nisancioglu et al., 2003; Schmidt, 2007; Lunt et al., 2008; Sepulchre et al., 2014; O'Dea et al., 2016). Moreover, evidence for a strong salinity contrast between the Pacific and Atlantic by ~4.2 Ma suggests that the Isthmus of Panama was mostly in place by the Early Pliocene (Billups et al., 1999; Schneider and Schmittner, 2006; O'Dea et al., 2016). It is important to note that our current interpretation of the Venice Elasmobranch Assemblage places it across, the Miocene–Pliocene boundary during the gradual closure of the CAS, and it does not represent a snapshot of elasmobranch diversity from before and directly after terminal CAS closure ~2.8 Ma.

It is highly likely that open connections between the Pacific, Caribbean, and Atlantic in place prior to the Middle Miocene would have enabled more frequent dispersal of larger, nektonic taxa, as well as planktonic larvae, between these ocean basins. Further narrowing and shallowing of the CAS led to decreased dispersal and a greater degree of isolation among marine populations, while increasing terrestrial mammal interchange between North and South American continents (i.e., Great American Biotic Interchange; Marshall et al., 1982; Webb, 1991; Morgan, 2005; Woodburne, 2010; Leigh et al., 2014; O'Dea et al., 2016). The gradual closure of the CAS initially caused geographic isolation between benthic organisms that subsequently progressed to an increasing number of invertebrates and vertebrates including shallow water and planktonic taxa (Keigwin, 1982; Lear et al., 2003; Lunt et al., 2008; O'Dea et al., 2016). In fact, it has been proposed that the diversification and dispersal of *Aetobatus* spp., as well as other marine fishes, is related to the closure of the Isthmus of Panama during the Pliocene (~3.6–1.8Ma) (e.g., Schultz et al., 2008; Chabot and Allen, 2009; Sales et al., 2019). Allopatric speciation associated with the formation of the Isthmus of Panama has also been documented and corroborated by molecular divergence estimates for numerous taxa including bivalves, gastropods, echinoderms, and crustaceans (e.g., Knowlton et al., 1993; Lessios, 2008; Leigh et al., 2014).

During the late stages of CAS closure (~7–4 Ma), nutrient dispersal and ocean current flow paths and strengths were noticeably different between the Pacific and Caribbean/Atlantic oceans, and numerous sea-level regressions during this same interval likely compounded stressors to organisms in the shallow marine environment (e.g., Schneider and Schmittner, 2006; Schmidt, 2007; Lunt et al., 2008; O'Dea et al., 2016; Haq and Ogg, 2024). Oceanographic changes associated with the gradual closure of the CAS, when combined with global climatic events, indicate an overall cooling trend and reduction in shallow marine habitat along most continental shelves, including that of southwestern Florida (e.g., Zachos et al., 2008; Hine et al., 2017; Miller et al., 2020; Westerhold et al., 2020; Haq and Ogg, 2024). These changes associated with the late-stage CAS closure have also been implicated with the onset of northern hemisphere glaciation beginning ~3 Ma; however, they are likely not the driving factor (Schneider and Schmittner, 2006; Schmidt, 2007; Molnar, 2008; Ruddiman, 2014; O'Dea et al., 2016).

While it is possible that larger, nektonic marine organisms including bony fish, elasmobranchs, and marine mammals would be capable of shifting their ranges, dispersal between the Pacific Ocean and Caribbean–Atlantic waters would have been greatly reduced as a result of late-stage and terminal CAS closure. In particular, most elasmobranchs and bony fish are ectothermic and have adapted to environments with certain temperature ranges to optimize their physiological performance (e.g., Pörtner and Farrell, 2008; Castro, 2011; Last et al., 2016a; Payne and Smith, 2017; Pinsky et al., 2019; Abel and Grubbs, 2020; Ebert et al., 2021; Harding et al., 2021). Dispersal

between the Pacific and Atlantic Ocean basins after CAS closure would have required large scale distribution shifts either southwards around Cape Horn, northwards through the Arctic Ocean, or eastwards across the Atlantic and Indian Oceans. These types of long-distance dispersals in the late Cenozoic would have exposed taxa to drastic differences in latitudinal temperatures, habitats, and prey availability. The majority of the elasmobranch taxa in the Venice assemblage are represented by ectothermic, nearshore species adapted to subtropical and tropical environments that would not have been readily capable of largescale, transoceanic migrations. In fact, while many extant elasmobranch taxa are globally ubiquitous, some form geographically restricted subpopulations with minimal gene flow between ocean basins (e.g., Castro et al., 2007; Castro, 2011; Blower et al., 2012; O'Leary et al., 2015; Andreotti et al., 2016; Bernard et al., 2016; Hillary et al., 2018; Sales et al., 2019; DeGroot et al., 2021). It seems likely that this situation would have also occurred between elasmobranchs in the Gulf of Mexico and eastern Pacific during the late stages of CAS closure across the Miocene–Pliocene boundary and that isolated, less mobile taxa were subsequently driven towards local extirpation.

CONCLUSIONS

The Venice Elasmobranch Assemblage consists of at least 45 taxa and is: 1) the most diverse elasmobranch assemblage reported by SCUBA diving submerged outcrop exposures known globally; 2) represents the most diverse, time-averaged elasmobranch assemblage reported from a single collecting region Florida; 3) is one of the most diverse late Cenozoic elasmobranch assemblages known from the USA, and 4) is one of several elasmobranch assemblages presently known to reflect the Miocene–Pliocene boundary in the USA (Tables 2–3). The 45 taxa in the Venice Elasmobranch Assemblage consist of benthic, neritic, and oceanic forms that are similar to extant species found in the Gulf of Mexico and Western North Atlantic Ocean today (e.g., Table 1; Bigelow and Schroeder, 1948a, 1948b, 1953; Castro, 2011; Last et al., 2016a; Ebert et al., 2021). The majority of the taxa in the Venice Elasmobranch Assemblage are represented by ectothermic, shallow water, tropical–subtropical species, including some with Indo-Pacific affinities, and 37 of 45 taxa are still represented in the modern oceans. The eight globally extinct taxa in the Venice Elasmobranch Assemblage are represented by carcharhiniform and lamniform sharks including the megatoothed shark, *O. megalodon*. Also apparent in the Venice Elasmobranch Assemblage is a mixing of large, macrophagous lamniform shark teeth with those from smaller carcharhiniform and batoid taxa.

Elasmobranch teeth are exceptionally abundant on the shallow Venice continental shelf because they are composed of durable, biogenic fluorapatite and have been concentrated into residual lag deposits as a result of shifting erosion and deposition largely driven by changes in climate and sea-level during the late Cenozoic (e.g., Haq and Ogg, 2024). These lag deposits represent the concentration and mixing of durable remains, including fossils, over several hundred thousand to several million years of time (e.g., Scott, 1988; Becker et al., 1998; Boessenecker et al., 2014; Maisch et al., 2015, 2018, 2019a, 2019b). Differing amounts of reworking has resulted in variable amounts of taphonomic wear and bioerosion on elasmobranch teeth across the Venice shelf (e.g., Maisch et al., 2019a).

In addition to influencing the concentration and preservation of fossil elasmobranch teeth on the Venice shelf, climatic and sea-level changes occurring during the late Cenozoic also impacted habitat availability, dispersal, and migratory abilities of many of the Venice taxa. In particular, the narrowing and shallowing of the CAS led to increased geographic isolation and restructured ocean currents, while cooling global temperatures and sea-level regression associated with increased ice sheet formation in the northern and southern hemispheres reduced shallow marine habitat, increased latitudinal temperature gradients, strengthened ocean currents, and redistributed nutrients. Collectively, these large-scale changes likely contributed to the global extinction of many macrophagous lamniform sharks including *O. megalodon* and the localized extirpation of smaller, benthic and neritic species from the Gulf of Mexico during the Pliocene, including *Heterodontus*, *Rhynchobatus*, and *Anoxypristis*.

ACKNOWLEDGMENTS

We would like to thank Captains B. Morrow and M. Konecnik for their assistance with field work, marine transportation, and allowing us to review their Venice fossil collections. We also thank C. Merrill, E. Hepworth, A. Lundberg, E. Schuth, M. Ryan, R. Miller, E. Reed, D. Pecora, M. Ellis, N. Hauser, G. Ayala, K. Geissinger, B. Judson, and P. Bakker for field and laboratory assistance. R. Scimeca and O. Yagy are thanked for

their assistance with graphic design. R. Narducci is thanked for creating a repository for the Venice specimens at FLMNH. Reviewers J. Kriwet and G. Cuny and editors O. Kovalchuk, Z. Barkaszi, and J. Rumford, helped improve an earlier version of this study. This research was funded in part by an FGCU Water School Grant, FGCU Career Advancement Award, and FGCU Whitaker Center for STEM Education Grant awarded to HMM.

REFERENCES

Abel, D. and Grubbs, R. 2020. Shark Biology and Conservation: Essentials for Educators, Students, and Enthusiasts. Johns Hopkins University Press, 430 p.

Adams, D., Mitchell, M., and Parsons, G. 1994. Seasonal occurrence of the white shark, *Carcharodon carcharias,* in waters off the Florida west coast, with notes on its life history. Marine Fisheries Review, 56:24–28.

Adnet, S. 2006. Nouvelles faunes de Sélaciens (Elasmobranchii, Neoselachii) de l'Éocène moyen des Landes (Sud-Ouest, France). Implication dans la connaissance des communautés de sélaciens d'eaux profondes. Palaeo Ichthyologica, 10:1–128.

Adnet, S., Cappetta, H., Guinot, G., and Notarbartolo di Sciara, G. 2012. Evolutionary history of the devilrays (Chondrichthyes: Myliobatiformes) from fossil and morphological inference. Zoological Journal of the Linnean Society, 166:132–159. https://doi.org/10.1111/j.1096-3642.2012.00844.x

Agassiz, L. 1833–1844. Recherches sur les Poissons fossiles. Imprimerie de Petitpierre. Neuchâtel and Soleure, Switzerland, 1–5. https://doi.org/10.5962/bhl.title.4275

Aines, A., Carlson, J., Boustany, A., Mathers, A., and Kohler, N. 2018. Feeding habits of the tiger shark, *Galeocerdo cuvier*, in the northwest Atlantic Ocean and Gulf of Mexico. Environmental Biology of Fishes, 101:403–415. https://doi.org/10.1007/s10641-017-0706-y

Allmon, W., Emslie, S., Jones, D., and Morgan, G. 1996. Late Neogene oceanographic change along Florida's west coast: evidence and mechanisms. The Journal of Geology, 104:143–162. https://doi.org/10.1086/629811

Andreotti, S., Rutzen, M., Van der Walt, S., Von der Heyden, S., Henriques, R., Meÿer, M., Oosthuizen, H., and Matthee, C. 2016. An integrated mark-recapture and genetic approach to estimate the population size of white sharks in South Africa. Marine Ecology Progress Series, 552:241–253. http://doi.org/:10.3354/meps11744

Andrianavalona, T., Ramihangihajason, T., Rasoamiaramanana, A., Ward, D., Ali, J., and Samonds, K. 2015. Miocene shark and batoid fauna from Nosy Makamby (Mahajanga Basin, Northwestern Madagascar). PLoS ONE, 10:e0129444. https://doi.org/10.1371/journal.pone.0129444

Antunes, M. and Balbino, A. 2004. Os carcharhiniformes (Chondrichthyes, Neoselachii) da Bacia de Alvalade (Portugal). Spanish Journal of Palaeontology, 19:73–92.

Antunes, M. and Balbino, A. 2006. Latest Miocene Myliobatids (Batoidei, Selachii) from the Alvalade Basin, Portugal. Cainozoic Research, 4:41–49.

Antunes, M. and Balbino, A. 2007. Rajiformes (Neoselachii, Batomorphii) from the Alvalade basin, Portugal. Annales de paléontologie, 93:107–119. https://doi.org/10.1016/j.annpal.2007.03.002

Antunes, M. and Jonet, S. 1970. Requins de l'Helvétien superieur et du Tortonien de Lisbonne. Revista da Faculdade de Ciências, Universidade de Lisboa 2. Série C, 16:119–280.

Antunes, M., Balbino, A., and Cappetta, H. 1999. Sélaciens du Miocene terminal du bassin d'Alvalade (Portugal), Essai de synthèse. Ciências Da Terra/Earth Sciences Journal, 13:115–129.

Apolín, J., González, G., and Martínez, J. 2004. Seláceos del Mioceno Superior de Quebrada Pajaritos (Piura, Perú). In Actas XII Congreso Peruano De Geología; Sociedad Geológica del Perú: Lima, Peru, pp. 401–404.

Applegate, S. 1972. A revision of the higher taxa of orectolobids. Journal of the Marine Biological Association of India, 14:743–751.
Applegate, S. 1978. Phyletic studies. Part. I. Tiger sharks. Universidad Nacional Autonoma de Mexico, Instituto de Geologia, Revista, 2:55–64.
Applegate, S. 1986. The El Cien Formation, strata of Oligocene and Early Miocene age in Baja California Sur. Universidad Nacional Autonoma de Mexico, Instituto de Geologia, Revista, 6:145–162.
Applegate, S. 1992. The case for dignathic heterodonty in fossil specimens of the tiger shark genus *Galeocerdo*. Journal of Vertebrate Paleontology, 12 (Supplement to Number 3), 16A.
Applegate, S. and Espinosa-Arrubarrena, L. 1996. The fossil history of *Carcharodon* and its possible ancestor, *Cretolamna*: a study in tooth identification, p. 19–36. In Klimley, A. and Ainley, D. (ed.), Great White Sharks: The Biology of *Carcharodon carcharias*. Academic Press, San Diego.
http://doi.org/10.1016/B978-012415031-7/50005-7
Aschliman, N. 2011. The Batoid Tree of Life: Recovering the Patterns and Timing of the Evolution of Skates, Rays and Allies (Chondrichthyes: Batoidea). Electronic Theses, Treatises and Dissertations. Paper 242.
Attrill, M. and Power, M. 2002. Climatic influence on a marine fish assemblage. Nature, 417: 275–278.
https://doi.org/10.1038/417275a
Ávila, S., Ramalho, R., and Vullo., R. 2012. Systematics, palaeoecology and palaeobiogeography of the Neogene fossil sharks from the Azores (Northeast Atlantic). Annales de Paléontologie, 98:167–189.
https://doi.org/10.1016/j.annpal.2012.04.001
Ayres, J. 1961. Fossil shark teeth near Venice, Fla. Rocks and Minerals, 36:512.
Bacon, C., Silvestro, D., Jaramillo, C., Smith, B., Chakrabarty, P., and Antonelli, A. 2015. Biological evidence supports an early and complex emergence of the Isthmus of Panama. Proceedings of the National Academy of Sciences, 112:6110–6115.
https://doi.org/10.1073/pnas.1423853112
Ball, M., Shinn, E., and Stockman, K. 1967. The geologic effects of Hurricane Donna in south Florida. The Journal of Geology, 75:583–597.
https://doi.org/10.1086/627283
Bancroft, E. 1831. On several fishes of Jamaica. Proceedings of the Committee of Science and Correspondence of the Zoological Society of London, 1:134–135.
Bangley, C., Edwards, M., Mueller, C., Fisher, R., Aguilar, R., Heggie, K., Richie, K., Ahr, B., and Ogburn, M. 2021. Environmental associations of cownose ray (*Rhinoptera bonasus*) seasonal presence along the US Atlantic Coast. Ecosphere, 12: p.e03743.
https://doi.org/10.1002/ecs2.3743
Bassos-Hull, K., Wilkinson, K., Hull, P., Dougherty, D., Omori, K., Ailloud, L., Morris, J., and Hueter, R. 2014. Life history and seasonal occurrence of the spotted eagle ray, *Aetobatus narinari*, in the eastern Gulf of Mexico. Environmental biology of fishes, 97:1039–1056.
https://doi.org/10.1007/s10641-014-0294-z
Becker, M., Slattery, W., and Chamberlain, J., Jr. 1996. Reworked Campanian and Maastrichtian macrofossils in a sequence bounding transgressive lag deposit, Monmouth County, New Jersey. Northeastern Geology and Environmental Science, 18:234–252.
Becker, M., Slattery, W., and Chamberlain, J., Jr. 1998. Mixing of Santonian and Campanian chondrichthyan and ammonite macrofossils along a transgressive lag deposit, Greene County, western Alabama. Southeastern Geology, 37:205–216.
Becker, M., Chamberlain, J., Jr., and Wolf, G. 2006. Chondrichthyans from the Arkadelphia Formation (Upper Cretaceous: upper Maastrichtian) of Hot Spring County, Arkansas. Journal of Paleontology, 80:700–716.
https://doi.org/10.1666/0022-3360(2006)80[700:CFTAFU]2.0.CO;2
Berg, L. 1937. A classification of fish-like vertebrates. Izvestiya Akademii Nauk USSR, Seriya Biologischeskaya, 4:1277–1280. (In Russian)
Berg, L. 1940. Classification of fishes, both recent and fossil. Trudy Zoologicheskogo Instituta, Akademiia Nauk SSSR, 5:87–345. (In Russian)
Berg, L. 1958. System rezenten und fossilen Fischartigen und Fisch. Hochschulbücher für Biologie. Deutscher Verlag der Wissenschaften, Berlin, Germany, 310 p.

Berkovitz, B. and Shellis, P. 2017. The Teeth of Non-Mammalian Vertebrates. Academic Press, 354 p.
https://doi.org/10.1016/C2014-0-02210-1

Bernard, A., Feldheim, K., Heithaus, M., Wintner, S., Wetherbee, B., and Shivji, M. 2016. Global population genetic dynamics of a highly migratory, apex predator shark. Molecular Ecology, 25:5312–5329.
https://doi.org/10.1111/mec.13845

Betancort, J., Lomoschitz, A., and Meco, J. 2016. Early Pliocene fishes (Chondrichthyes, Osteichthyes) from Gran Canaria and Fuerteventura (Canary Islands, Spain). Estudios Geológicos, 72:e054.
https://doi.org/10.3989/egeol.42380.399

Bice, K. and Shimada, K. 2016. Fossil marine vertebrates from the Codell Sandstone Member (middle Turonian) of the Upper Cretaceous Carlile Shale in Jewell County, Kansas, USA. Cretaceous Research, 65:172–198.
https://doi.org/10.1016/j.cretres.2016.04.017

Bigelow, H. and Schroeder, W. 1948a. Fishes of the western North Atlantic, Part I: Lancelets, Cyclostomes, Sharks, p. 59–576. In Tee-Van, J., Breder, C., Hildebrand, S., Parr, A., and Schroeder, W. (eds.), Fishes of the Western North Atlantic. Part 1. Sears Foundation for Marine Research, Yale University, New Haven.

Bigelow, H. and Schroeder, W. 1948b. New genera and species of batoid fishes. Journal of Marine Research, 7:543–566.

Bigelow, H. and Schroeder, W. 1951. Three new skates and a new chimaerid fish from the Gulf of Mexico. Journal of the Washington Academy of Sciences, 41:383–392.

Bigelow, H. and Schroeder, W. 1953. Sharks, sawfishes, guitarfishes, skates and rays. Chimaeroids, p. 1–514. In Tee-Van, J., Breder, C., Hildebrand, S., Parr, A., and Schroeder, W. (eds.), Fishes of the Western North Atlantic. Part 2. Sears Foundation for Marine Research, Yale University, New Haven.

Billups, K., Ravelo, A., Zachos, J., and Norris, R. 1999. Link between oceanic heat transport, thermohaline circulation, and the Intertropical Convergence Zone in the early Pliocene Atlantic. Geology, 27:319–322.
https://doi.org/10.1130/0091-7613(1999)027<0319:LBOHTT>2.3.CO;2

Blainville, H. 1816. Prodrome d'une nouvelle distribution systematique de regne animal. Bulletin de Sciences de la Société Philomatique de Paris, 8:113–124.

Blake, C. 1862. Shark's teeth at Panama. Geologist, 5:316.

Bloch, M. and Schneider, J. 1801. M.E. Blochii Systema Ichthyologiae iconibus ex illustratum. Post obitum auctoris opus inchoatum absolvit, correxit, interpolavit. J.G. Schneider, Saxo, 584 p., 110 pl.
https://doi.org/10.5962/bhl.title.5750

Blower, D., Pandolfi, J., Bruce, B., Gomez-Cabrera, M., and Ovenden, J. 2012. Population genetics of Australian white sharks reveals fine-scale spatial structure, transoceanic dispersal events and low effective population sizes. Marine Ecology Progress Series, 455:229–244.
https://doi.org/10.3354/meps09659

Boessenecker, R. 2011. A new marine vertebrate assemblage from the Late Neogene Purisima Formation in central California, Part I: fossil sharks, bony fish, birds, and implications for the age of the Purisima Formation west of the San Gregorio Fault. Palarch's Journal of Vertebrate Palaeontology, 8:1–30.

Boessenecker, R. 2016. First record of the megatoothed shark Carcharocles megalodon from the Mio-Pliocene Purisima Formation of Northern California. PaleoBios, 33:1–7.
http://doi.org/10.5070/P9331032076

Boessenecker, R., Perry, F., and Schmitt, J. 2014. Comparative Taphonomy, Taphofacies, and Bonebeds of the Mio-Pliocene Purisima Formation, Central California: Strong Physical Control on Marine Vertebrate Preservation in Shallow Marine Settings. PLoS ONE, 9:e91419.
https://doi.org/10.1371/journal.pone.0091419

Boessenecker, S., Boessenecker, R., and Geisler, J. 2018. Youngest record of the extinct walrus Ontocetus emmonsi from the Early Pleistocene of South Carolina and a review of North Atlantic walrus biochronology. Acta Palaeontologica Polonica, 63:279–286.
https://doi.org/10.4202/app.00454.2018

Boessenecker, R., Ehret, D., Long, D., Churchill, M., Martin, E., and Boessenecker, S. 2019. The Early Pliocene extinction of the mega-toothed shark Otodus megalodon: a view from the eastern North Pacific. PeerJ, 7:e6088. https://doi.org/10.7717/peerj.6088

Bonaparte, C. 1832–1841. Iconografia della fauna Italica, per le quattro classi degli animali vertebrati. 3 (Pesci). Rome, Tipographia Salviucci, 78 color plates.

Bonnaterre, J. 1788. Ichthyologie. Tableau encyclopédique et méthodique des trois règnes de la nature. Paris, 215 p., pl. A–B + 1–100.

Bor, T., Reinecke, T., and Verschueren, S. 2012. Miocene Chondrichthyes from Winterswijk-Miste, the Netherlands. Palaeontos, 21:1–136.

Boss, S., Hoffman, C., and Cooper, B. 2002. Influence of fluvial processes on the Quaternary geologic framework of the continental shelf, North Carolina, USA. Marine Geology, 183:45–65.

Boyd, B. 2016. Fossil sharks and rays of Gainesville creeks Alachua County, Florida: Hawthorn Group (middle Miocene to lower Pliocene). Florida Paleontological Society Special Papers, p.1–40.

Branstetter, S. 1981. Biological notes on the sharks of the north central Gulf of Mexico. Contributions in Marine Science, 24:13–24.

Branstetter, S. 1987. Age, growth and reproductive biology of the silky shark, *Carcharhinus falciformis*, and the scalloped hammerhead, *Sphyrna lewini*, from the northwestern Gulf of Mexico. Environmental Biology of Fishes, 19:161–173.

Breder, C. 1952. On the utility of the saw of the sawfish. Copeia, 1952:90–91.

Brodkorb, P. 1963. Miocene birds from the Hawthorne Formation. Quarterly Journal of the Florida Academy of Sciences, 26:159–167.

Brown, R., 1988. Florida's Fossils: Guide to Location, Identification, and Enjoyment. Pineapple Press, 216 p.

Browning, J., Miller, K., Sugarman, P., Kominz, M., McLaughlin, P., Kulpecz, A., and Feigenson, M. 2008. 100 Myr record of sequences, sedimentary facies and sea level change from Ocean Drilling Program onshore coreholes, US mid?Atlantic coastal plain. Basin Research, 20:227–248. https://doi.org/10.1111/j.1365-2117.2008.00360.x

Bryan, J., Scott, T., and Means, G. 2008. Roadside Geology of Florida. Mountain Press Publishing Company, Missoula, Montana, 376 p.

Byler, J. 2017. The identification, structure, care, and conservation of sawfish rostra (Rhinopristiformes: Pristidae). Society for the Preservation of Natural History Collections. Collection Forum, 31:1–14.

Cahill, B., Eckert, R., Bassos-Hull, K., Ostendorf, T., Voss, J., DeGroot, B., and Ajemian, M. 2023. Diet and feeding ecology of the whitespotted eagle ray *(Aetobatus narinari)* from Florida coastal waters revealed via DNA barcoding. Fishes, 8:388. https://doi.org/10.3390/fishes8080388

Cappetta, H. 1970. Les Sélaciens du Miocène de la région de Montpellier. Palaeovertebrata, Mémoire extraordinaire, 1–139 p.

Cappetta, H. 1980. Modification du statut générique de quelques espèces de sélaciens crétacés et tértiares. Palaeovertebrata, 10:29–42.

Cappetta, H. 1986. Myliobatidae nouveaux (Neoselachii, Batomorphii) de l'Yprésien des Ouled Abdoun, Maroc. Geologica et Palaeontologica, 20:185–207.

Cappetta, H. 2012. Chondrichthyes (Mesozoic and Cenozoic Elasmobranchii: Teeth, In Schultze H., Handbook of Paleoichthyology, Vol. 3E. Verlag F. Pfeil, München, 512 p.

Cappetta, H. and Case, G. 2016. A selachian fauna from the middle Eocene (Lutetian, Lisbon Formation) of Andalusia, Covington County, Alabama, USA. Palaeontographica Abteilung A, 307:43–103. https://doi.org/10.1127/pala/307/2016/43

Cappetta, H. and Cavallo, O. 2006. Les sélaciens du Pliocène de la région d'Alba (Piémont, Italie Nord-Ouest). Rivista Piemontese di Storia Naturale, 27:261–304.

Carnevale, G., Marsili, S., Caputo, D., and Egisti, L. 2006. The silky shark *Carcharhinus falciformis* (Bibron, 1841) in the Pliocene of Cava Serredi (Fine Basin, Italy). Neues Jahrbuch für Geologie und Palaontologie, Abhandlungen, 242:357–370.

Carrier, J. 2017. Sharks of the Shallows: Coastal Species in Florida and the Bahamas. Johns Hopkins University Press, 212 p.

Carrillo-Briceno, J., Gonzalez-Barba, G., Landaeta, M., and Nielsen, S. 2013. Condrictios fósiles del Plioceno Superior de la Formación Horcón Región de Valparaíso, Chile central. Revista chilena de historia natural, 86:191–206. https://doi.org/10.4067/S0716-078X2013000200008

Carrillo-Briceño, J., Aguilera, O., and Rodriguez, F. 2014. Fossil chondrichthyes from the central eastern Pacific Ocean and their paleoceanographic significance. Journal of South American Earth Sciences, 51:76–90. https://doi.org/10.1016/j.jsames.2014.01.001

Carrillo-Briceno, J., De Gracia, C., Pimiento, C., Aguilera, O., Kindlimann, R., Santamarina, P., and Jaramillo, C. 2015a. A new Late Miocene chondrichthyan assemblage from the Chagres Formation, Panama. Journal of South American Earth Sciences, 60:56–70. https://doi.org/10.1016/j.jsames.2015.02.001

Carrillo-Briceño, J., Maxwell, E., Aguilera, O., Sánchez, R., and Sánchez-Villagra, M. 2015b. Sawfishes and other elasmobranch assemblages from the Mio-Pliocene of the South Caribbean (Urumaco sequence, northwestern Venezuela). PLoS ONE, 10:e0139230. https://doi.org/10.1371/journal.pone.0139230

Carrillo-Briceño, J., Aguilera, O., De Gracia, C., Aguirre-Fernández, G., Kindlimann, R., and Sánchez-Villagra, M. 2016a. An Early Neogene Elasmobranch fauna from the southern Caribbean (Western Venezuela). Palaeontologia Electronica 19.2.27A:1–32. https://doi.org/10.26879/664

Carrillo-Briceño, J., Argyriou, T., Zapata, V., Kindlimann, R., and Jaramillo, C. 2016b. A new Early Miocene (Aquitanian) Elasmobranchii assemblage from the La Gaujira Peninsula, Colombia. Ameghiniana, 53:77–99. https://doi.org/10.5710/AMGH.26.10.2015.2931

Carrillo-Briceño, J., Carillo, J., Aguilera, O.A., and Sanchez-Villagra, M. 2018. Shark and ray diversity in the Tropical America (Neotropics)—an examination of environmental and historical factors affecting diversity. PeerJ, 6:e5313. https://doi.org/10.7717/peerj.5313

Carrillo-Briceño, J., Luz, Z., Hendy, A., Kocsis, L., Aguilera, O., and Vennemann, T. 2019. Neogene Caribbean elasmobranchs: diversity, paleoecology and paleoenvironmental significance of the Cocinetas Basin assemblage (Guajira Peninsula, Colombia). Biogeosciences, 16:33–56. https://doi.org/10.5194/bg-16-33-2019

Cartmell, C. 1988. Let's go fossil shark tooth hunting: a guide for identifying sharks and where and how to find their superbly formed fossilized teeth. Natural Science Research, 76 p.

Case, E. 1934. A specimen of long-nosed dolphin from the Bone Valley gravels of Polk County, Florida. Contributions from the Museum of Paleontology, University of Michigan, 4:105–113.

Case, G. 1980. A selachian fauna from the Trent Formation, Lower Miocene (Aquitanian) of Eastern North Carolina. Palaeontographica Abteilung A: Palaozoologie-Stratigraphie, 171:75–103.

Casier, E. 1954. Essai de Paléobiogéographie des Euselachii. Mémoir Jubilaire V. Van Straelen 2:575–640.

Castro, J. 2011. The Sharks of North America. Oxford University Press, 613 p.

Castro, A., Stewart, B., Wilson, S., Hueter, R., Meekan, M., Motta, P., Bowen, B., and Karl, S. 2007. Population genetic structure of Earth's largest fish, the whale shark (*Rhincodon typus*). Molecular Ecology, 16:5183–5192. https://doi.org/10.1111/j.1365-294X.2007.03597.x

Castro-Aguirre, J., Antuna-Mendiola, A., González-Acosta, A., and de La Cruz-Agüero, J. 2005. *Mustelus albipinnis* sp. nov. (Chondrichthyes: Carcharhiniformes: Triakidae) de la costa surroccidental de Baja California Sur, México. Hidrobiológica, 15:123–130.

Cathcart, J. 1989. Economic Geology of the Land Pebble Phosphate District and its Southern Extension, p. 18–38. In Scott, T., and Cathcart, J. (eds.), Florida Phosphate Deposits, International Geologic Congress, 28th, Washington D.C., Field trip guidebook T 178.

Chabot, C. and Allen, L. 2009. Global population structure of the tope (*Galeorhinus galeus*) inferred by mitochondrial control region sequence data. Molecular Ecology, 18:545–552. https://doi.org/10.1111/j.1365-294X.2008.04047.x

Chandler, A. 1921. A new species of ray from the Texas coast, and report of the occurrence of a top minnow new to the fauna of eastern Texas. Proceedings of the United States National Museum, 59:657–658.

Chandler, R., Chiswell, K., and Faulkner, G. 2006. Quantifying a possible Miocene phyletic change in *Hemipristis* (Chondrichthyes) teeth. Palaeontologia Electronica, 9:1–14.

Chirichigno, F. 1973. Nuevas especies de peces de los generos *Mustelus* (Fam. Triakidae), *Raja* (Fam. Rajidae) y *Schedophilus* (Fam. Centrolophidae). Informes Especiales, Instituto del Mar del Perú, 42:1–40.

Cicimurri, D. and Ebersole, J. 2015. Two new species of *Pseudaetobatus* Cappetta, 1986 (Batoidei: Myliobatidae) from the southeastern United States. Palaeontologia Electronica, 18.1.15A:1–17.
https://doi.org/10.26879/524

Cicimurri, D. and Knight, J. 2009. Late Oligocene sharks and rays from the Chandler Bridge Formation, Dorchester County, South Carolina, USA. Acta Palaeontologica Polonica, 54:627–647.

Cigala-Fulgosi, F. and Mori, D. 1979. Osservazioni tassonomiche sul genere *Galeocerdo* (Selachii, Carcharhinidae) con particolare riferimento a *Galeocerdo cuvieri* (Péron & Lesueur) nel Pliocene del Mediterraneo. Bollettino della Società Paleontologica Italiana, 18:117–132.

Cigala-Fulgosi, F., Casati, S., Orlandini, A., and Persico, D. 2009. A small fossil fish fauna, rich in *Chlamydoselachus* teeth, from the Late Pliocene of Tuscany (Siena, central Italy). Cainozoic Research, 6:3–23.

Cione, A., Cozzuol, M., Dozo, M., and Acosta Hospitaleche, C., 2011. Marine vertebrate assemblages in the southwest Atlantic during the Miocene. Biological Journal of the Linnean Society, 103:423–440.
https://doi.org/10.1111/j.1095-8312.2011.01685.x

Cione, A., Cabrera, D., and Barla, M. 2012. Oldest record of the great white shark (Lamnidae, *Carcharodon*; Miocene) in the Southern Atlantic. Geobios, 45:167–172.
https://doi.org/10.1016/j.geobios.2011.06.002

Clark, E. and von Schmidt, K. 1965. Sharks of the central Gulf coast of Florida. Bulletin of Marine Science, 15:13–83, figs. 1–18.

Clinton, J., Visaggi, C., Perez, V., Tweet, J., and Santucci, V. 2023. Fossil chondrichthyans and other new paleontological resources at Gulf Islands National Seashore, p. 143–154. In Lucas, S., Morgan, G., Hunt, A., and Lichtig, A. (Eds.), Fossil Record 9, Volume 94 of the New Mexico Museum of Natural History and Science Bulletin.

Coates, A., Collins, L., Aubry, M., and Berggren, W. 2004. The geology of the Darien, Panama, and the late Miocene–Pliocene collision of the Panama arc with northwestern South America. Geological Society of America Bulletin, 116:1327–1344.
https://doi.org/10.1130/B25275.1

Collareta, A., Landini, W., Chacaltana, C., Valdivia, W., Altamirano-Sierra, A., Urbina-Schmitt, M., and Bianucci, G. 2017a. A well preserved skeleton of the fossil shark *Cosmopolitodus hastalis* from the late Miocene of Peru, featuring fish remains as fossilized stomach contents. Rivista Italiana di Paleontologia e Stratigrafia, 123:11–22.

Collareta, A., Casati, S., Catanzariti, R., and Di Cencio, A. 2017b. First record of the knifetooth sawfish *Anoxypristis* (Elasmobranchii: Rhinopristiformes) from the Pliocene of Tuscany (central Italy). Neus Jahrbuch Für Geologie Und Paläontologie. Abhandlungen, 284:289–297.
https://doi.org/10.1127/njgpa/2017/0663

Collareta, A., Casati, S., and Di Cencio, A. 2017c. A pristid sawfish from the lower Pliocene of Lucciolabella (Radicofani basin, Tuscany, central Italy). Atti della Società Toscana di Scienze Naturali, Memorie, Serie A, p. 49–55.
https://doi.org/10.2424/ASTSN.M.2017.18

Collareta, A., Merella, M., Casati, S., Coletti, G., and Di Cencio, A. 2021. Another thermophilic "Miocene survivor" from the Italian Pliocene: A geologically young occurrence of the pelagic eagle ray *Aetobatus* in the Euro-Mediterranean region. Carnets de Geologie, 21:203–214.
https://doi.org/10.2110/carnets.2021.2110

Collareta, A., Casati, S., and Di Cencio, A. 2023. The palaeobiology of the false mako shark, *Parotodus benedenii* (Le Hon, 1871): A view from the Pliocene Mediterranean Sea. Journal of Marine Science and Engineering, 11:1990.
https://doi.org/10.3390/jmse11101990

Collins, A., Heupel, M., Hueter, R., and Motta, P. 2007. Hard prey specialists or opportunistic generalists? An examination of the diet of the cownose ray, *Rhinoptera bonasus*. Marine and

Freshwater Research, 58:135–144.
http://doi.org/10.1071/MF05227
Compagno, L. 1973. Interrelationships of living elasmobranchs. Journal of the Linnaean Society (Zoology), 53:63–98.
Compagno, L. 1988. Sharks of the Order Carcharhiniformes. Blackburn Press, 570 p.
Compagno, L. and Last, P. 1999. Order Pristiformes, p. 1397–2068. In Carpenter, K. and Niem, V. (eds.), The living marine resources of the western central Pacific Vol 3. Batoid fishes, chimaeras and bony fishes, part 1 (Elopidae to Linophyroidae). FAO, Rome.
Compagno, L., Dando, M., and Fowler, S. 2005. Sharks of the World. Princeton University Press, Princeton, N.J, 496 p.
Compton, J. 1997. Origin, age, and paleoceanographic significance of Florida's phosphorite deposits, p. 195–216. In Randazzo, A.F. and Jones, D. (eds.), The Geology of Florida. University Press of Florida, Gainesville, Florida.
Compton, J., Hodell, D., Garrido, J., and Mallinson, D. 1993. Origin and age of phosphorite from the south-central Florida Platform: Relation of phosphogenesis to sea-level fluctuations and $\delta^{13}C$ excursions. Geochimica et Cosmochimica Acta, 57:131–146.
Conan, A., Dennis, M., Gilbert, K., Lenain, E., Bruns, S., and Henderson, A. 2023. Occurrence of the endangered whitespotted eagle ray *Aetobatus narinari* around the Lesser Antilles island of Saint Kitts: a photo-identification study. Environmental Biology of Fishes, 106:1529–1538.
https://doi.org/10.1007/s10641-023-01431-z
Cook, T., Murray, A., Simons, E., Attia, Y., and Chatrath, P. 2010. A Miocene selachian fauna from Moghra, Egypt. Historical Biology, 22:78–87.
https://doi.org/10.1080/08912960903249329
Cooke, C. 1945. Geology of Florida. Bulletin of the Florida Geological Survey, 29:1–339.
Cope, E. 1867. An addition to the vertebrate fauna of the Miocene period, with a synopsis of the extinct Cetacea of the United States. Proceedings of the Academy of Natural Sciences of Philadelphia, 19:138–156.
Cortés, E., Brooks, E., Apostolaki, P., and Brown, C. 2006. Stock assessment of dusky shark in the US Atlantic and Gulf of Mexico. Panama City Laboratory Contribution, 6:1–155.
Covington, J. 1992. Neogene nannofossils of Florida, p. 52. In Harris, W. and Zullo, V. (eds.), The Florida Neogene, Abstract Volume, The Third Bald Head Island Conference on Coastal Plains Geology.
Cumbaa, S., Shimada, K., and Cook, T. 2010. Mid-Cenomanian vertebrate faunas of the Western Interior Seaway of North America and their evolutionary, paleobiogeographical, and paleoecological implications. Palaeogeography, Palaeoclimatology, Palaeoecology, 295:199–214.
https://doi.org/10.1016/j.palaeo.2010.05.038
Cunningham, K., Locker, S., Hine, A., Bukry, D., Barron, J., and Guertin, L. 2003. Interplay of late Cenozoic siliciclastic supply and carbonate response on the southeast Florida platform. Journal of Sedimentary Research, 73:31–46.
https://doi.org/10.1306/062402730031
Curtis, T., Adams, D., and Burgess, G. 2011. Seasonal distribution and habitat associations of bull sharks in the Indian River Lagoon, Florida: a 30-year synthesis. Transactions of the American Fisheries Society, 140:1213–1226.
https://doi.org/10.1080/00028487.2011.618352
Cuvier, G. 1816. Le Règne Animal distribué d'après son organisation pour servir de base à l'histoire naturelle des animaux et d'introduction à l'anatomie comparée. Les reptiles, les poissons, les mollusques et les annélides. Deterville, Paris, 532 p.
Cuvier, G. 1829. Le règne animal, distribué d'après son organisation, pour servir de base à l'histoire naturelle des animaux et d'introduction à l'anatomie comparée. Edition 2. Paris, Déterville, de l'Impr. de A. Belin.
da Silva Rodrigues-Filho, L., da Costa Nogueira, P., Sodré, D., da Silva Leal, J., Nunes, J., Rincon, G., Lessa, R., Sampaio, I., Vallinoto, M., Ready, J., and Sales, J. 2023. Evolutionary history and taxonomic reclassification of the critically endangered daggernose shark, a species endemic to the Western Atlantic. Journal of Zoological Systematics and Evolutionary Research, 2023:4798805.
https://doi.org/10.1155/2023/4798805
Daimeries, A. 1889. Notes ichthyologiques. IV. Annales de la Société royale malacologique de Belgique, Bulletin des des Séances, 24:5–10.

Dames, W. 1883. Über eine tertiäre Wirbelthierfauna von der westlichen Insel der Birket-El-Qrûn im Fajum (Aegypten). Sitzungsberichte der Königlich Preussischen Akademie der Wissenschaften zu Berlin, 6:129–153.
Darteville, E. and Casier, E. 1943. Les poissons fossiles du Bas-Congo et des régions voisines. Annales du Musée du Congo Belge, Sér. A (Minéralogie Géologie, Paléontologie), 3:1–200.
Darteville, E. and Casier, E. 1959. Les poissons fossiles du Bas-Congo et des régions voisines. Annales du Musée du Congo Belge, Sér. A (Minéralogie Géologie, Paléontologie) 3, 2:257–568.
Davies, D. 1964. The Miocene shark fauna of the southern St. Lucia area. Oceanographic Research Institute, 1–16.
Dawdy, A., Peterson, C., Keller, B., and Grubbs, R. 2022. Tidal and diel effects on the movement and space use of bull sharks (*Carcharhinus leucas*) and bonnetheads (*Sphyrna tiburo*) in a Florida Estuary. Environmental Biology of Fishes, 105:1713–1727. https://doi.org/10.1007/s10641-022-01264-2
Day, T., 1886. Phosphate Rock. United States Geological Survey, Mineral Resources of the United States for 1885. United States Geological Survey, p. 445–454.
De Muizon, C. and De Vries, T. 1985. Geology and paleontology of the Late Cenozoic marine deposits in the Sacaco area (Peru). Geologische Rundschau, 74:547–563.
De Schutter, P., Van der Vliet, R., Bor, T. 2021. Dental evolution of the 'serrated' mako shark, *Isurus subserratus* aka *I. escheri* (Chondrichthyes, Lamnidae) in the late Neogene of the North Sea Basin. Cainozoic Research, 21:173–192.
Dean, M., Bizzarro, J., Clark, B., Underwood, C., and Johanson, Z. 2017. Large batoid fishes frequently consume stingrays despite skeletal damage. Royal Society Open Science, 4:170674. https://doi.org/10.1098/rsos.170674
DeGroot, B., Bassos-Hull, K., Wilkinson, K., Lowerre-Barbieri, S., Poulakis, G., and Ajemian, M. 2021. Variable migration patterns of whitespotted eagle rays *Aetobatus narinari* along Florida's coastlines. Marine Biology, 168:1–21. https://doi.org/10.1007/s00227-021-03821-2
del Moral-Flores, L., Ramírez-Antonio, E., Angulo, A., Pérez-Ponce de León, G. 2015. *Ginglymostoma unami* sp. nov. (Chondrichthyes: Orectolobiformes: Ginglymostomatidae): una especie nueva de tiburón gata del Pacífico oriental tropical. Revista Mexicana de Biodiversidad, 86:48–58. https://doi.org/10.7550/rmb.46192
Delfortrie, E. 1871. Les broyeurs du Tertiaire aquitanien. Actes de la Société linnéenne de Bordeaux, 23:213–236.
Dodd Jr, C. and Morgan, G. 1992. Fossil sea turtles from the early Pliocene Bone Valley Formation, central Florida. Journal of Herpetology, 26:1–8.
Dodrill, J. 1977. A hook and line survey of the sharks of Melbourne Beach, Brevard County, Florida. Masters Thesis. Florida Institute of Technology, Melbourne, 304 p.
Doyle, T., Smith, T., III, and Robblee, M. 1995. Wind damage effects of Hurricane Andrew on mangrove communities along the southwest coast of Florida, USA. Journal of Coastal Research, Special Issue Number 21: Impacts of Hurricane Andrew on the Coastal Zones of Florida and Louisiana, p. 159–168.
Driggers, III, W., Hoffmayer, E., and Hickerson, E. 2011. Validating the occurrence of Caribbean reef sharks, *Carcharhinus perezi* (Poey), (Chondrichthyes: Carcharhiniformes) in the northern Gulf of Mexico, with a key for sharks of the family Carcharhinidae inhabiting the region. Zootaxa, 2933:65–68. https://doi.org/10.11646/zootaxa.2933.1.6
Dudley, S., Anderson-Reade, M., Thompson, G., and McMullen, P. 2000. Concurrent scavenging off a whale carcass by great white sharks, *Carcharodon carcharias*, and tiger sharks, *Galeocerdo cuvier*. Fishery Bulletin–National Oceanic and Atmospheric Administration, 98:646–649.
Dulvy, N., Davidson, L., Kyne, P., Simpfendorfer, C., Harrison, L., Carlson, J., and Fordham, S. 2016. Ghosts of the coast: global extinction risk and conservation of sawfishes. Aquatic Conservation: Marine and Freshwater Ecosystems, 26:134–153. https://doi.org/10.1002/aqc.2525
Ebersole, J., Ebersole, S., and Cicimurri, D. 2017. The occurrence of early Pleistocene marine fish remains from the Gulf Coast of Mobile County, Alabama, USA. Palaeodiversity, 10:97–

115.
https://doi.org/10.18476/pale.v10.a6
Ebersole, J., Cicimurri, D., and Stringer, G. 2019. Taxonomy and biostratigraphy of the elasmobranchs and bony fishes (Chondrichthyes and Osteichthyes) of the lower-to-middle Eocene (Ypresian to Bartonian) Claiborne Group in Alabama, USA, including an analysis of otoliths. European Journal of Taxonomy, 585:1–274.
https://doi.org/10.5852/ejt.2019.585
Ebersole, J., Kelosky, A., Huerta-Beltrán, B., Cicimurri, D., and Drymon, J. 2023. Observations on heterodonty within the dentition of the Atlantic Sharpnose Shark, *Rhizoprionodon terraenovae* (Richardson, 1836), from the north-central Gulf of Mexico, USA, with implications on the fossil record. PeerJ, 11:e15142.
https://doi.org/10.7717/peerj.15142
Ebert, D., Dando, M., and Fowler, S., 2021. Sharks of the world: a complete guide. Princeton University Press, Princeton, New Jersey, 608 p.
Ehrenbaum, E. 1915. Über Küstenfische von Westafrika, besonders von Kamerun. Friedrichsen & Co., Hamburg, 85 p.
Ehret, D., Hubbell, G., and MacFadden, B. 2009. Exceptional preservation of the white shark *Carcharodon* (Lamniformes, Lamnidae) from the early Pliocene of Peru. Journal of Vertebrate Paleontology, 29:1–13.
https://doi.org/10.1671/039.029.0113
Ehret, D., MacFadden, B., Jones, D., Devries, T., Foster, D., and Salas-Gismondi, R. 2012. Origin of the white shark *Carcharodon* (Lamniformes: Lamnidae) based on recalibration of the upper Neogene Pisco Formation of Peru. Palaeontology, 55:1139–1153.
https://doi.org/10.1111/j.1475-4983.2012.01201.x
Ercolani, C., Muller, J., Collins, J., Savarese, M., and Squiccimara, L. 2015. Intense Southwest Florida hurricane landfalls over the past 1000 years. Quaternary Science Reviews, 126:17–25.
https://doi.org/10.1016/j.quascirev.2015.08.008
Euphrasen, B. 1790. *Raja (Narinari).* Kongliga Vetenskaps Akademiens nya Handlingar, Stockholm, 11: 217–219, Pl. 10.
Everhart, M. 2007. New stratigraphic records (Albian-Campanian) of *Rhinobatos* sp. (Chondrichthyes; Rajiformes) from the Cretaceous of Kansas. Transactions of the Kansas Academy of Science, 110:225–235.
https://doi.org/10.1660/0022-8443(2007)110[225:NSRAOR]2.0.CO;2
Evermann, B. and Jenkins, O. 1891. Report upon a collection of fishes made at Guaymas, Sonora, Mexico, with descriptions of new species. Proceedings of the United States National Museum, 14:121–164.
Fagherazzi, S., Howard, A., and Wiberg, P. 2004. Modeling fluvial erosion and deposition on continental shelves during sea level cycles. Journal of Geophysical Research: Earth Surface, 109:F03010.
https://doi.org/10.1029/2003JF000091
Faria, V., McDavitt, M., Charvet, P., Wiley, T., Simpfendorfer, C., and Naylor, G. 2013. Species delineation and global population structure of Critically Endangered sawfishes (Pristidae). Zoological Journal of the Linnean Society, 167:136–164.
https://doi.org/10.1111/j.1096-3642.2012.00872.x
Fernandez-Carvalho, J., Imhoff, J., Faria, V., Carlson, J., and Burgess, G. 2014. Status and the potential for extinction of the largetooth sawfish *Pristis pristis* in the Atlantic Ocean. Aquatic Conservation: Marine and Freshwater Ecosystems, 24:478–497.
https://doi.org/10.1002/aqc.2394
Fialho, P., Balbino, A., and Antunes, M. 2019. Langhian rays (Chondrichthyes, Batomorphii) from Brielas, Lower Tagus Basin, Portugal. Geologica Acta, 17:1–16.
Fialho, P., Balbino, A., Legoinha, P., and Antunes, M. 2021. Shark fossil diversity (Squalomorphii, Squatinomorphii, and Galeomorphii) from the Langhian of Brielas (Lower Tagus Basin, Portugal). Geological Journal, 56:405–421.
https://doi.org/10.1002/gj.3965
Fink, B. 2004. Fossil Shark's Teeth and Other Fossils: A Photo Identification Guide, 28 p. Florida Dept. of State. Accessed 9/25/2024:
https://dos.fl.gov/historical/archaeology/projects/manasota-key-offshore/

Flemming, C. and McFarlane, D. 1998. New Caribbean locality for the extinct Great White Shark *Carcharodon megalodon*. Caribbean Journal of Science, 34:317–318.
FLMNH Vertebrate Fossil Sites. Accessed 9-25-2024: https://www.floridamuseum.ufl.edu/florida-vertebrate-fossils/sites/
Forsskål, P. 1775. Descriptiones animalium, avium, amphibiorum, piscium, insectorum, vermium, quae in itinere orientali observavit. –20 + XXXIV + 164pp.; Hauniae (ex officina Mölleri).
Fountain, R., Hurst, M. and Brown, D., 1993. The Geology of the Central Florida Phosphate District: A Comparison of the Bone Valley Deposits vs. the Southern Extension Deposits. Chp. 17, p. 165–169. In El-Shall, H., Moudgill, B., and Wiegel, R. (eds.), Beneficiation of Phosphate: Theory and Practice.
Frazier, T., Wood, N., Yarnal, B., and Bauer, D. 2010. Influence of potential sea level rise on societal vulnerability to hurricane storm-surge hazards, Sarasota County, Florida. Applied Geography, 30:490–505. https://doi.org/10.1016/j.apgeog.2010.05.005
Fuqua, R. 2011. Hunting Fossil Shark Teeth in Venice, Florida: The Complete Guide: On the Beach, SCUBA Diving, and Inland, 80 p.
Fuqua, R. 2017. Fossil Shark Teeth of Venice, Florida: The Paleontology Behind How Shark Teeth, and other Fossils, Ended up in the Venice Area. 70 pp.
Fuqua, R. 2020. Florida Fossil Shark Teeth Identification Guide: The Fossil Shark Teeth Most Commonly Found in Florida, 36 p.
Garcia, F. and Miller, D., 1998. Discovering fossils: How to find and identify remains of the prehistoric past. Stackpole Books, 212 p.
Garman, S. 1880. Synopsis and descriptions of the American Rhinobatidae. Proceedings of the United States National Museum, 3:516–523.
Garman, S. 1881. Reports on the results of dredging, under the Supervision of 'Alexander Agassiz, along the Atlantic coast of the United States during the summer of 1880, by the U. S. Coast Survey Steamer "Blake," Commander J. R. Bartlett, U. S. N., commanding. XII. Reports on the Selachians. Bulletin of the Museum of Comparative Zoology at Harvard College, 8:231–237.
Garman, S. 1885. Notes and descriptions taken from selachians in the U. S. National Museum. Proceedings of the United States National Museum, 8:39–44.
Garman, S. 1908. New Plagiostomia and Chismopnea. Bulletin of the Museum of Comparative Zoology at Harvard College, 51:249–256.
Garrick, J. 1982. Sharks of the Genus *Carcharhinus*. National Marine Fisheries Service, National Oceanographic and Atmospheric Administration, (NOAA) Technical Report 445, 194 p.
Garrick, J. and Springer, S. 1964. *Isistius plutodus*, a new squaloid shark from the Gulf of Mexico. Copeia, 1964:678–682.
Gibbes, R. 1849. Monograph of the fossil squalidae of the United States. Journal of the Academy of Natural Sciences of Philadelphia series 2, 1:139–147, 191–206, plates 18–21; 25–27.
Gill, T. 1862. Analytical synopsis of the Order of Squali and revision of the nomenclature of the genera. Annals of the Lyceum of Natural History of New York, 7:367–408.
Gill, T. 1863. On the classification of the families and genera of the Squali of California. Proceedings of the Academy of Natural Sciences of Philadelphia, 14:483–501.
Gill, T. 1864. Second contribut ion to the Selachology of California. Proceedings of the Academy of Natural Sciences of Philadelphia, 16:147–151.
Gill, T. 1865a. Synopsis of the eastern American sharks. Proceedings of the Academy of Natural Sciences of Philadelphia, 16:258–265.
Gill, T. 1865b. Note on the family of myliobatoids, and on a new species of *Aetobatis*. Annals of the Lyceum of Natural History of New York, 8:135–138.
Gillette, D. 1984. A marine ichthyofauna from the Miocene of Panama, and the Tertiary Caribbean faunal province. Journal of Vertebrate Paleontology, 4:172–186.
Girard, C. 1855. Characteristics of some cartilaginous fishes of the Pacific coast of North America. Proceedings of the Academy of Natural Sciences of Philadelphia, 7:196–197.
Glikman, L. 1964. Sharks of Paleogene and their stratigraphic significance. Nauka Press, Moscow, 229 p., 76 fig., 31 pl. (In Russian).
Godfrey, S., Ellwood, M., Groff, S., and Verdin, M. 2018. *Carcharocles*-bitten odontocete caudal vertebrae from the Coastal Eastern United States. Acta Palaeontologica Polonica, 63:463–

468.
https://doi.org/10.4202/app.00495.2018
Gonzalez, C., Postaire, B., Driggers, W., Caballero, S., and Chapman, D. 2024. Sphyrna alleni sp. nov., a new hammerhead shark (Carcharhiniformes, Sphyrnidae) from the Caribbean and the Southwest Atlantic. Zootaxa, 5512:491–511.
https://doi.org/10.11646/zootaxa.5512.4.2
Goodbred, S., Jr. and Hine, A. 1995. Coastal storm deposition: Salt-marsh response to a severe extratropical storm, March 1993, west-central Florida. Geology, 23:679–682.
https://doi.org/10.1130/0091-7613(1995)023%3C0679:CSDSMR%3E2.3.CO;2
Goode, G. and Bean, T. 1896. Oceanic ichthyology, a treatise on the deep-sea and pelagic fishes of the world, based chiefly upon the collections made by the steamers Blake, Albatross, and Fish Hawk in the northwestern Atlantic, with an atlas containing 417 figures. Special Bulletin U. S. National Museum, 2: Text: i–xxxv + 1–26 + 1–553, Atlas: i–xxiii, 1–26, 123 pls.
Goodrich, E. 1909. Vertebrata Craniata (First fascicle: Cyclostomes and Fishes). In Lankester, R. (ed.), A treatise on Zoology. Adam and Charles Black, London, part IX, pp. i–xvi, 1–518, figs 1–514.
Goto, M., Kikuchi, T., Sekimoto, S., and Noma, T. 1984. Fossil teeth of the great white shark, Carcharodon carcharias, from the Kazusa and Shimosa Groups (Pliocene to Pleistocene) in Boso Peninsula and Shimosa Upland, Central Japan. Earth Science [Chikyu Kagaku], 38:420–426.
https://doi.org/10.15080/agcjchikyukagaku.38.6_420
Govender, R. and Chinsamy, A. 2013. Early Pliocene (5 Ma) shark–cetacean trophic interaction from Langebaanweg, western coast of South Africa. Palaios, 28:270–277.
https://doi.org/10.2110/palo.2012.p12-058r
Grace, M. 2001. Field guide to requiem sharks (Elasmobranchiomorphi: Carcharhinidae) of the Western North Atlantic (Vol. 153). US Government Printing Office, 32 p.
Gray, J. 1851. List of the specimens of fish in the collection of the British Museum. Part I. Chondropterygii. British Museum (Natural History), London, 160 p.
Green, R., Campbell, K., Arthur, J., Scott, T. 1997. Geologic Map of the Western Portion of the U.S.G.S 1:100,000 Scale Sarasota Quadrangle. Florida Geological Survey, Open File Map Series 86-01.
Griffith, E. and Smith, C. 1834. Supplemental additions. In Cuvier B. The Animal Kingdom, Vol. 10, 680 p., 62 pls.
Griffiths, M., Eagle, R., Kim, S., Flores, R., Becker, M., Maisch IV, H., Trayler, R., Chan, R., McCormack, J., Akhtar, A., and Tripati, A. 2023. Endothermic physiology of extinct megatooth sharks. Proceedings of the National Academy of Sciences, 120:e2218153120.
https://doi.org/10.1073/pnas.2218153120
Guertin, L., Missimer, T., and McNeill, D. 2000. Hiatal duration of correlative sequence boundaries from Oligocene–Pliocene mixed carbonate/siliciclastic sediments of the south Florida Platform. Sedimentary Geology, 134:1–26.
https://doi.org/10.1016/S0037-0738(00)00011-7
Guitart-Manday, D. 1966. Nueva nombre para una especie de tiburon del genero Isurus (Elasmobranchii: Isuridae) de aguas Cubanas. Poeyana, Serie A, 15:1–9.
Günther, A. 1870. Catalogue of the fishes in the British Museum, Vol. 8. British Museum (Natural History), London, 549 p.
Hallam, A. and Wignall, P.B. 1999. Mass extinctions and sea-level changes. Earth-Science Reviews, 48:217–250.
Hamon, N., Sepulchre, P., Lefebvre, V., and Ramstein, G. 2013. The role of eastern Tethys seaway closure in the Middle Miocene Climatic Transition (ca. 14 Ma). Climate of the Past, 9:2687–2702.
https://doi.org/10.5194/cp-9-2687-2013
Haq, B. and Ogg., J. 2024. Retraversing the Highs and Lows of Cenozoic Sea Levels. GSA Today, 34:4–11.
https://doi.org/10.1130/GSATGG593A.1
Harding, L., Jackson, A., Barnett, A., Donohue, I., Halsey, L., Huveneers, C., Meyer, C., Papastamatiou, Y., Semmens, J.M., Spencer, E., and Watanabe, Y. 2021. Endothermy makes fishes faster but does not expand their thermal niche. Functional Ecology, 35:1951–1959.
https://doi.org/10.1111/1365-2435.13869

Hasse, C. 1879. Das natürliche System der Elasmobranchier auf Grundlage des Baues und der Entwicklung ihrer Wirbelsäule. Eine morphologische und paläontologische Studie. I. Allgemeiner Theil, 1–76.

Hastings, A. and Dooley, A. 2017. Fossil-collecting from the middle Miocene Carmel Church Quarry marine ecosystem in Caroline County, Virginia, p. 77–88. In Bailey, C. and Jaye, S. (eds.), From the Blue Ridge to the Beach: Geological Field Excursions across Virginia. Field Guide 47. The Geological Society of America, Boulder, Colorado.

Hay, O. 1902. On a collection of Upper Cretaceous fishes from Mount Lebanon, Syria, with descriptions of four new genera and nineteen new species. Bulletin of the American Museum of Natural History, 19:395–452.

Heck, K., Jr., Hays, G., and Orth, R. 2003. Critical evaluation of the nursery role hypothesis for seagrass meadows. Marine Ecology Progress Series, 253:123–136. https://doi.org/10.3354/meps253123

Heemstra, P. 1997. A Review of the Smooth-Hound Sharks (Genus *Mustelus*, Family Triakidae) of the Western Atlantic Ocean, with Descriptions of Two New Species and a New Subspecies. Bulletin of Marine Science, 60:894–928.

Herman, J., Hovestadt-Euler, M., Hovestadt, D. 1989. Contributions to the study of the comparative morphology of teeth and other relevant ichthyodorulites in living superspecific taxa of Chondrichthyan fishes. Part A: Selachii. No. 3: Order: Squaliformes – Families: Echinorhinidae, Oxynotidae and Squalidae. Bulletin de l'Institut Royal des Sciences Naturelles de Belgique, Biologie, 59:101–158.

Herman, J., Hovestadt-Euler, M., Hovestadt, D. 1992. Contributions to the study of the comparative morphology of teeth and other relevant ichthyodorulites in living superspecific taxa of Chondrichthyan fishes. Part A: Selachii. No. 4: Order: Orectolobiformes Families: Brachaeluridae, Giglymostomatidae, Hemiscylliidae, Orectolobidae, Parascylliidae, Rhiniodontidae, Stegostomatidae. Order: Pristiophoriformes – Family: Pristiophoridae Order: Squatiniformes – Family: Squatinidae. Bulletin de l'Institut Royal des Sciences Naturelles de Belgique, Biologie, 62:193–254.

Herman, J., Hovestadt-Euler, M., and Hovestadt, D. 1993. Contributions to the study of the comparative morphology of teeth and other relevant ichthyodorulites in living superaspecific taxa of Chondrichthyan fishes. Addendum to Part A, No. 1b: Hexanchiformes – Family: Chlamidoselachidae; No. 5: Order: Heterodontiformes – Family: Heterodontidae; No. 6: Order: Lamniformes – Families: Cetorhinidae, Megachasmidae; Addendum 1 to No. 3: Order: Squaliformes; Addendum 1 to No. 4: Order Orectolobiformes; General Glossary; Summary Part A. Bulletin de l'Institut Royal des Sciences Naturelles de Belgique, Biologie, 63:185–256.

Herman, J., Hovestadt-Euler, M., Hovestadt, D., and Stehmann, M. 1997. Contributions to the study of the comparative morphology of teeth and other relevant ichthyodorulites in living superaspecific taxa of Chondrichthyan fishes. Part B: Batomorphii No. 2: Order: Rajiformes – Suborder: Pristoidei – Family: Pristidae – Genera: *Anoxypristis* and *Pristis*; No. 3: Suborder: Rajoidei – Superfamily: Rhinobatoidea – Families: Rhinidae – Genera: *Rhina* and *Rhynchobatus* and Rhinobatidae – Genera: *Aptychotrema*, *Platyrhina*, *Plathyrhinoidis*, *Rhinobatos*, *Trygonorrhina*, *Zanobatus* and *Zapteryx*. Bulletin de l'Institut Royal des Sciences Naturelles de Belgique, Biologie, 67:107–162.

Herman, J., Hovestadt-Euler, M., Hovestadt, D., and Stehmann, M. 1998. Contributions to the study of the comparative morphology of teeth and other relevant ichthyodorulites in living supra-specific taxa of Chondrichthyan fishes. Part B: Batomorphii No. 4a: Order Rajiformes – Suborder Myliobatoidei – Superfamily Dasyatoidea – Family Dasyatidae – Subfamily Dasyatinae – Genera: *Amphotistius*, *Dasyatis*, *Himantura*, *Pastinachus*, *Pteroplatytrygon*, *Taeniura*, *Urogymnus* and *Urolophoides* (incl. supraspecific taxa of uncertain status and validity), Superfamily Myliobatoidea – Family Gymnuridae – Genera: *Aetoplatea* and *Gymnura*, Superfamily Plesiobatoidea – Family Hexatrygonidae – Genus: *Hexatrygon*. Bulletin de l'Institut Royal des Sciences Naturelles de Belgique, Biologie, 68:145–197.

Herman, J., Hovestadt-Euler, M., Hovestadt, D., and Stehmann, M. 1999. Contributions to the study of the comparative morphology of teeth and other relevant ichthyodorulites in living supraspecific taxa of chondrichthyan fishes. Part B: Batomorphii. No.4b: Order Rajiformes – Suborder Myliobatoidei – Superfamily Dasyatoidea – Family Dasyatididae – Subfamily Dasyatinae – Genus: *Taeniura*, *Urogymnus*, *Urolophoides* – Subfamily Potamotrygoninae – Genera: *Disceus*, *Pleisiotrygon*, and *Potamotrygon* (incl. supraspecific taxa of uncertain

status and validity), Family Urolophidae – Trygonoptera, Urolophus and Urotrygon – Superfamily Myliobatidea – Family: Gymnuridae – Genus: *Aetoplatea*. Bulletin de l'Institut Royal des Sciences Naturelles de Belgique, Biologie, 69:161–200.

Herman, J., Hovestadt-Euler, M., Hovestadt, D., and Stehmann, M. 2000. Contributions to the study of the comparative morphology of teeth and other relevant ichthyodorulites in living superaspecific taxa of Chondrichthyan fishes. Part B: Batomorphii 4c: Order: Rajiformes – Suborder Myliobatoidei – Superfamily Dasyatoidea – Family Dasyatidae – Subfamily Dasyatinae – Genus: *Urobatis*, Subfamily Potamotrygoninae – Genus: *Pomatotrgon*, Superfamily Plesiobatoidea – Family Plesiobatidae – Genus: *Plestiobatis*, Superfamily Myliobatoidea – Family Myliobatidae Subfamily Myliobatinae – Genera: *Aetobatus*, *Aetomylaeus*, *Myliobatis* and *Pteromylaeus*, Subfamily Rhinopterinae – Genus: *Rhinoptera* and Subfamily Mobulinae – Genera: *Manta* and *Mobula*. Addendum 1 to 4a: erratum to Genus *Pteroplatytrygon*. Bulletin de l'Institut Royal des Sciences Naturelles de Belgique, Biologie, 70:5–67.

Herold, N., Huber, M., and Müller, R. 2011. Modeling the Miocene climatic optimum. Part I: Land and atmosphere, Journal of Climatology, 24:6353–6372. https://doi.org/10.1175/2011JCLI4035.1

Herold, N., Huber, M., Müller, R., and Seton, M. 2012. Modeling the Miocene climatic optimum: Ocean circulation. Paleoceanography, 27:1209. https://doi.org/10.1029/2010PA002041

Herraiz, J., Ribé, J., Botella, H., Martínez-Pérez, C. and Ferrón, H. 2020. Use of nursery areas by the extinct megatooth shark *Otodus megalodon* (Chondrichthyes: Lamniformes). Biology Letters, 16:20200746. https://doi.org/10.1098/rsbl.2020.0746

Heupel, M. and Simpfendorfer, C. 2008. Movement and distribution of young bull sharks *Carcharhinus leucas* in a variable estuarine environment. Aquatic Biology, 1:277–289. https://doi.org/10.3354/ab00030

Heupel, M. and Simpfendorfer, C. 2011. Estuarine nursery areas provide a low-mortality environment for young bull sharks *Carcharhinus leucas*. Marine Ecology Progress Series, 433:237–244. https://doi.org/10.3354/meps09191

Heupel, M., Simpfendorfer, C., Collins, A., and Tyminski, J. 2006. Residency and movement patterns of bonnethead sharks, *Sphyrna tiburo*, in a large Florida estuary. Environmental Biology of Fishes, 76:4–67. https://doi.org/10.1007/s10641-006-9007-6

Hildebrand, S. and Schroeder, W. 1928. Fishes of Chesapeake Bay. Bulletin of the United States Bureau of Fisheries, 43:1–366.

Hillary, R., Bravington, M., Patterson, T., Grewe, P., Bradford, R., Feutry, P., Gunasekera, R., Peddemors, V., Werry, J., Francis, M., and Duffy, C. 2018. Genetic relatedness reveals total population size of white sharks in eastern Australia and New Zealand. Scientific Reports, 8:2661. https://doi.org/10.1038/s41598-018-20593-w

Hine, A. 1997. Structural and paleoceanographic evolution of the margins of the Florida Platform, p. 169–194. In Randazzo, A. and Jones, D. (eds.), Geology of Florida. University Press of Florida, Gainesville, Florida.

Hine, A. 2013. Geologic History of Florida, Major Events that Formed the Sunshine State. University Press of Florida, 256 p.

Hine, A. and Belknap, D. 1986. Recent geological history and modern sedimentary processes of the Pasco, Hernando and Citrus county coastlines: west central Florida. Florida Sea Grant Report 79.

Hine, A. and Snyder, S.W. 1985. Coastal lithosome preservation: evidence from the shoreface and inner continental shelf off Bogue Banks, North Carolina. Marine Geology, 63:307–330.

Hine, A., Brooks, G., Davis, R., Jr, Duncan, D., Locker, S., Twichell, D., and Gelfenbaum, G. 2003. The west-central Florida inner shelf and coastal system: a geologic conceptual overview and introduction to the special issue. Marine Geology, 200:1–17. https://doi.org/10.1016/S0025-3227(03)00161-0

Hine, A., Martin, E., Jaeger, J., and Brenner, M. 2017. Paleoclimate of Florida, p. 457–484. In Chassignet, E., Jones, J., Misra, V., and Obeysekera, J. (eds.), Florida's climate: Changes,

variations, & impacts. Gainesville, FL: Florida Climate Institute. https://doi.org/10.17125/fci2017.ch15

Hoffmayer, E., Franks, J., Driggers, W., McKinney, J., Hendon, J., and Quattro, J. 2014. Habitat, movements and environmental preferences of dusky sharks, *Carcharhinus obscurus*, in the northern Gulf of Mexico. Marine Biology, 161:91–924. https://doi.org/10.1007/s00227-014-2391-0

Holec, P., Hornacek, M., and Sykora, M. 1995. Lower Miocene shark (Chondrichthyes, Elasmobranchii) and whale faunas (Mammalia, Cetacea) near Mučín, Southern Slovakia. Geologické práce, Správy, 100:37–52.

Hovestadt, D. and Hovestadt-Euler, M. 2013. Generic assessment and reallocation of Cenozoic Myliobatinae based on new information of tooth, tooth plate and caudal spine morphology of extant taxa. Palaeontos, 24:1–66.

Howell Rivero, L. 1936. Some new, rare and little-known fishes from Cuba. Proceedings of the Boston Society of Natural History, 41:41–76.

Hoyos-Padilla, E., Papastamatiou, Y., O'Sullivan, J., and Lowe, C. 2013. Observation of an attack by a cookiecutter shark (*Isistius brasiliensis*) on a white shark (*Carcharodon carcharias*). Pacific Science, 67:129–134. https://doi.org/10.2984/67.1.10

Hulbert Jr., R. 2001. The fossil vertebrates of Florida. University Press of Florida, Gainesville, Florida, 368 p.

Hunt, M. and Doering, P. 2013. Salinity preferences and nursery habitat considerations for blue crab (*Callinectes sapidus*), bull shark (*Carcharhinus leucas*), and smalltooth sawfish (*Pristis pectinata*) in the Caloosahatchee Estuary. South Florida Water Management District, Technical Publication: WR-2013-001, 20 p.

Huxley, T. 1880. On the application on the laws of evolution to the arrangement of the vertebrata and more particularly of the Mammalia. Zoological Society of London, Scientific Memoirs 4:457–472.

Itoigawa, J. and Nishimoto, H. 1974. Fossil elasmobranchs (shark teeth) from the Miocene series of Mizunami. Bulletin of the Mizunami Fossil Museum, 1:243–262.

Iturralde-Vinent, M., Hubbell, G., and Rojas, R. 1996. Catalogue of Cuban fossil Elasmobranchii (Paleocene to Pliocene) and paleogeographic implications of their Lower to middle Miocene occurrence. Boletín de la Sociedad Jamaicana de Geología, 31:7–21

Joleaud, L. 1912. Géologie et paléontologie de la Plaine du Comtat et de ses abords. Description des terrains néogènes. Montpellier, Imprimerie Montane, Sicardi et Valentin, 2:255–285.

Jordan, D. and Bollman, C. 1889. Descriptions of new species of fishes collected at the Galápagos Islands and along the coast of the United Status of Colombia, 1877–88. Proceedings of the United States National Museum, 12:149–183.

Jordan, D. and Evermann, B. 1896. The fishes of North and Middle America: a descriptive catalogue of the species of fish-like vertebrates found in the waters of North America, north of the Isthmus of Panama. Part I. Bulletin of the United States National Museum, 47:1–1240.

Jordan, D. and Evermann, B. 1898. The fishes of North and Middle America: a descriptive catalogue of the species of fish-like vertebrates found in the waters of North America north of the Isthmus of Panama. Part III. Bulletin of the United States National Museum, 47:2183–3136.

Jordan, D. and Gilbert, C. 1879. Notes on the fishes of Beaufort Harbor, North Carolina. Proceedings of the United States National Museum, 1:365–388.

Jordan, D. and Gilbert, C. 1880. Description of a new ray (*Platyrhina triseriata*), from the coast of California. Proceedings of the United States National Museum, 3:36–38.

Jordan, D. and Gilbert, C. 1882. Description of four new species of sharks, from Mazatlan, Mexico. Proceedings of the United States National Museum, 5:102–110.

Kajiura, S. and Tricas, T. 1996. Seasonal dynamics of dental sexual dimorphism in the Atlantic stingray *Dasyatis sabina*. Journal of Experimental Biology, 199:2297–2306.

Kajiura, S., Sebastian, A., and Tricas, T. 2000. Dermal bite wounds as indicators of reproductive seasonality and behaviour in the Atlantic stingray, *Dasyatis sabina*. Environmental Biology of Fishes, 58:23–31. https://doi.org/10.1023/A:1007667108362

Karas, C., Nürnberg, D., Bahr, A., Groeneveld, J., Herrle, J., Tiedemann, R. and Demenocal, P. 2017. Pliocene oceanic seaways and global climate. Scientific Reports, 7:39842. https://doi.org/10.1038/srep39842

Kast, E., Griffiths, M., Kim, S., Rao, Z., Shimada, K., Becker, M., Maisch IV, H., Eagle, R., Clarke, C., Neumann, A., and Karnes, M. 2022. Cenozoic megatooth sharks occupied extremely high trophic positions. Science Advances, 8:eabl6529. https://doi.org/10.1126/sciadv.abl6529

Keigwin, L. 1982. Isotopic paleoceanography of the Caribbean and East Pacific: role of Panama uplift in late Neogene time. Science, 217:350–353.

Kemp, N. 1991. Chondrichthyans in the Cretaceous and Tertiary of Australia, p. 497–568. In Vickers-Rich, P., Baird, R., and Rich, T. (eds.), Vertebrate Palaeontology of Australasia. Pioneer Design Studios and Monash University Publications Committee, Melbourne.

Kent, B. 2018. The cartilaginous fishes (chimaeras, sharks, and rays) of Calvert Cliffs, Maryland, USA. The Geology and Vertebrate Paleontology of Calvert Cliffs, Maryland, USA. Smithsonian Contributions to Paleobiology, 100:45–157.

Kent, B. and Powell, G. 1999. Reconstructed dentition of the rare lamnoid shark *Parotodus benedeni* (le Hon) from the Yorktown Formation (Early Pliocene) at Lee Creek Mine, North Carolina. The Mosasaur, 6:1–10.

Kimel, E. 2019. Manasota Key Offshore site was active 8,000 years ago. Sarasota Herald Tribune, May 16, 2019. Accessed: 9/25/2024. https://www.heraldtribune.com/story/news/local/venice/2019/05/16/ancient-burial-site-off-manasota-key-is-1000-years-older-than-estimated/5142533007/

Kimmel, P. and Purdy, R. 1984. Fossil fish of the Calvert and Eastover Formations. Stratigraphy and Paleontology of the Outcropping Tertiary Beds in the Pamunkey River Region, Central Virginia Coastal Plain. Guidebook for Atlantic Coastal Plain Geological Association, p. 205–215.

Kiraly, S., Moore, J., and Jasinski, P. 2003. Deepwater and Other Sharks of the U.S. Atlantic Ocean Exclusive Economic Zone. Marine Fisheries Review, 65:1–63.

Klunzinger, C. 1871. Synopsis der Fische des Rothen Meeres II. Theil. Verhandlungen der Königlischen Zoologischen–Botanischen Gesellschaft in Wien, 21:441–688.

Knowlton, N., Weigt, L., Solorzano, L., Mills, D., and Bermingham, E. 1993. Divergence in proteins, mitochondrial DNA, and reproductive compatibility across the Isthmus of Panama. Science, 260:1629–1632.

Kocsis, F. 2002. Vertebrate fossils: A neophyte's guide. IBIS Graphics, Palm Harbor, FL, 184 p.

Kocsis, L. 2007. Central Paratethyan shark fauna (Ipolytarnóc, Hungary). Geologica Carpathica, 58:27–40.

Kocsis, L., Vennemann, T., Ulianov, A., and Brunnschweiler, J. 2015. Characterizing the bull shark Carcharhinus leucas habitat in Fiji by the chemical and isotopic compositions of their teeth. Environmental Biology of Fishes, 98:1609–1622. https://doi.org/10.1007/s10641-015-0386-4

Kocsis, L., Razak, H., Briguglio, A., and Szabó, M. 2018. First report on a diverse Neogene cartilaginous fish fauna from Borneo (Ambug Hill, Brunei Darussalam). Journal of Systematic Palaeontology, 17:791–819. https://doi.org/10.1080/14772019.2018.1468830

Kohler, N., Casey, J., and Turner, P. 1998. NMFS cooperative shark tagging program, 1962–93: an atlas of shark tag and recapture data. Marine Fisheries Review, 60:1–87.

Kriwet, J. and Klug, S. 2009. Fossil record and origin of squaliform sharks (Chondrichthyes, Neoselachii), p. 19–38. In Gallucci, V., McFarlane, G., and Bargmann, G. (eds), Biology and management of dogfish sharks. American Fisheries Society. Bethesda, Maryland.

Kriwet, J., Mewis, H., and Hampe, O. 2015. A partial skeleton of a new lamniform mackerel shark from the Miocene of Europe. Acta Palaeontologica Polonica, 60:857–875. https://doi.org/10.4202/app.00066.2014

Lacepède, B. 1800. Histoire Naturelle des Poissons. Plassan, Paris, 2: i–lxiv, 1–632, pls 1–20.

Landini, W., Altamirano-Sierra, A., Collareta, A., Di Celma, C., Urbina, M., and Bianucci. G. 2017a. The late Miocene elasmobranch assemblage from Cerro Colorado (Pisco Formation, Peru). Journal of South American Earth Sciences, 73:168–190. https://doi.org/10.1016/j.jsames.2016.12.010

Landini, W., Collareta, A., Pesci, F., Di Celma, C., Urbina, M., and Bianucci, G., 2017b. A secondary nursery area for the copper shark *Carcharhinus brachyurus* from the late Miocene

of Peru. Journal of South American Earth Sciences, 78:164–174. https://doi.org/10.1016/j.jsames.2017.07.003

Last, P., Naylor, G., Séret, B., White, W., Stehmann, M., Carvalho, M. 2016a. Rays of the World, CSIRO Publishing. 832 pp.

Last, P., Naylor, G., and Manjaji-Matsumoto, B. 2016b. A revised classification of the family Dasyatidae (Chondrichthyes: Myliobatiformes) based on new morphological and molecular insights. Zootaxa, 4139:345–368. https://doi.org/10.11646/zootaxa.4139.3.2

Latham, J. 1794. An essay on the various species of Sawfish. Transactions of the Linnean Society of London, 2:273–282.

Laurito Mora, C. 1996. El Género *Isistius* (Squalidae) en el Alto Guayacán. Formación Uscari (Mioceno Superior-Plioceno Inferior), Provincia de Limón, Costa Rica. Revista Geológica de América Central, 19/20:87–92.

Laurito Mora, C. 1999. Los selaceos fosiles de la localidad de Alto Guayacan (y otros ictiolitos associados). Mioceno Superior-Plioceno Inferior de Limon, Costa Rica. Guila Imprenta, San José, 125 p, 13 fig., 44 pl.

Laurito Mora, C. 2004. Ictiofauna de la Formación Punta Judas, Mioceno Medio, Provincia de Puntarenas, Costa Rica. Brenesia, 62:57–74.

Laurito Mora, C. and Valerio, A. 2008. Ictiofauna de la localidad de San Gerardo de Limoncito, Formación Curré, Mioceno Superior, cantón de Coto Brus, provincia de Puntarenas, Costa Rica. Revista Geológica de América Central, 39:65–85.

Laurito Mora, C. and Valerio, A. 2021. Review of the taxonomic status of fossil Batomorphii from Southern Limon Basin, Costa Rica and description of a new species of Dasyatidae. Revista Geológica de América Central, 65:44–71. https://doi.org/10.15517/rgac.v0i65.46685

Laurito Mora, C., Valerio, A., and Calvo, C. 2022. Nuevos registros de Otodontidae Glickman 1964B (Chondrichthyes) para el sur de la Península de Nicoya, Puntarenas, Costa Rica. Revista Geológica de América Central, 66:1–14. https://doi.org/10.15517/rgac.v66i0.49759

Le Hon, H. 1871. Préliminaires d'un mémoire sur les poissons tertiaires de Belgique. Préliminaire d'un mémoire sur les poissons fossiles tertiaires de Belgique, 15 p.

Lear, C., Rosenthal, Y., and Wright, J. 2003. The closing of a seaway: ocean water masses and global climate change. Earth and Planetary Science Letters, 210:425–436. https://doi.org/10.1016/S0012-821X(03)00164-X

Leidy, J., 1896. Fossil vertebrates from the Alachua Clays of Florida (Vol. 4). Wagner Free Institute of Science, 61 p., 19 pl.

Leigh, E., O'Dea, A., and Vermeij, G. 2014. Historical biogeography of the Isthmus of Panama. Biological Reviews, 89:148–172. https://doi.org/10.1111/brv.12048

Leriche, M. 1926. Les poissons Neogenes de la Belgique. Memoires du Musee Royal d'Histoire Naturelle de Belgique, 32:367–472, figures 161–228.

Lessios, H. 2008. The great American schism: divergence of marine organisms after the rise of the Central American Isthmus. Annual Review of Ecology, Evolution, and Systematics, 39:63–91. https://doi.org/10.1146/annurev.ecolsys.38.091206.095815

Lesueur, C. 1817. Description of three new species of the genus *Raja*. Journal of the Academy of Natural Sciences of Philadelphia, 1:41–45.

Lesueur, C. 1818. Description of several new species of North American fishes. Journal of the Academy of Natural Sciences of Philadelphia, 1:222–235.

Lesueur, C. 1824. Description of several species of the Linnaean genus Raia of North America. Journal of the Academy of Natural Sciences of Philadelphia, 4:100–121.

Lin, C., Lin, C., and Shimada, K. 2022. A previously overlooked, highly diverse early Pleistocene elasmobranch assemblage from southern Taiwan. PeerJ, 10:e14190. https://doi.org/10.7717/peerj.14190

Linck, H. 1790. Versuch einer Eintheilung der Fische nach den Zähnen. Magazin für das Neueste aus der Physik und Naturgeschichte, 6:28–38.

Linnaeus, C. 1758. Systema Naturae per regna tria naturae, regnum animale, secundum classes, ordines, genera, species, cum characteribus differentiis synonymis, locis. Stockholm.

Lira-Beltrán, R., González-Barba, G., Macías, J., Solis-Añorve, A., García-Tenorio, F., García-Sánchez, L., and Osorio-Ocampo, S. 2020. Fauna de tiburones y rayas de la formación tirabuzón (plioceno) en el Canón El Álamo, sierras de La reforma–el aguajito, Baja California sur, México. Revista Mexicana De Ciencias Geológicas, 37:40–63. https://doi.org/10.22201/cgeo.20072902e.2020.1.1421

Lloyd, R. 1908. On two new species of eagle-rays (Myliobatidae), with notes on the skull of the genus *Ceratoptera*. Records of the Indian Museum, 2:175–180.

Locker, S., Hine, A., and Brooks, G. 2003. Regional stratigraphic framework linking continental shelf and coastal sedimentary deposits of west-central Florida. Marine Geology, 200:351–378. https://doi.org/10.1016/S0025-3227(03)00191-9

Long, D.J. 1993. Late Miocene and Early Pliocene fish assemblages from the north central coast of Chile. Tertiary Research, 14:117–126.

Longbottom, A. 1979. Miocene shark's teeth from Ecuador. Bulletin of the British Museum of Natural History, Geology, 32:57–70.

Ludt, W. and Rocha, L.A. 2015. Shifting seas: The impacts of Pleistocene sea?level fluctuations on the evolution of tropical marine taxa. Journal of Biogeography, 42:25–38. https://doi.org/10.1111/jbi.12416

Lunt, D., Valdes, P., Haywood, A., and Rutt, I. 2008. Closure of the Panama Seaway during the Pliocene: implications for climate and Northern Hemisphere glaciation. Climate Dynamics, 30:1–18. https://doi.org/10.1007/s00382-007-0265-6

MacFadden, B., Jones, D., Jud, N., Moreno-Bernal, J., Morgan, G., Portell, R., Perez, V., Moran, S., Wood, A. 2017. Integrated Chronology, Flora and Faunas, and Paleoecology of the Alajuela Formation, Late Miocene of Panama. PLoS ONE 12: e0170300. https://doi.org/10.1371/journal.pone.0170300

MacFadden, B. and Webb, S. 1982. The succession of Miocene (Arikareean through Hemphillian) terrestrial mammalian localities and faunas in Florida, p.186–199. In Scott, T. and Upchurch, S. (eds.), Miocene of the Southeastern United States. Florida Department of Natural Resources, Division of Resource Management, Bureau of Geology, Tallahassee, Florida.

Maisch, H., IV, Becker, M., Raines, B., and Chamberlain, J., Jr. 2014. Chondrichthyans from the Lisbon–Tallahatta Formation Contact (Middle Eocene), Choctaw County, Silas, Alabama. Paludicola, 9:183–209.

Maisch, H., IV, Becker, M., Chamberlain, J., Jr. 2015. Chondrichthyans from a lag deposit between the Shark River Formation (Middle Eocene) and Kirkwood Formation (Early Miocene), Monmouth County, New Jersey. Paludicola, 10:149–183.

Maisch, H., IV, Becker, M., and Chamberlain, J., Jr. 2018. Lamniform and carcharhiniform sharks from the Pungo River and Yorktown formations (Miocene–Pliocene) of the submerged continental shelf, Onslow Bay, North Carolina, USA. Copeia, 106:353–374. https://doi.org/10.1643/OT-18-016

Maisch, H., IV, Becker, M. and Chamberlain Jr, J. 2019a. Macroborings in *Otodus megalodon* and *Otodus chubutensis* shark teeth from the submerged shelf of Onslow Bay, North Carolina, USA: implications for processes of lag deposit formation. Ichnos, 27:122–141. https://doi.org/10.1080/10420940.2019.1697257

Maisch, H., IV, Becker, M., and Griffiths, M. 2019b. Chondrichthyans from the Lower Clayton Limestone Unit of the Midway Group (Paleocene) near Malvern, Arkansas, USA with Comments on the K/Pg boundary. PalZ (Paläontologische Zeitschrift), 94:561–593. https://doi.org/10.1007/s12542-019-00494-7

Maisch, H., IV, Becker, M., and Shimada, K. 2021. Fossil fishes from a lag deposit within the Upper Cretaceous Mancos Shale in New Mexico, USA, with comments on correlative Turonian–Coniacian time-transgressive lags in the Western Interior Seaway of North America. Cretaceous Research, 126:104886. https://doi.org/10.1016/j.cretres.2021.104886

Maisch, H., IV, Ellis, M., Bakker, P., Ayala, G., Pecora, D., Merrill, C., Judson, B., and Becker, M. 2023. Analysis of Submerged Fossiliferous Lag Deposits from Venice, Sarasota County, FL, USA. Geological Society of America, Spring 2023 conference, Reston, VA.

Maisch, H., IV, Ellis, M., Merrill, C., Pecora, D., Bapst, C., Hepworth, E., and Becker, M. 2024. Microfossil Analysis of Submerged Lag Deposits from Venice, Sarasota County, FL, USA.

Geological Society of America, Southeastern Section Meeting, Spring 2024, Asheville, North Carolina.
Marie, A. and Justine, J. 2005. Monocotylids (Monogenea: Monopisthocotylea) from *Aetobatus* cf. *narinari* off New Caledonia, with a description of *Decacotyle elpora* n. sp. Systematic Parasitology, 60:175–185. https://doi.org/10.1007/s11230-004-6345-7
Marlowe, S. 2014. Florida Fossils: Vol. 1 Shark Teeth and Marine Animals, 32 p.
Marshall, L., Webb, S., Sepkoski, J., Jr., and Raup, D. 1982. Mammalian evolution and the great American interchange. Science, 215:1351–1357. https://doi.org/10.1126/science.215.4538.1351
Marsili, S. 2007. Revision of the teeth of the genus *Carcharhinus* (Elasmobranchii; Carcharhinidae) from the Pliocene of Tuscany, Italy. Rivista Italiana di Paleontologia e Stratigrafia, 113:79–95.
Marsili, S., Carnevale, G., Danese, E., Bianucci, G., and Landini, W. 2007. Early Miocene vertebrates from Montagna della Maiella, Italy. Annales de Paléontologie, 93:27–66.
Martin, T. and Muller, J. 2021. The geologic record of Hurricane Irma in a Southwest Florida back-barrier lagoon. Marine Geology, 441:106635. https://doi.org/10.1016/j.margeo.2021.106635
Matson, G. 1915. The phosphate deposits of Florida. United States Geological Survey Bulletin 604. US Government Printing Office, 101 p.
Matson, G. and Clapp, F. 1909. A preliminary report on the geology of Florida with special reference to the stratigraphy. Florida Geological Survey Annual Report, 2, p. 25–173.
Matyas, C. and Cartaya, M. 2009. Comparing the rainfall patterns produced by Hurricanes Frances (2004) and Jeanne (2004) over Florida. Southeastern Geographer, 49:132–156. https://doi.org/10.1353/sgo.0.0046
Maul, G. 1955. Five species of rare sharks new for Madeira including two new to science. Notulae Naturae, 279:1–13.
McArthur, J., Howarth, R., Shields, G. and Zhou, Y., 2020. Strontium isotope stratigraphy, p. 211–238. In Gradstein, F., Ogg, J., Schmitz, M., and Ogg, G. (eds.), Geologic Time Scale 2020. Elsevier.
McCartan, L. and Moy, W., 1995. Geologic map of the Sarasota and Arcadia, Florida 30 by 60-minute quadrangles (No. 95-261). US Geological Survey.
McCormack, J., Feichtinger, I., Fuller, B., Jaouen, K., Griffiths, M., Bourgon, N., Maisch IV, H., Becker, M., Pollerspöck, J., Hampe, O. Rössner, G., Assemat, A., Müller, W., and Shimada, K. 2025. Miocene marine vertebrate trophic ecology reveals megatooth sharks as opportunistic supercarnivores. Earth and Planetary Science Letters, 664: 119392. https://doi.org/10.1016/j.epsl.2025.119392
McCormack, J., Griffiths, M., Kim, S., Shimada, K., Karnes, M., Maisch IV, H., Pederzani, S., Bourgon, N., Jaouen, K., Becker, M., and Jöns, N. 2022. Trophic position of *Otodus megalodon* and great white sharks through time revealed by zinc isotopes. Nature Communications, 13:2980. https://doi.org/10.1038/s41467-022-30528-9
McKinney, M. 1984. The Cenozoic stratigraphic record of peninsular Florida: how complete is it?. Florida Scientist, 1984:35–43.
Mearns, D., Hine, A., and Riggs, S. 1988. Comparison of sonographs taken before and after hurricane Diana, Onslow Bay, North Carolina. Geology, 16:267–270. https://doi.org/10.1130/0091-7613(1988)016%3C0267:COSTBA%3E2.3.CO;2
Merrett, N. 1973. A new shark of the genus Squalus (Squalidae: Squaloidea) from the equatorial western Indian Ocean; with notes on *Squalus blainvillei*. Journal of Zoology, 171:93–110. https://doi.org/10.1111/j.1469-7998.1973.tb07518.x
Miller, K., Schmelz, W., Browning, J., Kopp, R., Mountain, G., and Wright, J. 2020. Ancient sea level. Oceanography, 33:32–41.
Minaglia, S. and Liegl, M. 2024. Moonless night sky increases *Isistius* species (cookiecutter shark) and live human contact. PLoS ONE, 19:e0291852. https://doi.org/10.1371/journal.pone.0291852
Missimer, T. 1978. The Tamiami Formation—Hawthorn Formation contact in southwest Florida. Florida Scientist, 41:31–39.
Missimer, T. 1992. Stratigraphic relationships of sediment facies within the Tamiami Formation of southwest Florida: proposed intraformational correlations. The Plio–Pleistocene stratigraphy

and paleontology of southern Florida: Florida Geological Survey Special Publication, 36:63–92.
Missimer, T. 1999. Sequence stratigraphy of the late Miocene–early Pliocene Peace River Formation, southwestern Florida. Gulf Coast Association of Geological Societies Transactions, 49:358–369.
Missimer, T. 2001. Late Paleogene and Neogene Chronostratigraphy of Lee County, Florida, p. 67–90. In Missimer, T. and Scott, T. (eds.), Geology and Hydrology of Lee County, Florida, Durward H. Boggess Memorial Symposium, Florida Geological Survey Special Publication No. 49.
Missimer, T. and Maliva, R. 2017. Late Miocene fluvial sediment transport from the southern Appalachian Mountains to southern Florida: an example of an old mountain belt sediment production surge. Sedimentology, 64:1846–1870. https://doi.org/10.1111/sed.12377
Mitchill, S. 1815. The fishes of New York described and arranged. Transactions of the Literary and Philosophical Society of New York, 1:355–492.
Mitchill, S. 1825. The hedgehog-ray — a species of Fish taken occasionally near New York, in the Atlantic Ocean, and now, as is believed, for the first time described. American Journal of Science and Arts, 9:290–293.
Molnar, P. 2008. Closing of the Central American Seaway and the Ice Age: A critical review. Paleoceanography, 23:PA2201. https://doi.org/10.1029/2007PA001574
Montes, C., Cardona, A., Jaramillo, C., Pardo, A., Silva, J., Valencia, V., Ayala, C., Pérez-Angel, L., Rodriguez-Parra, L., Ramirez, V., and Niño, H. 2015. Middle Miocene closure of the Central American seaway. Science, 348:226–229. https://doi.org/10.1126/science.aaa2815
Morgan, G. 1994. Miocene and Pliocene marine mammal faunas from the Bone Valley Formation of Central Florida, p. 239–268. In Berta, A. and Deméré, T. (eds.), Contributions in Marine Mammal Paleontology Honoring Frank C. Whitmore, Jr. San Diego Natural History Society, San Diego.
Morgan, G. 2005. The great American biotic interchange in Florida. Bulletin of the Florida Museum of Natural History, 45:271–311.
Morgan, G. and Hulbert, R., 1995. Overview of the geology and vertebrate biochronology of the Leisey Shell Pit local fauna, Hillsborough County, Florida. Bulletin of the Florida Museum of Natural History, 37:1–92.
Morgan, G. and Pratt, A. 1983. Recent discoveries of late Tertiary marine mammals in Florida. The Plaster Jacket, a publication of the Florida Paleontological Society, 43:4–30.
Morrissey, J. and Gruber, S. 1993. Habitat selection by juvenile lemon sharks, *Negaprion brevirostris*. Environmental Biology of Fishes, 38:311–319.
Morton, R. 1988. Nearshore responses to great storms, p. 7–22. In Clifton, H. (ed.), Sedimentologic Consequences of Convulsive Geologic Events, Geological Society of America Special Publication, Vol. 229.
Müller, J. 1836. Vergleichende Anatomie der Myxinoiden, der Cyclostomen mit durchbohrtem Gaumen. Erster Theil. Osteologie und Myologie. Abhandlungen der Königlichen Akademie der Wissenschaften zu Berlin, 1834:65–340.
Müller, J. and Henle, F. 1837. Gattungen der Haifische und Rochen nach einer von ihm mit Hrn. Henle unternommenen gemeinschaftlichen Arbeit über die Naturgeschichte der Knorpelfische. Berichte der Königlichen Preussischen Akademie der Wissenschaften zu Berlin, 1837:111–118.
Müller, J. and Henle, J. 1838–41 [1838]. Systematische Beschreibung der Plagiostomen. Verlag, Berlin.
Mullins, H., Gardulski, A., Wise Jr, S., and Applegate, J. 1987. Middle Miocene oceanographic event in the eastern Gulf of Mexico: implications for seismic stratigraphic succession and Loop Current/Gulf Stream circulation. Geological Society of America Bulletin, 98:702–713.
Nardo, G. 1827. Prodromus observationum et disquisitionum Adriaticae ichthyologiae. Giornale di fisica, chimica e storia naturele, medicina, ed arti, 10:22–40.
Naylor, G. and Marcus, L. 1994. Identifying isolated shark teeth of the genus *Carcharhinus* to species: relevance for tracking phyletic change through the fossil record. American Museum novitates; no. 3109, 53 p.

Naylor, G., Caira, J., Jensen, K., Rosana, K., Straube, N., and Lakner, C. 2012. Elasmobranch Phylogeny: A Mitochondrial Estimate Based on 595 Species, p. 31–56. In Carrier, J., Musick, J., and Heithaus, M. (eds.), Biology of Sharks and their Relatives (2nd ed.). CRC Press, Boca Raton, Florida.

Neer, J. and Thompson, B. 2005. Life history of the cownose ray, *Rhinoptera bonasus*, in the northern Gulf of Mexico, with comments on geographic variability in life history traits. Environmental Biology of Fishes, 73:321–331. https://doi.org/10.1007/s10641-005-2136-5

Nelson, J. 1984. Fishes of the World, 2nd edition. John Wiley and Sons, Inc., New York, 523 p.

Nevatte, R., Wueringer, B., Jacob, D., Park, J., and Williamson, J. 2017. First insights into the function of the sawshark rostrum through examination of rostral tooth microwear. Journal of Fish Biology, 91:1582–1602. https://doi.org/10.1111/jfb.13467

Nieves-Rivera, A., Ruiz-Yantin, M., and Gottfried, M. 2003. New record of the Lamnid Shark *Carcharodon megalodon* from the middle Miocene of Puerto Rico. Caribbean Journal of Science, 39:223–227.

Nisancioglu, K., Raymo, M., and Stone, P. 2003. Reorganization of Miocene deep water circulation in response to the shoaling of the Central American Seaway. Paleoceanography, 18:1006. https://doi.org/10.1029/2002PA000767

Nishida, K. 1990. Phylogeny of the suborder Myliobatidoidei. Memoirs of the faculty of fisheries Hokkaido University, 37:1–108.

NOAA Historical Hurricane Tracks: Accessed: 9-25-2024. https://coast.noaa.gov/hurricanes/#map=4/32/-80

Notarbartolo-di-Sciara, G. 1987. A revisionary study of the genus *Mobula* Rafinesque, 1810 (Chondrichthyes: Mobulidae), with the description of a new species. Zoological Journal of the Linnean Society, 91:1–91. https://doi.org/10.1111/j.1096-3642.1987.tb01723.x

Nyberg, K., Ciampaglio, C., and Wray, G. 2006. Tracing the ancestry of the great white shark, *Carcharodon carcharias*, using morphometric analyses of fossil teeth. Journal of Vertebrate Paleontology, 26:806–814. https://doi.org/10.1671/0272-4634(2006)26[806:TTAOTG]2.0.CO;2

O'Dea, A., Lessios, H., Coates, A., Eytan, R., Restrepo-Moreno, S., Cione, A., Collins, L., De Queiroz, A., Farris, D., Norris, R., and Stallard, R. 2016. Formation of the Isthmus of Panama. Science Advances, 2:e1600883. https://doi.org/10.1126/sciadv.1600883

O'Leary, S., Feldheim, K., Fields, A., Natanson, L., Wintner, S., Hussey, N., Shivji, M., and Chapman, D. 2015. Genetic diversity of white sharks, *Carcharodon carcharias*, in the Northwest Atlantic and Southern Africa. Journal of Heredity, 106:258–265. https://doi.org/10.1093/jhered/esv001

Ogburn, M., Bangley, C., Aguilar, R., Fisher, R., Curran, M., Webb, S., and Hines, A. 2018. Migratory connectivity and philopatry of cownose rays *Rhinoptera bonasus* along the Atlantic coast, USA. Marine Ecology Progress Series, 602:197–211. https://doi.org/10.3354/meps12686

Olsen, S. 1959. Fossil mammals of Florida. Florida Geological Survey, Special Publication, 6:1–74.

Olsen, S. 1964. The stratigraphic importance of a lower Miocene vertebrate fauna from north Florida. Journal of Paleontology, 38:477–482.

Olsson, A. 1968. A review of late Cenozoic stratigraphy of southern Florida. Late Cenozoic stratigraphy of southern Florida—a reappraisal. Miami Geological Survey, Miami, p. 66–82.

Olsson, A. and Harbison., A. 1953. Pliocene Mollusca of southern Florida with special reference to those from North Saint Petersburg. Academy of Natural Sciences of Philadelphia, Monographs, 8:1–457.

Ortega, L., Heupel, M., Beynen, P., and Motta, P. 2009. Movement patterns and water quality preferences of juvenile bull sharks (*Carcharhinus leucas*) in a Florida estuary. Environmental Biology of Fishes, 84:361–373. https://doi.org/10.1007/s10641-009-9442-2

Osborn, A., Portell, R., and Mooi, R. 2020. Neogene echinoids of Florida. Bulletin of the Florida Museum of Natural History, 57:1–465.

Papastamatiou, Y., Wetherbee, B., O'Sullivan, J., Goodmanlowe, G., and Lowe, C. 2010. Foraging ecology of Cookiecutter Sharks (*Isistius brasiliensis*) on pelagic fishes in Hawaii, inferred from prey bite wounds. Environmental Biology of Fishes, 88:361–368. https://doi.org/10.1007/s10641-010-9649-2

Papastamatiou, Y., Grubbs, R., Imhoff, J., Gulak, S., Carlson, J., and Burgess, G. 2015. A subtropical embayment serves as essential habitat for sub-adults and adults of the critically endangered smalltooth sawfish. Global Ecology and Conservation, 3:764–775. https://doi.org/10.1016/j.gecco.2015.03.003

Partarrieu, D., Villafaña, J., Pinto, L., Mourgues, F., Oyanadel-Urbina, P., Rivadeneira, M., and Carrillo-Briceño, J. 2018. Neogene 'horn sharks' *Heterodontus* (Chondrichthyes: Elasmobranchii) from the Southeastern Pacific and their paleoenvironmental significance. Ameghiniana, 55:651–667. https://doi.org/10.5710/AMGH.19.10.2018.3202

Pawellek, T., Adnet, S., Cappetta, H., Metais, E., Salem, M., Brunet, M., and Jaeger, J. 2012. Discovery of an earliest Pliocene relic tropical fish fauna in a newly detected cliff section (Sabratah Basin, NW Libya). Neues Jahrbuch fur Geologie und Palaontologie-Abhandlungen, 266:93–114. https://doi.org/10.1127/0077-7749/2012/0272

Payne, N. and Smith, J. 2017. An alternative explanation for global trends in thermal tolerance. Ecology Letters, 20:70–77. https://doi.org/10.1111/ele.12707

Peck, D., Slater, D., Missimer, T., Wise Jr, S., and O'Donnell, T. 1979. Stratigraphy and paleoecology of the Tamiami Formation in Lee and Hendry Counties, Florida. Transactions of the Gulf Coast Association of Geological Societies, 39:328–341.

Perez, V. 2022. The chondrichthyan fossil record of the Florida Platform (Eocene–Pleistocene). Paleobiology, 48:622–654. https://doi.org/10.1017/pab.2021.47

Perez, V. and Marks, K. 2017. The first documented fossil records of *Isistius* and *Squatina* (Chondrichthyes) from Florida, with an overview of the associated vertebrate fauna. Bulletin of the Florida Museum of Natural History, 55:139–155. https://doi.org/10.58782/flmnh.ewxq4679

Perez, V., Pimiento, C., Hendy, A., González-Barba, G., Hubbell, G., and MacFadden, B. 2017. Late Miocene chondrichthyans from Lago Bayano, Panama: functional diversity, environment and biogeography. Journal of Paleontology, 91:512–547. https://doi.org/10.1017/jpa.2017.5

Perez, V., Leder, R., and Badaut, T. 2021. Body length estimation of Neogene macrophagous lamniform sharks (*Carcharodon* and *Otodus*) derived from associated fossil dentitions. Palaeontologia Electronica, 24:a09. https://doi.org/10.26879/1140

Perón, F. and C. Lesueur. 1822. Description of a Squalus, of a very large size, which was taken on the coast of New Jersey. Journal of the Philadelphia Academy of Natural Sciences, 2:343–352.

Petuch, E. 1994. Atlas of Florida Fossil Shells (Pliocene and Pleistocene Marine Gastropods). Graves Museum of Archaeology and Natural History, 394 p.

Petuch, E. and Berschauer, D. 2021. Ancient Seas of Southern Florida: The Geology and Paleontology of the Everglades Region. CRC Press, 266 p.

Pfleger, M., Grubbs, R., Cotton, C., and Daly-Engel, T. 2018. *Squalus clarkae* sp. nov., a new dogfish shark from the Northwest Atlantic and Gulf of Mexico, with comments on the *Squalus mitsukurii* species complex. Zootaxa, 4444:101–119. https://doi.org/10.11646/zootaxa.4444.2.1

Pimiento, C. and Balk, M. 2015. Body-size trends of the extinct giant shark *Carcharocles megalodon*: a deep-time perspective on marine apex predators. Paleobiology, 41:479–490. https://doi.org/10.1017/pab.2015.16

Pimiento, C. and Clements, C. 2014. When did *Carcharocles megalodon* become extinct? A new analysis of the fossil record. PLoS ONE, 9:e111086. https://doi.org/10.1371/journal.pone.0111086

Pimiento, C., González-Barba, G., Ehret, D., Hendy, A., MacFadden, B., and Jaramillo, C. 2013. Sharks and rays (Chondrichthyes, Elasmobranchii) from the late Miocene Gatun formation of

Panama. Journal of Paleontology, 87:755–774. https://doi.org/10.1666/12-117
Pimiento, C., MacFadden, B., Clements, C., Varela, S., Jaramillo, C., Velez-Juarbe, J., and Silliman, B. 2016. Geographical distribution patterns of *Carcharocles megalodon* over time reveal clues about extinction mechanisms. Journal of Biogeography, 43:1645–1655. https://doi.org/10.1111/jbi.12754
Pino, J. 2014. Fossil tooth of a cookie cutter shark (*Isistius triangulus*) from the late Miocene of Panama. Puente Biológico, 6:41–49.
Pinsky, M., Eikeset, A., McCauley, D., Payne, J., and Sunday, J. 2019. Greater vulnerability to warming of marine versus terrestrial ectotherms. Nature, 569:108–111. https://doi.org/10.1038/s41586-019-1132-4
Pledge, N. 1967. Fossil elasmobranch teeth of South Australia and their stratigraphic distribution. Transactions of the Royal Society of South Australia, 91:135–160.
Poey, F. 1860. L. Conspectus piscium cubensis. Memorias sobra la historia natural de la Isla de Cuba, 2:357–404, pl. 19.
Poey, F. 1861. Memorias sobra la historia natural de la Isla de Cuba, a compañados de sumarios Latinos y extractos en Francés. Tomo 2, p. 337–442.
Poey, F. 1868. Synopsis piscium cubensium. Catalogo razonado de los peces de la isla de Cuba. Repertorio Fisico–Natural de la Isla de Cuba, 2:279–484.
Poey, F. 1875. Enumeratio piscium cubensium. Anales de la Sociedad Española de Historia Natural, 4:75–161.
Poey, F. 1876. Enumeratio piscium cubensium (Parte III). Anales de la Sociedad Española de Historia Natural, 5:373–404.
Pollerspöck, J. and Shimada, K. 2024. The first recognition of the enigmatic fossil shark genus Megalolamna (Lamniformes, Otodontidae) from the lower Miocene of Europe and *M. serotinus* (Probst, 1879) as the newly designated type species for the genus. Zitteliana, 98:1–9. https://doi.org/10.3897/zitteliana.98.131387
Pollerspöck, J. and Unger, E. 2022. “Beiträge zur Kenntniss der fossilen Fische aus der Molasse von Baltringen” – Revision zum 200. Geburtstag von Pfarrer Josef Probst. Teil Batoidei (Probst 1877). Jahreshefte der Gesellschaft für Naturkunde Württemberg, 178:149–204. https://doi.org/10.26251/jhgfn.178.2022.149-204
Poortvliet, M., Olsen, J., Croll, D., Bernardi, G., Newton, K., Kollias, S., O’Sullivan, J., Fernando, D., Stevens, G., Magaña, F., and Seret, B. 2015. A dated molecular phylogeny of manta and devil rays (Mobulidae) based on mitogenome and nuclear sequences. Molecular Phylogenetics and Evolution, 83:72–85. https://doi.org/10.1016/j.ympev.2014.10.012
Portell, R. 2004. Eocene, Oligocene, and Miocene decapod crustaceans. Florida Paleontological Society, Florida Fossil Invertebrates, Part 5, 27 p.
Portell, R. and Agnew J. 2004. Pliocene and Pleistocene decapod crustaceans. Florida Paleontological Society, Florida Fossil Invertebrates, Part 4, 29 p.
Portell, R., Polites, G., Schmelz, G. 2006. Mollusca: Shoal River Formation (Middle Miocene). Florida Paleontological Society, Florida Fossil Invertebrates, Part 9, 52 p.
Portell, R., Hubbell, G., Donovan, S., Green, J., Harper, D., and Pickerill, R. 2008. Miocene sharks in the Kendeace and Grand Bay formations of Carriacou, The Grenadines, Lesser Antilles. Caribbean Journal of Science, 44:279–286. https://doi.org/10.18475/cjos.v44i3.a2
Pörtner, H. and Farrell, A. 2008. Physiology and climate change. Science, 322:690–692. https://doi.org/10.1126/science.1163156
Posey, M., Lindberg, W., Alphin, T., and Vose, F. 1996. Influence of storm disturbance on an offshore benthic community. Bulletin of Marine Science, 59:523–529.
Poulakis, G., Stevens, P., Timmers, A., Wiley, T., and Simpfendorfer, C. 2011. Abiotic affinities and spatiotemporal distribution of the endangered smalltooth sawfish, *Pristis pectinata*, in a south-western Florida nursery. Marine and Freshwater Research, 62:1165–1177. https://doi.org/10.1071/MF11008
Price, M. 2023. Sea level rise and a Florida mortuary pond: how oysters (*Crassostrea virginica*) reveal past climate change at the Manasota key offshore archaeological site. Doctoral dissertation. Leiden University, The Netherlands, 209 p.

Probst, J. 1877. Beiträge zur Kenntniss der fossilen Fische aus der Molasse von Baltringen. II: Batoidei A. Günther. Jahreshefte des Vereins für vaterländische Naturkunde in Württemberg, 33:69–103.
Probst, J. 1878. Beiträge zur Kenntniss der fossilen Fische aus der Molasse von Baltringen. Hayfische. Jahreshefte des Vereins für vaterländische Naturkunde in Württemberg, 34:113–154.
Probst, J. 1879. Beiträge zur Kenntniss der fossilen Fische aus der Molasse von Baltringen. Jahreshefte des Vereins für vaterländische Naturkunde in Württemberg, 35:127–191.
Purdy, R., Schneider, V., Applegate, S., McLellan, J., Meyer, R., and Slaughter, R. 2001. The Neogene sharks, rays, and bony fish from Lee Creek Mine, Aurora, North Carolina, p. 71–202. In Ray, C. and Bohaska, D. (eds.), Geology and Paleontology of the Lee Creek Mine, North Carolina, III Smithsonian Contributions to Paleobiology, No. 90. Smithsonian Institution Press, Washington, D.C.
Quoy, J. and Gaimard, J. 1824. Description des Poissons. Chapître IX. In Freycinet, L. de, Voyage autour du monde, entrepris par ordre du roi. Exécuté sur les corvettes de S.M. l'Uranie et la Physicienne, pendant les années 1817, 1818, 1819 et 1820. Paris. Description des Poissons. Description des Poissons. Chapter IX.: 192–401 [1–328 in 1824; 329–616 in 1825], Atlas pls. 43–65.
Rafinesque, C. 1810. Caraterri di alcuni nuovi generi e nuove specie di animali piante. Della Sicilia, con varie osservazioni sopra i medisimi, lère partie, p. [i–iv] 3–69.
Rafinesque, C. 1818. (Review of) Journal of the Academy of Natural Sciences of Philadelphia. Vol. I. Part I. American Monthly Magazine and Critical Review, 3:269–274.
Rangel, B., Rodrigues, S., Favaron, P., Amorim, A., and Rici, R. 2014. Structure and dental sexual dimorphism in *Dasyatis hypostigma* (Santos & Carvalho, 2004) (Myliobatiformes, Dasyadae). Microscopy: advances in scientific research and education. Microscopy book series—2014 edition. FORMATEX, Badajoz, p.89–94.
Ranzani, C. 1839. De novis speciebus piscium. Dissertatio prima. Novi Commentarii Academiae Scientiarum Instituti Bononiensis, 4:65–83, pl. 8–13.
Razak, H. and Kocsis, L. 2018. Late Miocene *Otodus* (*Megaselachus*) *megalodon* from Brunei Darussalam: Body length estimation and habitat reconstruction. Neues Jahrbuch für Geologie und Paläontologie-Abhandlungen, 288:299–306. https://doi.org/10.1127/njgpa/2018/0743
Reinecke, T. 2015. Batoids (Rajiformes, Torpediniformes, Myliobatiformes) from the Sülstorf Beds (Chattian, Late Oligocene) of Mecklenburg, northeastern Germany: a revision and description of three new species. Palaeovertebrata, 39:e2. https://doi.org/10.18563/pv.39.2.e2
Reinecke, T. and Radwański, A. 2015. Fossil sharks and batoids from the Korytnica-clays, early Badenian (Langhian, Middle Miocene), Fore-Carpathian basin, central Poland – a revision and updated record. Palaeontos, 28:1–32.
Reinecke, T., Moths, H., Grant, A., and Breitkreuz, H. 2005. Die Elasmobranchier des norddeutschen Chattiums, insbesondere des Sternberger Gesteins (Eochattium, Oligozän). Palaeontos, 8:1–135.
Reinecke, T., von der Hocht, F., and Gürs, K. 2008. Die Elasmobranchier des Vierlandiums, Unteres Miozän, im Nordwestdeutschen Becken aus Bohrungen und glaziofluviatilen Geröllen („Holsteiner Gestein") der Vierlande-Feinsande (Holstein) und der Kakert-Schichten (Niederrhein). Palaeontos, 14:1–54.
Reinecke, T., Louwye, S., Havekost, U., and Moths, H. 2011. The elasmobranch fauna of the late Burdigalian, Miocene, art Werder-Uesen, Lower Saxony, Germany, and its relationship with early Miocene faunas in the North Atlantic, Central Paratethys, and Mediterranean. Palaeontos, 20:1–170.
Reinecke, T., Mollen, F., Seitz, J., Motomura, H., Hovestadt, D., and Hoedemakers, K. 2023. Iconography of jaws and representative teeth of extant rhinopristiform and dasyatoid batoids (Chondrichthyes, Elasmobranchii) for comparison with fossil batoid material. Palaeontos, 34:1–158.
Reinhart, R. 1976. Fossil sirenians and desmostylians from Florida and elsewhere. Bulletin of the Florida Museum of Natural History, 20:187–300. https://doi.org/10.58782/flmnh.bywr8066
Renaud, P., Ambrose Jr., W., Riggs, S., and Syster, D. 1996. Multi-level effects of severe storms on an off-shore temperate reef system: benthic sediments, macroalgae, and implications for

fisheries. Marine Ecology, 17:383–396.
https://doi.org/10.1111/j.1439-0485.1996.tb00516.x
Renaud, P., Riggs, S., Ambrose, W. Jr, Schmid, K., and Snyder, S. 1997. Biological-geological interactions: storm effects on macroalgal communities mediated by sediment characteristics and distribution. Continental Shelf Research, 17:37–56.
https://doi.org/10.1016/0278-4343(96)00019-2
Renz, M. 1999. Fossiling in Florida: A Guide for Diggers and Divers. University Press of Florida, 202 p.
Renz, M. 2002. Megalodon: hunting the hunter. PaleoPress, 159 p.
Renz, M. 2005. Giants in the Storm. PaleoPress, 263 p.
Richards, V., Henning, M., Witzell, W., and Shivji, M. 2009. Species delineation and evolutionary history of the globally distributed spotted eagle ray (*Aetobatus narinari*). Journal of Heredity, 100:273–283.
https://doi.org/10.1093/jhered/esp005
Richardson, J. 1836. The Fish. In Fauna Boreali–Americana; or the zoology of the northern parts of British America: containing descriptions of the objects of natural history collected on the late northern land expeditions, under the command of Sir John Franklin, R.N. Fauna Boreali–Americana; or the zoology of the northern parts of British America: Part 3: i–xv + 1–327, Pls. 74–97.
Riggs, S. 1979. Phosphorite sedimentation in Florida; a model phosphogenic system. Economic Geology, 74:285–314.
https://doi.org/10.2113/gsecongeo.74.2.285
Riggs, S. 1984. Paleoceanographic model of Neogene phosphorite deposition, U.S. Atlantic continental margin. Science, 223:123–131.
https://doi.org/10.1126/science.223.4632.123
Riggs, S., Ambrose, W., Cook, J., Snyder, S.W., and Snyder, S.W. 1998. Sediment production on sediment-starved continental margins: the interrelationship between hardbottoms, sedimentological and benthic community processes, and storm dynamics: Journal of Sedimentary Research, 68:155–168.
https://doi.org/10.2110/jsr.68.155
Risso, A. 1810. Ichthyologie de Nice, ou histoire naturelle des poissons du département des Alpes Maritimes. Paris: F. Schoell, i–xxxvi + 1–388, pls. 1–11.
Roedel, P. and Ripley, W. 1950. California sharks and rays. California Fish and Game Bulletin, No. 75, 88 p., 65 figs.
Ruddiman, W. 2014. Earth's Climate: Past and Future, 3rd Edition. W.H. Freeman, 445 p.
Rüppell, W. 1837. Neue Wirbelthiere zu der Fauna von Abyssinien gehörig: Fische des rothen Meeres. Frankfurt am Main, 1837:53–80, pls. 15–21.
Sahni, A. and Mehrotra, D.K. 1981. Elasmobranch from the coastal Miocene sediments of peninsular India. Biological Memoirs, 5:83–121.
Sales, J., de Oliveira, C., dos Santos, W., Rotundo, M., Ferreira, Y., Ready, J., Sampaio, I., Oliveira, C., Cruz, V., Lara-Mendoza, R., and da Silva Rodrigues-Filho, L. 2019. Phylogeography of eagle rays of the genus *Aetobatus: Aetobatus narinari* is restricted to the continental western Atlantic Ocean. Hydrobiologia, 836:169–183.
https://doi.org/10.1007/s10750-019-3949-0
Schmidt, D. 2007. The closure history of the Central American seaway: evidence from isotopes and fossils to models and molecules, p. 429–444. In Williams, M., Haywood, A., Gregory, F., and Schmidt, D. (eds.), Deep-Time Perspectives on Climate Change: Marrying the Signal from Computer Models and Biological Proxies. The Micropalaeontological Society, Special Publications. The Geological Society, London.
https://doi.org/10.1144/TMS002.19
Schneider, B. and Schmittner, A. 2006. Simulating the impact of the Panamanian seaway closure on ocean circulation, marine productivity and nutrient cycling. Earth and Planetary Science Letters, 246:367–380.
https://doi.org/10.1016/j.epsl.2006.04.028
Schultz, J., Feldheim, K., Gruber, S., Ashley, M., McGovern, T., and Bowen, B. 2008. Global phylogeography and seascape genetics of the lemon sharks (genus *Negaprion*). Molecular Ecology, 17:5336–5348.
https://doi.org/10.1111/j.1365-294X.2008.04000.x

Schwartz, F. 1990. Mass Migratory Congregations and Movements of Several Species of Cownose Rays, Genus *Rhinoptera*: A World-wide Review. Journal of the Elisha Mitchell Scientific Society, 106:10–13.

Scott, T. 1985a. The Geology of the Florida Peninsula and its Relationship to Economic Phosphate Deposits, p. 97–113. In Snyder, S. (ed.), International Geological Correlation Project No. 156, Phosphorites; Guidebook of the eighth international field workshop and symposium (southeastern United States).

Scott, T. 1985b. The lithostratigraphy of the Central Florida Phosphate District and its southern extension, p. 28–37. In Cathcart, J. and Scott, T. (eds.), Florida Land-Pebble Phosphate District, Field Trip Guidebook. Geological Society of American Annual Meeting, Orlando, Florida.

Scott, T. 1986. A Revision of the Miocene Lithostratigraphic Nomenclature, Southwestern Florida. Gulf Coast Association of Geological Societies Transactions, 36:553–560.

Scott, T. 1988. The lithostratigraphy of the Hawthorne Group (Miocene) of Florida. Florida Geological Survey Bulletin, No. 59, 148 p.

Scott, T. 1990. The Lithostratigraphy of the Hawthorn Group of Peninsular Florida, p. 325–336. In Burnett, W. and Riggs, S. (eds.), Phosphate Deposits of the World. Cambridge University Press, Cambridge, UK.

Scott, T. 1997. Miocene to Holocene history of Florida, p. 57–68. In Randazzo, A. and Jones, D. (eds.), The Geology of Florida, University Press of Florida, Gainesville, Florida.

Scott, T. 2011. Geology of the Florida Platform, Pre-Mesozoic-Recent, p. 17–31. In Buster, N. and Holmes, C. (eds.), Geology of the Florida Platform. Gulf of Mexico Origin, Waters, and Biota: Volume 3, Geology. A&M Press, Texas.

Scott, T. and Allmon, W. 1992. Plio-Pleistocene stratigraphy and paleontology of southern Florida (No. 36). Published for the Florida Geological Survey. 194p.

Scott, T., Campbell, K., Rupert, F., Arthur, J., Green, R., Means, G., Missimer, T., Lloyd, J., Yon, J., and Duncan, J. 2001. Geologic Map of the State of Florida. Map Series 146, Florida Geological Survey.

Scudder, S., Simons, E., and Morgan, G., 1995. Chondrichthyes and Osteichthyes from the early Pleistocene Leisey Shell Pit local fauna, Hillsborough County, Florida. Bulletin of the Florida Museum of Natural History, 37:251–272.

Seitz, J. and Waters, J. 2018. Clarifying the Range of the Endangered Largetooth Sawfish in the United States. Gulf and Caribbean Research, 29:15–22. https://doi.org/10.18785/gcr.2901.05

Sepulchre, P., Arsouze, T., Donnadieu, Y., Dutay, J., Jaramillo, C., Le Bras, J., Martin, E., Montes, C., and Waite, A. 2014. Consequences of shoaling of the Central American Seaway determined from modeling Nd isotopes. Paleoceanography, 29:176–189. https://doi.org/10.1002/2013PA002501

Sharma, K. and Patnaik, R. 2013. Additional fossil batoids (skates and rays) from the Miocene deposits of Baripada Beds, Mayurbhanj District, Orissa, India. Earth Science India, 6:160–184.

Sharma, K. and Patnaik, R. 2014. Miocene fishes from Baripada beds, Orissa and their palaeoenvironmental, palaeobiogeographic and palaeoclimatic significance. Special Publication of the Palaeontological Society of India, 5:291–323.

Sharma, K., Singh, N., Patnaik, R., Tiwari, R., Singh, N., Singh, Y., Choudhary, D., and Lalotra, S. 2021. Sharks and rays (chondrichthyes, elasmobranchii) from the Miocene sediments of Kutch, Gujarat, India: paleoenvironmental and paleobiogeographic implications. Historical Biology, 34:10–29. https://doi.org/10.1080/08912963.2021.1893712

Shimada, K. 1987. Elasmobranchs from the Early Pliocene Naarai Formation, Choshi City, Chiba Prefecture, and from the Middle Miocene Tokigawa Group, Higashimatsuyama City, Saitama Prefecture, Japan. Thirtieth Japanese Students Science Prize Complete Works, Japan Home Teacher Center, Tokyo, p. 354–357.

Shimada, K. 2021. The size of the megatooth shark, *Otodus megalodon* (Lamniformes: Otodontidae), revisited. Historical Biology, 33:904–911. https://doi.org/10.1080/08912963.2019.1666840

Shimada, K., Chandler, R., Lam, O., Tanaka, T., and Ward, D. 2016. A new elusive otodontid shark (Lamniformes: Otodontidae) from the lower Miocene, and comments on the taxonomy

of otodontid genera, including the 'megatoothed' clade. Historical Biology, 29:704–714. https://doi.org/10.1080/08912963.2016.1236795

Shimada, K., Becker, M., and Griffiths, M. 2020. Body, jaw, and dentition lengths of macrophagous lamniform sharks, and body size evolution in Lamniformes with special reference to 'off-the-scale' gigantism of the megatooth shark, *Otodus megalodon*. Historical Biology, 33:2543–2559. https://doi.org/10.1080/08912963.2020.1812598

Shimada, K., Motani, R., Wood, J., Sternes, P., Tomita, T., Bazzi, M., Collareta, A., Gayford, J., Türtscher, J., Jambura, P., Kriwet, K., Vullo, R., Long, D., Summers, A., Maisey, J., Underwood, C., Ward, D., Maisch IV, H., Perez, V., Feichtinger, I., Naylor, G., Moyer, J., Higham, T., da Silva, J., Bornatowski, H., González-Barba, G., Griffiths, M., Becker, M., Siversson, M. 2025. Reassessment of the possible size, form, weight, cruising speed, and growth parameters of the extinct megatooth shark, *Otodus megalodon* (Lamniformes: Otodontidae), and new evolutionary insights into its gigantism, life history strategies, ecology, and extinction. Palaeontologia Electronica, 28.1.a12 https://doi.org/10.26879/1502

Shimada, K., Maisch, H., IV, Perez, V., Becker, M., and Griffiths, M. 2022. Revisiting body size trends and nursery areas of the Neogene megatooth shark, *Otodus megalodon* (Lamniformes: Otodontidae), reveals Bergmann's rule possibly enhanced its gigantism in cooler waters. Historical Biology, 35:208–217. https://doi.org/10.1080/08912963.2022.2032024

Shimada, K., Bonnan, M., Becker, M., and Griffiths, M. 2021. Ontogenetic growth pattern of the extinct megatooth shark *Otodus megalodon*—implications for its reproductive biology, development, and life expectancy. Historical Biology, 33:3254–3259. https://doi.org/10.1080/08912963.2020.1861608

Simons, E., MacKenzie, K., and Hulbert, R. 2014. Osteichthyes and Chondrichthyes from the Early Pliocene Palmetto Fauna, Central Florida Phosphate Mining Region. The Paleontological Society Special Publications, 13:37–37. https://doi.org/10.1017/S2475262200010777

Simpson, G. 1930. Tertiary Land Mammals of Florida. Bulletin of the American Museum of Natural History, 59:149–211.

Sinibaldi, R. 1998. Fossil diving in Florida's Waters or Any Other Waters Containing Prehistoric Treasures, 118 p.

Smith, T., Anderson, G., Balentine, K., Tiling, G., Ward, G., and Whelan, K. 2009. Cumulative impacts of hurricanes on Florida mangrove ecosystems: sediment deposition, storm surges and vegetation. Wetlands, 29:24–34. https://doi.org/10.1672/08-40.1

Snelson, F. and Williams, S. 1981. Notes on the occurrence, distribution, and biology of elasmobranch fishes in the Indian River lagoon system, Florida. Estuaries, 4:110–120.

Snodgrass, R. and Heller, E. 1905. Papers from the Hopkins-Stanford Galapagos Expedition, 1898-1899. XVII. Shore fishes of the Revillagigedo, Clipperton, Cocos and Galapagos islands. Proceedings of the Washington Academy of Sciences, 6:333–427.

Snyder, S., Hine, A., and Riggs, S. 1990. The seismic stratigraphic record of shifting Gulf Stream flow paths in response to Miocene glacioeustacy: implications for phosphogenesis along the North Carolina Continental Margin, p. 396–423. In Burnett, W. and Riggs, S. (eds.), Phosphate Deposits of the World, Volume III: Neogene to Modern Phosphorites. Cambridge University Press, Cambridge, UK.

So, S., Juarez, B., Valle-Levinson, A., and Gillin, M. 2019. Storm surge from hurricane Irma along the Florida peninsula. Estuarine, Coastal and Shelf Science, 229:106402. https://doi.org/10.1016/j.ecss.2019.106402

Sorenson, L., Santini, F., and Alfaro, M. 2014. The effect of habitat on modern shark diversification. Journal of Evolutionary Biology, 27:1536–1548. https://doi.org/10.1111/jeb.12405

Soto, L. 2016. Systematics and Paleoecology of a new chondrichthyan fauna from the middle Miocene (Barstovian) Torreya Formation, Gadsen County, Florida, USA. Unpublished M.S. Thesis, 110 p.

Soto, L. and MacFadden, B. 2014. Paleoecology of new chondrichthyan fauna from middle Miocene (Barstovian) Gadsen County, Florida, USA. North American Paleontological Convention. Session 24-Poster 51.

Springer, S. 1939. Two new Atlantic species of dog sharks, with a key to the species of *Mustelus*. Proceedings of the United States National Museum, 86:461–468.
Springer, S. 1940. Three new sharks of the genus *Sphyrna* from the Pacific coast of tropical America. Stanford Ichthyological Bulletin, 1:161–172.
Springer, S. 1950a. Natural history notes on the lemon shark, *Negaprion brevirostris*. Texas Journal of Science, 2:349–359.
Springer, S. 1950b. A revision of north American sharks allied to the genus *Carcharhinus*. American Museum Novitates, 1451:1–13.
Springer, S. 1960. Natural history of the sandbar shark *Eulamia milberti*. Fishery Bulletin, 61:1–38.
Springer, S. 1966. A review of Western Atlantic Cat Sharks, Scyliorhinidae, with descriptions of a new genus and five new species. Fishery Bulletin, 65:581–624.
Springer, S. and Lowe, R. 1963. A new smooth dogshark, *Mustelus higmani*, from the Equatorial Atlantic coast of South America. Copeia, 1963:245–251.
Springer, V. 1964. A revision of the carcharhinid shark genera *Scoliodon*, *Loxodon*, and *Rhizoprionodon*. Proceedings of the United States National Museum, 115:559–632.
Staig, F., Hernández, S., López, P., Villafaña, J., Varas, C., Soto, L., and Carrillo-Briceño, J. 2015. Late Neogene elasmobranch fauna from the Coquimbo formation, Chile. Revista Brasileira de Paleontologia, 18:261–272. https://doi.org/10.4072/rbp.2015.2.07
Sternes, P., Wood, J., and Shimada, K. 2022. Body forms of extant lamniform sharks (Elasmobranchii: Lamniformes), and comments on the morphology of the extinct megatooth shark, *Otodus megalodon*, and the evolution of lamniform thermophysiology. Historical Biology, 35:139–151. https://doi.org/10.1080/08912963.2021.2025228
Sternes, P., Jambura, P., Türtscher, J., Kriwet, J., Siversson, M., Feichtinger, I., Naylor, G., Summers, A., Maisey, J., Tomita, T., Moyer, J., Higham, T., da Silva, J., Bornatowski, H., Long, D., Perez, V., Collareta, A., Underwood, C., Ward, D., Vullo, R., González-Barba, G., Maisch IV, H., Griffiths, M., Becker, M., Wood, J., and Shimada, K. 2024. White shark comparison reveals a slender body for the extinct megatooth shark, *Otodus megalodon* (Lamniformes: Otodontidae). Palaeontologia Electronica, 27.1:a7. https://doi.org/10.26879/1345
Steurbaut, E. and Herman, J. 1978. Biostratigraphie et poissons fossiles de la formation de l'Argile de Boom (Oligocène moyen du Bassin belge). Geobios, 11:297–325.
Stevens, G., Fernando, D., Dando, M., and Notarbolo di Sciara, G. 2018. Guide to the Manta and Devil Rays of the World. Princeton University Press, 144 p.
Stockdon, H., Doran, K., Thompson, D., Sopkin, K., Plant, N., and Sallenger, A. 2012. National Assessment of Hurricane-induced Coastal Erosion Hazards: Gulf of Mexico. U.S. Geological Survey Open-file Report 2012-1084, 51 p.
Stone, N. and Shimada, K. 2019. Skeletal anatomy of the bigeye sand tiger shark, *Odontaspis noronhai* (Lamniformes: Odontaspididae), and its implications for lamniform phylogeny, taxonomy, and conservation biology. Copeia, 107:632–652. https://doi.org/10.1643/CG-18-160
Strasburg, D. 1958. Distribution, abundance, and habits of pelagic sharks in the central Pacific Ocean. Fishery Bulletin 138. Fishery Bulletin of the Fish and Wildlife Service, 58:335–361.
Strasburg, D. 1963. The diet and dentition of *Isistius brasiliensis*, with remarks on tooth replacement in other sharks. Copeia, 1963:33–40. https://doi.org/10.2307/1441272
Straube, N., Li, C., Claes, J., Corrigan, S., and Naylor, G. 2015. Molecular phylogeny of Squaliformes and first occurrence of bioluminescence in sharks. BioMed Central Evolutionary Biology, 15:162. https://doi.org/10.1186/s12862-015-0446-6
Stromer, E. 1905. Die Fischreste des Mittleren und Oberen Eocäns von Ägypten. I. Teil: Die Selachier, A. Myliobatiden und Pristiden. Beiträge zur Paläontologie und Geologie Österreich-Ungarns, 18:37–58.
Suárez, M., Encinas, A., and Ward, D. 2006. An Early Miocene elasmobranch fauna from the Navidad Formation, Central Chile, South America. Cainozoic Research, 4:3–18.
Szabó, M. and Kocsis, L. 2016. A new Middle Miocene selachian assemblage (Chondrichthyes, Elasmobranchii) from the Central Paratethys (Nyirád, Hungary): implications for temporal

turnover and biogeography. Geologica Carpathica, 67:573–594. https://doi.org/10.1515/geoca-2016-0036

Szabó, M., Kocsis, L., Bosnakoff, M., and Sebe, K. 2021. A diverse Miocene fish assemblage (Chondrichthyes and Osteichthyes) from the Pécs-Danitzpuszta sand pit (Mecsek Mts, Hungary). Földtani Közlöny, 151:363–409. https://doi.org/10.23928/foldt.kozl.2021.151.4.363

Szabó, M., Kocsis, L., Tóth, E., Szabó, P., Németh, T., and Sebe, K. 2022. Chondrichthyan (Holocephali, Squalomorphii and Batomorphii) remains from the Badenian of southern Hungary (Tekeres, Mecsek Mountains): the first deepwater cartilaginous fishes from the Middle Miocene of the Central Paratethys. Papers in Palaeontology, 8:e1471. https://doi.org/10.1002/spp2.1471

Szabó, M., Kocsis, L., Szabó, P., Békési, Z., and Gulyás, P. 2023. New records and specimens to the Badenian fish fauna of Nyirád (Hungary), including the first report of *Galeocerdo cuvier* from the Middle Miocene of Europe. Fragmenta Palaeontologica Hungarica, 38:53–74. https://doi.org/10.17111/FragmPalHung.2023.38.53

Takakuwa, Y. 2014. A dense occurrence of teeth of fossil ‘‘mako’’ shark (‘‘*Isurus*’’ *hastalis*: Chondrichthyes, Lamniformes), associated with a balaenopterid-whale skeleton of the Late Miocene Pisco Formation, Peru, South America. Bulletin of Gunma Museum of Natural History, 18:77–86.

Talling, P. 1998. How and where do incised valleys form if sea level remains above the shelf edge?. Geology, 26:87–90. https://doi.org/10.1130/0091-7613(1998)026%3C0087:HAWDIV%3E2.3.CO;2

Taylor, L. 1972. A revision of the shark family Heterodontidae (Heterodontiformes, Selachii). Ph.D. Thesis, U. California, San Diego, xiii, 176 p. University Microfilms International.

Taylor, L. and Castro-Aguirre, J. 1972. *Heterodontus mexicanus*, a new horn shark from the Golfo de California. Anales de la Escuela Nacional de Ciencias Biologicas México, 19:123–143.

Thomas, M. 1965. Let’s Find Fossils on the Beach. Sunshine Press, 51 p.

Türtscher, J., López-Romero, F., Jambura, P., Kindlimann, R., Ward, D., and Kriwet, J. 2021. Evolution, diversity, and disparity of the tiger shark lineage *Galeocerdo* in deep time. Paleobiology, 47:574–590. https://doi.org/10.1017/pab.2021.6

Underwood, C. and Cumbaa, S. 2010. Chondrichthyans from a Cenomanian (Late Cretaceous) bonebed, Saskatchewan, Canada. Palaeontology, 53:903–944. https://doi.org/10.1111/j.1475-4983.2010.00969.x

Underwood, C., Johanson, Z., Welten, M., Metscher, B., Rasch, L., Fraser, G., and Smith, M. 2015. Development and evolution of dentition pattern and tooth order in the skates and rays (Batoidea; Chondrichthyes). PLoS ONE, 10:e0122553. https://doi.org/10.1371/journal.pone.0122553

Uyeno, T. 1978. A preliminary report on fossil fishes from Ts’o-chen Tainan. Science Report Geology and Paleontology, 1:5–17.

Uyeno, T., Kondo, K., and Inoue, K. 1990. A nearly complete tooth set and several vertebrae of the lamnid shark *Isurus hastalis* from the Pliocene in Chiba, Japan. Journal of the Natural History Museum and Institute, 1:15–20.

Van den Bosch, M. 1978. On shark teeth and scales from the Netherlands and the biostratigraphy of the Tertiary of the eastern part of the country. Mededelingen Van De Werkgroep Voor Tertiaire En Kwartaire Geologie, 15:129–136.

Van den Bosch, M., Cadee, M., and Janssen, A. 1975. Lithostratigraphical and biostratigraphical subdivision of Tertiary deposits (Oligocene-Pliocene) in the Winterswijk-Almelo region (eastern part of the Netherlands). Scripta Geologica, 29:1–167.

Van Hasselt, J. 1823. Uittreksel uit een brief van Dr. J.C. van Hasselt aan den Heer C.J. Temminck. Algemeene Konst- en Letter-Bode Deel, 1(20): 315–317;(21): 328–331.

Vélez-Juarbe, J., Wood, A., and Pimiento, C. 2016. Pygmy sperm whales (Odontoceti, Kogiidae) from the Pliocene of Florida and North Carolina, Journal of Vertebrate Paleontology, 36:e1135806. https://doi.org/10.1080/02724634.2016.1135806

Vialle, N., Adnet, S., and Cappetta, H. 2011. A new shark and ray fauna from the Middle Miocene of Mazan, Vaucluse (southern France) and its importance in interpreting the paleoenvironment of marine deposits in the southern Rhodanian Basin. Swiss Journal of

Palaeontology, 130:241–258.
https://doi.org/10.1007/s13358-011-0025-4
Villafaña, J., Marramà, G., Hernandez, S., Carrillo-Briceño, J., Hovestadt, D., Kindlimann, R., and Kriwet, J. 2019. The Neogene fossil record of *Aetomylaeus* (Elasmobranchii, Myliobatidae) from the southeastern Pacific. Journal of Vertebrate Paleontology, 39:e1577251.
https://doi.org/10.1080/02724634.2019.1577251
Voight, M. and Weber, D. 2011. Field guide for sharks of the genus *Carcharhinus*. Verlag Dr. Friedrich Pfeil, München, 151 p.
Walbaum, J. 1792. Petri Artedi sueci genera piscium. In quibus systema totum ichthyologiae proponitur cum classibus, ordinibus, generum characteribus, specierum differentiis, observationibus plurimis. Redactis speciebus 242 ad genera 52. Ichthyologiae pars III. Ant. Ferdin. Rose, Grypeswaldiae [Greifswald].
Walker, R. and Plint, A. 1992. Wave-and storm- dominated shallow marine systems, p. 219–238. In Walker, R. and James, N. (eds.), Facies Models: Response to Sea Level Change, Geological Association of Canada, St. John's.
Waller, T. 2018. Systematics and Biostratigraphy of *Chesapecten* and *Carolinapecten* (Mollusca: Bivalvia: Pectinidae) in the Upper Miocene and Pliocene "Lower Tamiami Formation" of Southwestern Florida. Bulletin of the Florida Museum of Natural History, 56:1–47.
https://doi.org/10.58782/flmnh.ublr4862
Ward, D. 1979. Additions to the fish fauna of the English Paleogene. 2. A new species of *Dasyatis* (sting ray) from the London Clay (Eocene) of Essex, England. Tertiary Research, 2:75–81.
Ward, D. and Bonavia, C. 2001. Additions to, and a review of, the Miocene shark and ray fauna of Malta. The Central Mediterranean Naturalist, 3:131–146.
Ward, L. 1992. Diagnostic mollusks from the APAC Pit, Sarasota, Florida, p. 28–72. In Allmon, W. and Scott, T. (eds.), The Plio-Pleistocene stratigraphy and paleontology of southern Florida (Florida Geological Survey Special Publication, 36).
Webb, D., MacFadden, B., and Baskin, J. 1981. Geology and paleontology of the Love Bone Bed from the late Miocene of Florida. American Journal of Science, 281:513–544.
Webb, S. 1974. Pleistocene Mammals of Florida. University Press of Florida, Gainesville, Florida, 270 p.
Webb, S. 1991. Ecogeography and the great American interchange. Paleobiology, 17:266–280.
https://doi.org/10.1017/S0094837300010605
Webb, S. and Crissinger, D. 1983. Stratigraphy and vertebrate paleontology of the central and southern phosphate districts of Florida, p. 28–72. In Central Florida Phosphate District Field Trip Guidebook (Geological Society of America, Southeastern Section).
Webb, S. and Tessman, N., 1968. A Pliocene vertebrate fauna from low elevation in Manatee County, Florida. American Journal of Science, 266:777–811.
Weigel, R. 1962. Fossil vertebrates of Vero, Florida. Florida Geological Survey, Special Publication 10, 59 p.
Weisbord, N. 1971. Corals from the Chipola and Jackson Bluff Formations of Florida. Florida Geological Survey Bulletin No. 53, 100 p.
Welton, M., Smith, M., Underwood, C., and Johanson, Z. 2015. Teeth outside the mouth? Evolution and development of the sawfish and sawshark rostral dentitions (Elasmobranchii; Chondrichthyes). Royal Society Open Science, 2:150189.
https://doi.org/10.1098/rsos.150189
Wenzel, F. and López Suárez, P. 2012. What is known about cookiecutter shark (*Isistius* spp.) interactions with cetaceans in Cape Verde seas?. Zoologia Caboverdiana, 3:57–66.
Westerhold, T., Marwan, N., Drury, A., Liebrand, D., Agnini, C., Anagnostou, E., Barnet, J., Bohaty, S., De Vleeschouwer, D., Florindo, F., and Frederichs, T. 2020. An astronomically dated record of Earth's climate and its predictability over the last 66 million years. Science, 369:1383–1387.
https://doi.org/10.1126/science.aba6853
White, E. 1926. Eocene fishes from Nigeria. Bulletin of the Geological Survey of Nigeria, 10:1–82.
White, E. 1955. Notes on African Tertiary sharks. Bulletin of American Palaeontology, 5:319–325.

White, E. and Moy-Thomas, J. 1941. Notes on the nomenclature of fossil fishes. Part III. Homonyms MZ. Annals and Magazine of Natural History, 11:395–400.
White, W. 2014. A revised generic arrangement for the eagle ray family Myliobatidae, with definitions for the valid genera. Zootaxa, 3860:149–166. https://doi.org/10.11646/zootaxa.3860.2.3
White, W. and Last, P. 2013. Notes on shark and ray types at the South China Sea Fisheries Research Institute (SCSFRI) in Guangzhou, China. Zootaxa, 3752:228–248. https://doi.org/10.11646/zootaxa.3752.1.14
White, W. and Naylor, G. 2016. Resurrection of the family Aetobatidae (Myliobatiformes) for the pelagic eagle rays, genus *Aetobatus*. Zootaxa, 4139:435–438. https://doi.org/10.11646/zootaxa.4139.3.10
White, W., Furumitsu, K., and Yamaguchi, A. 2013. A New Species of Eagle Ray *Aetobatus narutobiei* from the Northwest Pacific: An Example of the Critical Role Taxonomy Plays in Fisheries and Ecological Sciences. PLoS ONE, 8:e83785. https://doi.org/10.1371/journal.pone.0083785
White, W., Corrigan, S., Yang, L., Henderson, A., Bazinet, A., Swofford, D., and Naylor, G. 2018. Phylogeny of the manta and devilrays (Chondrichthyes: Mobulidae), with an updated taxonomic arrangement for the family. Zoological Journal of the Linnean Society, 182:50–75. https://doi.org/10.1093/zoolinnean/zlx018
Whitenack, L. and Gottfried, M. 2010. A morphometric approach for addressing tooth-based species delimitation in fossil Mako Sharks, *Isurus* (Elasmobranchii: Lamniformes). Journal of Vertebrate Paleontology, 30:17–25. https://doi.org/10.1080/02724630903409055
Whitley, G. 1929. Addition to the check list of the fishes of New South Wales. The Australian Zoologist, 5:353–357.
Whitley, G. 1939. Taxonomic notes on sharks and rays. The Australian Zoologist, 9:227–262.
Whitley, G. 1940. The Nomenclator Zoologicus and some new fish names. The Australian Naturalist, 10:241–243.
Williams, M., Haywood, A., Harper, E., Johnson, A., Knowles, T., Leng, M., Lunt, D., Okamura, B., Taylor, P., and Zalasiewicz, J. 2009. Pliocene climate and seasonality in North Atlantic shelf seas. Philosophical Transactions of the Royal Society A: Mathematical, Physical and Engineering Sciences, 367:85–108. https://doi.org/10.1098/rsta.2008.0224
Winkler, T. 1874. Deuxième mémoire sur des dents de poissons fossiles du terrain bruxellien. Archives du Musée Teyler, 4:16–48.
Wirsing, A., Heithaus, M., and Dill., L. 2007. Fear factor: do dugongs (*Dugong dugon*) trade food for safety from tiger sharks (*Galeocerdo cuvier*)?. Oecologia, 153:1031–1040. https://doi.org/10.1007/s00442-007-0802-3
Woodburne, M. 2010. The Great American Biotic Interchange: dispersals, tectonics, climate, sea level and holding pens. Journal of Mammalian Evolution, 17:245–264. https://doi.org/10.1007/s10914-010-9144-8
Wright, C. 1893. The Phosphate industry of the United States. Sixth Special Report of the Commissioner of Labor, 145 p.
Wueringer, B., Squire, L., and Collin, S. 2009. The biology of extinct and extant sawfish (Batoidea: Sclerorhynchidae and Pristidae). Reviews in Fish Biology and Fisheries, 19:445–464. https://doi.org/10.1007/s11160-009-9112-7
Yeiser, B., Heupel, M., and Simpfendorfer, C. 2008. Occurrence, home range and movement patterns of juvenile bull (*Carcharhinus leucas*) and lemon (*Negaprion brevirostris*) sharks within a Florida estuary. Marine and Freshwater Research, 59:489–501. https://doi.org/10.1071/MF07181
Zachos, J., Pagani, M., Sloan, L., Thomas, E., and Billups, K. 2001. Trends, rhythms, and aberrations in global climate 65 Ma to present. Science, 292:686–693. https://doi.org/10.1126/science.1059412
Zachos, J., Dickens, G., and Zeebe, R. 2008. An early Cenozoic perspective on greenhouse warming and carbon-cycle dynamics. Nature, 451:279–283. https://doi.org/10.1038/nature06588
Zbyszewski, G. 1947. Découverte d'un rostre de grand *Pristis* dans l'Helvétien de Lisbonne. Boletim da Sociedade Geológica de Portugal, 6:237–242.

Zhang, L., Hay, W., Wang, C., and Gu, X. 2019. The evolution of latitudinal temperature gradients from the latest Cretaceous through the Present. Earth-Science Reviews, 189:147–158. https://doi.org/10.1016/j.earscirev.2019.01.025

Zidowitz, H., Fock, H., Pusch, C., and von Westernhagen, H. 2004. A first record of *Isistius plutodus* in the north-eastern Atlantic. Journal of Fish Biology, 64:1430–1434. https://doi.org/10.1111/j.0022-1112.2004.00382.x

Ziegler, M., Jaeger, J., Steadman, D., Perez, V., and MacFadden, B. 2019. Paleoenvironmental Analysis of an Unusual Fossil Locality from the Late Miocene in Northern Florida, USA. Society of Vertebrate Paleontology Conference, B90, p. 224.